VOLCANIC FRAMEWORK AND GEOCHEMICAL EVOLUTION OF THE ARCHEAN HOPE BAY GREENSTONE BELT, NUNAVUT, CANADA

by
ANDREW J. SHANNON
B.Sc.Hon. University of Waterloo, 2005

A THESIS SUBMITTED IN PARTIAL FULFILMENT
OF THE REQUIREMENTS FOR THE DEGREE OF

MASTER OF SCIENCE

in

THE FACULTY OF GRADUATE STUDIES

(Geological Sciences)

THE UNIVERSITY OF BRITISH COLUMBIA
(Vancouver)
April 2008

Abstract

Part of the Slave Structural Province, the Hope Bay Greenstone Belt is a 82 km long north-striking sequence of supracrustal rocks dominated by mafic volcanic rocks with lesser felsic volcanic and sedimentary rocks. Mapping of two transects in the southern section and two transects in the northern section have contributed to a robust stratigraphic framework the belt. Three recently discovered Archean lode gold deposits in the Hope Bay Greenstone belt have associations with major structures and specific lithologies (Fe-Ti enriched basalts).

The Flake Lake and the Clover Transects are in the southern part of the belt and the Wolverine and Doris-Discovery Transects are in the northern part of the belt. This work subdivides the volcanic rocks into distinct suites based upon field, petrologic, geochemical, and geochronologic criteria. Some of the suites are stratigraphically continuous and can be correlated tens of kilometres along strike thereby linking the two parts of the Hope Bay Greenstone Belt.

U-Pb geochronology supports work by Hebel (1999) concluded that virtually all the supracrustal rocks in the Hope Bay Greenstone Belt were deposited over at least 53 m.y. (2716-2663 Ma), with the majority of the volcanism occurring after 2700 Ma.

A number of basalt groups are identified and include the normal basalt, the LREE-enriched basalt, the Ti-enriched basalt and the Ti-enriched Al-depleted basalt groups. They have chemical signatures that vary in trace elements particularly HFSE and REE's, and can be easily be distinguished by geochemical screening. The felsic volcanic suites are also divided into three main groups, tholeiitic rhyolite, calc-alkaline dacite and calc-alkaline rhyolite groups. Nd and Hf isotope signatures are consistent with trace element

signatures in identifying mafic and felsic volcanic groups, with the tholeiitic rhyolite showing highly variable signature.

The Hope Bay Greenstone Belt has been show to have a number of felsic and volcanic cycles. An early construction phase of the belt is made up of primarily mafic volcanics which is followed by felsic volcanism equalled mafic volcanism which lacks basalts enriched in Ti. The geodynamic environment that created the Hope Bay Greenstone Belt can be explained by plume influenced subduction zone.

TABLE OF CONTENTS

CHAPTER 3
Geochemical Evolution of the Hope Bay Greenstone Belt

CHAPTER 4

Conclusions and Suggestions for Further Work

Appendices

List of Tables

List of Figures

Acknowledgments

In the past two years several organizations and numerous people have supported me in various ways and without them this project would not have been possible.
Generous financial support was provided by Miramar Hope Bay Limited, National Science and Engineering (NSERC) and Society of Economic Geology (SEG). My two seasons of field work in Nunavut would not have been possible with out the logistical support provided by Miramar Hope Bay Limited.
I would like to thank the faculty at the Department of Earth and Ocean Science at UBC for always having door open and helpful comments. I would particularly like to thank James Scoates, Greg Dipple and Ken Hickey for their time they spent with chatting about geology and answering questions. My committee members of Jim Mortensen, Dominique Weis and Dick Tosdal were instrumental in guiding my goals in this thesis. In the field many people who work for Miramar Hope Bay Limited were instrumental assisting me in work and developing my geologic understand of the Hope Bay Greenstone Belt, particularly Mike, Richard, Blair, Elli, and Darren. I greatly appreciate the contribution of Ross Sherlock. His guidance and assistance has kept me on track and fostered growth as a field geologist. To my supervisor Richard (Dick) Tosdal, thank you for getting me through. You have taught me a great deal about putting together a good academic document and your feedback and time are greatly appreciated.

I would like to thank my family and friends who have supported me so many ways through my work. I would like to thank Ashley and Sarah for their time reading drafts and giving feedback.

CHAPTER 1

Introduction

CHAPTER 1

1.1 Objective of Thesis

Despite over ten years geologic study of the Archean Hope Bay Greenstone Belt, no synthesis paper or mapping based study has been conducted encompassing the entire greenstone belt. Building upon previous detailed geological work and geochronology, this study provides constraints on the evolution of the Hope Bay Greenstone Belt with regards to petrogenesis and tectonic setting of the volcanic successions that host gold deposits. Occurrences of gold in the belt are hosted in, or spatially related to, particular lithologic suites. Geological mapping along with volcanic stratigraphy was integrated with lithogeochemistry, radiogenic isotopes, and geochronology to place the main lithologic suites of the belt into a temporal framework. Using these tools, identified gold deposits can be placed in a regional context which will reduce exploration risk by focusing exploration on stratigraphically favorable rock suites.

1.2 Location, Physiography and Access

The Hope Bay Greenstone Belt is located in the Nunavut Territory, which was created on April 1, 1999, as the largest and newest of the Canadian territories. The Hope Bay Greenstone Belt, informally referred to as “the belt”, is situated 750 km northeast of Yellowknife and 150 km southwest of the community of Cambridge Bay (Figure 1.1).

Roughly rectangular in shape, the belt is approximately 16 km wide and 82 km long and borders on Melville Sound, which is part of the Arctic Ocean (Figure 1.1). Located 140 km above the Arctic Circle, this greenstone belt is situated in the tundra biome where the soil is permanently frozen in the subsurface. Trees do not grow but vegetation such as berries, lichens, Arctic Willows, moss, grass, and small willow shrubs survive.

Supracrustal rocks of the belt make up north trending ridges with the valleys filled with till overlain by marine clays. Surrounding the belt are granitoids which are resistive to weathering processes and form plateaus with close to 100% outcrop. The southern half of the belt has subdued topography with the north-trending ridges usually only representing ten's of meters of relief. Linear ridges in the northern half of the belt typically have greater relief, although rarely more than 100 m, with the highest point in the study area being approximately 150 m above sea level.

Access to the Hope Bay Greenstone Belt is by air and water. In the summer, bulk supplies are shipped by barge to Roberts Bay, from the Great Slave Lake along the Mackenzie River and along the coast (Figure 1.1). Personnel and other supplies are flown from Cambridge Bay or Yellowknife to all weather landing strips, lakes in the summer months or an ice runway in the winter.

1.3 Methods and Sources of Data

Field mapping is the foundation of this study and is complimented by geochronology, lithogeochemistry, and isotope geochemistry. In addition to collecting original data, a thorough review of existing documentation was conducted.

Field mapping of six geologic transects is the foundation of this study. Transects were mapped at a scale of 1:10,000. Individual transect lengths range from 3 to 10 km long and an average width of several hundred meters. Each transect was selected to include the suites that occur between east granites and west granites and collectively encompass virtually the entire stratigraphy in the Hope Bay Greenstone Belt. These transects are described in Chapter 2, where variations in volcanic textures, distribution of the suites, contact relationships and structural geology are presented along with the overall stratigraphic framework.

U-Pb geochronology on intermediate and felsic rocks provide age constraints on the mapped units. The high precision of this method as well as the robust nature and high blocking temperatures (~ 900°C) of zircon crystals make it ideal for dating Archean felsic rocks (Lee et al., 1997). Six samples were collected from surface outcrops during the course of fieldwork and analyzed by the Pacific Centre for Isotopic and Geochemical Research at the University of British Columbia. Results of new geochronology complement by published U-Pb ages (Bevier and Gebert 1991; Hebel, 1999; Sherlock, 2001) are integrated with field relationships in Chapter 2 of this thesis.

Major and trace element chemistry was conducted on a set of surface samples collected during the mapping of the six transects. Major element concentrations were determined by X-Ray florescence (XRF) and trace element concentrations were determined by Induced Coupled Plasma - Mass Spectrometry (ICP-MS). Detailed descriptions of analytical methods, presentation of data and interpretation can be found in Chapter 3 and Appendix B.

Sm-Nd and Lu-Hf isotopic systems aid in understanding of the variation in the volcanic regime though time. Isotopic analyses were conducted on pulps from rock samples previously collected and analyzed by ALS Chemex. The Sm-Nd system has been extensively used in greenstone belts as isotopic tracers while the relatively newly established Lu-Hf technique has been previously used to a lesser extent on Archean rocks. Sm-Nd and Lu-Hf systems are considered to be relatively immobile and suitable for petrogenetic studies despite the low grade metamorphism and hydrothermal alteration in the study area (Ayer et al., 2002). Analytical methods and procedures as well as presentation of data and interpretation are presented in Chapter 3.

1.4 Geology of the Slave Structural Province

The Slave Structural Province (SSP) is located in the northwest portion of the Canadian Shield. This Archean craton, with an area of ~210,000 km^2, is comprised of ~50% granitoid rocks, ~35% metasedimentary, ~10% gneissic rocks, and ~5% metavolcanic rocks, with a geologic history that spans ~4500 to 2590 Ma (Figure 1.2) (Padgham and Fyson, 1992; King and Helmstaedt, 1997; Stubley, 2005). The SSP is bounded to the east by the Paleoproterozoic Thelon Orogen (2.02-1.91 Ga) and to the west by the Wopmay Orogen (1.95-1.84 Ga) (Hoffman, 1988).

Early work, by Henderson (1970), on the supracrustal rocks of the SSP subdivided as part of the Yellowknife Supergroup. Supracrustal units both older and younger than the Yellowknife Supergroup have since been identified and are referred to as pre- and post- Yellowknife Supergroup (Kusky, 1989; Isachsen and Bowring, 1994; Bleeker, 1999). Utilizing U/Pb geochronology and newly identified field relationships, a number of authors (e.g., Kusky, 1989; Padgham and Fyson, 1992; Isachsen and Bowring, 1994; Bleeker, 2006) have re-examined the Yellowknife Supergroup and produced a revised stratigraphy of the SSP. This stratigraphy should be applied with caution to the Hope Bay Greenstone Belt as it was based on a greenstone belt from the western Slave.

These greenstone belts are many hundreds of kilometres away but are the best studied in the SSP (Figure 1.3).

The oldest identified portions of the SSP (4.03 to 2.86 Ga) are found on the west side of the craton. This crystalline basement, known as the Central Slave Basement Complex, has previously been known as the Anton and Sleepy Dragon Terrane (Kusky, 1989; Bleeker, 1999). Based on geochronological and isotopic evidence, the Central Slave Basement Complex is inferred to underlie the central and western portion of the SSP (Bleeker, 1999). The Central Slave Basement Complex consists of polymetamorphic gneisses and, most commonly, heterogeneous dioritic to tonalitic gneisses with some migmatites, that yield protolith ages of up to 4.03 Ga (Stern and Bleeker, 1998; Bowring and Williams, 1999; Bleeker, 1999).

In the eastern part of the SSP, much work has been done to understand the relationship between the Central Slave Basement Complex and the supracrustal rocks of the Yellowknife Supergroup. This work may have only limited applicability to the eastern half of the SSP, and the Hope Bay Greenstone Belt. Based on Pb and Nd isotopic compositions there is differing basement rock in the western and eastern parts the SSP (Thorpe et al., 1992; Davis and Hegner, 1992). The $^{207}Pb/^{204}Pb$ signatures from the eastern Slave are lower (more juvenile) than those found in the west, which suggests that the source in the west is an older, more evolved crust. Other researchers suggest that based on geologic evidence there is little difference between the eastern and western parts of the SSP (Padgham and Fyson, 1992; Padgham, 1995).

The Central Slave Basement Complex is overlain by a discontinuous veneer of the autochthonous sedimentary rocks named the Slave Cover Group (2.9 to 2.8 Ga).

Preserved in a number of localities, this group is dominated by quartzite and banded iron formation (BIF) with lesser pebble conglomerates (Helmstaedt and Padgham, 1986; Kusky, 1990). These deposits are distributed within the vicinity of the Central Slave Basement Complex and represent remnants of a continental shelf assemblage (Ketchum et al., 2004). A thin cover succession marks the onset of the Neoarchean cycle of supracrustal development in the SSP (Bleeker et al., 1999a).

Greenstone belts of the SSP are separated into two broad categories: the Yellowknife-type and the Hackett River-type (Padgham, 1985). Yellowknife-type belts, which are mostly found in the western Slave, are characterized by a thick succession of massive to pillowed tholeiitic basalt flows that may also be interleaved with calc-alkaline felsic volcanic and volcaniclastic rocks. These greenstone belts are seen throughout the western Slave and occur between 2734 and 2697 Ma (Isachsen and Bowring, 1997; Mortensen et al., 1988). There are also minor amounts of sandstone, shale, conglomerates, carbonate units and intra-volcanic sedimentary rocks. The Elu and Hope Bay Greenstone Belt s are the only Yellowknife-type belts found in the eastern SSP. Hackett River-type greenstone belts are characterized by intermediate to felsic calc-alkaline volcaniclastic rocks. These arc-like rocks are somewhat younger (post 2700 Ma) and are found mainly in eastern side of the SSP (Mortensen et al., 1988).

In the Yellowknife area sedimentation of the Burwash Formation buried some of the volcanic successions (Figure 1.3). This sedimentary sequence is common across the SSP where they form a relatively unmetamorphosed and deformed package of rocks and are considered one of the best preserved Archean deep marine succession in the world (Ferguson et al., 2005). The Burwash Formation around Yellowknife, where it’s type section if found, consists of metamorphosed sandstones and shale with thin felsic tuff layers (Bleeker, 2004). The thinly bedded sandstone-shale units of the Burwash Formation display Bouma sequences, as well as thicker (2-10 m), bedded units (Ferguson et al. 2005). The main phase of sedimentation in the south part of the SSP occurred from 2680 to 2660 Ma, however, in the north part of the SSP, older ages of 2695 and 2671 Ma in High Lake are encountered (Henderson et al., 1994). These ages suggest an older onset of turbidite sedimentation in the far north of the province (Bleeker, 2004). In the SSP, the Burwash-equivalent sedimentary rocks have been given different formational names depending on location; they include the Contwoyto Formation, the Itchen Formation, and the Beechey Lake Group (King and Helmstaedt, 1997; Bleeker, 2006).

The youngest sedimentary rocks in the SSP are identified in a number of greenstone belts, the Jackson Lake Formation in the Yellowknife belt, the String Lake conglomerate in the Anialik belt, and the Beauliue River Formation in the Beaulieu belt (King and Helmstaedt, 1997). These late orogenic sedimentary rocks are mainly composed of polymictic conglomerates, cross-bedded sandstones, and some argillite deposited in an alluvial fan sequence (Henderson, 1985; Martel and Lin, 2006). The Jackson Lake Formation (JLF) has been dated at 2605 ± 6 Ma. Similar evidence suggests that the String Lake conglomerate was deposited ca. 2.6 Ga (Isachsen and Bowring, 1994; King and Helmstaedt, 1997). In the Yellowknife Greenstone Belt, these late orogenic sedimentary rocks are found over a length of 37 km some 60 m.y. after the end of widespread volcanism.

At a craton scale, the oldest deformation event, D1, is attributed to the closing of the Burwash Basin at ~2650 Ma (Bleeker, 2006). A LITHOPROBE seismic survey of the western SSP has shown a northeast-southwest structural grain (D1) in the lithospheric mantle (Davis et al., 2003). The second deformation event (D2) commenced ca. 2600 Ma, and manifests itself as broadly north-south structural trends (Bleeker, 2006). The onset of D_2 also saw the over-thickening of the crust, which led to the generation of S-type granites (Kusky, 1989; Bleeker, 2004). The late felsic intrusives can be grouped into 2620–2605 Ma tonalite to granodiorite plutons followed by ca. 2600–2580 Ma, syn- to late kinematic granites, including two-mica leucogranites, and extensive pegmatites (Villeneuve et al., 1997; Davis and Bleeker, 1999). Granite plutonism at this time shows no regional changes through time and no regional zonation across the SSP (van Breemen et al., 1992; Davis and Bleeker, 1999).

After a Proterozoic collisional event with the Rae Province to form the Thelon orogen and creation of the accretionary Wopmay orogen, the Slave Province was accreted to the larger Precambrian Shield of North America (Hoffman, 1989). Two mafic magmatic events affect the SSP in the Early Proterozoic: the intrusion of dike swarms, and minor intrusive complexes. At 2.03 Ga, a swarm of diabase dikes with a variety of orientations were intruded into the central and southern areas of the SSP. At 1.27 Ga, the Mackenzie dike swarm intruded the entire SSP, whereas the Franklin magmatic event at ~ 720 Ma affected only the northern areas (LeCheminant and Heaman, 1989). Kimberlitic magmatism in the Slave occurred during the Cambrian (~ 535 Ma) and the Cretaceous to Tertiary (~ 150 Ma to 40 Ma) (Heaman et al., 2003).

1.4.1 The Bathurst Block

At the northeast corner of the SSP is a terrain named the Bathurst Block (Figure 1.2). Separating the Bathurst Block from the rest of the SSP is the northwest striking Bathurst

Fault. The Bathurst Fault is not well exposed and for the most part is covered by Proterozoic sediments of the Kilohigok Basin (Fraser, 1964). The rocks that make up the Bathurst Block are similar to those that make up the rest of the SSP and include granitoids, sedimentary rocks and supracrustal rocks forming linear north trending belts. There is little know about the basement in the Bathurst Block but Bleeker (2006) interprets it a being similar to the basement of eastern SSP which is younger than the Central Slave Basement Complex.

1.5 General Geology of the Hope Bay Greenstone Belt

The Hope Bay Greenstone Belt is in the north-central part of the Bathurst block. Striking approximately north-south, the Hope Bay Greenstone Belt is dominated by mafic volcanic rocks with lesser felsic volcanic and sedimentary rocks (Figure 1.4), making it analogous to a Yellowknife-type greenstone belt (Padgham, 1985). The metamorphic grade in the Hope Bay Greenstone Belt is mainly greenschist facies increasing to amphibolite facies along the belt margins near the granitoid contacts. For the purposes of this discussion the prefix of meta will be excluded from descriptions of lithologies as the protolith is commonly evident. Available U-Pb geochronology provides a broad temporal framework of the belt which will be complimented by additional geochronology (Figure 1.5). Ages of all the previous geochronology is found on Table 1.1 and the spatial distribution ages determined on felsic volcanic and sedimentary rock suites is found on Figure 2.18.

1.5.1 Mafic Volcanic Rocks

Submarine mafic volcanic rocks intruded by gabbro dominate the Hope Bay Greenstone Belt. The mafic flows have a wide range of preserved primary textures, including pillowed flows, pillow breccias, hyaloclastite, varioles, amygdules, peperitic textures, gas cavities and pillow selvage (hyaloclastic pillow rims). It is not uncommon to observe massive sections grading into pillowed flows capped by hyaloclastite and breccia (Therriault, 2006). The mafic volcanic rocks suites can be separated based on physical characteristics, geographic location or stratigraphic position and chemical composition. Chapter 2 discusses the physical characteristics and geographic-stratigraphic position of the mafic volcanic suites, and Chapter 3 presents the geochemical characterisation of the mafic volcanic units.

Mafic volcanic rocks can not be directly dated, but a relative age can be inferred by their relative stratigraphic position with respect to felsic intervals which have been dated. Hebel (1999) assigned all mafic volcanism to the Hayden Formation which is older than 2.7 Ga (Figure 1.6). Within this formation, he identified three distinct mafic suites based on geochemistry called the BG-1, BG-2 and BG-3 which correspond to the Normal, LREE, and Ti-enriched basalts of this study. Gebert (1999) suggests that there are two episodes of mafic volcanism; the first is that described above by Hebel (1999), and the second is a minor suite of basalts at approximately 2660 Ma. In the Madrid-Wolverine corridor, Sherlock et al. (2003) identified a group of Fe-Ti -rich tholeiitic basalts, the Doris Group, as the oldest mafic volcanic rocks in the north part of the Hope Bay Greenstone Belt. These are overlain by a succession of normal basalts (Wolverine Group and Windy Basalts) and Ti-enriched mafic rocks (Patch Group). Few true ultramafic volcanic rocks are observed in the Hope Bay Greenstone Belt; where present the ultramafic volcanic rocks may contain harrisite also known as "Rhum harrisite" texture which is a randomly oriented spinifex (Donaldson, 1982; Lindsay, 1998; Therriault, 2006).

1.5.2 Felsic Volcanic Rocks

Five episodes of felsic magmatism are recognized in the Hope Bay Greenstone Belt between 2716 Ma to 2665 Ma (Figure 1.5) (Hebel, 1999). In order of decreasing age they are named the Flake Lake, Square Lake, Windy Lake, Koignuk, and Clover Lake suites. Primary volcanic textures in the felsic rocks permit identification of the coherent, volcaniclastic or epiclastic facies.

The Flake Lake Suite (2716 Ma; Hebel, 1999), Square Lake Suite (2690 Ma; Hebel, 1999) and Clover Lake Suite (2662 Ma; Hebel, 1999) are geographically restricted suites. Whereas the Windy Lake Felsic Suite (2686 Ma; Hebel, 1999) and Koignuk Felsic Suite (2677 Ma; Hebel, 1999) are regionally extensive units that can be mapped almost the entire length of the Hope Bay Greenstone Belt. These regionally extensive suites vary in thickness between several hundred meters to over a kilometer.

1.5.3 Sedimentary Rocks

Sedimentary rocks in the Hope Bay Greenstone Belt are interbedded with the volcanic rocks and also form thick packages that are interpreted to have been deposited in post- or intra- volcanic sedimentary basins. Sedimentary rocks which are intercalated with volcanic rocks include thinly bedded wacke, argillite and rarely carbonate rhythmites and iron formation. They are found through the mafic and felsic stratigraphy as relatively thin beds or units on a scale of tens of meters. They are usually recessively weathering, so less is known about their distribution (Gebert, 1993; Therriault, 2006).

The thicker packages of sediments which are interpreted to have been deposited in post- or intra- volcanic sedimentary basins are noted in a number of localities including the Clover Lake, Spyder Lake, the Windy Lake, Conglomerate Hill and Discovery. These sedimentary rocks consist of greywacke to shale as well as conglomerate. Detrital zircon U-Pb ages indicate a maximum depositional age of 2675 Ma (Hebel, 1999) some of the sedimentary rocks. Some very old zircons (2804 Ma and 3281 Ma) are identified in one sample; however, no rocks of that age have been identified in eastern SSP (Hebel, 1999).

Two late- to post- volcanic sedimentary successions containing conglomerate , the Hope Bay Sedimentary Suite and the Conglomerate Hill Sedimentary Suite, are found in the northern part of the belt (Hebel, 1999; Gebert, 1999). The Hope Bay Sedimentary Suite is a polymictic conglomerate with up to 30% rounded granitoid boulders exposed on an island north of Discovery Bay with a maximum depositional age of 2647 Ma (Hebel, 1999), based on detrital zircons from sandy beds in the conglomerate. This formation has been compared by Gebert (1999) and Hebel (1999) to the post-Yellowknife Supergroup conglomerates of the Jackson Lake Formation of the Yellowknife Greenstone Belt and the Timiskaming sedimentary rocks of the Abitibi Greenstone Belt. However as the outcrop is isolated on an island in the ocean its geologic context is unknown and the relationship to the rest of the belt is uncertain. The Conglomerate Sedimentary Hill Suite is located south of the Hope Bay Sedimentary Suite lacks granitoid boulders and contains a smaller variety of clast types. Gebert, 1999) suggests the conglomerate may have formed from the erosion of the upper felsic volcanic rocks of the Hope Bay Greenstone Belt shortly after the end of volcanism.

1.5.4 Plutonic Rocks

Felsic plutonic rocks surround the Hope Bay Greenstone Belt and can be separated into a granitoid series based on field relationships, plutonic textures and geochronology. The first comprehensive study of the granitoids surrounding the Hope Bay Greenstone Belt was conducted by Thompson (1996, 1997) who divided the granitoids into three main groups (Figure 1.7) (Table 1.2). Sherlock and Sandeman (2004b) revised the suites (Table 1.3).

Thompson (1996, 1997) outlined Group I as metagranitoids, migmatites and a gneisses complex dated at 2650 +2.9/-2.5 Ma (Hebel, 1999). This high-grade metamorphic suite lies along the southeastern part of the Hope Bay Greenstone Belt where it is in contact with low metamorphic grade supracrustal rocks that cross a zone of ductile deformation (Thompson, 1997). A titanite U-Pb age of 2589 Ma (Hebel, 1999) is thought to represent cooling from the peak metamorphism for this suite. Thompson (1997) interprets the Group I rocks to be much older than the lower greenschist facies rocks that they are in contact with, and favors an unconformity. This idea conflicts with geochronology results mentioned above, which suggests a syn-metamorphic fault.

Sherlock and Sandeman (2004b) name this suite of rocks Group II (Table 1.3). This is based on the observations that the rocks comprising Group I, outline by Thompson (1997, 1998), are not as metamorphosed as previously thought and is likely a syn- to late-D2 intrusion. The gneissosity is believed to have developed by a biotitic schleiren and amphibolite- inclusion charged granodioritic magma that was intruded by widespread veins and sheets of monzogranite that were subsequently flattened.

Thompson (1996, 1997) outlined Group II intrusives as a syn-volcanic suite that is situated to the east of the Hope Bay Greenstone Belt, where they have been dated at 2672 +3/-1 Ma (Bevier and Gebert, 1991). A variety of rock types compose this group including a mafic metaplutonic suite and a metatonalite suite. These rocks may extend eastward as far as the Elu Greenstone Belt (Figure 1.7). The Group II rocks intruded prior to the main phase of metamorphism and deformation, and are interpreted to be the plutonic components of the magmatic event that produced the volcanic rocks of the Hope Bay Greenstone Belt. The volume of syn-volcanic granitoids is inferred to be much larger than that reported from anywhere else in the Slave Province (Thompson, 1997). Sherlock and Sandeman (2004b) has renamed this granitoid suite Group I based on the observation in the metagranitoid suite as well as the geochronology.

Thompson (1996, 1997) outlined Group III granitoids, which lie along the west side of the belt, as an undeformed or unmetamorphosed suite (Figure 1.7). Group III rocks dated at 2608±5 Ma (Bevier and Gebert 1991) include a monzodiorite suite, a biotite tonalite suite, and a biotite granite suite (Thompson, 1997). Thompson (1997) suggests that Group III granitoids intruded after the volcanic rocks and older granitoids following significant deformation and metamorphism, but before regional deformation ceased. The observation by Thompson (1997) and geochronologic constrains are consistent with the observations elsewhere in the SSP (van Breemen et al., 1992).

Proterozoic magmatic events that have affected the Hope Bay Greenstone Belt include the ca. 2000 Ma Beechey dikes, the 1267 Ma Mackenzie dikes, and the 723 Ma Franklin Diabase (Gebert, 1993).

1.5.5 Metamorphism and Deformation

Low-metamorphic grades dominate the Hope Bay Greenstone Belt, except for the margins of the belt where the rocks are metamorphosed to amphibolite facies. Metamorphic mineral assemblages of hornblende + plagioclase ± garnet characterize the rocks along the belt margin, whereas chlorite+ albite + epidote + quartz + actinolite characterize the rocks in the interior of the belt. Timing of regional metamorphism is partially constrained by the granites to the west, dated at 2609 Ma (Bevier and Gebert, 1991), which are unaffected by metamorphism (Thompson, 1997). A titanite U-Pb age of 2589 Ma from metagranitoid (Group I, Thompson (1997), Group II, Sherlock and Sandeman (2004b)) is interpreted to date cooling after a peak of regional metamorphism (Hebel, 1999). Contact metamorphism is observed as centimeter to meter wide aureoles of hornfels around syn-volcanic and post-volcanic dikes.

Locally penetrative cleavages cut the deformed rocks of the Hope Bay Greenstone Belt. The oldest deformation event is poorly constrained, but is marked by a foliation (S_1) that is subparallel to the dominant foliation (S_2) (Gebert, 1999). A second cleavage, S_2, is the most strongly developed fabric in the belt. It generally strikes between 030° and 330° and is steeply dipping.

The D_2 deformation produced folding (F_2) as a result of east-west shortening and S_2 is the north-trending axial planar cleavage to these folds The Doris anticline can be traced for ten's of kilometers is a prominent F_2 fold pattern in the north part of the belt (Sherlock and Carpenter, 2003). All the earlier fabrics are affected by a third deformation event (D_3) which locally forms complex fold interference patterns. The F_3 folds are observed south of Flake Lake in the River Bend area. The north-south shortening during D_3 may also account for doubly plunging geometry of the Doris anticline (Gebert, 1999).

1.5.6 Gold Deposits

The Hope Bay Greenstone Belt contains three gold deposits and numerous prospects. Th gold deposits (Doris, Madrid, Boston) (Figure 1.4) and showings are hosted mainly in the mafic volcanic rock and, to a lesser extent, in sedimentary and plutonic rocks. The Doris and Madrid deposits are located in the north part of the belt whereas the Boston is located in the south part of the belt (Figure 1.4). Currently being permitted for mining, the Doris deposits resource contains a total of ~1.5 Million oz Au. Deposits in the Madrid area have resources of ~ 7.8 Million oz Au whereas the Boston deposit contains a ~1.5 Million oz Au resource (Miramar, 2007). Minor base metal occurrences are and Au-rich syn-volcanic alteration assemblages are associated with felsic volcanic units (Gebert, 1999; Sherlock and Lindsay, 2002).

The Doris deposit, in the north part of the Hope Bay Greenstone Belt, occurs as a quartz-carbonate vein system traceable for 3 km (Carpenter et al., 2003). The deposit is hosted by amygdaloidal pillowed basalt succession with minor gabbro. The contact between the Fe-Ti rick basalts (hangingwall) and a gabbro (footwall) is the host to the quartz carbonate veins. Basalt and gabbro of the deposit have been folded into a tight, doubly plunging, north-striking anticline (Carpenter et al., 2003). Two of the mineralized veins, known as the Central and Lakeshore veins, contain slivers of tourmaline-ankerite-pyrite altered wall rock, this wall rock typically host the ore (pyrrhotite, pyrite, and gold). The strongest sericite-dolomite/ankerite-quartz ±tourmaline ±rutile ±hematite ±pyrite ±gold alteration is at the vein selvage. Distal hydrothermal alteration is characterized by quartz-chlorite-calcite-albite ± actinolite-tremolite ±epidote ±magnetite ±rutile. Pyrite is ubiquitous throughout the altered wall rock and increases in concentration proximal to the vein (Sterritt, 2003).

Located in the northern part of the Hope Bay Greenstone Belt between Windy and Patch Lake, are the Madrid group of deposits (Naartok, Rand, Suluk and South Suluk) (Figure 1.4). Gold is occurs in quartz-ankerite-sericite-albite-pyrite volcanic rocks cut by complex network of quartz stockwork veins (Sherlock 2003; Therriault 2006; Madsen et al., 2007). Volcanic stratigraphy in the Madrid area includes mafic volcanic flows, gabbros, argillitic sedimentary rocks and feldspar porphyric rocks (Sherlock et al., 2003; Therriault, 2006, Madsen et al., 2007). The deposits lies in the hanging wall of a regional structure called the Deformation Zone (DEFZ) is an important feature controlling gold occurrences with lenses along the hanging wall contact and as pods within it, but no gold has been recognized in the footwall of the DEFZ (Madsen et al., 2007).

Gold is present in carbonatized, albiteized and silicified breccia zones with quartz stockwork veins and disseminated pyrite (Madsen et al., 2007). The deposits are hosted in altered mafic volcanic flows and flow breccias characterized by intense albitization, brecciation, and iron-carbonate flooding (Therriault, 2006). The most intense alteration is characterized by carbonate minerals (ankerite, magnesite or ferroan dolomite), quartz, chlorite, rutile, sericite, albite, hematite, and pyrite (Sterritt, 2003; Therriault, 2006). Gold is typically in carbonate located at the quartz vein margins, where it is often associated with pyrite and trace chalcopyrite (Therriault, 2006). The large alterations system in the Madrid area gives way to typical greenschist mineral assemblages on the periphery, including hornblende, actinolite, chlorite, albite, calcite, quartz, epidote, and titanite (Sterritt, 2003).

The Boston deposit, southernmost in the belt, is a mafic volcanic-hosted, multistage, mesothermal quartz-ankerite-sulphide vein system (Stemler, 2000; Stemler et al., 2006). The host mafic volcanic rocks and interflow sedimentary rocks are deformed in a tightly folded anticline with sub vertical lithologic contacts. Proximal alteration destroyed the primary volcanic textures, and is characterized by quartz, ankerite, sericite, paragonite and pyrite (Sherlock and Sandeman, 2004a). Gold is hosted in pillowed basalt flows, volcaniclastic rocks and sedimentary rocks and is controlled by anastomozing axial planar shear zones (Sherlock and Sandeman, 2004a). Vein formation was accompanied by widespread wall rock alteration in the form of carbonitization, hydrolysis, hydration, and sulfidation (Stemler, 2000). In a fluid inclusion study Stemler et al. (2006) shows that auriferous fluid responsible for mineralization at Boston were similar to those in other greenstone belts, (low salinity (4.6 ± 1.4 eq. wt.% NaCl) H_2O-CO_2 trapped at 320ºC and pressures 2 to 3 kbar).

Table 1.1: Summary of rock suites in the Hope Bay Greenstone Gebert (1993, 1999), Bevier and Gebert (1991), Hebel (1999), Carpenter et al. (2003), Sherlock et al. (2003), Sherlock and Sandeman (2004), Therriault (2006)

Rock Type and Suite Name	U/Pb age (Ma)	2σ Error (Ma)	Distribution	Referance
Ultramafic Volcanic Rocks				
Patch komatiitic basalts	-	-	meter scale flows around Madrid	Therriault 2006
Mafic Volcanic Rocks				
Patch High Ti-Fe Basalts	-	-	~150m wide striking north with a length of ~10km	Sherlock et al. 2003
Doris High Ti-Fe Basalts	-	-	~100m wide striking north exposed at surface 1km	Carpenter et al. 2003
Normal Tholities	-	-	belt wide distribution	Hebel 1999, Gebert 1999
Boston High Ti Basalts	-	-	found within the Boston Anticline	Sherlock and Sandeman 2004
Intermediate Volcanic Rocks				
Son Voit Suite	-	-	Found at the south central end of the belt	Hebel 1999
Felsic Volcanic Rocks				
Flake Lake suite	2716	+3.1 -2.6	restricted to the south central east	Hebel 1999
Square Lake suite	avg 2690	n/a	restricted to the central west portion of the belt	Hebel 1999
Wolverine suite	2689.4	+4.0 -3.6	restricted to the area around Madrid	Sherlock unpublished data 2001, Sherlock et al. 2003
Windy Lake suite	avg 2685	n/a	belt wide destribution along the center of the belt	Hebel 1999, Sherlock et al. 2003
Koignuk suite	avg 2677	n/a	belt wide destribution at the west margin of the belt	Bevier and Gebert 1991, Hebel 1999,
Clover Lake suite	2663	+3.4 -2.8	restricted to two outcrops 3km northwest of Boston	Hebel 1999, Sherlock and Sandeman 2004
Sedementry Rocks				
Wilko Sedimentry Suite	max 2675	±3.0	belt wide destribution along the center of the belt	Hebel 1999
Conglomerat Hill Sedimentry Suite	max 2670	±2.5	confined to the north half of the belt in the center of the belt	
Hope Bay Sedimentry Suite	max 2647	±2.8	confined an island to the north of the belt	Hebel 1999

Table 1.2: Summary of Granitic rocks surrounding the Hope Bay Greenstone Belt (after Thompson 1997)

	U/Pb Age	Field observation	Subgroup	Description
Group I	2650Ma	pre-volcanic?	Metagranitoid-migmatite-gneiss complex	foliated, recrystallized granite to tonalite, granitic to tonalitic granitoid migmatite, quartzofeldspathic gneiss, tonalite, granitic to tonalitic granitoid migmatite, quartzofeldspathic gneiss, mettagabbro
Group II	2672Ma	syn-volcanic	Mafic metaplutonic suite	biotite/hornblende diorite, tonalite to quartz diorite, leucogabbro, gabbro, anorthosite; massive to moderately foliated, variably recrystallized
			Metatonalite suite	biotite/hornblende tonalite, some granodiorite; intensely foliated and recrystallized
			Pitted metatonalite suite	hornblende/biotite tonalite, minor granodiorite; massive to moderately foliated, variably recrystallized; differential weathering of coarse-grained biotite forms pits
Group III	2608Ma	post-volcanic, syn-D2	Monzodiorite suite	biotite-hornblende quartz monzodiorite, monzodiorite, granodiorite, diorite; typically foliated and recrystallized with lenticular inclusions of metavolcanic rocks near contact with greenstone belt
			Biotite tonalite suite	granodiorite to tonalite; schistose to gneissic metasedimentary and metavolcanic inclusions which define a foliation.
			Biotite granite suite	biotite granite to granodiorite, K-feldspar megacrysts typical; weakly foliated locally; 8a - relatively fine-grained, inclusions of granitoid migmatite, quartzofeldspathic gneiss, foliated metatonalite, mafic metavolcanic rocks, and/or metagabbro

Table 1.3: Summary of Granitic rocks surrounding the Hope Bay Greenstone Belt (after Sherlock and Sandeman 2004b)

	U/Pb Age	Field observation	Description
Group I	2672Ma	syn-volcanic	fine- to medium-grained biotite-magnetite-bearing granodiorite to monzogranite
Group II	2650Ma	post-volcanic, syn-D2	medium- to coarse-grained biotite-titanite ± hornblende ± epidote-bearing tonalite
Group III	2608Ma	post-D2	leucocratic, medium-grained, microcline porphyritic, biotite ± magnetite ± hornblende-bearing granodiorite to monzogranite

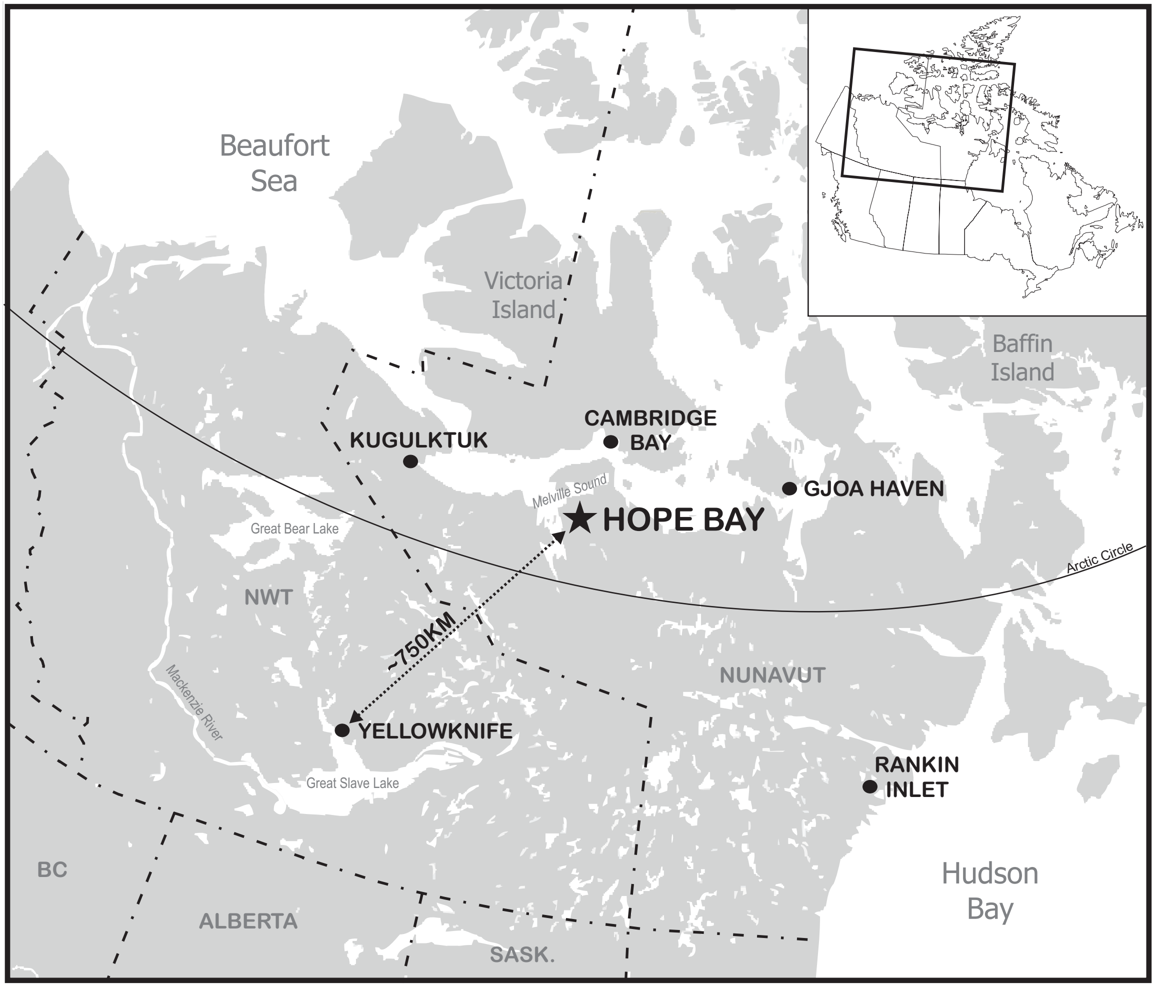

Figure 1.1: Location map of the Hope Bay Greenstone Belt (modified Miramar Figure)

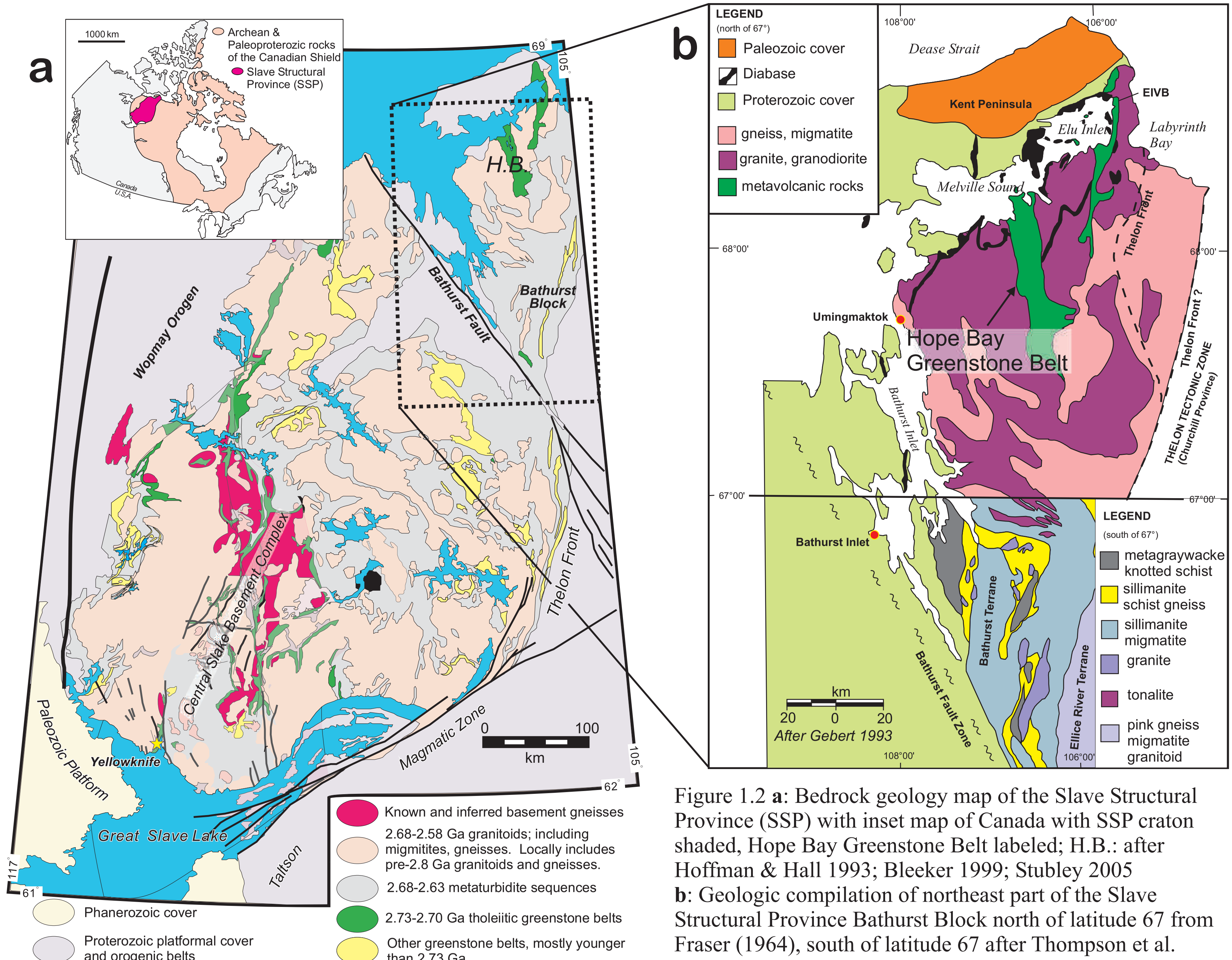

Figure 1.2 **a**: Bedrock geology map of the Slave Structural Province (SSP) with inset map of Canada with SSP craton shaded, Hope Bay Greenstone Belt labeled; H.B.: after Hoffman & Hall 1993; Bleeker 1999; Stubley 2005
b: Geologic compilation of northeast part of the Slave Structural Province Bathurst Block north of latitude 67 from Fraser (1964), south of latitude 67 after Thompson et al. (1986), figure modified after Gebert (1993)

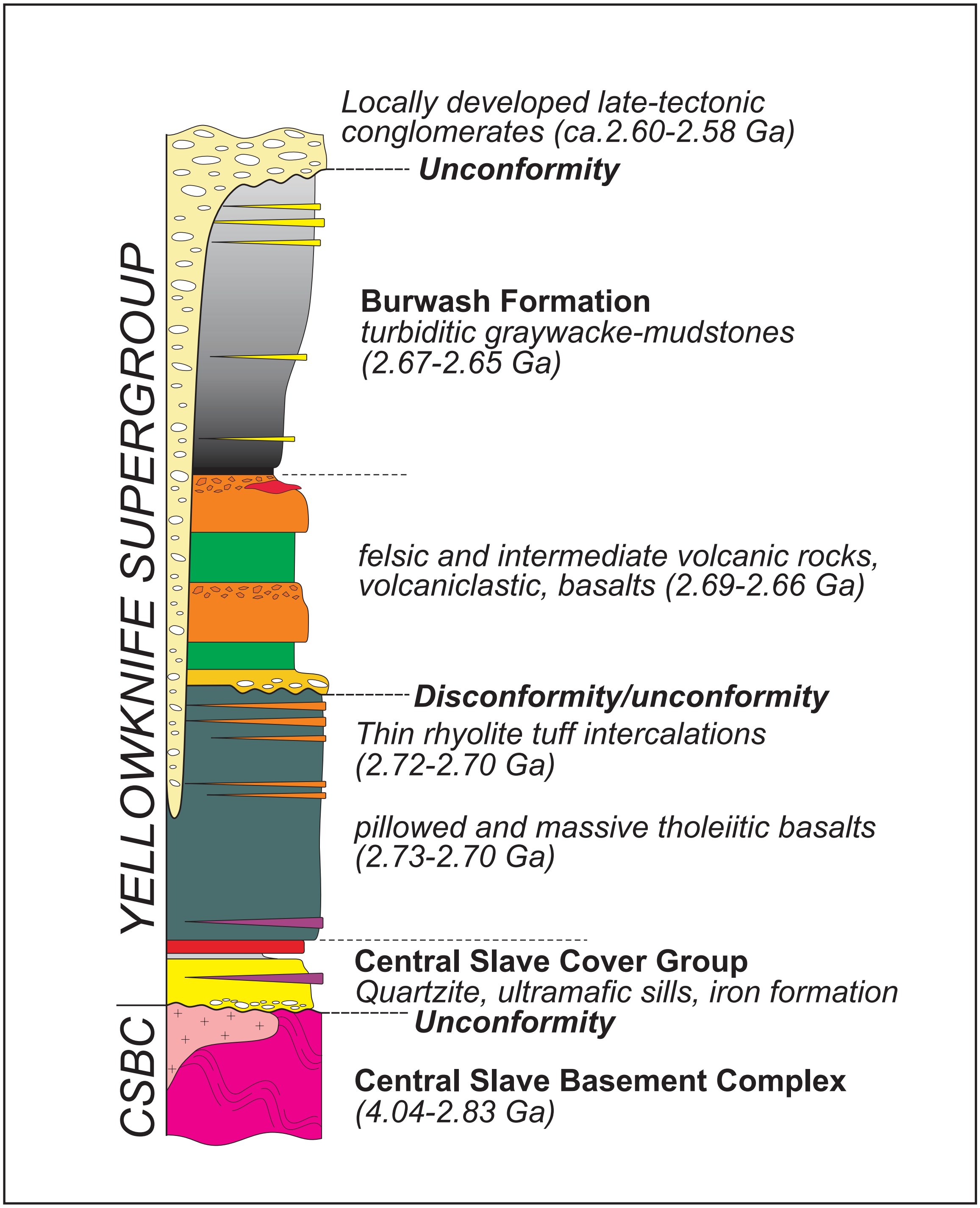

Figure 1.3: Generalized stratigraphic column for the Central and Western SSP (modified Henderson 1970; Bleeker et al. 1999; Bleeker et al. 2001)

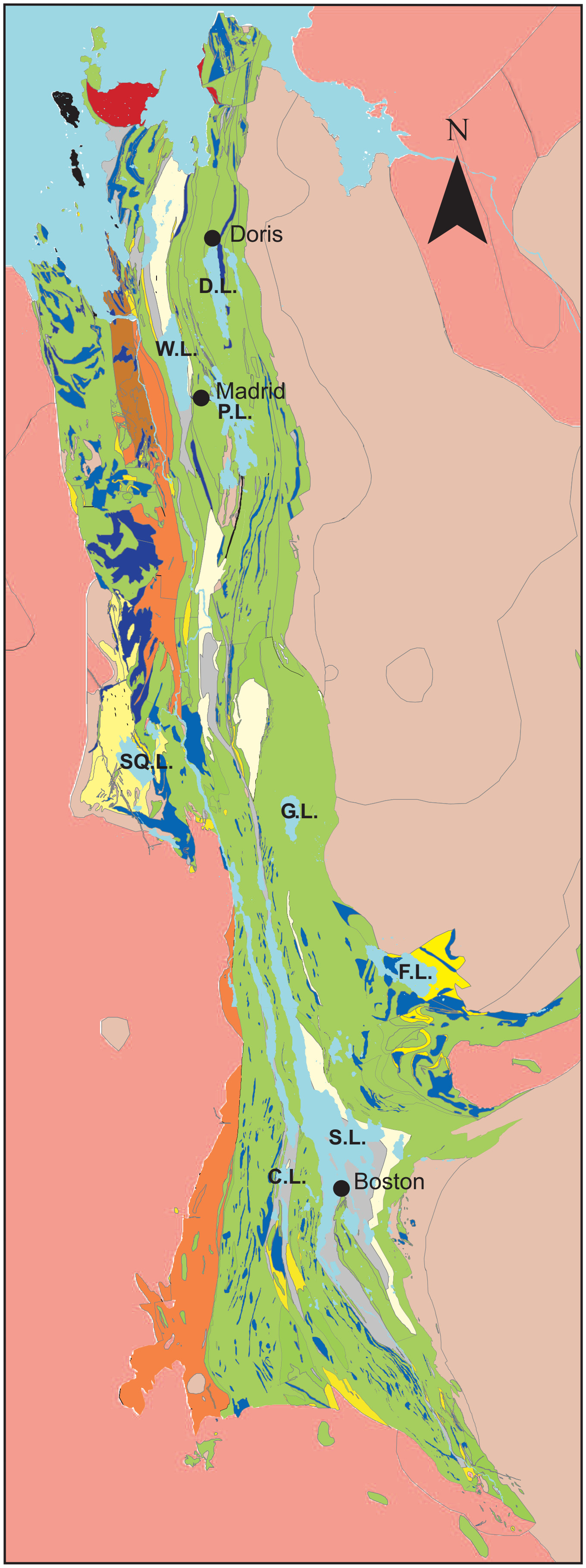

Figure 1.4: General geology of the Hope Bay Greenstone Belt with selected lakes, D.L.: Doris Lake, W.L.: Windy Lake, SQ.L.: Square Lake, G.L. Gascache Lake, F.L.: Flake Lake, S.L.: Spyder Lake, C.L.: Clover Lake

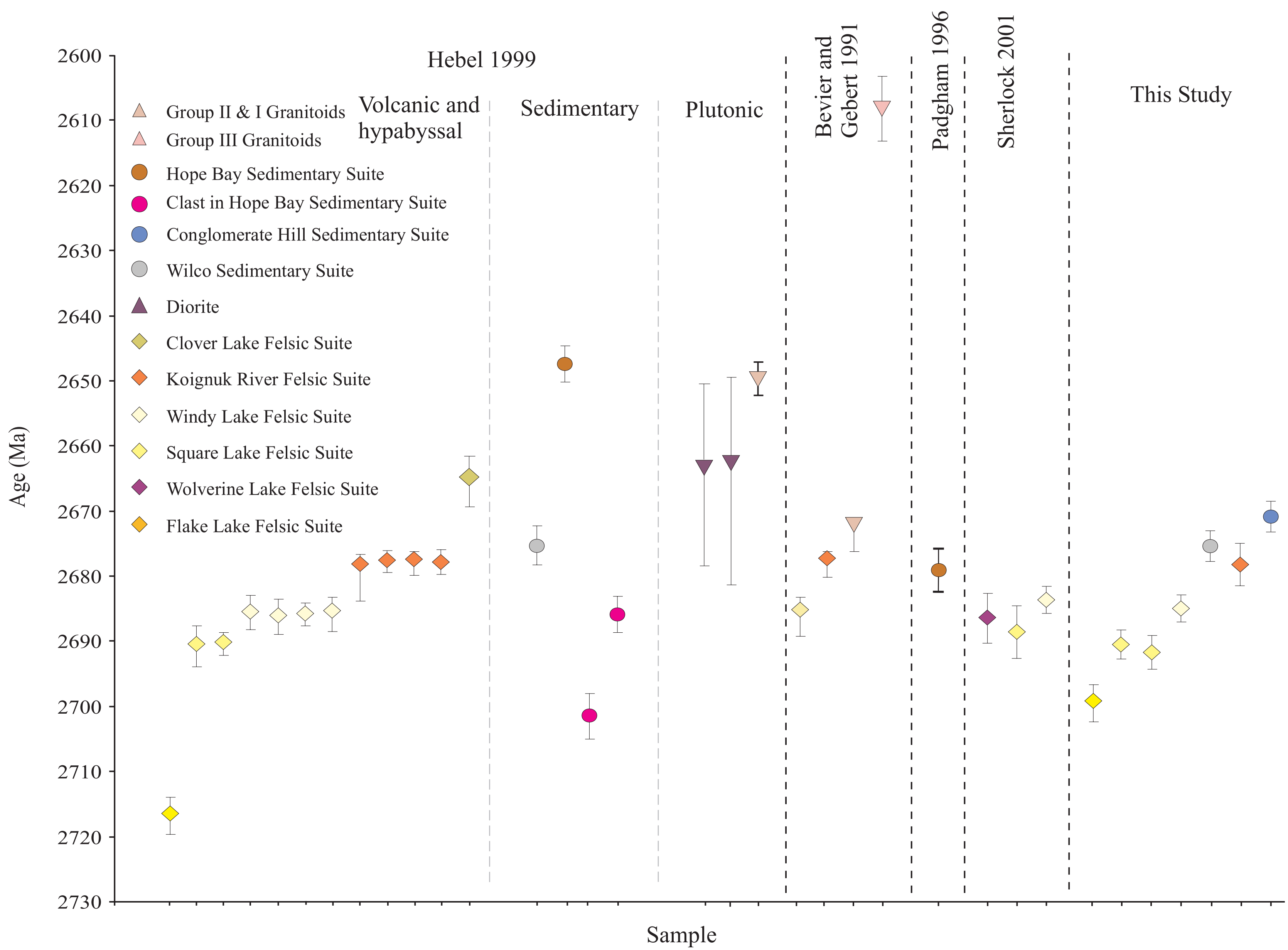

Figure 1.5 U/Pb ages of felsic and sedimentary suites (after Bevier and Gebert 1991; Padgham 1996; Hebel 1999; Sherlock 2001; Sherlock 2001 (unpublished data) , Shannon 2008 (this study):

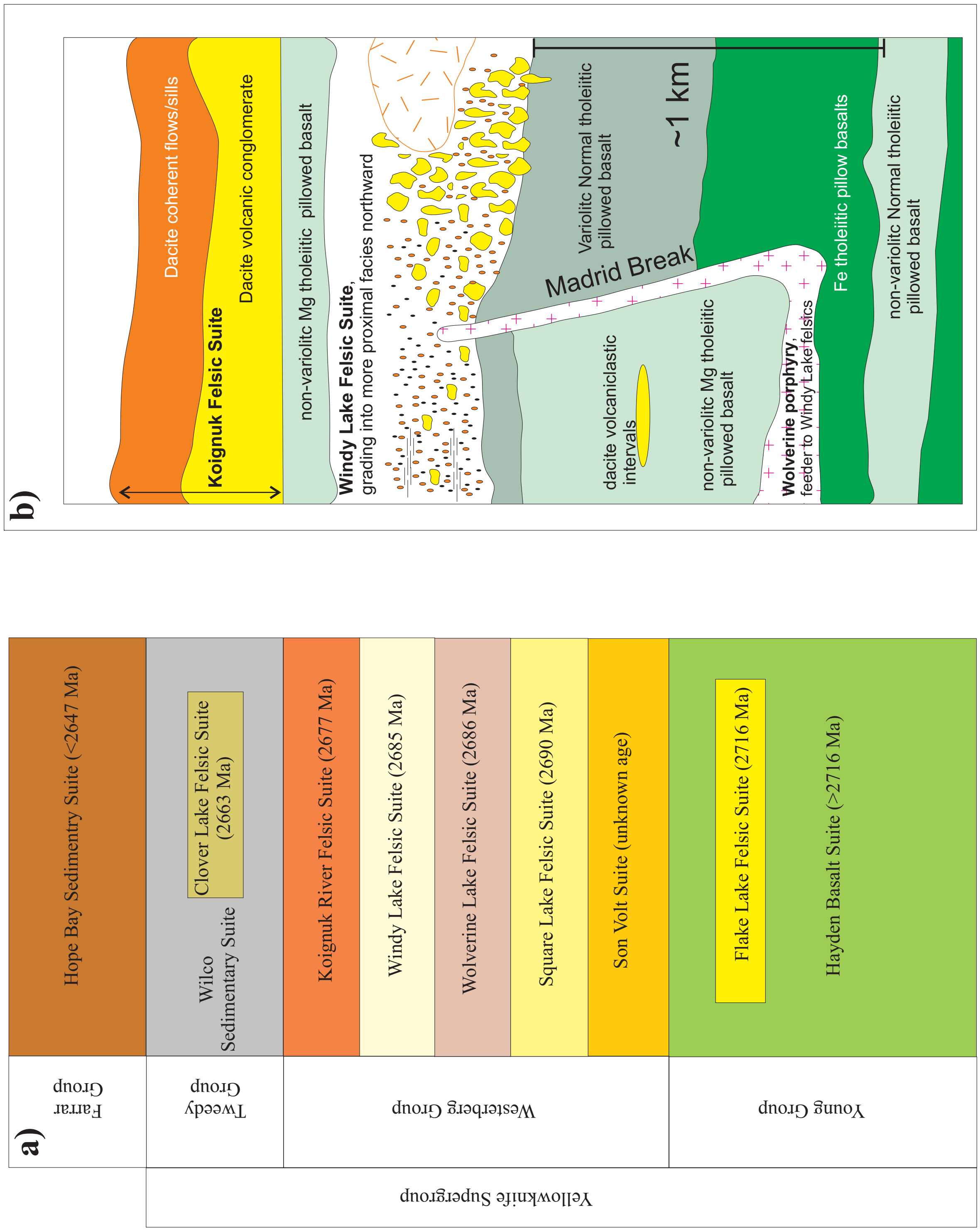

Figure 1.6: a) Generalized stratigraphic column for the Hope Bay Greenstone Belt with original stratigraphic nomenclature of formations replaced by suites (after Hebel 1999; Gebert 1999) b) stratigraphic column for the Patch Doris corridor with (after Sherlock et al. 2003; Therriault 2006)

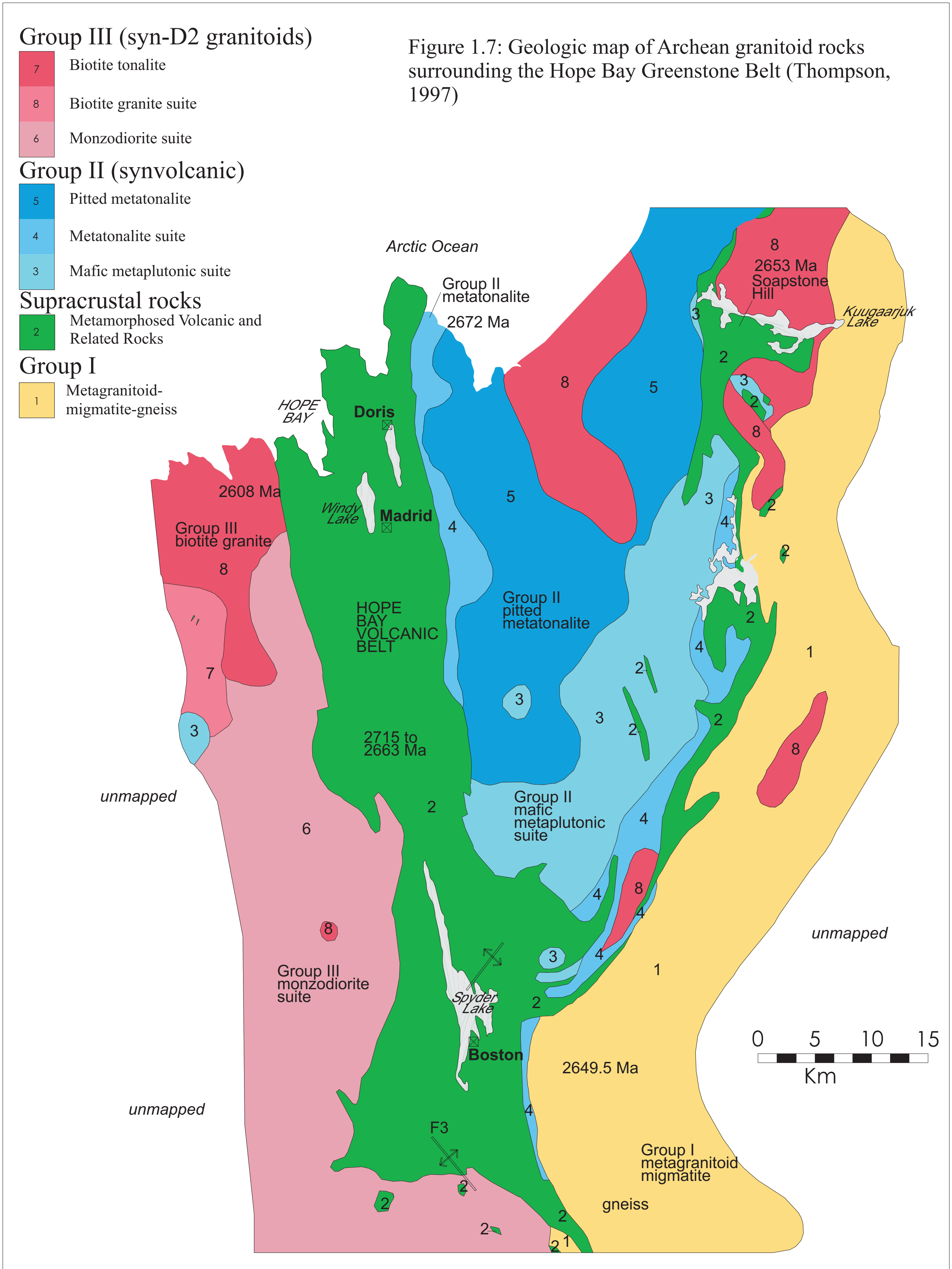

Figure 1.7: Geologic map of Archean granitoid rocks surrounding the Hope Bay Greenstone Belt (Thompson, 1997)

CHAPTER 2

Volcanic Architecture and Stratigraphic Framework of The Hope Bay Greenstone Belt

2.1 Introduction

This chapter combines field relationships and U-Pb geochronology from discrete transects across the belt to create a composite stratigraphic framework. Understanding the volcanic architecture of the Hope Bay Greenstone Belt places the gold deposits in a stratigraphic context and reduces risk by focusing exploration efforts.

2.2 Descriptions of Geologic Transects

Six geologic transects were mapped across the Hope Bay Greenstone Belt. They were selected to include virtually the entire stratigraphy of the Hope Bay Greenstone Belt (Figure 2.1). Three transects were mapped in the northern and three transects in the southern parts of the belt to illustrate the stratigraphic differences along strike. The stratigraphic and structural relationships of each volcanic suite in each transects is described. A number of assemblages and formations have been previously described by Hebel (1999), which was considered but not necessarily incorporated here as the understanding of the belt scale stratigraphy has evolved since Hebel's work Instead, rock units sharing similar physical, chemical or geographic characteristics will be referred to informally as suites. The transects in the south part of the belt are presented first and the transects in the north are presented second. Within each transect the suites will be discussed in stratigraphic order, from oldest to youngest.

2.2.1 Flake Lake Transect

The Flake Lake Transect covers the area from Flake Lake to the east side of Spyder Lake (Figure 2.1 and 2.2). Rock units in this transect include the Flake Lake Felsic Suite, a feldspar porphyritic gabbro, the Windy Lake Felsic Suite, and at least three mafic volcanic suites. The volcanic stratigraphy of this transect forms two homoclinal successions, with pillows facing to the northeast, that are juxtaposed by a fault. In this transect three mafic volcanic suites were subdivided on textural differences and supported by geochemistry.

An inferred fault divides the transects into two domains. The older domain lies to the northeast and contains the Flake Lake Felsic Suite and Bend Basalt Suite, and the younger domain lies to the southwest and contains the Windy Lake Felsic Suite, Spyder Arm Basalt Suite and the Member Basalt Suite (Figure 2.2). Although some suites are intercalated, the following descriptions focus on characterising of the individual suites and their stratigraphic and structural relationships.

2.2.1.1 Flake Lake Felsic Suite

The majority of the Flake Lake Felsic Suite is found on the northeast side of Flake Lake, but is also found south of the lake in the 'River Bend' area where it is intercalated with the Bend Basalt Suite (Figure 2.2). This suite, on the north shore of Flake Lake, is massive rhyolite with up to 0.5cm in diameter blue quartz phenocrysts making up 20% of the rock. In the same area, rare volcaniclastic textures, including a number of quartz phyric lapilli in a quartz porphyritic matrix, are observed (Figure 2.4a). The Flake Lake Felsic Suite is bounded to the north and east by granites and to the south and west by basalts. It has subsequently been intruded by a large gabbro body on the southeast margin of the suite. Gabbro dikes, related to this intrusion, cross cut the Flake Lake Felsic Suite. The Flake Lake Felsic Suite is also found to the southwest of the large gabbro as a thin strip of rhyolitic volcaniclastic rock and minor sedimentary beds less than 20 cm thickness (Figure 2.2).

The Flake Lake Felsic Suite is the oldest felsic suite in this transect, with a volcanic two age dates indicating that felsic volcanism spanned from at least 2716±7.8 Ma (Hebel 1999) to 2697.6±8.9 Ma (AJS 1, Table 2.1 and Figure 2.17). The volcaniclastic sections dated at 2697.6±8.9 Ma are intercalated with the Bend Basalt Suite which shows that part of the Flake Lake Felsic was coeval with mafic volcanism. These ages, along with field relationships, show that the Flake Lake Suite is the oldest suite of felsic volcanic rocks and lie in the lower portion of the stratigraphy of the Flake Lake Transect (Figure 2.3).

2.2.1.2 Bend Basalt Suite

Pillow basalts, named the Bend Basalt Suite, stratigraphically underlie and are intercalated with a thin volcaniclastic rock section of Flake Lake Felsic Suite on the southwest side of the feldspar porphyritic gabbro (Figure 2.2). This basalt suite is approximately 1.5 km thick with a consistent northeast facing direction determined from pillow tops. This suite is dominantly composed of moderately well formed pillows with local sections of megapillows (>2.5 m). The pillows commonly have amygdules, as well as small (~0.5mm) plagioclase phenocrysts. Fresh surfaces of these basalts are usually dark green with medium to dark brown weathered surface. Pillow selvages range in size from 15 cm to less than 3 cm (Figure 2.4b). Within the pillowed unit, there is a minor component of medium-grained massive sections, interpreted to be either massive flows or syn-volcanic dikes or sills.

A felsic dyke with the same chemical composition as the Flake Lake Suite, intruded the Bent Basalt Suite, suggesting that the Bend Basalt Suite is older than the Flake Lake Suite (Figure 2.3). This porphyritic dike has irregular contacts with the surrounding mafic pillows and has abundant quartz phenocrysts. The regional magnetic data shows a strong lineament at the base of the Bend Basalt Suite, which is interpreted as a fault.

2.2.1.3 Eastern Granites

To the east of the supracrustal rocks of the Flake Transect is a suite of felsic intrusives. This suite of intrusive rocks is located along the majority of the east side of the Hope Bay Greenstone Belt and is made up of a medium-grained granodiorite ± biotite. Bevier and Gebert (1991) dated this group of granites at 2672+3/-1 Ma and suggesting a syn-volcanic origin.

2.2.1.4 Windy Lake Felsic Suite

Stratigraphically below the Member Basalt Suite is a 100 m interval of dacitic volcaniclastic rocks, dated at 2685±2.0 Ma (AJS 3, Table 2.1 and Figure 2.17). These rocks are considered part of the Windy Lake Felsic Suite and have massive porphyritic and breccia facies (Figure 2.2). The porphyritic section has 40-55%, 1-5 mm feldspar phenocrysts in a grey matrix and is likely a flow or sill. The breccia section has fragments of quartz up to 4 cm, and feldspar porphyritic clasts in a grey matrix. It is separated from the main portion of the Windy Lake Felsic Suite by the Spyder Arm Basalt Suite (Figure 2.3).

The base of the stratigraphy of the younger domain of the Flake Lake transect is formed by a thick (750 m) portion of the Windy Lake Felsic Suite that lies against the edge of the north arm of Spyder Lake (Figure 2.2). This suite is characterized by two facies; a primary volcanic facies, and a resedimented syn-eruptive volcaniclastic facies.

This terminology used to classify volcanic rocks has been created by such workers as Easton et al. 1989; McPhie et al. 1994. In this area, the volcanic portion of the Windy Lake Felsic Suite is composed of a dark grey porphyritic dacite with 1 to 3 mm quartz phenocrysts. This monotonous portion of the Windy Lake Felsic Suite lacks clasts or bedding, and has been dated at 2685+4/-2 Ma (Bevier and Gebert 1991). The second facies of the Windy Felsic Suite is a volcaniclastic facies, with significant sedimentary textures, found stratigraphically below the primary volcanic facies. At the top of the section that is less than 100 m thick a monomictic conglomerate is interpreted as a resedimented syn-eruptive volcaniclastic deposit (Figure 2.4e). Stratigraphically below the volcanic conglomerate are volcanogenic sedimentary deposits ranging from wacke to siltstones (Figure 2.4f). Sedimentary features, including graded beds, cross beds and flame structures, indicate stratigraphic younging is to the northeast. From the field relationships and U/Pb geochronology, the Windy Lake Suite is the oldest stratigraphic unit in the younger domain of the Flake transect (Figure 2.3).

2.2.1.5 Spyder Arm Basalt Suite

The Spyder Arm Basalt Suite, named after the adjacent lake, overlies the majority of Windy Lake Felsic Suite but is locally overlain by a unit of Windy Lake Suite age dacite dated at 2685±2.0 Ma (AJS 3, Table 2.1 and Figure 2.17) (Figure 2.2). This basalt suite differs from the Member Basalts Suite in color and geochemistry; it is much lighter in color on both the fresh and weathered surface, and contains varioles and gas cavities (Figure 2.4d). Locally this basalt suite is light rare earth enriched, discussed further in Chapter 3.1, supporting it's distinction from the other basalt suites in this transect. This unit is composed almost entirely of pillowed flows with minor massive flows or sills.

An isolated discontinuous gabbro intruded along the contact of a 14 m wide felsic unit is intercalated with the Spyder Arm Basalt Suite. This minor felsic volcaniclastic unit has abundant feldspar phenocrysts with small amounts of quartz phenocrysts and many lapilli fragments, as well as local quartz clasts (up to 5 cm). This unit stratigraphically lies within the Windy Lake Felsic Suite indicating that it was deposited at the same time ca. 2685 Ma (Figure 2.3).

2.2.1.6 Member Basalt Suite

Southwest of the Bend Basalt Suite is a package of mafic volcanic rocks named the Member Basalt Suite (Figure 2.2). The majority of this 2 km thick suite is pillowed, and locally has subequal proportions of massive and pillowed flows. This suite is ~2 km in thickness and has similar size and shaped pillows as the Bend Basalt Suite unit discussed above. This unit has a green color on the fresh surface and consistently thin (<5cm) pillow selvages. Almost all the pillowed and massive flows lack notable quantity of phenocrysts, amygdules or varioles. A few intervals containing amygdules or very small plagioclase phenocrysts have been observed (Figure 2.4c). This suite of volcanic rocks clearly faces to the northeast as shown by numerous pillow tops as well as gas cavities. Gas cavities also know as pillow shelves are the result of repeated filling and empting of pillow lava tubes (Batiza and White 2000). They are flat bottomed with a top that is concave down and are excellent younging indicators. The absolute age of this unit is not known but from field relationships it stratigraphically overlies the Windy Lake Felsic Suite (2685 Ma) (Figure 2.3).

2.2.1.7 Feldspar Megacrystic Gabbro

This gabbro pluton and has intruded much of the Flake Lake Suite (Figure 2.2). This gabbro is medium to coarse grained with abundant pink feldspar phenocrysts that range in size from <1 mm to 10 cm. This plutonic body has numerous large (>10 m) roof pendents/ xenoliths as inclusions of rock with mineralogy and textures consistent with Flake Lake Suite. Also observed are rare macroscopic blue quartz crystals. These are likely xenocrysts due to presence of xenoliths as well as composition of this gabbro not allowing it to crystallize quartz.

Equivalent gabbro dykes with or without feldspar, are found intruding the stratigraphy throughout the belt. The absolute age of this unit is unknown, but from field relationships, it is one of the youngest intrusions in the Hope Bay Greenstone Belt and has no comparable volcanic suite (Figure 2.3).

2.2.1.8 Structural Geology

The earliest fabric (S_0) is seen as bedding in sedimentary rocks and can also be approximated by pillow younging feature (pillow tops and gas cavities). The dominant fabric observed in this transect, and the rest of the belt, is a single penetrative foliation, and is termed S_2. S_2 is fairly consistently trends approximately north-south and steeply dipping. Folding is locally observed in the Member Basalt Suite as well as near inferred or mapped faults. In the Flake Lake Transect S_3 is observed as crenulation of S_2 and in the area adjacent to the transect F_3 is observed as complicated fold interference pattern of lithologic units. The feldspar megacrystic gabbro south of Flake Lake contains a system of close-spaced fractures trending east-north-east and commonly has alteration along their margins. There are no large scale folds identified that affect the rocks in this transect and this is supported by lack of changes in facing direction or foliation. Geochronology supports two homoclinal sequence with the Flake Lake Felsic Suite (2697 Ma and 2716 Ma) juxtaposed below the Windy Lake Felsic Suite (2686 Ma). The fault that juxtaposes the Bend Basalt Suite against the Member Lake Basalts is not directly observed as it lies in a valley but no rotation in the foliation is observed.

2.1.2 Clover Lake Transect

The Clover Lake Transect extends west of Spyder Lake to the edge of the granites that form the the west margin of the Hope Bay Greenstone Belt, a length of approximately 6.5 km (Figure 2.1). The transect starts on the shore of Spyder Lake and proceeded west to include the area around Clover Lake and the Koignuk River (Figure 2.5). A wide range of mafic volcanic, felsic volcanic and sedimentary rocks form the transect.

Similar to the Flake Lake Suite, there are two different age sequences of rocks separated by a fault. On the west side there is an older domain which is made up of the Koignuk Felsic Suite (2677 Ma) and Clover West Basalt Suite. The east (younger) domain is made up of the Cover East Basalt Suite, Clover Sedimentary Suite and Clover Felsic Suite (2662 Ma). The break between the two domains is mapped as a fault lying at the east side of the Clover West Basalt Suite. This fault juxtaposes the younger Clover Sedimentary Suite rocks against the Clover West Basalt Suite (Figure 2.6).

2.2.2.1 Koignuk Felsic Suite

The westernmost felsic volcanic package observed on this transect is the Koignuk Felsic Suite (Figure 2.5). On the regional scale, the Koignuk Felsic Suite appears to be in angular contact with the mafic volcanic rocks to the east . A late fault cuts the east portion of the Koignuk Felsic Suite where diabase dikes are displaced. This suite stratigraphically youngs to the east based on graded beds in the sedimentary rocks at the top of the suite. The strtagraphic base of this suite contains a series of aphanitic to quartz phyric epidote altered felsic flows, flow breccias and tuffs. Stratigraphically above this is the feldspar porphyry, dated at 2677 +2.5/-1.1 Ma (Hebel 1999), is the dominant rock type of the Koignuk Felsic Suite, (~1.2 km thick) and contains few primary features aside from occasional bedding. The rocks are interpreted as crystal tuffs and grade into a volcaniclastic succession dominated by lapilli stone with lesser breccia (Figure 2.7e and f). Stratigraphically above the volcanic rocks is a facies dominated by volcanic-derived sedimentary rocks ranging from immature feldspar and minor quartz phyric tuff to more mature sedimentary rocks, such as argillite, siltstone and wacke. The stratigraphic base of the sedimentary facies is defined by a dolomite unit. This unit is massive dolomite to dolomite rhythmite with a maximum thickness of 20 meters, and grades up stratigraphy to a siltstone (Figure 2.7d). The massive dolomite ranges in thickness, but averages approximately 2 meters. The rhythmite section has centimeter scale bedding that alternates between dolomite and quartz-cemented siltstone. In this dolomite unit numerous graded beds indicate stratigraphic younging is eastwards, which is consistent with the overlying sedimentary rocks. The The Koignuk Felsic Suite is the oldest (2677 Ma) and thickest felsic suite in the Clover Transect (Figure 2.6).

2.2.2.2 Clover West Basalt Suite

West of the Clover Valley Sedimentary Suite is a suite of mafic rocks informally named the Clover West Basalt Suite (Figure 2.5). The contact between this package and the Clover Valley sedimentary rocks is interpreted as a ductile fault, although the exact relationship between the two units has not been totally resolved. The Clover West Basalt is composed of well formed, pillowed flows with a significant amount of mafic intrusions and lesser mafic volcaniclastic rocks. Stratigraphically on the top of this suite, the rocks are weakly variolitic. The pillows in the center of the unit lack primary features, whereas the west side has some amygdaloidal sections. Numerous facing reversals in the pillowed flows and repetition of the gabbro and a volcaniclastic rock unit suggest that this unit is tightly folded. The contact relationship between the Clover West Basalt Suite and the Koignuk Felsic Suite to the west is not observed, but new data suggest that it is faulted in places but likely part of the stratigraphy (R. Sherlock, pers comm, 2006). Field relationships and geochronology show that the West Clover Basalt Suite stratigraphically overlies the Koignuk Felsic Suite (2677 Ma) (Figure 2.6).

2.2.2.3 Clover East Basalt Suite

The package of rock directly west of Spyder Lake is dominated by light green, normal and light rare earth enriched pillowed basalt (see Chapter 3). This package lies along the western shore of Spyder Lake, and is named the Clover East Basalt Suite (Figure 2.5). It is a mixture of pillowed, and lesser massive, flows, as well as syn-volcanic mafic intrusions. A thin felsic dike intrudes the middle of the suite, and numerous pillow top directions suggest that stratigraphy youngs to the west. The top of this package contains the highest density of varioles seen in this transect and is lighter in color compared to underlying flows. A dacite breccia approximately 25 m thick is interbedded in the upper 100 m of the mafic package. This rock ranges from 10 to 70% clasts in a matrix of altered soft and dark brown material. The feldspar phyric clasts, which range in size from 0.5 to 10 cm, are sub-rounded. The breccia is overlain by a unit of strongly foliated pillows, and variolitic pillows greater than 1 m in diameter. This unit stratigraphically underlies the Clover Valley Sedimentary Suite which has an inferred age of ca. 2663 Ma (Hebel 1999) (Figure 2.6).

2.2.2.4 Clover Valley Sedimentary Suite

To the west of the Clover East Basalt Suite is a package of sedimentary rocks named the Clover Valley Sedimentary Suite as it lies in the Clover Valley (Figure 2.5). A number of facies make up this suite including resedimented syn-eruptive volcaniclastic rocks and sedimentary rocks ranging from conglomerate to argillite. A 25 m thick volcanic sandstone recognized south of Clover Lake forms the stratigraphic base of this suite. This sandstone unit contains a number of porphyritic clasts but is dominated by rounded feldspar grains and few quartz grains (Figure 2.7b). Above the sandstone unit is a heterolithic pebble conglomerate with clasts of sedimentary, volcaniclastic and coherent volcanic rock (Figure 2.7a). Rocks in the upper part of this unit include argillite with lesser greywacke. Graded bedding indicates stratigraphic younging is to the west. Along strike to the north, outside of the transect area, contradictory facing directions are mapped, suggesting structural complexity in that locality (B. Hrabi, pers comm., 2005). There is a great deal of structural complexity but overall the Clover Valley Sedimentary

Suite grossly faces to the west and the stratigraphically overlies the Clover East Basalt Suite (Figure 2.6).

2.2.2.5 Clover Lake Felsic Suite

The Clover Lake Felsic Suite lies within the argillite facies of the Clover Sedimentary Suite, and outcrops on the north shore of Clover Lake (Figure 2.5). The Clover Lake Suite has two parts: the first is coherent feldspar porphyry, dated at 2663 +3.4/-2.8 Ma (Hebel 1999); and the second is a breccia unit. The coherent portion of this unit is a massive rhyolite that is quartz and feldspar porphyritic and likely represents a sub-volcanic intrusion or core of a dome. The breccia facies of this felsic suite has angular rhyolite clasts that range in size from 0.5 to 6 cm set in an argillite matrix (Figure 2.7c). These textures are consistent with felsic magma intruding into wet sediments and creating complex lava-sediment breccia called peperite. Sherlock and Sandeman (2004a) suggested these rocks were a carapace breccia. The felsic volcanic rocks are interpreted as having intruded and are intercalated with the Clover Valley Sedimentary Suite (Figure 2.6).

2.2.2.6 Western Granitoid

A felsic intrusive unit is encountered at the west margin of the Koignuk Suite and marks the edge of the greenstone belt (Figure 2.5). This massive, fresh, medium grained tonalite to granodiorite has up to 15% hornblende and has no fabric. These observations are consistent with Group III (post-volcanic) granitoids found on the west side of the belt (Thompson 1997; Sherlock and Sandeman 2004b). The contact between the intrusives and the dacite flows is sharp and has little alteration or deformation along it. This unit has been dated at 2608 ±5 Ma (Bevier and Gebert 1991), which is much younger than volcanism in the belt, and is not represented in the stratigraphic column (Figure 2.6).

2.2.2.7 Structural Geology

The earliest fabric (S_0) is seen as bedding in sedimentary rocks and can also be approximated by pillow younging feature (pillow tops and gas cavities). The dominant deformation event D_2 is observed as the S_2 which trends approximately north. There is transposed bedding in thinly bedded argillite of the Clover Valley sedimentary Suite which is called S_3.

The folding in the Clover Transect is identified in Clover West Basalt Suite as well as outcrop scale parasitic folding in the Clover Lake Sedimentary Suite. The folding in the Clover West Basalt Suite has a number of north trending fold which are indicated by unit repetition and changes in facing direction, are shallowly plunging. Geochronology of this transect suggests that a fault exists that juxtaposes the older domain (the Koignuk Felsic and Clover West Basalt Suites) against the younger domain (Clover Sedimetry and Clover East Basalt Suites). This fault is located at the west side of the Clover Valley between the Clover Sedimentary Suite and the Clover West Basalts.

2.2.3 Boston Area Transect

The Boston area transect lies south of the Boston deposit (Figure 2.1), located on a peninsular near the south end of Spyder Lake between the south arm of Spyder Lake and Stickleback lake (Figure 2.8). The geology of this area is well understood due to its potential economic importance (Clark 1996; Stemler; 2000; Sherlock and Sandeman 2004a, Stemler et al., 2006). Field relationships and extensive drilling have defined an approximately north trending anticline with mafic rocks in the core, overlain by sedimentary rocks (Figure 2.9). The oldest rocks in the area are a suite of normal and Ti-enriched basalts, which are folded into either a synformal anticline or an overturned anticline (Sherlock and Sandeman 2004a). A succession of normal pillow basalts with locally variolitic pillowed flows are found stratigraphically overlying the other basalts. Mafic volcaniclastic rocks overlain by sedimentary rocks with an age of 2675±2.5 Ma (LMB055, Table 2.1 and Figure 2.17) form the top of the sequence.

2.2.3.1 Boston Basalt Suite

The core of the Boston anticline is composed of green, normal pillowed basalts cross cut by syn-volcanic dikes (Figure 2.8). The rocks found at the north end of the Boston anticline are highly iron carbonate altered and have experienced ductile shearing, despite this some volcanic textures including pillows can be recognized (Figure 2.10a). The mafic volcanic flows are composed of pillows with thin black pillow selvages. Although variable, this unit is approximately 150 m thick. The pillowed basalt unit grades into a section of variolitic pillowed flows. The variolitic pillows are a medium to light green, and have up to 5 cm pillow selvages (Figure 2.10b). Varioles in the pillows are commonly coalesced in the center of the pillow, with some less variolitic pillows having a few varioles occurring around the outer edge of the pillow. Stratigraphically above the variolitic mafic volcanic rocks is a unit of mafic volcaniclastic rocks which is a volcaniclastic clast supported breccia that is usually deformed (Figure 2.9).

2.2.3.2 Boston Sedimentary Suite

Stratigraphically above the mafic volcaniclastic rocks is a sedimentary package informally named the Boston Sedimentary Suite. These rocks underlie Spyder lake and are found on the east and west limb of the Boston anticline (Figure 2.8). This package consists of argillite and wacke deposited as turbidites. The rocks that stratigraphically overlie the volcanic rocks in the Boston Area have a maximum depositional age of 2675±2.5 Ma (AJS 6, Table 2.1 and Figure 2.17). The contact between the sediments and the volcanics is not observed on surface; but the reconstructed geometry from diamond drilling indicates the Boston Sedimentary Suite is in parallel with the Boston Basalt Suite (E. Alesi, pers. comm. 2007) (Figure 2.7).

2.2.3.3 Structural Geology

The geology of the Boston Area is dominated by a large scale south plunging fold (Sherlock and Sandeman 2004a). This anticline, which is defined by graded beds and pillowing facings, has a core of the Boston Basalt Suite overlain by the Boston Sedimentary Suite. The deformation in the area is complex, S_2 is well developed and trends from northeast to northwest. There is a well developed steeply south plunging stretch lineation. The sedimentary rocks preserve the best record of deformations including S_0 (bedding), S_1 (transposed bedding), S_2. There are at two generations of folds observed F_2 and F_3 , F_3 is acute to F_2. The age of the sedimentary rocks on the west limb of the Boston Anticline is 2675.8±2.5 Ma and the rocks on the east limb include the Windy Lake Felsic Suite (2686 Ma) (Figure 2.9). This relationship indicates a disconformity between the sedimentary rocks and the underlying mafic volcanic rocks in the Boston Area.

2.2.4 Wolverine Transect

The Wolverine transect, in the north part of the Hope Bay Greenstone Belt, starts between Patch Lake and Wolverine Lake (Figure 2.1 and 2.11), and ends at the Koignuk River. A variety of rock units including pillowed mafic volcanic and felsic volcanic suites underlie this transect.

The Wolverine transect is underlain by a homoclinal package of volcanic, intrusive and sedimentary rocks. The base of the stratigraphy in this transect is bounded by a north-striking fault, the Hope Bay Deformation Zone. West of the Hope Bay Deformation Zone lies a thick package of pillow basalts called the Wolverine Basalt Suite, which is intercalated with a hetrolithic breccia and dacite tuffs, the tuffs are dated at ca. 2690 Ma. Near the base of this basalt unit is the Wolverine Intrusive dated at 2686 Ma (Sherlock, unpublished data). Stratigraphically above the Wolverine Basalt Suite is a suite called the Kennet Tarn Basalt Suite that is dominantly Ti-enriched basalts. These rocks are overlain by a sedimentary portion of the Windy Lake Felsic Suite. The Windy Lake Felsic Suite is overlain by the Koig Basalt Suite which is the complex mix of normal and Ti-enriched basalts, which is in turn overlain by the Koignuk Felsic Suite (2677 Ma), the youngest rocks in the transect. The package of rocks in this transect are in normal stratigraphic succession, and represent a large part of the stratigraphy in the north part of the belt. U-Pb ages indicate volcanism in this transect occurred between 2690 and 2677 Ma.

2.2.4.1 Wolverine Basalt Suite

The Wolverine Basalt Suite is an interval of pillowed basalts which is over 1 km-thick. It has been intruded by the Wolverine Porphyry (2684.2±3.6 Ma), and is intercalated with a number of felsic beds, dated at ca. 2690 Ma, and is bounded to the east by the Hope Bay Deformation Zone. In this transect the Wolverine Basalt Suite consists of well formed pillows with consistent stratigraphic younging to the west with local massive flows preserved. These pillows have weathered to a dark brown color, have thick selvages and lack varioles. This suite also contains massive flows and mafic intrusives.

2.2.4.2 2690 Ma Dacite Unit

The Wolverine Basalt Suite is intercalated with at least two volcaniclastic facies of ca. 2690 Ma age rocks. Two north striking feldspar phyric tuff beds have been dated at 2691.1±2.0 Ma and 2691.7 ±2.5 Ma (AJS 4 and AJS 5, Table 2.1 and Figure 2.17). Stratigraphically below these tuffs is a unit containing a heterolithic breccia and lapilli tuff facies. The lapilli tuff portion has been dated at 2689 +4.0/-3.6 Ma (Sherlock, 2003). These felsic rocks are stratigraphic equivalents as the Square Lake Felsic Suite is found ~20 km to the southwest.

2.2.4.3 Kennet Tarn Basalt Suite

West of the Wolverine Basalt Suite is a sequence of dark green pillowed basalts and massive flows (Figure 2.11) informally named the Kennet Tarn Basalt Suite. This suite contains Ti-enriched basalts which will be discussed further in Chapter 3. Facing directions are not directly found in this poorly outcropping suite but it is inferred to face west based on the enclosing strata (Figure 2.12).

2.2.4.4 Windy Lake Felsic Suite

To the west of the Kennet Tarn Basalt Suite lies a volcanic-derived sedimentary package, correlated with the Windy Lake Felsic Suite, dated ~3 km to the north at 2685 +2.0/-2.5 Ma (Figure 2.11). In this area, the Windy Lake Felsic Suite is made up of the volcanic-derived sedimentary rocks composed of siltstone and wacke. The unit is approximately 250 m thick, and contains well preserved graded beds that face west. The Windy Lake Felsic Suite stratigraphically overlies the Kennet Tarn Basalt Suite (Figure 2.12).

2.2.4.5 Koig Basalt Suite

Stratigraphically above the Windy Lake Felsic Suite are mafic volcanic rocks called the Koig Basalt Suite (Figure 2.11). This unit is made up of large (~1 m), well formed pillow basalts that are locally light rare earth enriched and Ti-enriched (discussed in Chapter 3). This unit has abundant pillow breccia and vesicles, with the east side of the unit containing the majority of pillow breccia textures. Pillow tops face stratigraphically to the west and were deposited on top of Windy Lake Felsic Suite (Figure 2.12).

2.2.4.6 Koignuk Felsic Suite

The Koignuk Felsic Suite, stratigraphically overlies the Koig Basalt Suite, it is the uppermost unit in the Wolverine transect (Figure 2.11). Here, the Koignuk Felsic Suite is composed of a monomictic volcanic breccia which grades upward over a short stratigraphic distance into a lapilli bearing volcaniclastic rock within tens of meters of the base of the unit and then grades into a feldspar porphyritic volcaniclastic rock over the next 100 m (Figure 2.12). The Koignuk fault, which cuts the Koignuk Suite, bounds the western margin of the transect. The Koignuk Suite, dated at 2677.4+1.9/-1.5 Ma (Hebel 1999), is the youngest suite in the Wolverine transect.

2.2.4.7 Structural Geology

The structural geology of this transect is relatively simple; it is a homocline sequence of basalt, dacite and sedimentary rocks laid in stratigraphic order. The tops are consistently to east, determined from graded beds, pillow tops and gas cavities. There are no parasitic folds, changes in facing direction or rotated foliations to suggest large scale folding. The only large scale structural feature of this transect is found at the base which is bounded by the Hope Bay Deformation Zone. In the volcanic derived siltstones of the Windy Lake Felsic Suite the S_0/S_1 relationship is observed, where S_1 is parallel to S_0. The dominant fabric observed is the result of D_2, it is named S_2, it overprint all earlier fabrics and is acute to S_1/S_0 transposed fabrics

2.2.5 Doris-Discovery Transect

The Doris-Discovery Transect extends to the west from the Doris deposit to the shore of Hope Bay (Figure 2.1 and 2.13). This 7 km long doglegged transect is underlain by of a number of intervals of felsic, mafic and sedimentary rocks. Felsic volcanic and sedimentry rocks include the Windy Lake Felsic Suite, Koignuk Felsic Suite and Conglomerate Hill Sedimentary Suite.

The Discovery area is highly faulted, and comprises at least three different lithologic units. The Discovery Basalt Suite can be correlated with the Koig Basalt Suite in the Wolverine Transect.

The Doris anticline is an extremely large structural feature traceable over 5 km north and south of the transect (Figure 2.13). The stratigraphic lower part of the transect is made up of rocks on the west limb of the anticline, they are a series of basalts that are in stratigraphic succession, from youngest to oldest, the Doris Basalt Suite, Mesa Basalt Suite, variolitic Doris Basalt Suite, Mesa Basalt Suite, Patch Basalt Suite and variolitic Windy Basalt Suite. The top of the Windy Basalt Suite is in stratigraphic contact with the Windy Lake Felsic Suite in one location, whereas in other locations it is separated by an intrusive component of the Windy Lake Felsic Suite (Figure 2.14). The relationship between the Windy Lake Felsic Suite and units in the Discovery Area is not directly observed in this transect, but the stratigraphic relationship to the south can be traced to the Discovery Area. The oldest rocks in the discovery area are part of the sedimentary facies of the Windy Lake Felsic Suite (the Glen Lake Sedimentary Suite), which is structurally overlain by Discovery Basalt Suite, and the Conglomerate Hill Suite. Outside this transect area, to the south, this structural contact are known to be stratigraphic.

2.2.5.1 Doris Basalt Suite

The Doris gold deposit is located at the north end of Doris Lake, and is hosted in the Doris Basalt Suite at the core of a north striking doubly plunging anticline (Figure 2.13). The Doris Basalt Suite is composed of dark green mafic flows made up of pillowed basalts, vesicular pillowed basalt, and massive basalt (Figure 10d). The vesicular pillowed flows are moderate to highly vesicular, with vesicles up to 0.5 cm (Figure 10c). The thickness of these flows range from 10 to 60 m, with the total thickness of the Doris Basalt Suite being 250m. At the core of the anticline, a fine to medium grained massive to pillowed flow (Carpenter et al. 2003). The Doris Basalt Suite has magnetic and non-magnetic sections that are stratigraphically continuous. Individual flows can be mapped, and the center of each flow is more magnetic than the top and bottom of the flow. This magnetic pattern represents primary petrogenetic controls rather than destruction of magnetite during hydrothermal alteration. These basalts are the oldest volcanic rocks in the northern part of the belt (Figure 2.14). At the top of the Doris Basalt suite is a 200 to 300 m thick unit of highly variolitic dark green pillowed basalt is found. This basalt is similar to the Doris Basalt Suite in pillow size, colour and chemistry. It is characterized by stretched varioles that measure 0.2 to 1 cm in diameter and plunge steeply to the north. It is separated from the non-variolitic vesicular Doris Basalts by a 150 m unit pillows texturally similar to the overlying Mesa Basalt Suite. This intercalation of the Doris Basalt Suite and Mesa Basalt suite suggests that the deposition of these two suites overlapped.

2.2.5.2 Mesa Basalt Suite

Stratigraphically overlying the Doris Basalt Suite is a suite named the Mesa Basalt Suite, after a geographic feature to the north (Figure 2.10 and 2.13). The Mesa Basalt Suite is the largest stratigraphic unit in the Doris-Discovery transect, with an approximate thickness of 1 km. The Mesa Basalt Suite is almost entirely composed of green, well-formed pillows, with minor pillow breccia (Figure 2.10e). Locally, there are sections of megapillows (pillows over 2m in diameter), which are found close to the top of the unit (Figure 2.16d). All pillow tops give a west facing direction and there is no evidence of internal folding of this suite.

Minor meter scale sections of massive basalt and pillow breccia form part of the Mesa Basalt Suite. A number of large, up to 30m wide, gabbro dikes with chilled margins intruded the upper parts of the Mesa Mafic Suite.

2.2.5.3 Patch Basalt Suite

To the west of the Mesa Basalt Suite lies a chemically and texturally distinct group of rocks referred to as the Patch Basalt Suite (Figure 2.13). This basalt suite is host to a number of gold deposits further south in the Madrid area. These rocks are susceptible to weathering, and usually lie in valleys under cover and rarely crop out. In the Doris Transect, the majority of this suite is pillowed basalt, with few massive basalt sections. In the Madrid area, along strike and outside the transect, a variety of textures are also present, including peperitic and harrisitic (a pseudo-spinifex texture) textures, as well as a variety of auto breccias (Therriault 2006; Madsen et al., 2007). Pillows in this suite are extremely dark in some cases almost black on the fresh surface (Figure 2.16b). Pillows are round and amoeboid in shape, and are characteristically smaller than the majority of pillowed basalts in the Hope Bay Greenstone Belt (Figure 2. 16a). This rock type is preferentially mineralized compared to the suites of basalts nearby (Windy Basalt and Mesa Basalt Suites) (Madsen et al., 2007). Poor pillow shapes of this unit do not allow direct determination of younging directions, but it is inferred to young westward based on stratigraphic relationships of the enclosing strata (Figure 2.14).

2.2.5.4 *Windy Basalt Suite*

West of the Patch Basalt Suite is a highly variolitic pillowed unit called the Windy Basalt Suite (Figure 2.13). It is dominantly composed of large pillow basalts, approximately 1 m in diameter, which are light green on the fresh surface, with thin and light brown pillow selvages. This group of basalts has abundant gas cavities, and facing directions are consistently west. There are also sections of discontinuous flow breccia as well as fine- to medium-grained massive basalt. Varioles are few at the pillow rim but increase in abundance several centimetres from the pillow rim to form coalesced varioles at the center of the pillow (Figure 2.16c). The unit conformably overlies the Patch Basalt Suite (Figure 2.14).

2.2.5.5 *Windy Lake Felsic Suite*

To the west of the Windy Basalt Suite is the Windy Lake Felsic Suite (Figure 2.13). This transect lacks the contact between the Windy Basalt Suite and Windy Lake Felsic Suite due to the intrusion of a quartz diorite, but along strike the contact is observed to be stratigraphic . On the Discovery transect, an intrusive portion of the Windy Lake Felsic Suite is observed, and is interpreted as a sub-volcanic portion of this suite (Sherlock et al. 2003). This porphyritic intrusion has a wide range of feldspar and quartz phenocryst content and size (0.01 to 10 mm). Epidote alteration is also common. Quartz ranges from 0 to 20% of the rocks where as, the feldspar laths compose 10 to 45% of the rock. To the west of the intrusion, the volcaniclastic portion of the Windy Lake Felsic Suite is a polymictic breccia with abrupt vertical facies changes (Figure 2.16 e and f). This breccia has clast-poor and clast-rich facies, and has a wide range of matrix compositions, from aphanitic to quartz and feldspar rich. The breccia portion of the

Windy Lake Felsic Suite grades rapidly into a massive quartz feldspar porphyritic unit. In some locations, this unit is homogeneous, but elsewhere distinct beds are characterized by changes in grain size and differing phenocryst content (Figure 2.14).

2.2.5.6 Glen Lake Sedimentary Suite

To the west of the Glen Lake is a group of sedimentary rocks called the Glen Lake Sedimentary Suite (Figure 2.13). The Glen Lake Sedimentary Suite is made up of immature siltstones with lesser argillite. Graded beds show facing is to the west and it has a maximum depositional age of 2678.4±2.8 Ma (LMB-55, Table 2.1 and Figure 2.17) based on U-Pb ages of detrital zircon. To the south it can be correlated with sedimentary rocks so this unit is not actually a distinct sedimentary suite but instead it is part of the Windy Lake Felsic Suite. It represents the end of the sedimentation of Windy Lake Felsic Suite and gives an age range on the Windy Lake Felsic Suite.

2.2.5.7 Discovery Basalt Suite

To the west, and overlying the Windy Lake Suite is a package of mafic volcanic rocks refered to as the Discovery Basalt Suite (Figure 2.13). This unit is made up of pillowed mafic volcanic rocks and almost an equal volume of gabbro intrusions. Pervasive wide spread iron carbonate alteration is found in the Discovery area, as well as at least two well-developed, subparallel foliations, which obscure primary volcanic textures. Nonetheless, relic pillow shapes are locally observed in the Discovery Basalt Suite, but no facing indicators can be found. To the south, outside the transect area, good pillows face to the west in the Koig Basalt Suite and these facing directions can be correlated to the Discovery Basalt Suite. There is faulting in this area which forms north trending ridges and ~100 m wide valleys. The majority of these brittle-ductile faults are north-striking, but other perpendicular (west-striking) brittle faults are observed. The displacement on the north-striking faults is not known but the west-striking faults have tens of meters of offset. Due to this faulting, the primary contact relationships of the Discovery Basalt Suite and enclosing strata must be inferred from areas along strike where they can be observed (Figure 2.15).

2.2.5.8 Koignuk Felsic Suite

Stratigraphically overlying the Discovery Basalt Suite is a portion of felsic volcanic rocks that can be correlated south to the Koignuk Felsic Suite (2677 Ma). In this area these rocks exhibit volcano-sedimentary textures; the bottom of the unit is primarily a crystal tuff with some sections of lapilli tuff. Subangular plagioclase and quartz crystals, with few lithic fragments in a dark grey siliceous matrix characterize the rock. Westward, the unit lacks plagioclase, and clasts become round, suggesting a change from a resedimented syn-eruptive volcaniclastic deposit to a volcanogenic sedimentary deposit.

2.2.5.9 Conglomerate Hill Sedimentary Suite

Stratigraphically above the Koignuk Felsic Suite lies a package sedimentary rocks called the Conglomerate Hill Sedimentary Suite (Figure 2.13). The east side of this suite has portions of the Koignuk Felsic Suite intercalated with argillite of the Conglomerat Hill Sedimentary Suite. Further west and up stratigraphy, the tuffaceous rock of the Koignuk Felsic Suite disappears and the unit consists of thinly bedded argillites with some sandstone beds high in the sequence (Figure 2.15). Above the argillites are conglomerate, with 5 to 65 cm beds of a polymictic pebble conglomerate interbedded with graded course sandstone beds. Clasts in the conglomerate are felsic volcanic rocks, argillite to arenaceous sedimentary rocks, and few mafic volcanic rocks (Figure 2.16g). Round to sub-angular clasts have a maximum size of 30cm, but an average size of <10 cm. Bedding strikes approximately north and dips moderately to the west. Graded, course sandstone beds show that the unit is upright, and stratigraphically youngs to the west. One of these sandy beds has been dated by U-Pb methods and gives a maximum depositional age of 2670.6±2.5 Ma (LMB-56, Table 2.1 and Figure 2.17). The contact between the Conglomerate Hill Sedimentary Suite and the Discovery Basalt Suite is difficult to discern as it has been faulted on most localities. Along strike the contact is believed to be stratigraphic . In the Discovery area it is interpreted that the sedimentary rock suites stratigraphically overlie the Discovery Basalt Suite (Figure 2.15).

2.2.5.10 Late Mafic Intrusives

In the Discovery Area, the Conglomerate Hill Sedimentary Suite is intruded by north-striking diorite intrusions (Figure 2.13). These intrusions form thick sills that run approximately parallel to bedding, trending north. The xenolith-rich diorite is characterized by abundant hornblende and lesser plagioclase phenocrysts in an aphanitic matrix. Xenoliths are made up of rounded, equigranular granitoids material, mostly monzogranites but rare xenoliths of volcanic and sedimentary rocks are also noted. The xenolith size ranges from <5 cm to ~45 cm, with the average xenolith clast being ~20 cm in diameter. There is minimal wallrock alteration with the surrounding sedimentary rocks.

2.2.5.11 Structural Geology

The Doris Discovery transect encompasses the entire west limb of the Doris anticline, which is the largest structural feature in the northern part of the belt. This anticline fold hinge trends north under Doris Lake and is shallowly doubly plunging (Sherlock et al. 2003). The anticline is mapped based upon facing direction in the normal pillow basalts;

The earliest deformation event D_1 is observed in the sedimentary rocks of this transect, it is name S_1 and is transposed bedding S_0. The dominant penetrative fabric in the Doris-Discovery transect is S_2 which strikes north-north-east and is steeply dipping. S_2 is the result of east west compression which also formed the doris anticline and it is at an acute angle to S_1. This transect has some excellent examples of stretched varioles in the Doris Basalt Suite,. These stretching lineations are consistently north-north-west and steeply dipping. There is little evidence in this transect for D_3 but subtle larger scale F_3 patterns have been identified (Sherlock et al. 2003).

The Discovery Area consists of a number of fault blocks. These fault blocks include a number of homoclinal sequences. Found furthest to the east is a mixture of relatively fresh gabbro and iron carbonate altered basalts of the Discovery Basalt Suite. The fault block to the east contains a sequence from dacite pyroclastic and resedimented syn-eruptive volcaniclastic rocks of the Koignuk Felsic Suite, and argillites and conglomerates of the Conglomerate Hill Sedimentary Suite which appears to contain some F_2 folding, from parasitic folding along lithologic contacts. The most westerly fault block is composed of the Conglomerate Hill Sedimentary Suite with bedding upright and dipping moderately west which is intruded by the Late Mafic Intrusives.

2.3 Discussion

Mapping of the Hope Bay Greenstone Belt along six transects shows the belt to be composed of at least six felsic volcanic suites, thirteen mafic volcanic suites and three sedimentary rock suites. Geochronology data from this study supports work by Hebel (1999) which concluded that virtually all the supracrustal rocks in the Hope Bay Greenstone Belt were deposited over at least 53 m.y. (2716-2663 Ma). Felsic volcanism has been shown to occur episodically, commonly punctuating periods of mafic volcanism that may have occurred relatively consistently throughout the construction of the Hope Bay Greenstone Belt.

2.3.1 Correlating and Understanding Transects

The oldest felsic suite in the Hope Bay Greenstone Belt is the Flake Lake Felsic Suite, and now has two U/Pb dates of 2716±7.8 Ma (Hebel 1999) and 2697.6±8.9 Ma (AJS 1, Table 2.1 and Figure 2.17). The Flake Lake Felsic Suite is spatially restricted to the area in the south part of the belt around Flake Lake. Two samples from this suite that were processed for U/Pb geochronology indicate a 19 m.y. (2716 -2697 Ma) age range for the Flake Lake Felsic Suite, which is a large age range for a magmatic event. When the errors are included the age range may be as short as 7 m.y. which could be considered a reasonable range for a single magmatic event. The age range of the Flake Lake Suite most likely explained by a single magmatic event with several stages of magma generation though similar tectonic process

The Bend Basalt Suite is intercalated with the Flake Lake Felsic Suite at the location of the 2697 Ma date. Stratigraphic relationships suggest that much of the Bend

Basalt Suite is coeval with some of the Flake Lake Felsic Suite. The upper domain of the stratigraphy of the Flake Lake transect contains the Windy Lake Felsic Suite intercalated with the Spyder Arm Basalt Suite (Figure 2.4). This represents contemporaneous volcanism of the Windy Lake Felsic Suite and the Spyder Arm Basalt Suite which implies that the felsic volcanic cycles were discrete while the mafic volcanism was continuous thought the evolution of the belt. The Windy Lake Felsic Suite and Spyder Arm Basalt Suite are then overlain by the Member Basalt Suite.

The geochronology of the Clover Transect suggests that the rocks from this locality are younger than those from the Flake Lake Transect (west side of the belt) (Figure 2.6). In this transect, the Koignuk Felsic Suite is overlain by the Clover West Basalt Suite in the older volcanic sequence. The upper (younger) sequence is defined by mafic volcanic rocks that are overlain by sedimentary rocks (Clover Lake Sedimentary Suite) and the Clover Lake Felsic Suite (2663 Ma).

The overall stratigraphic position of the Boston Area could not be completely resolved through mapping. The disconformity between the sedimentary rocks and the underlying mafic volcanic rocks in the Boston Area is based on two U/Pb ages. The sedimentary rocks on the west limb of the Boston Anticline is 2675.8±2.5 Ma and the rocks on the east limb include the Windy Lake Felsic Suite (2686 Ma) (Figure 2.9). This relationship means that the Boston Basalts Suite is older than 2686 Ma. This relationship is consistent elsewhere in the belt where Ti-enriched basalt suites similar to the Boston Ti basalts usually lie in the lower portions of the stratigraphy, below the Windy Lake Felsic Suite (2686 Ma).

The north part of the belt the Wolverine Transect covers a similar portion of the stratigraphy as the Doris-Discovery transect. These two transects are separated by a fault called the Hope Bay Deformation Zone which juxtaposes distinct basalt suites (Figure 2.19). The Doris-Discovery transect and the Wolverine transect contains a similar mixture of small, dark green pillowed basalt suites (Doris Basalt Suite, Kennet Tarn Basalt Suite and Patch Basalt Suite) which are separated by light green well formed pillows (Mesa Basalt Suite, Windy Basalt Suite and Wolverine Basalt Suite). This indicates that the north part of the belt contains multiple cycles of small, dark green (Ti-enriched) pillowed basalts separated by "normal" pillowed basalt. These suites of small dark green pillow forms are Ti-enriched basalts and are an important group of rocks discussed further in Chapter 3. They host two gold deposits in the north part of the belt. On the south side of the Hope Bay Deformation Zone the Wolverine Basalt Suite is intercalated with felsic tuffs, dated at ca. 2690 Ma. There are no suitable units to collect geochronology data from the lower part of the Doris stratigraphy, but stratigraphic relations suggest that the Patch Basalt Suite is older than 2690 Ma as parts of it lie below the Wolverine Basalt Suite.

The uppermost part of the stratigraphy in the northern part of the belt is found in the Discovery Area. The age of the siltstone (2678 Ma) at discovery represents the end of the sedimentary part of the Windy Felsic Suite and gives a time range of 8 m.y. on this suite. The date of 2670 Ma on the Conglomerate Hill Suite is the youngest sedimentary rock in this study and represents sedimentation that is post-volcanic but likely pre-orogenic. Hebel (1999) dated a conglomerate suite bearing granitic clasts at 2647 Ma but there is no context how this suite relates to the rest of the Hope Bay Greenstone Belt.

There are two types of intrusives in the Discovery Area, a xenolith rich diorite and a gabbro. The gabbro is similar to gabbro seen throughout the basalt stratigraphy which is likely the same as the feldspar megacrystic gabbro at Flake Lake. The relationships in the Discovery Area suggest that all these gabbros are relatively young but likely still are within the time range of volcanism in the belt. The most interesting intrusive in the Discovery Area is the xenolith rich diorite which has a sill like geometry. These rounded xenoliths are up to 40cm in diameter. The rounding suggests mechanical abrasion or resorption as well as possible transport of significant distances. No feeder dykes have been identified and the lack of vesicles suggest a low velocity magma which would rule out mechanical abrasion.

The north and south parts of the belt contain similar stratigraphy which can be correlated in places (Figure 2.19). Koignuk Felsic Suite and the Windy Felsic Suites are regionally extensive units that can be correlated between the two transects, and a sequence of conglomerates and argillites that are the youngest rocks found in the belt can be broadly correlated based on geochronology. The base of the Clover Lake and Conglomerate Hill Sedimentary Suite define the end of regional volcanism. The most voluminous felsic volcanic rocks in the south part of the belt belong to the Koignuk Felsic Suite, whereas the north part of the belt contains equal proportions of Windy Lake Felsic Suite and Koignuk Felsic Suite rocks (Figure 1.4).

2.3.2 The Belt as a Whole and Comparison to Other Greenstone Belts

The original stratigraphic framework, by Hebel (1999), holds true with volcanism occurring over an interval of at least 53 million years. The felsic volcanic episodes which occur around 2716 Ma, 2697 Ma, 2690 Ma, 2686 Ma, 2677 Ma and 2663 Ma are separated by the deposition of mafic or sedimentary rocks. Turbiditic sedimentation and conglomerates are syn-volcanic and post-volcanic. The felsic to mafic cycles of volcanism seen in greenstone belts worldwide are observed here (Ayer et al. 2002).

The tectonics of the Archean are not well understood, we can only speculate on the geodynamic setting of greenstone belts. Despite our lack of understanding of the Archean some basic observations can be made; 1) almost all of the felsic and mafic volcanism is submarine indicated by pillowed volcanic rocks and reworking of felsic volcanic rocks and 2) there are complicated magma processes that results in mafic to felsic volcanic cycles.

The plutonic activity found on the margins of the Hope Bay Greenstone Belt is marked by synvolcanic (2672 Ma, Bevier and Gebert 1991), post-volcanic/syn-D2 (2650 Ma, Bevier and Gebert 1991) intrusives and post-deformation (2608 Ma, Bevier and Gebert 1991) intrusive rocks. Titanite U-Pb cooling ages from a gneiss bordering the south eastern margin of the Hope Bay Greenstone Belt suggest the peak of regional metamorphism had occurred by ca. 2589 Ma.

The temporal framework of the Hope Bay Greenstone Belt is similar to many other greenstone belts throughout the Canadian Shield. The Yellowknife Greenstone Belt has volcanism spanning 70 m.y. (2730 – 2660 Ma) as well as a significantly younger sequence of late orogenic sedimentary rocks (Henderson, 1970; Cousens et al., 2006; Martel and Lin, 2006; Davis and Bleeker 1999; Bleeker et al., 2004). The Abitibi Greenstone belt evolved over a longer time frame but is of similar age; it has volcanism spanning 45 m.y., between (2730 - 2685 Ma) and has significant late orogenic sedimentation of the Timiskaming Assemblage (Chown et al., 1992; Corfu, 1993; Ayer et al., 2002). The Hope Bay Greenstone Belt is similar to both of these well documented greenstone belts in age and span of volcanism. Only one isolated location with little geologic context of late orogenic sedimentary rocks has been identified as part of the Hope Bay Sedimentary Suite (Hebel 1999).

2.4 Summary

The combination of field relationships, from a number of discrete transects across the Hope Bay Greenstone Belt, and U-Pb geochronology has allowed the creation of a revised stratigraphic framework for the belt. This work confirms that volcanism occurred over an interval of at least 53 m.y. (2716 Ma to 2663 Ma) (Hebel 1999) but using field relationships and additional geochronology the majority of volcanism occurred over 33 m.y. (2700 – 2677 Ma).

The stratigraphy of the Hope Bay Greenstone Belt can be broken into two main parts, that older and younger than 2686 Ma. The time horizon of 2686 Ma is the first time belt wide felsic volcanism is observed and is chosen because it can be correlated throughout the belt. This age of 2686 Ma represents the transition period in the belt's history where mafic dominated volcanism is replaced by interbedded felsic and mafic volcanism with lesser sedimentation.

In the Hope Bay Greenstone Belt mafic volcanic rocks are almost entirely made up of pillow basalts with some pillow breccia, there are also sections of massive basalt or gabbro that are often difficult to determine it they are syn-volanic or post-volcanic intrusions. The volcanic textures in the pillow basalts include vesicles, gas cavities and varioles. The felsic volcanic rock packages show a wide range of volcanic textures including those consistent with pyroclastic, resedimented syn-eruptive volcanioclastic and volcanogenic sedimentary deposits. Volcanic textures of these suites show that all were deposited in a submarine environment.

The stratigraphic framework of the sedimentary suites of the Hope Bay Greenstone Belt includes syn-volcanic sedimentary and post-volcanic sedimentary rocks. The sedimentary rock suites include the Boston and Glen Lake Sedimentary Suites as well as the sedimentary portions of the Windy Lake and the Koignuk Felsic Suites. The younger sedimentary suites observed in this study include Clover Lake and Conglomerate Hill sedimentary suites. These younger sedimentary suites are made up of argillites and conglomerates.

In the north and south part of the belt the oldest rocks observed are found on the east side of the belt and the youngest rocks (sedimentary) are found in approximately the middle of the belt. Other than this, the north and south part of the belt differ due to the fact that the south part has a number of stratigraphic packages that are juxtaposed against each other by a number of faults, whereas in the north part of the belt the rocks are relatively stratigraphically continuous.

In the Hope Bay Greenstone Belt, gold deposits are broadly associated with favorable lithologic host rock and structural features (large scale folds or faults). In the north part of the Hope Bay Greenstone Belt the Doris Deposit and Madrid Area Deposits are hosted in high titanium mafic volcanic suites, these are located in the lower portions of the stratigraphy, (older than 2690 Ma). The Doris Deposit is hosted in the oldest known rocks in the north part of the belt, with the Madrid deposits hosted stratigraphically higher in the same mafic volcanic secession. The Boston Deposit which is located in the south part of the belt is hosted in sedimentary rocks, dated at 2675 Ma, as well as basalts older than 2686 Ma.

A major part of the exploration methodology in the Hope Bay Greenstone Belt has been based on identifying and understanding these favorable basalt rock suites, notably the Doris and Patch Basalt Suites. Less voluminous but similar suites to the Doris and Patch Basalt Suites exist elsewhere in the belt and may hold great exploration potential.

Understanding the supracrustal succession in the Hope Bay Greenstone Belt is complicated by its structural complexity and long history. The Hope Bay Greenstone Belt was created by a number felsic and mafic volcanic events, that have a variety of compositions, and the belt also contains syn-volcanic and post-volcanic sedimentation. These findings are consistent with that of numerous other greenstone belts in the Slave Structural Province, Canadian Shield and the World.

Table 2.1 U-Pb TIMS analytical data

Fraction[1]	Wt (µg)	U[2] (ppm)	Pb*[3] (ppm)	$^{206}Pb/^{204}Pb$[4]	Pb[5] (pg)	Th/U[6]	Isotopic ratios ±1σ,%[7] $^{206}Pb/^{238}U$	$^{207}Pb/^{235}U$	$^{207}Pb/^{206}Pb$	ρ[8]	%[9] discordant	Apparent ages ±2σ,Ma[7] $^{206}Pb/^{238}U$	$^{207}Pb/^{235}U$	$^{207}Pb/^{206}Pb$
a) AJS1 *(Nad83, Zone 13N 445023, 7515114)*														
A	6	31.4	18.7	2715	2.2	0.538	0.51967 ± 0.38	13.2510 ± 0.41	0.18494 ± 0.11	0.96640	0.0	2697.8 ± 16.9	2697.7 ± 7.7	2697.6 ± 3.5/3.5
B	7	29.8	18.0	308.3	22.8	0.574	0.52299 ± 0.40	13.3197 ± 0.51	0.18472 ± 0.26	0.866515	-0.7	2711.8 ± 17.8	2702.6 ± 9.6	2695.7 ± 8.4/8.5
C	7	28.9	17.5	2719	2.4	0.595	0.52041 ± 0.33	13.2267 ± 0.38	0.18433 ± 0.14	0.933982	-0.4	2700.9 ± 14.7	2696.0 ± 7.1	2692.3 ± 4.5/4.5
D	6	30.2	18.4	4003	1.5	0.626	0.52108 ± 0.42	13.2276 ± 0.45	0.18411 ± 0.11	0.970830	-0.6	2703.7 ± 18.6	2696.0 ± 8.6	2690.3 ± 3.6/3.6
b) AJS5 *(Nad83, Zone 13N 441634, 7510788)*														
A	7	65.7	39.7	4378	3.4	0.628	0.51768 ± 0.09	13.1049 ± 0.12	0.18360 ± 0.06	0.886331	-0.2	2689.3 ± 4.1	2687.2 ± 2.3	2685.7 2.0/2.0
B	5	52.7	32.4	3152	2.7	0.672	0.51550 ± 0.13	13.0533 ± 0.15	0.18365 ± 0.08	0.866261	0.3	2680.1 ± 5.6	2683.5 ± 2.9	2686.1 2.5/2.5
C	4	46.3	27.9	8117	0.7	0.636	0.51525 ± 0.10	13.0251 ± 0.13	0.18334 ± 0.05	0.918299	0.2	2679.0 ± 4.3	2681.5 ± 2.4	2683.3 1/8/1.8
D	4	91.9	55.0	7191	1.6	0.633	0.51189 ± 0.10	12.8871 ± 0.13	0.18259 ± 0.06	0.913657	0.5	2664.7 ± 4.2	2671.4 ± 2.4	2676.5 1.8/1.8
E	5	47.3	28.5	6678	1.1	0.610	0.51701 ± 0.13	13.0974 ± 0.15	0.18373 ± 0.07	0.903059	0.0	2686.5 ± 5.5	2686.7 ± 2.8	2686.8 2.1/2.1
c) AJS4 *(Nad83, Zone 13N 434907, 7546452)*														
A	5	175.6	93.2	11260	2.5	0.066	0.51335 ± 0.12	13.0386 ± 0.16	0.18421 ± 0.07	0.903831	0.9	2670.9 ± 5.0	2682.5 ± 3	2691.1 ± 2.4/2.4
B	5	186.9	98.2	20020	1.5	0.100	0.50407 ± 0.10	12.7811 ± 0.15	0.18390 ± 0.07	0.940886	2.6	2631.3 ± 4.3	2663.7 ± 2.8	2688.3 ± 2.2/2.2
D	2	312.3	172.4	5022	4.0	0.201	0.51779 ± 0.15	13.1464 ± 0.19	0.184144 ± 0.07	0.935317	0.0	2689.8 ± 6.4	2690.2 ± 3.5	2690.5 ± 2.3/2.3
d) AJS3 *(Nad83, Zone 13N 433414, 7549980)*														
A	4	110.5	59.9	9199	1.5	0.16	0.51266 ± 0.12	13.0197 ± 0.17	0.184191 ± 0.07	0.933907	1.0	2668.0 ± 5.3	2681.1 ± 3.1	2691.0 ± 2.2/2.2
B	2	92.6	49.8	1122	5.3	0.189	0.50573 ± 0.23	12.8449 ± 0.27	0.184211 ± 0.1	0.931284	2.4	2638.4 ± 10.1	2668.3 ± 5.2	2691.2 ± 3.4/3.4
C	7	40.7	20.8	1546	5.7	0.103	0.48980 ± 0.23	12.4039 ± 0.27	0.183672 ± 0.09	0.939666	5.3	2569.8 ± 9.9	2635.5 ± 5.0	2686.3 ± 3.1/3.1
D	2	119.6	66.4	4535	1.7	0.34	0.50495 ± 0.10	12.7969 ± 0.15	0.18380 ± 0.08	0.912976	2.4	2635.0 ± 4.3	2664.8 ± 2.9	2687.5 ± 2.5/2.5

[1]single grain analyses; all air abraded.

[2]U blank correction of 0.2 pg ± 20%; U fractionation corrections were measured for each run with a double $^{233\text{-}235}U$ spike.

[3]Radiogenic Pb; all raw Pb data corrected for fractionation of 0.32-0.23/amu ± 20% determined by repeated analysis of NBS-982 reference material.

[4]Measured ratio corrected for spike and Pb fractionation.

[5]Total common Pb in analysis based on blank isotopic composition: $^{206}Pb/^{204}Pb = 18.5 \pm 3\%$, $^{207}Pb/^{204}Pb = 15.8\text{-}15.5 \pm 3\%$, $^{208}Pb/^{204}Pb = 36.4 \pm 0.5\%$.

[6]Model Th/U derived from radiogenic ^{208}Pb and the $^{207}Pb/^{206}Pb$ age of fraction.

[7]Fractionation, blank and common Pb corrected; Pb procedural blanks were ~0.5-2.0 pg and U <0.2 pg. Common Pb compositions are based on Stacey-Kramers model Pb at the $^{207}Pb/^{206}Pb$ age of each fraction (Stacey and Kramers, 1975).

[8]Correlation coefficient.

[9]Discordance in % to origin.

H. Lin carried out mineral separations and provided assistance with mass spectrometry; assitance with grain selection, abrasion and in the cleanlab provided by R. Lishansky.

Table 2.1 continued. U-Pb TIMS analytical data

Fraction[1]	Wt (μg)	U^2 (ppm)	Pb^{*3} (ppm)	$^{206}Pb^4/^{204}Pb$	Pb^5 (pg)	Th/U^6	Isotopic ratios ±1σ,% [7] $^{206}Pb/^{238}U$	$^{207}Pb/^{235}U$	$^{207}Pb/^{206}Pb$	ρ^8	% [9] discordant	Apparent ages ±2σ,Ma [7] $^{206}Pb/^{238}U$	$^{207}Pb/^{235}U$	$^{207}Pb/^{206}Pb$
e) AJS6 detrital zircons		*(Nad 83, 13N 440607, 7503775)*												
A	6	141.8	87.0	674.9	41.0	0.801	0.50674 ± 0.10	12.8240 ± 0.18	0.183545 ± 0.12	0.781775	1.9	2642.7 ± 4.2	2666.8 ± 3.4	2685.2 ± 4.0/4.0
B	5	140.2	80.7	1921	11.2	0.696	0.48646 ± 0.09	12.2417 ± 0.13	0.182513 ± 0.07	0.840805	5.5	2555.3 ± 3.9	2623.1 ± 2.5	2675.8 ± 2.5/2.5
C	8	112.9	61.0	760.7	36.4	0.455	0.4795 ± 0.07	12.2092 ± 0.16	0.184672 ± 0.11	0.808635	7.6	2525.1 ± 2.7	2620.6 ± 2.9	2695.3 ± 3.6/3.6
D	3	59.0	37.1	951.2	6.0	0.960	0.50292 ± 0.13	12.7454 ± 0.23	0.183805 ± 0.18	0.599397	2.8	2626.3 ± 5.8	2661.0 ± 4.3	2687.5 ± 6.0/6.0
E	2	43.4	29.0	452.4	6.5	0.938	0.5182 ± 0.21	13.1515 ± 0.41	0.184065 ± 0.33	0.599456	-0.1	2691.6 ± 9.2	2690.6 ± 7.7	2689.8 ± 10.8/10.9
f) LMB055 detrital zircons			*(Nad83 13N 429456, 7558010)*											
A	6	58.6	55.9	5421	1.7	5.012	0.42977 ± 0.26	10.8320 ± 0.28	0.18280 ± 0.08	0.953237	16.6	2304.7 ± 10.1	2508.8 ± 5.1	2678.4 ± 2.8/2.8
B	8	53.6	32.5	9971	1.4	0.632	0.51872 ± 0.18	13.1158 ± 0.20	0.18338 ± 0.06	0.958597	-0.5	2693.8 ± 8.4	2688.0 ± 3.8	2683.7 ± 1.9/1.9
C	5	83.9	49.7	8579	1.6	0.557	0.51442 ± 0.08	12.9732 ± 0.11	0.18290 ± 0.05	0.914630	0.2	2675.5 ± 3.3	2677.7 ± 2.1	2679.4 ± 1.7/1.7
D	3	113.9	68.2	10380	1.1	0.581	0.51775 ± 0.25	13.0787 ± 0.27	0.18321 ± 0.06	0.977950	-0.3	2689.7 ± 11.2	2685.4 ± 5.0	2682.1 ± 1.9/1.9
E	3	110.5	65.3	13430	0.8	0.530	0.51632 ± 0.10	13.0517 ± 0.13	0.18334 ± 0.05	0.931670	0	2683.5 ± 4.5	2683.4 ± 2.4	2683.3 ± 1.7/1.7
g) LMB056 detrital zircons			*(Nad83 13N 429456, 7558010)*											
A	13	83.9	55.7	61800	0.6	1.100	0.51791 ± 0.19	13.1009 ± 0.21	0.18346 ± 0.06	0.964153	-0.3	2690.3 ± 8.4	2686.9 ± 3.9	2684.4 ± 1.8/1.8
B	6	27.3	15.7	8580	0.6	0.394	0.51620 ± 0.13	12.9898 ± 0.15	0.18251 ± 0.07	0.907404	-0.3	2683.1 ± 5.8	2678.9 ± 2.9	2675.8 ± 2.1/2.2
C	4	107.1	66.1	12550	1.1	0.763	0.51376 ± 0.08	12.9446 ± 0.12	0.18274 ± 0.05	0.916194	0.2	2672.7 ± 3.6	2675.6 ± 2.2	2677.9 ± 1.7/1.7
D	6	33.7	19.9	12500	0.5	0.539	0.51478 ± 0.15	12.9136 ± 0.17	0.18194 ± 0.08	0.897069	-0.3	2677.0 ± 6.8	2673.4 ± 3.2	2670.6 ± 2.5/2.5
E	3	45.4	26.8	5646	0.8	0.547	0.51405 ± 0.26	12.9853 ± 0.27	0.18321 ± 0.08	0.960957	0.4	2673.9 ± 11.4	2678.6 ± 5.1	2682.1 ± 2.5/2.5

[1]single grain analyses; all air abraded.

[2]U blank correction of 0.2 pg ± 20%; U fractionation corrections were measured for each run with a double $^{233-235}U$ spike.

[3]Radiogenic Pb; all raw Pb data corrected for fractionation of 0.32-0.23/amu ± 20% determined by repeated analysis of NBS-982 reference material.

[4]Measured ratio corrected for spike and Pb fractionation.

[5]Total common Pb in analysis based on blank isotopic composition: $^{206}Pb/^{204}Pb = 18.5 \pm 3\%$, $^{207}Pb/^{204}Pb = 15.8\text{-}15.5 \pm 3\%$, $^{208}Pb/^{204}Pb = 36.4 \pm 0.5\%$.

[6]Model Th/U derived from radiogenic ^{208}Pb and the $^{207}Pb/^{206}Pb$ age of fraction.

[7]Fractionation, blank and common Pb corrected; Pb procedural blanks were ~0.5-2.0 pg and U <0.2 pg. Common Pb compositions are based on Stacey-Kramers model Pb at the $^{207}Pb/^{206}Pb$ age of each fraction (Stacey and Kramers, 1975).

[8]Correlation coefficient.

[9]Discordance in % to origin.

H. Lin carried out mineral separations and provided assistance with mass spectrometry; assitance with grain selection, abrasion and in the cleanlab provided by R. Lishansky.

Table 2.2: Summary of published U/Pb geochronology

Suite Name	Rock Type	Age (Ma)	2 σ error (Ma)	Referance
Flake Lake	Rhyolite	2716.3	+3.1 / -2.6	(inheratence issues)Hebel 1999
Wolverine Lake	quartz-feldspar porphyry	2698.7	+6.1 / -3.7	(inheratence issues) Hebel 1999
Square Lake	Felsic Tuff	2690.2	+3.6 / -2.8	Hebel 1999
Square Lake	Felsic Flow	2690	+2.0 / -1.5	Hebel 1999
Windy Lake	felcis Tuff	2685.2	+2.9 / -2.5	Hebel 1999
Windy Lake	lapilli tuff	2685.8	+2.9 / -1.5	Hebel 1999
Son Volt	lapilli tuff	2685.6	+1.8 / -1.6	Hebel 1999
Windy Lake	quartz-feldspar porphyry	2685.1	+3.2 / -2.0	Hebel 1999
Koignuk	quartz-feldspar porphyry	2677.9	+5.8 / -1.4	Hebel 1999
Koignuk	Fesic Flow	2677.4	+1.9 / -1.5	Hebel 1999
Koignuk	Fesic Flow	2677.2	+2.5 / -1.1	Hebel 1999
Koignuk	Fesic Tuff	2677.6	+1.9 / -1.9	Hebel 1999
Clover Lake	Rhyolite	2662.7	+3.4 / -2.8	Hebel 1999
Sandusky	Diorite	2663.2	+15.1 / -10.1	Hebel 1999
Sandusky	Diorite	2662.4	+18.7 / -13.1	Hebel 1999
Group I	Foliated Gniess	2649.5	+2.9 / -2.5	Hebel 1999
Hope Bay	Granitoid clast	2701.1	+4.6 / -3.8	Hebel 1999
Hope Bay	Granitoid clast	2685.9	+2.4 / -2.3	Hebel 1999
Hope Bay	sandstone	2647.2	+2.8 / -2.8	Hebel 1999
Wilco	sandstone	2675	+3.0 / -3.0	Hebel 1999
Windy Lake	Foliated Quartz porphyry	2685	+4 / -2	Bevier and Gebert 1991
Koignuk River	feldspar porphyry	2677	+3 / -1	Bevier and Gebert 1991
Group II	hornblende granodiorite	2672	+3 / -1	Bevier and Gebert 1991
Group III	hornblende-biotite granite	2608	+5 / -5	Bevier and Gebert 1991
n/a	Granitic pegmatite	1910	+1.7 / -1.7	Bevier and Gebert 1991
Hope Bay	conglomerate	2715	+7 / -7	Padgham 1996 (no error from author)
Square Lake	volcaniclastic	2689.4	+4 / -3.6	Sherlock unpublished data 1998
QSP	dacite	2681.5	+4.9 / -4.9	Sherlock unpublished data 1999
Windy Lake	dacite	2683.4	+2.1 / -2.1	Sherlock unpublished data 2000
Wolverine Lake	quartz-feldspar porphyry	2686	+3.6 / -3.6	Sherlock unpublished data 2001

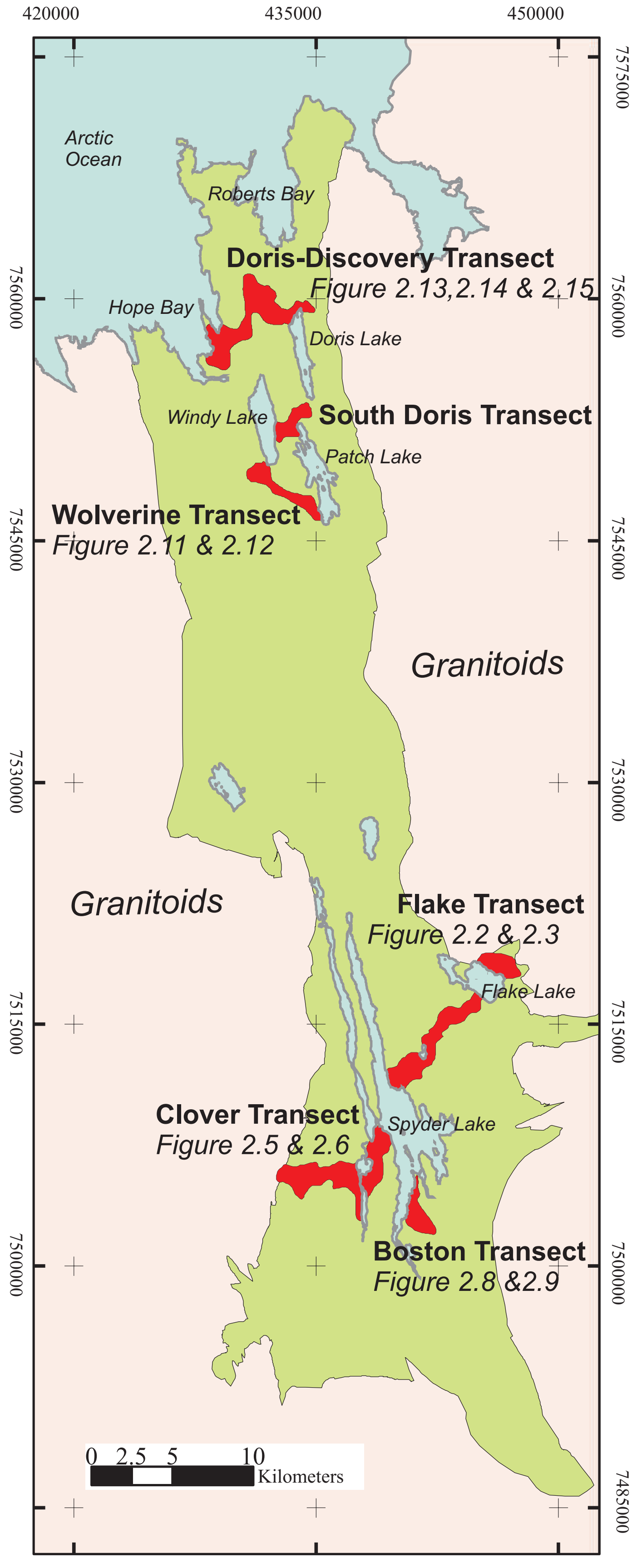

Figure 2.1: The Hope Bay Greenstone Belt with six transects mapped in this study outlined in red

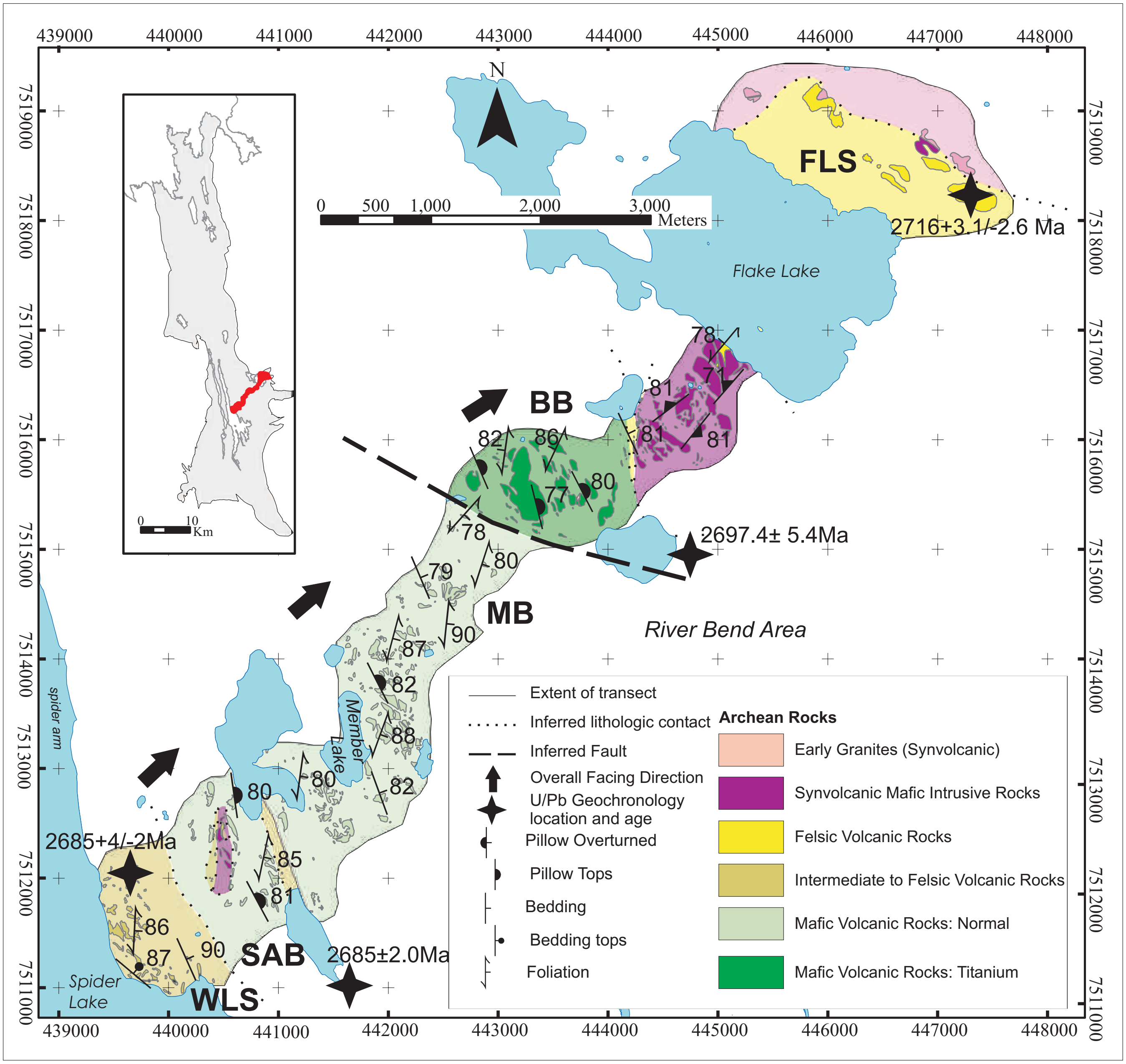

Figure 2.2 : Geology of the Flake Lake transect showing the distribution of rock types. The rocks are divided into suites based on field relationships and chemical composition. Suites: FLS: Flake Lake Felsic Suite, BB: Bend Basalt Suite, MB: Member Basalt Suite, SAB: Spider Arm Basalt Suite, WLS Windy Lake Felsic Suite. Inset map: Outline of the Hope Bay Greenstone Belt with mapped transect outlined in red

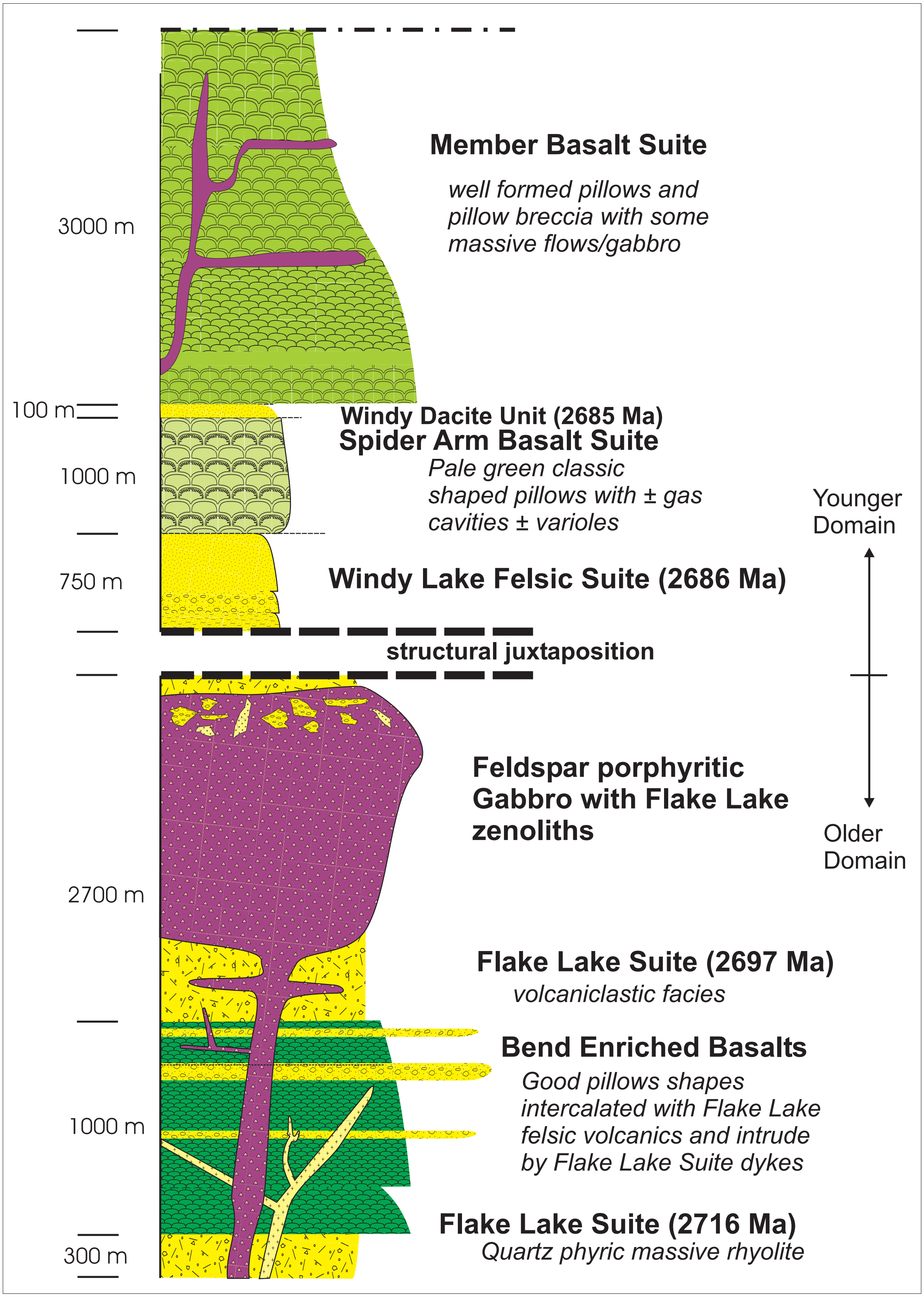

Figure 2.3 Reconstructed stratigraphic column for the Flake Lake Transect, suites are presented in proper stratigraphic order. Width of column does not represent clast or pillow size but instead is used to easily distinguish different packages for rocks.

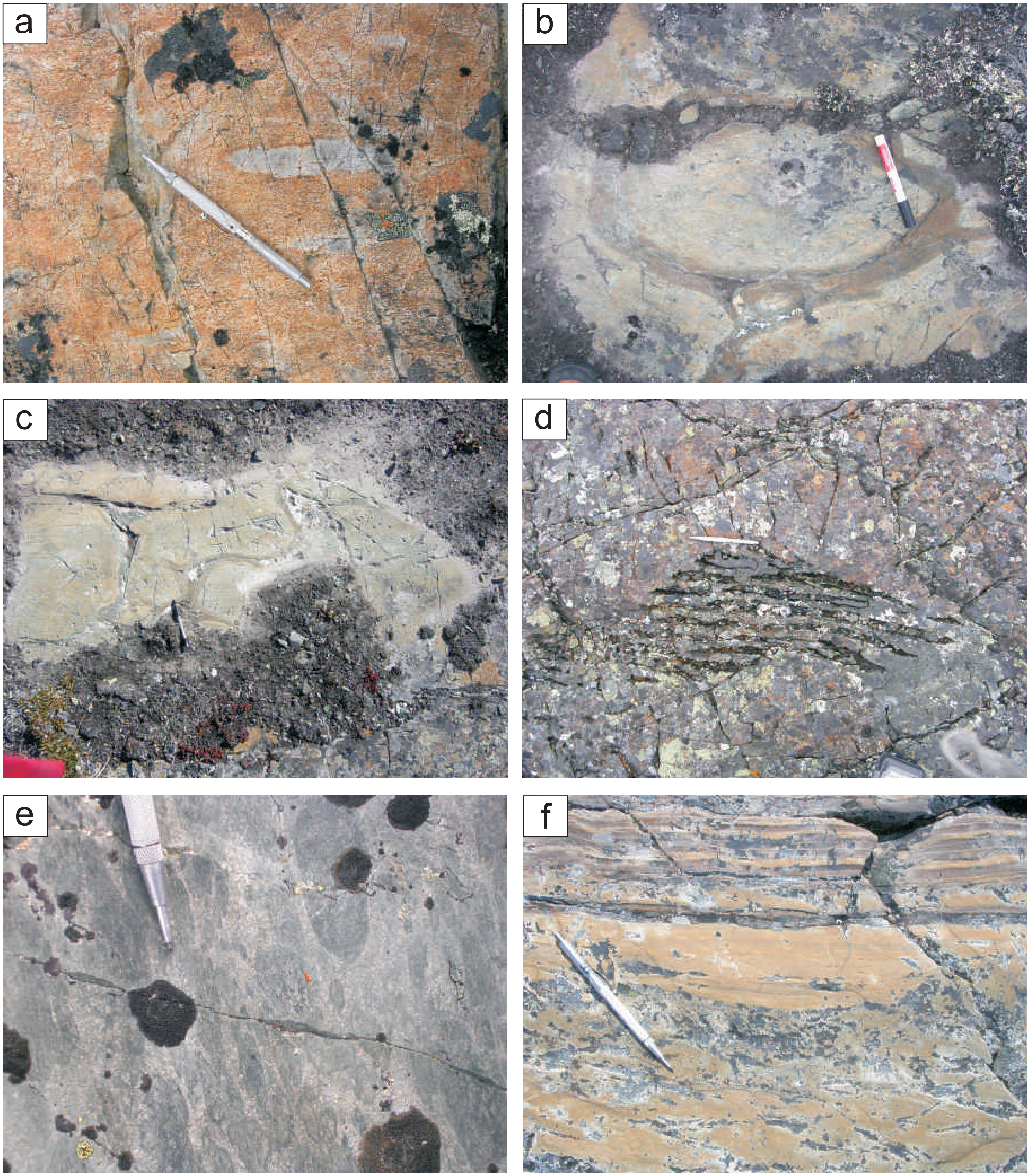

Figure 2.4 **a)** Field photograph of volcaniclastic rhyolite from the Flake Lake Suite, silica rich clast (light grey) in crystal (light grey) and ash (brown) matrix **b)** Field photograph of pillow from the Bend Basalt Suite, with 3cm dark brown pillow selvage **c)** Field photograph of vesicular-amygdaloidal and plagioclase porphyritic pillow basalt with ~1.5cm brown pillow selvage from Member Basalt Suite **d)** Field photograph of numerous gas cavities in pillow basalt from the Spider Arm Basalt Suite, pillow shapes obscured by lichen **e)** Field photograph of monomictic volcanic conglomerate with immature sand matrix, this facies is part of Windy Lake Felsic Suite **f)** Field photograph of well bedded siltstone showing crossbedding and flame structures, this is part of the sedimentary facies of the Windy Lake Felsic Suite (scribe for scale, length 15cm)

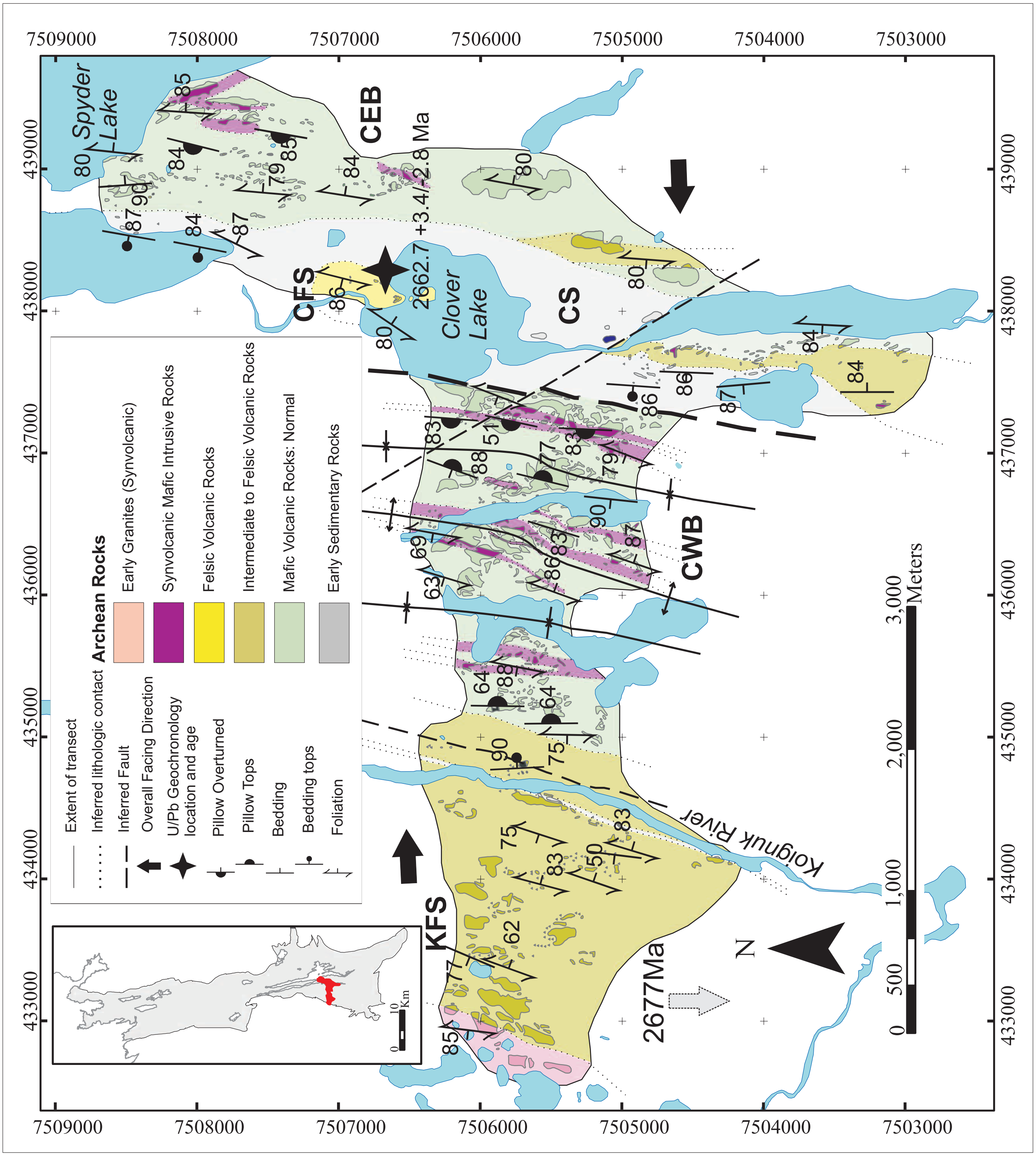

Figure 2.5: Geology of the Clover transect showing the distribution of rock types. The rocks are divided into suites based on field relationships and chemical composition. Suites: CEB: Clover East Basalt Suite, CS: Clover Sedimentary Suite, CFS Clover Felsic Suite, CWB: Clover West Basalt Suite, KFS: Koignuk Felsic Suite Inset map: Outline of the Hope Bay Greenstone Belt with transect outlined in red

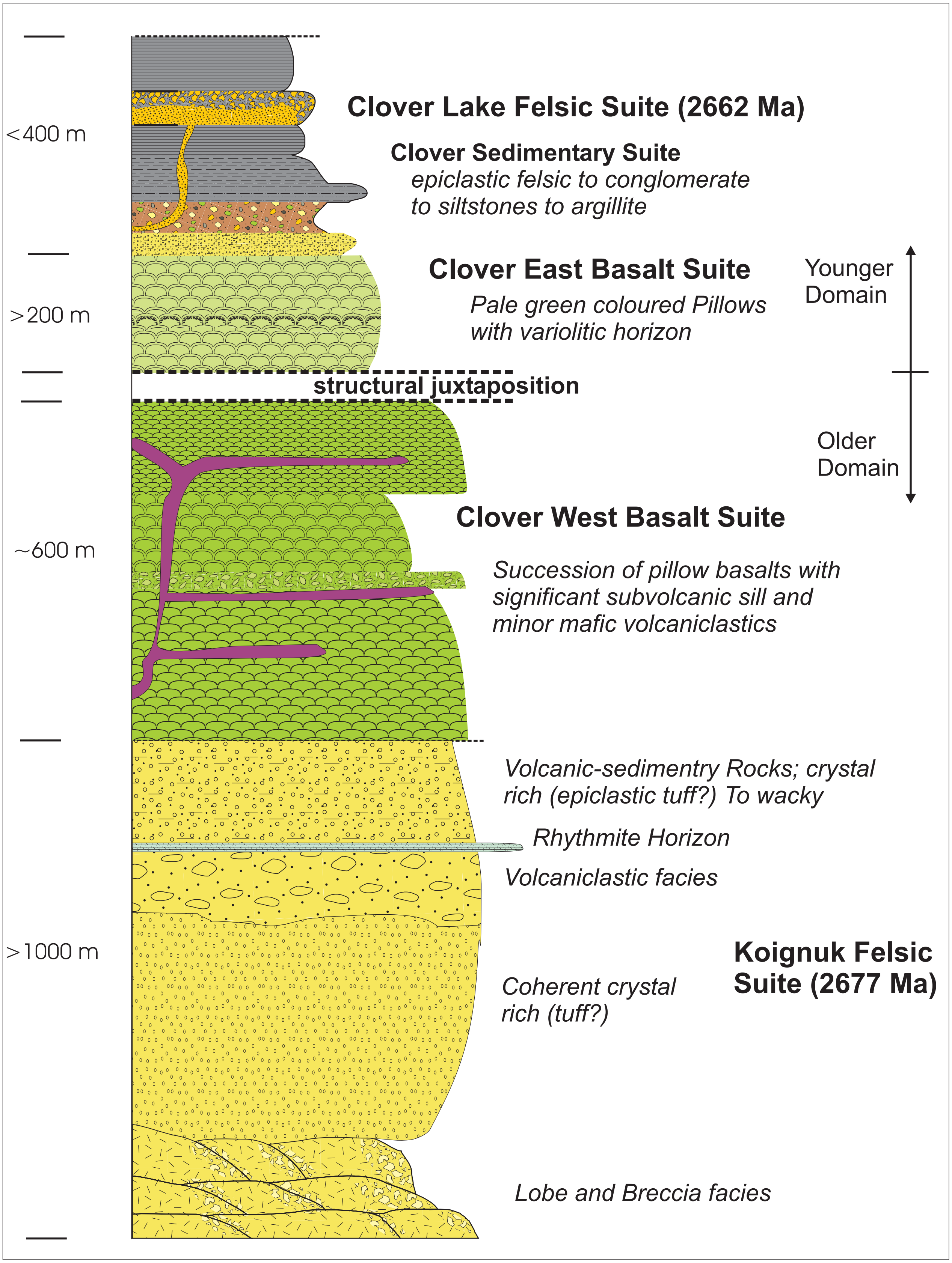

Figure 2.6 Reconstructed stratigraphic column for the Clover Transect. Width of column does not represent clast or pillow size but instead is used to easily distinguish different packages for rocks.

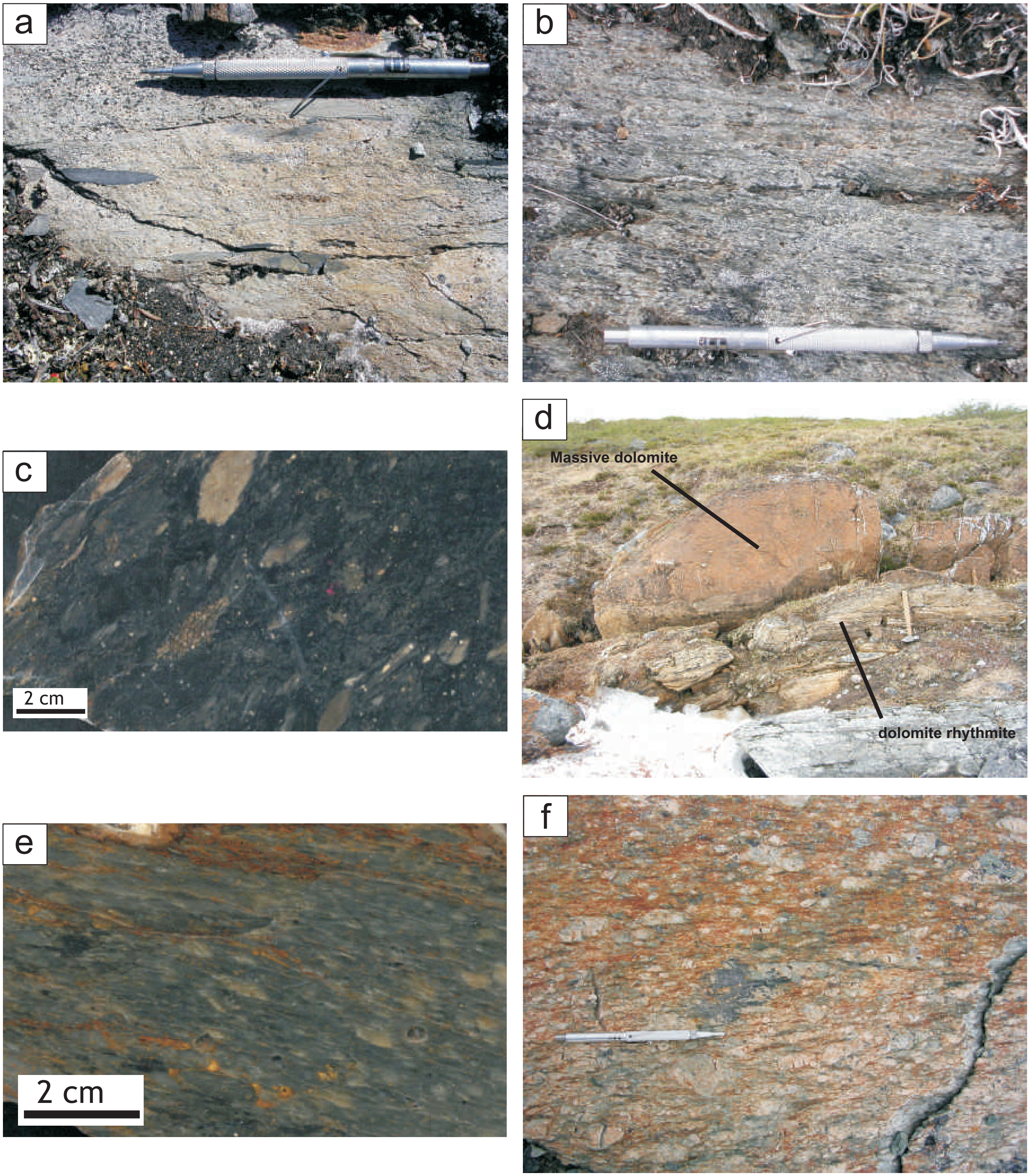

Figure 2.7 **a)** Field photograph of conglomerate with mostly sedimentary clasts in a immature sand matrix, from the Clover Sedimentary Suite **b)** Field photograph of a epiclastic volcaniclastic rock at the base of the Clover Sedimentary Suite **c)** Polished slab photograph of black matrix breccia, rhyolite clasts (porphyritic and choheent) in a black argillite matrix, from the Clover Felsic Suite, **d)** Field photograph of a massive dolomite bed and thinly bedded dolomite rhythmite of the to of the Koignuk Felsic Suite **e)** Polished slab photograph of the crystal tuff facies from the Koignuk Felsic Suite **f)** Field photograph of lapilli tuff from the Koignuk Felsic Suite (scribe for scale, length 15cm)

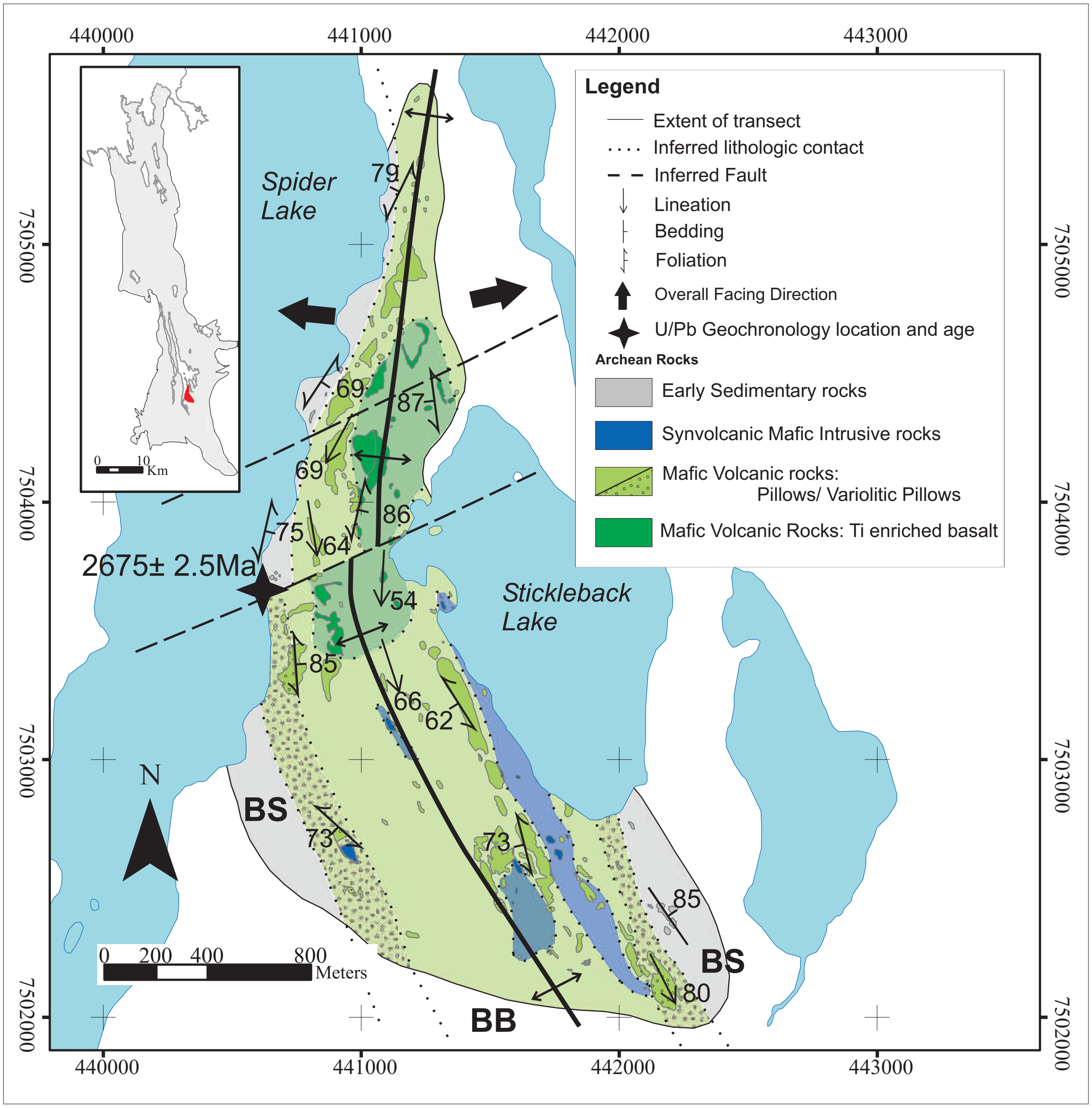

Figure 2.8: Geology of the Boston Area showing the distribution of rock types. The rocks are divided into suites based on field relationships and chemical composition.
Suites: BS Boston Sedimentary Suite, BB Boston Basalt Suite, which includes non-variolitic, variolitic and Ti-enriched basalts Inset map: Outline of the Hope Bay Greenstone Belt with transect in red

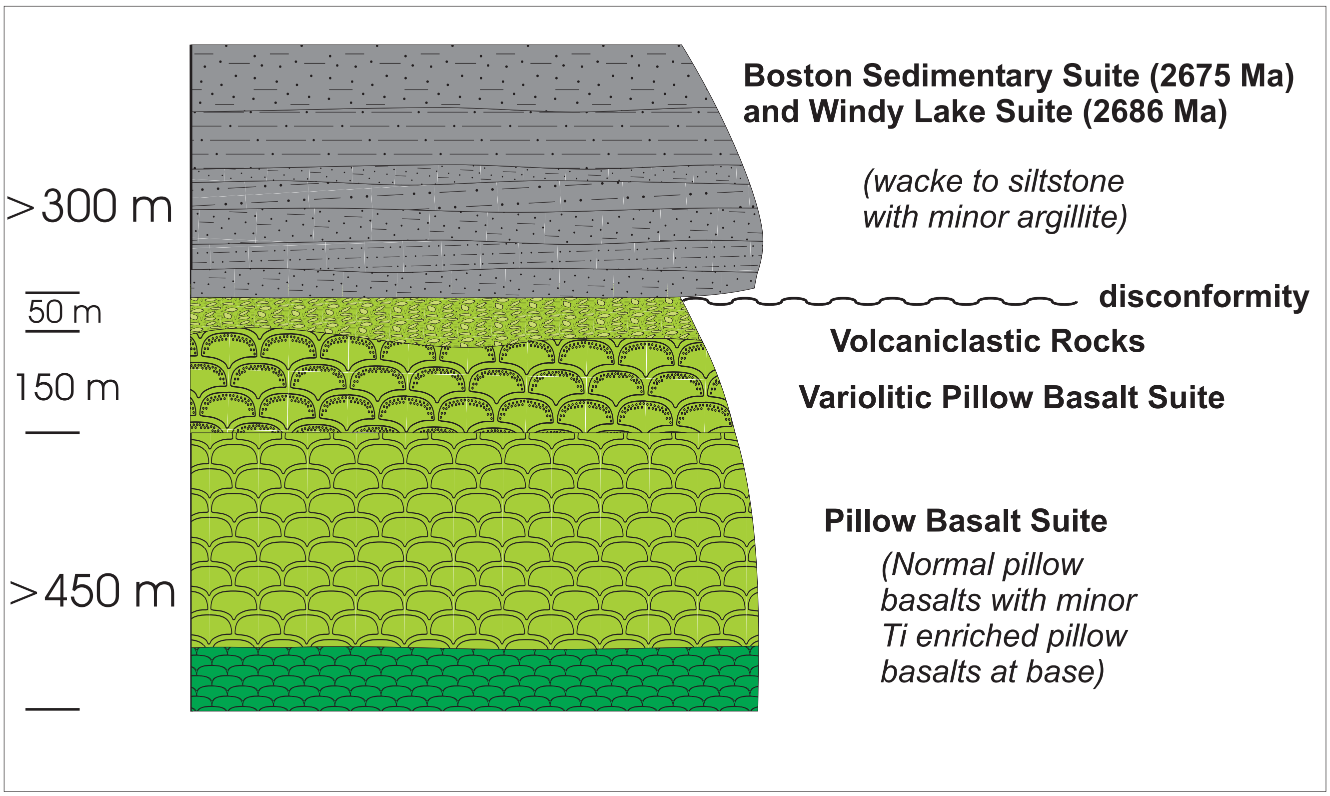

Figure 2.9: Reconstructed stratigraphic column for the Boston Area. Width of column does not represent clast or pillow size but instead is used to easily distinguish different packages for rocks.

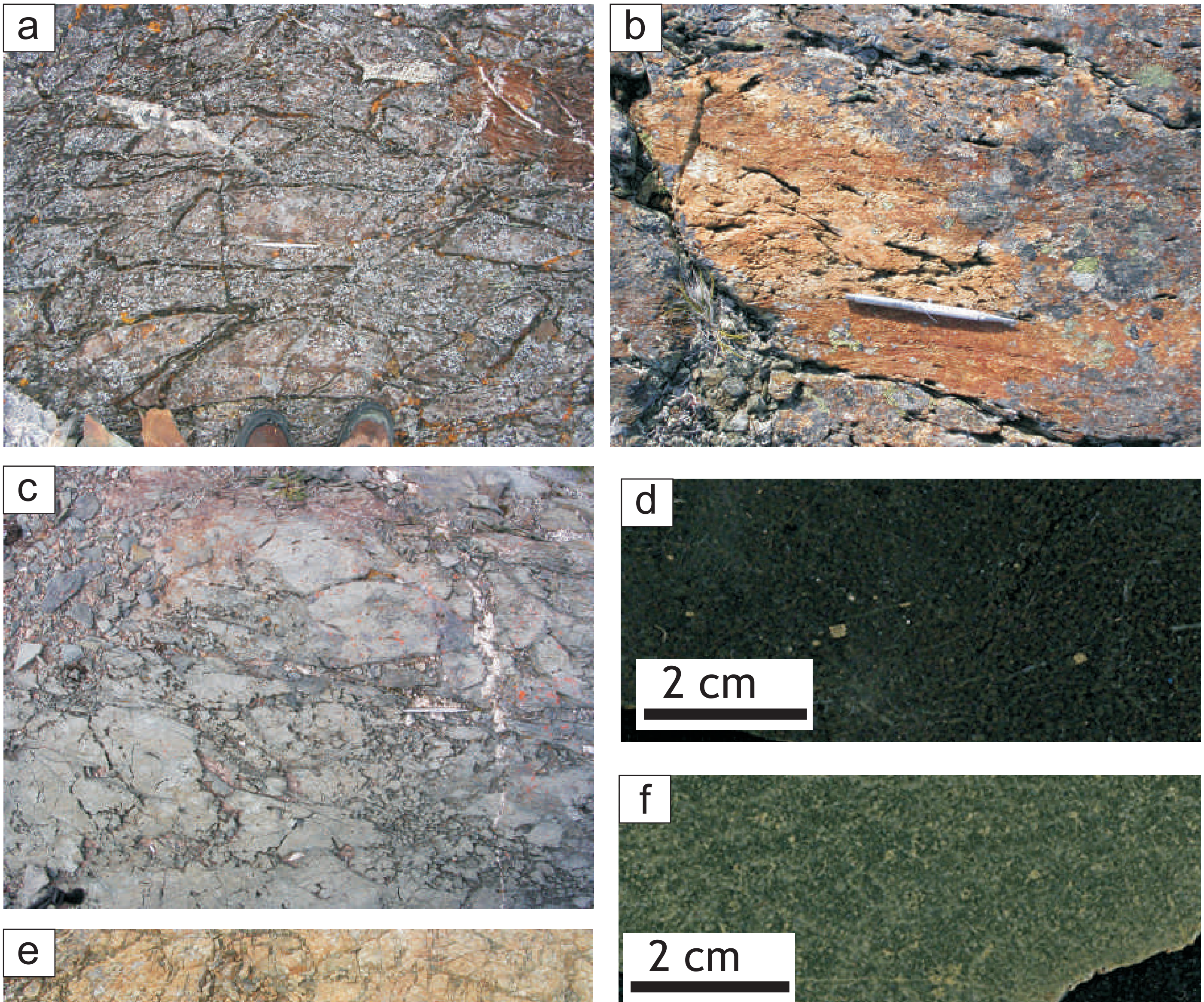

Figure 2.10 **a)** Field photograph of highly altered pillow basalts from the Boston Basalt Suite **b)** Field photograph variolitic pillow basalt from the Boston area, light brown coalesced varioles at center of pillow **c)** Field photograph of pillowed Ti basalt from the Doris Basalt Suite **d)** picture of polished slab of Doris Basalt Suite **e)** Field photograph of Mesa Basalt Suite, **f)** Picture of polished slab of Mesa Basalt Suite (scribe for scale, length 15cm)

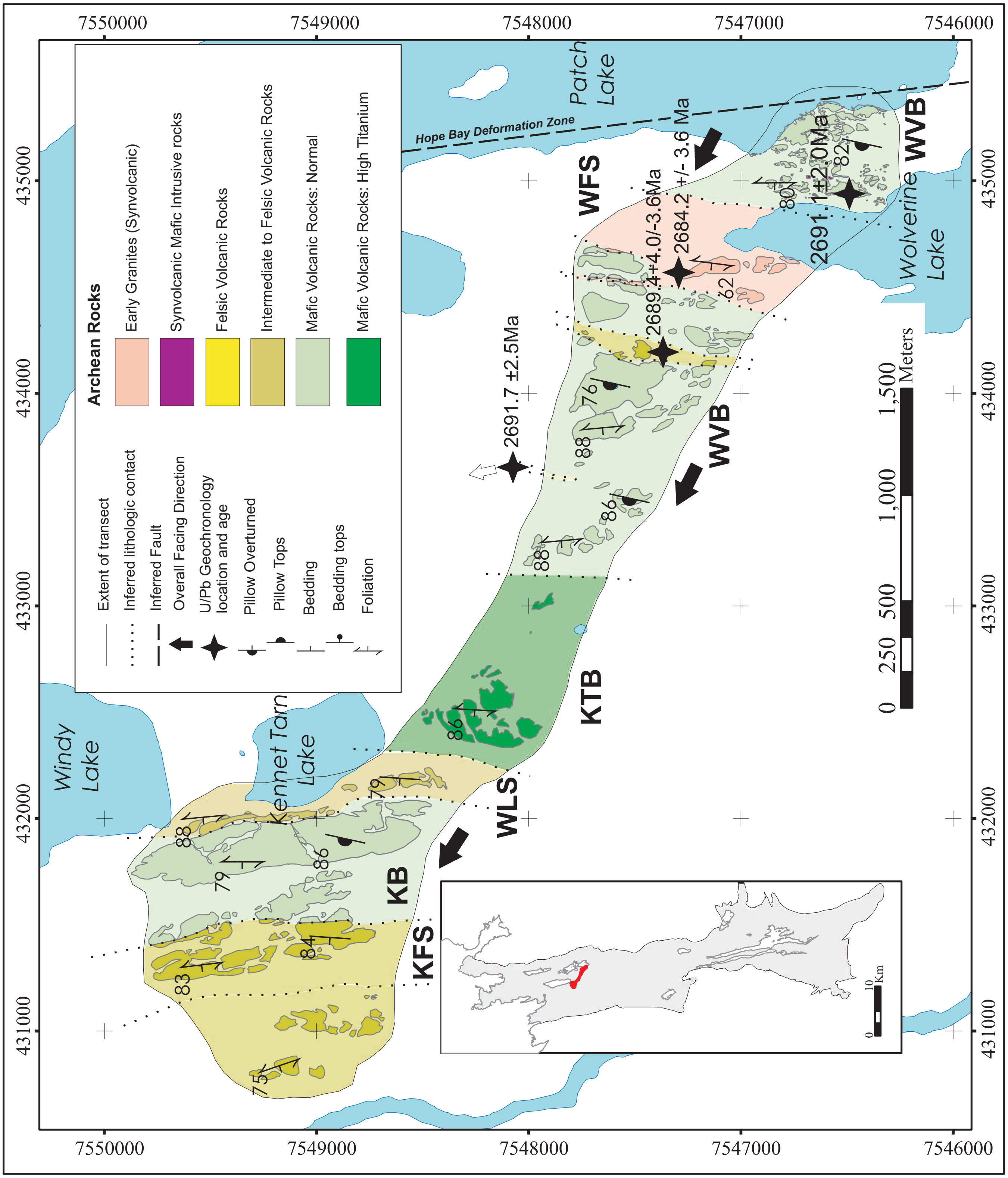

Figure 2.11: Geology of the Wolverine Transect showing the distribution of rock types. The rocks are divided into suites based on field relationships and chemical composition.
Suites: WVB Wolverine Basalts, WFS Wolverine Felsic Suite, KTB Kennet Tarn Basalts, WLS Windy Lake Felsic Suite, KB Koig Basalts, KFS Koignuk Felsic Suite,
Inset map: Outline of the Hope Bay Greenstone Belt with transect outlined in red

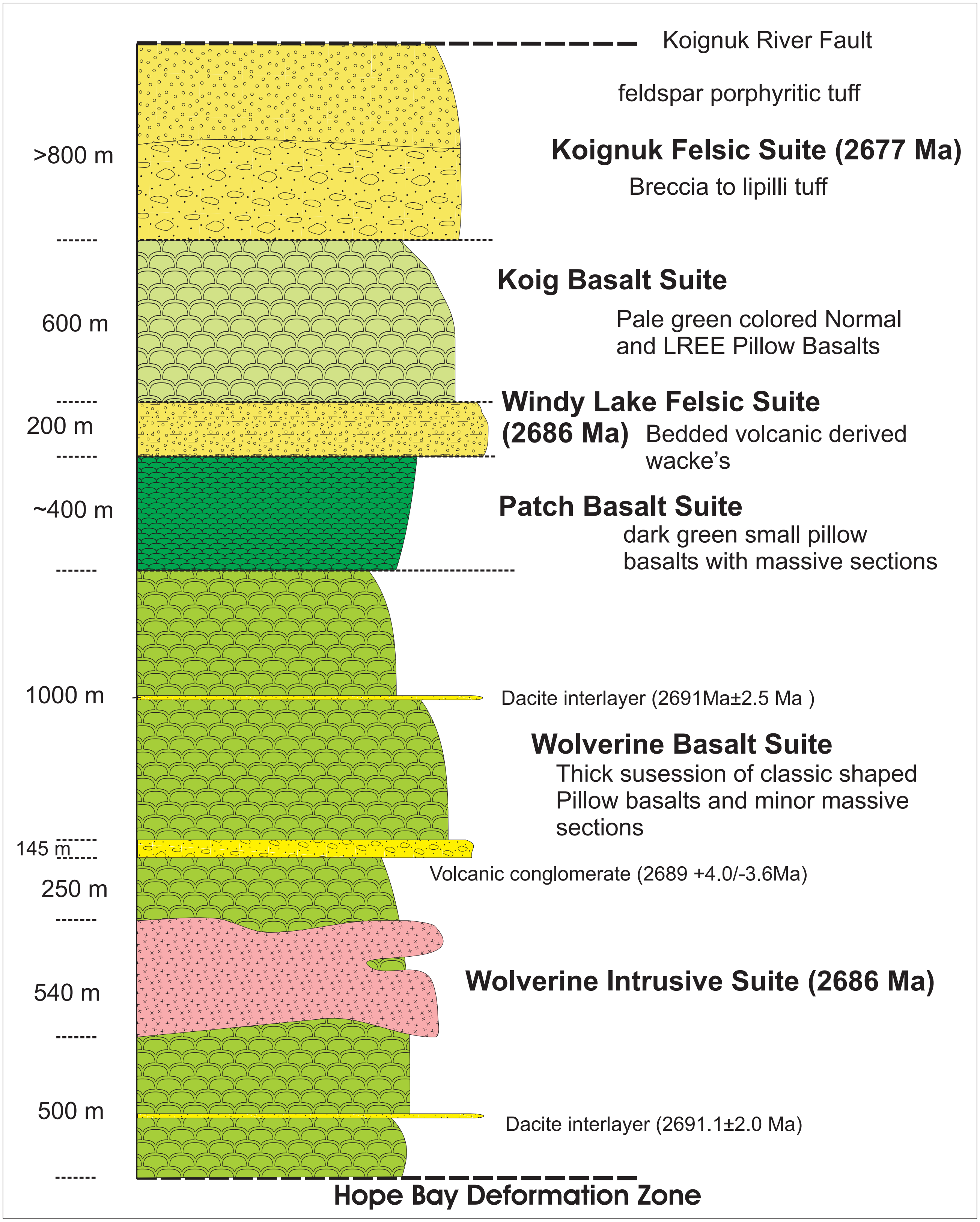

Figure 2.12 Stratigraphic column for the Wolverine Transect. Width of column does not represent clast or pillow size but instead is used to easily distinguish different packages for rocks.

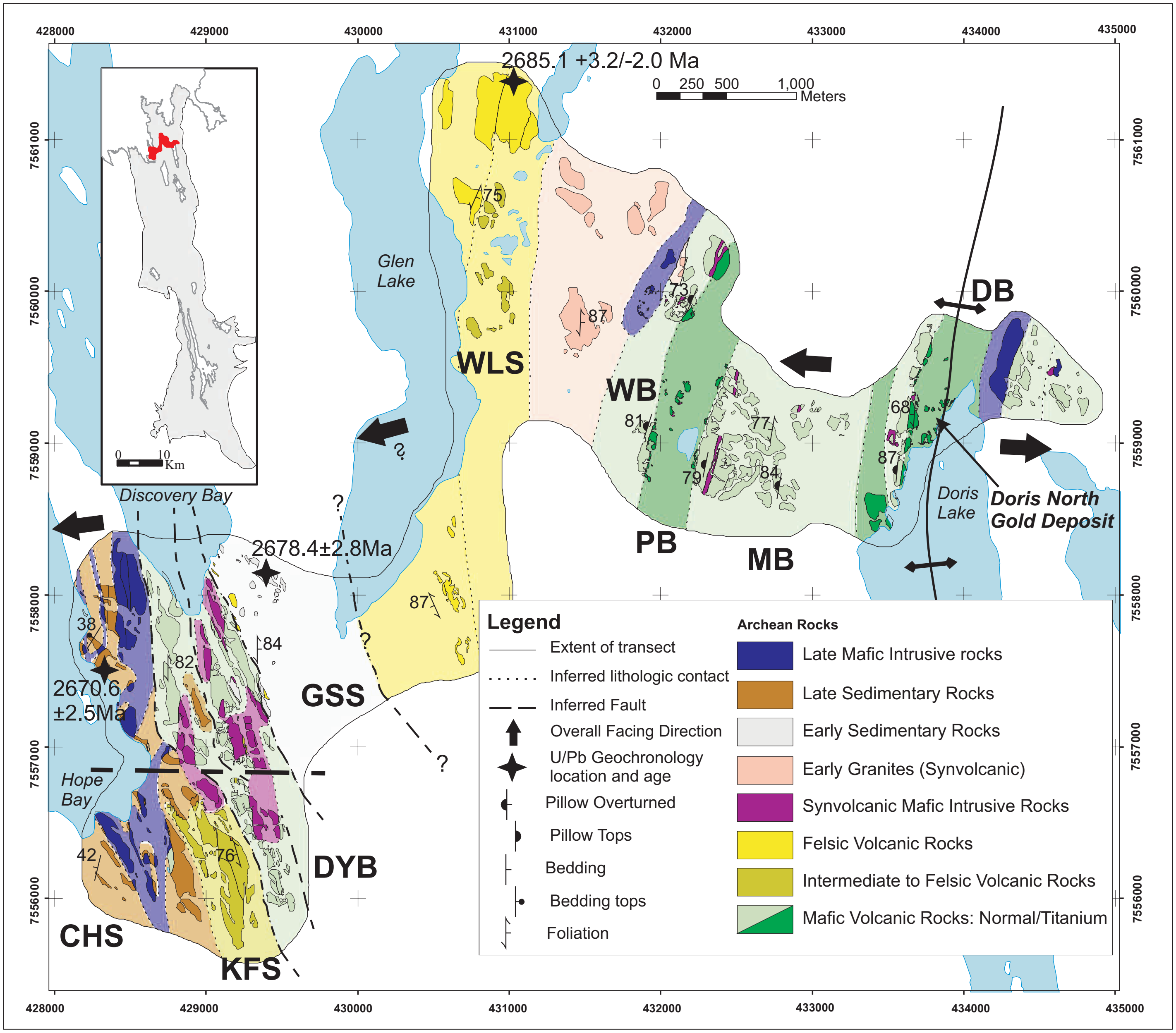

Figure 2.13: Geology of the Doris-Discovery Transect showing the distribution of rock types. The rocks are divided into suites based on field relationships and chemical composition. Suites: DB Doris Basalt Suite, MB Mesa Basalt Suite, PB Patch Basalt Suite, WB Windy Basalt Suite, WLS Windy Lake Felsic Suite, DYB Discovery Basalt Suite, GSS Glen Lake Sedimentary Suite, CHS Conglomerate Hill Sedimentary Suite, KFS Koignuk Felsic Suite

Inset map: Outline of the Hope Bay Greenstone Belt with transect in red

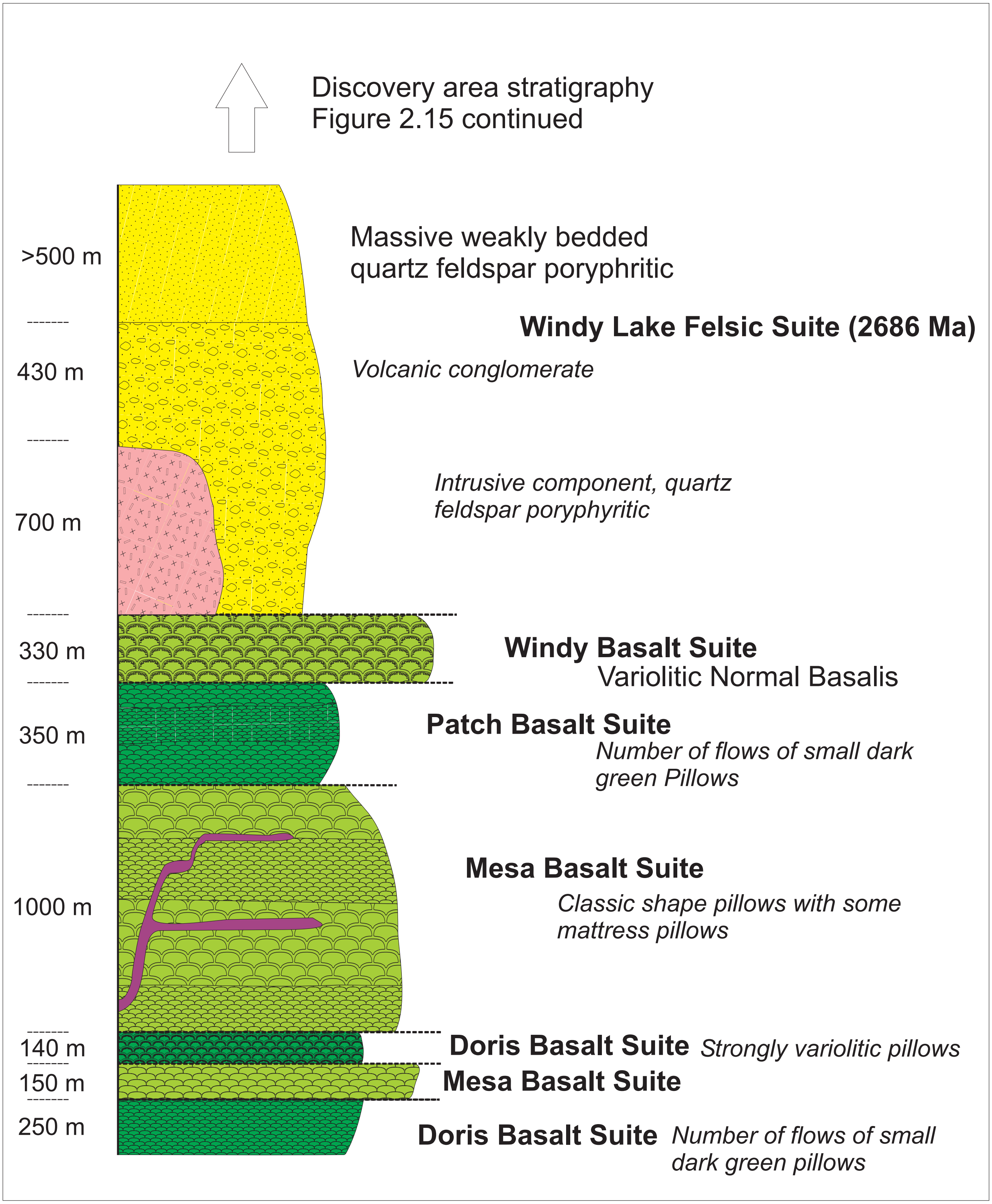

Figure 2.14 Stratigraphic column for the Doris-Discovery Transect. Width of column does not represent clast or pillow size but instead is used to easily distinguish different packages for rocks.

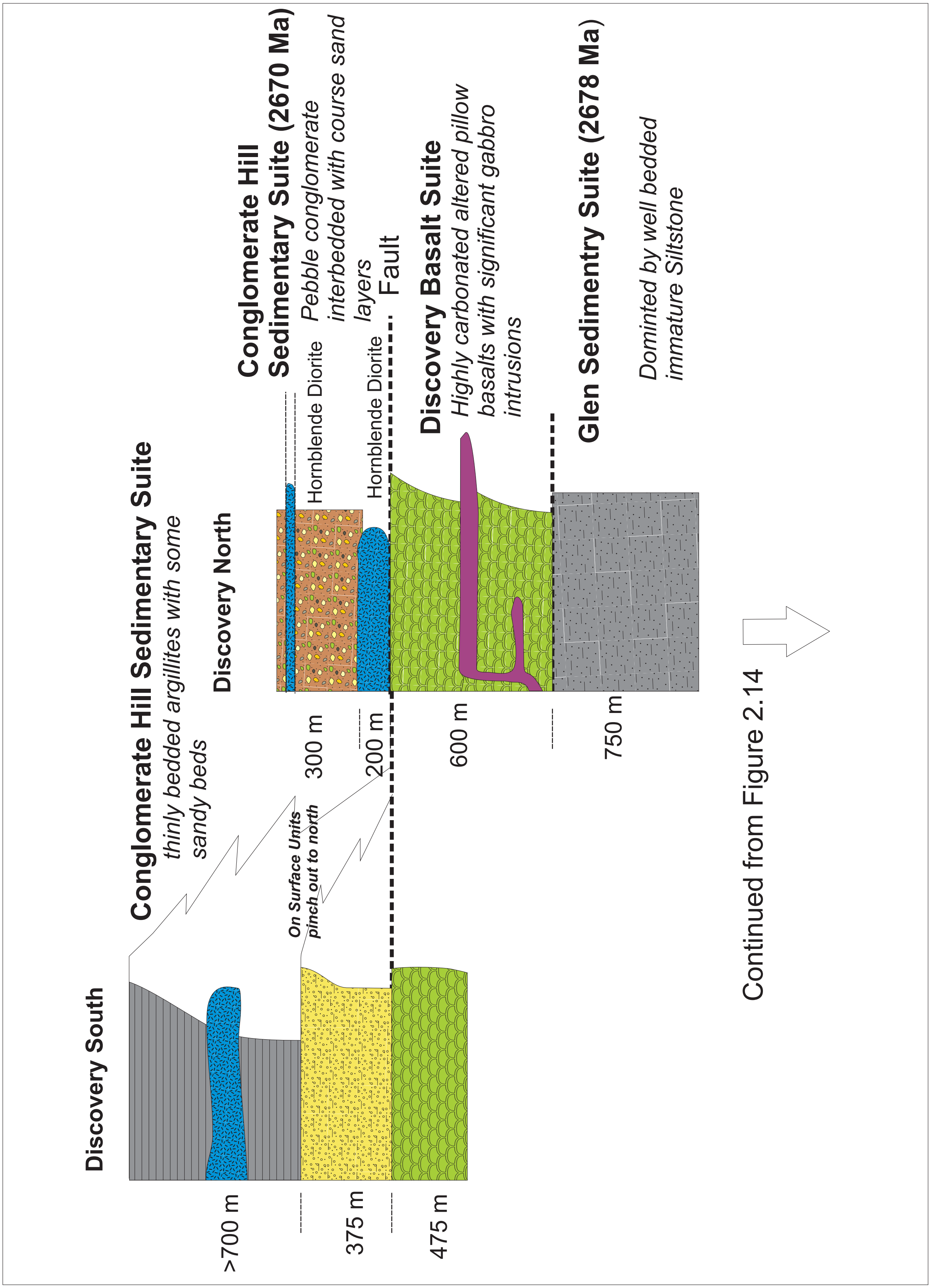

Figure 2.15 Stratigraphic column for the Doris-Discovery Transect. Width of column does not represent clast or pillow size but instead is used to easily distinguish different packages for rocks.

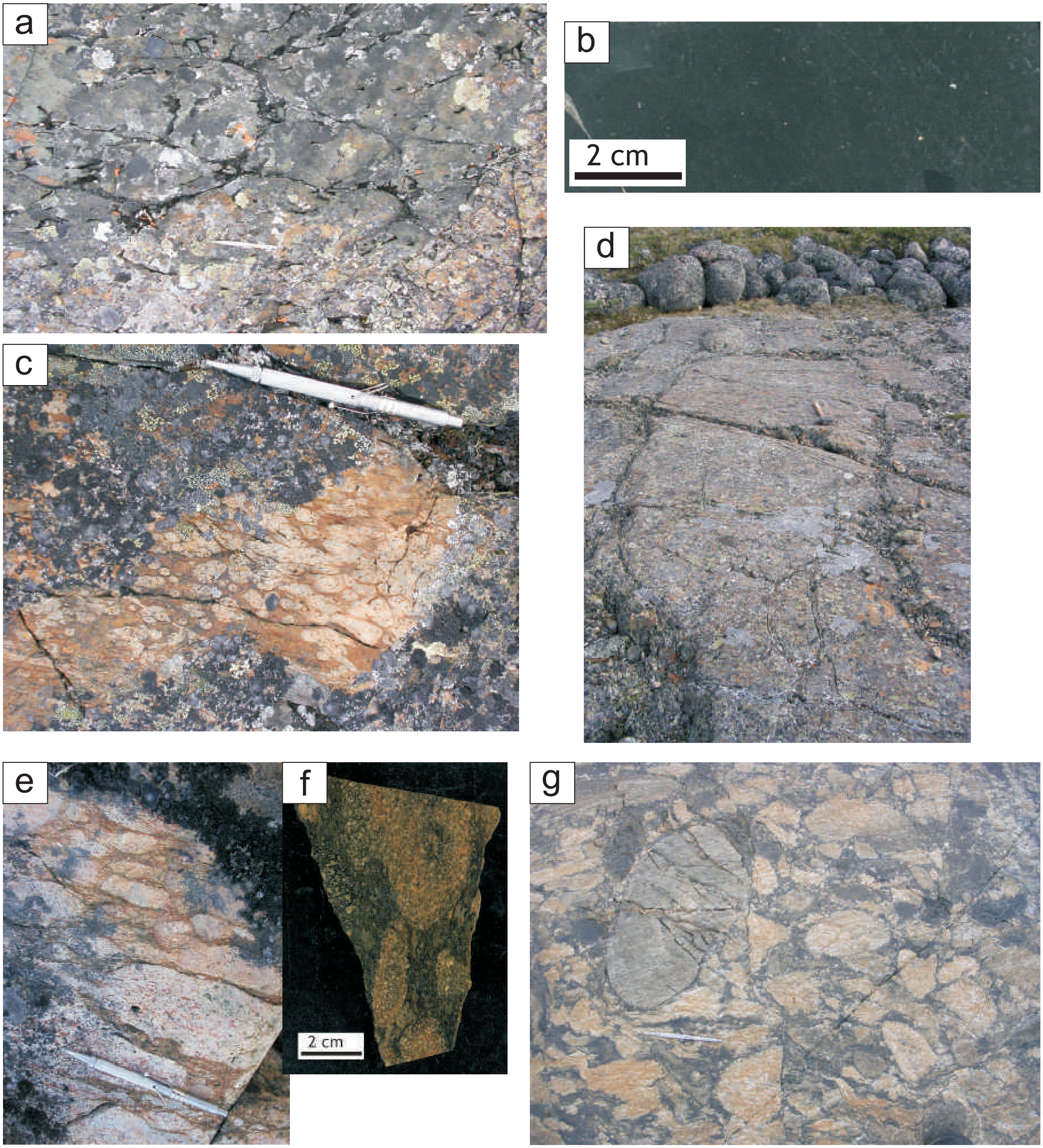

Figure 2.16 **a)** Field photograph of Ti pillow basalt of the Patch Basalt Suite **b)** Photograph of Ti basalts of the Patch Basalt Suite **c)** Field photograph varioles from Windy Basalt Suite **d)** Field photograph of mega pillow in the Mesa Basalt Suite **e)** Field photograph volcanic conglomerate of the Windy Lake Felsic Suite **f)** Photography of the volcanic conglomerate of the Windy Lake Felsic Suite **g)** Field photograph of pillowed Ti Basalt from the Doris Basalt Suite inset picture of polished slab of Doris Basalt Suite (scribe for scale, length 15cm)

Figure 2.18 Locations of U/Pb geochronology samples, Bold ages from this study (geology from Miramar Hope Bay compilation, 2003, Dating: Bevier and Gebert 1991; Hebel 1999; R. Sherlock, pers comm, 2001)

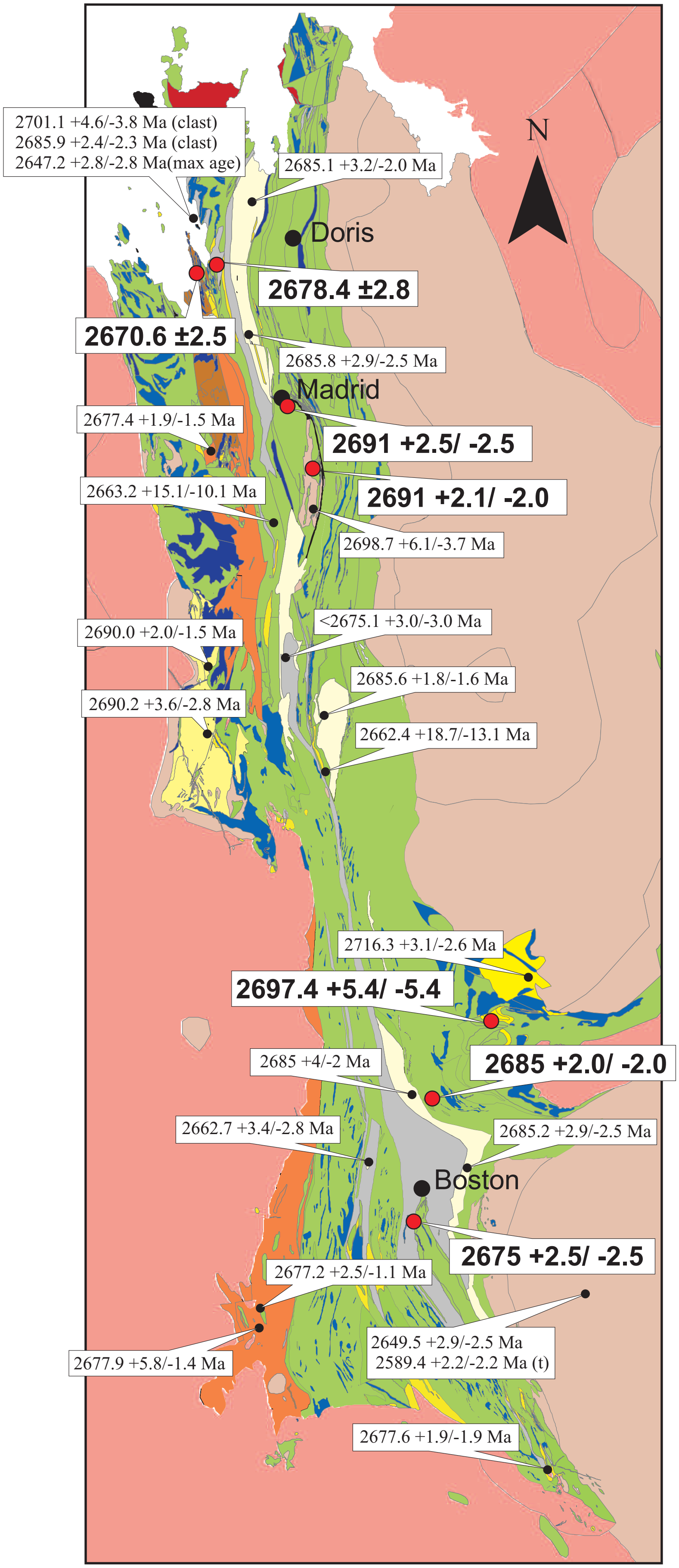

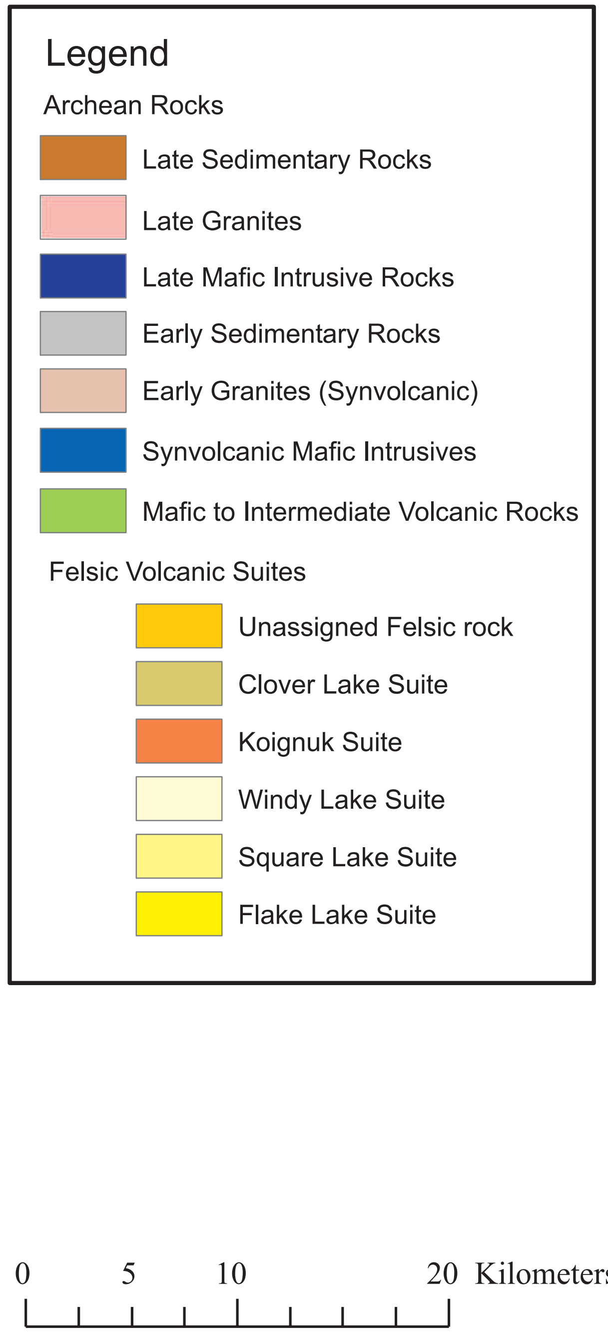

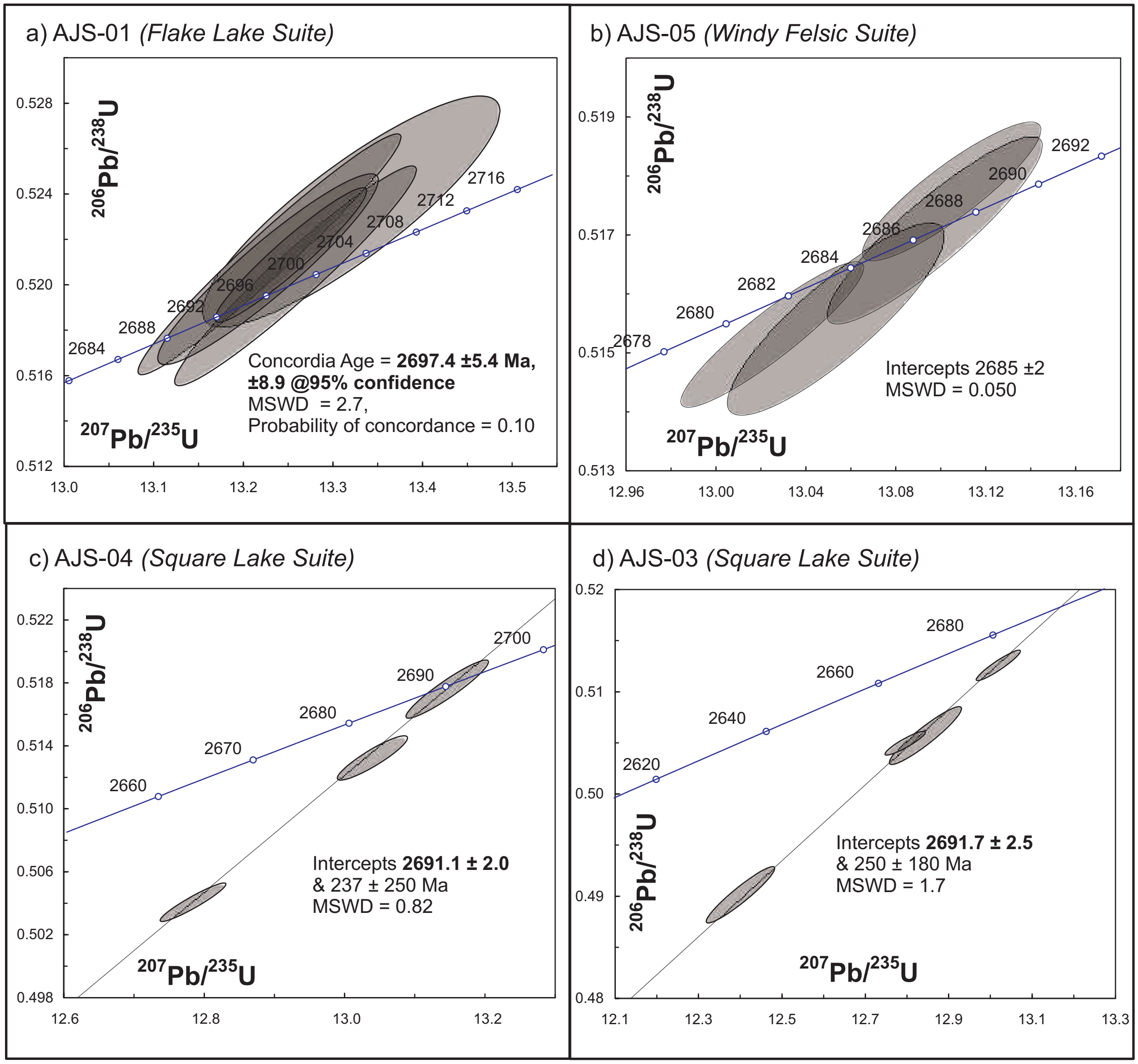

Figure 2.17 U/Pb concordia diagrams from volcanic rocks of the Hope Bay Greenstone belt

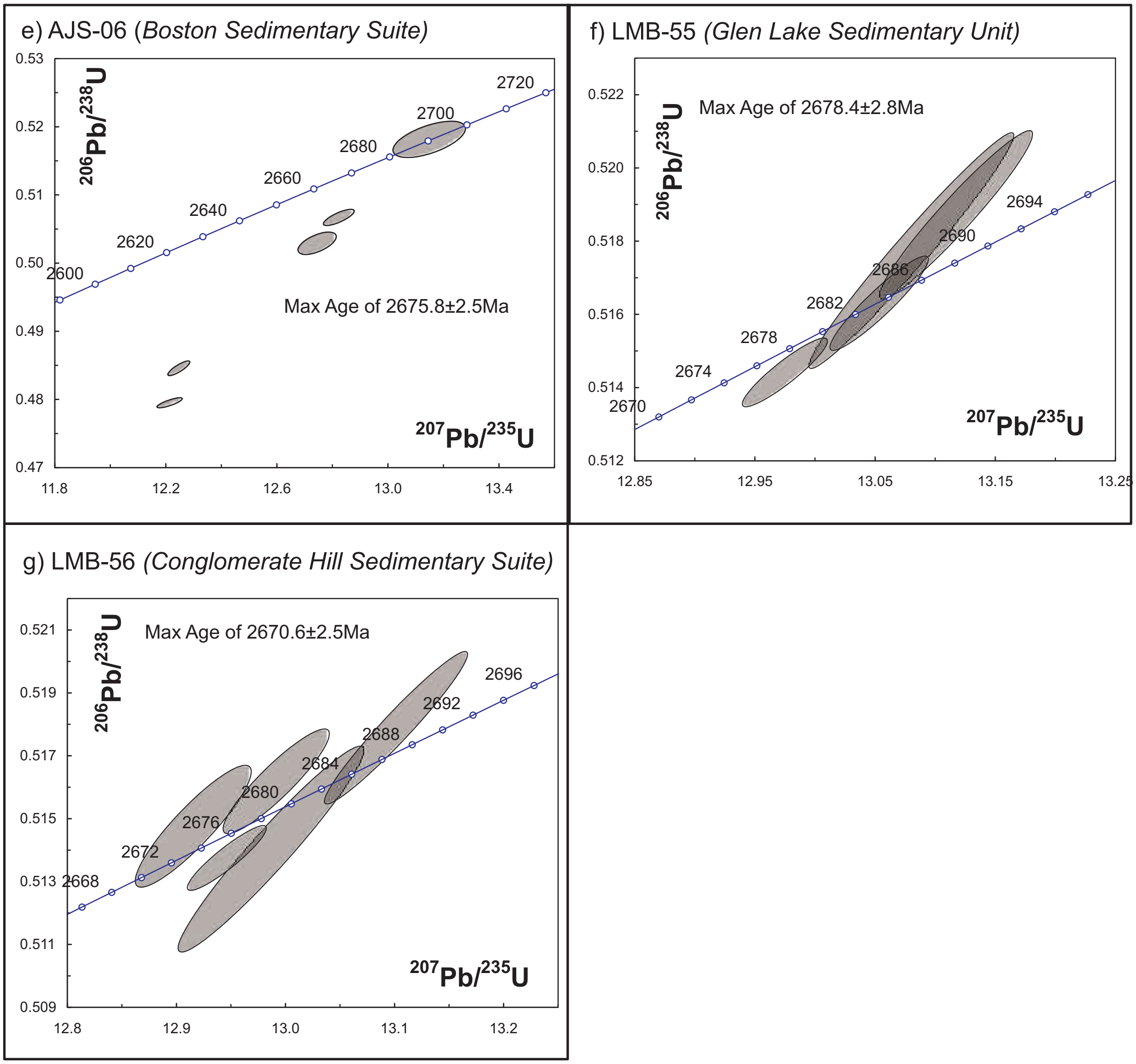

Figure 2.17 continued U/Pb concordia diagrams from sedimentary rocks of the Hope Bay Greenstone belt

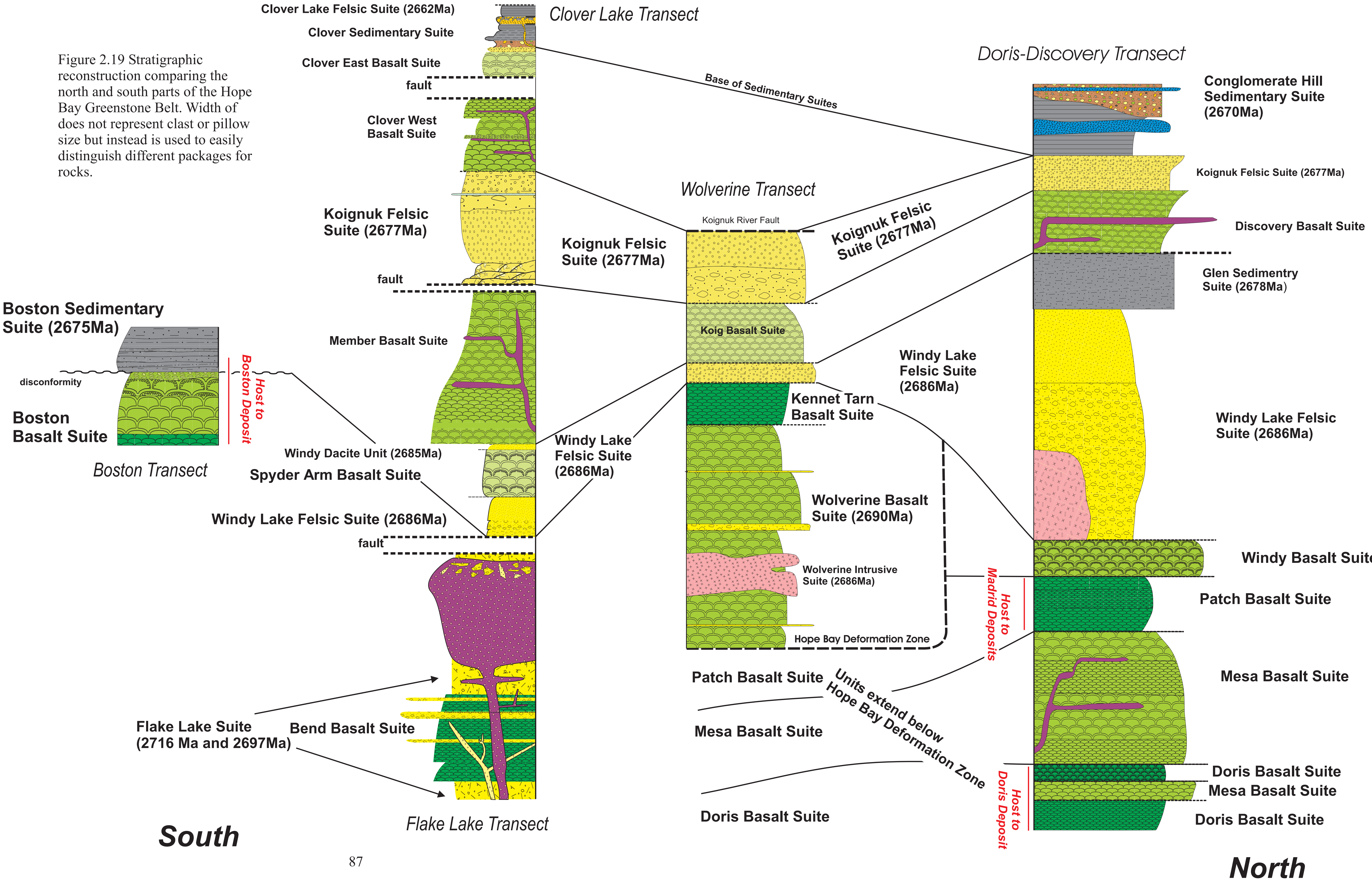

Figure 2.19 Stratigraphic reconstruction comparing the north and south parts of the Hope Bay Greenstone Belt. Width of does not represent clast or pillow size but instead is used to easily distinguish different packages for rocks.

CHAPTER 3

Geochemical Evolution of the Hope Bay Greenstone Belt

3.1 Introduction and Methodology

The late Archean Hope Bay Greenstone Belt is made up of a number of packages of mafic, felsic and sedimentary rocks. There is a gap in the understanding between the large amount of data from the deposits and the widely spaced geochemical sampling throughout the rest of the belt. The result of this study's well constrained sampling through the five transects, outlined in Chapter 2, will allow the results of regional and deposit geochemical sampling to be placed in a better context. Deriving a chemostratigraphic framework will aid in the understanding of the geochemical evolution of the Hope Bay Greenstone Belt. The correct geochemical characterization of rock groups will then allow a petrologic model of the belt to be created. Geochemical characterization of mafic volcanic rocks is particularly important since the three gold deposits in the Hope Bay Greenstone Belt are hosted in mafic volcanic rocks. Locally, a connection between basalts enriched in Ti and gold deposits has long been known in the Hope Bay Greenstone Belt (eg., Sherlock et al. 2002) but the hypothesis has not been tested on a regional scale. The regional distribution of these basalts enriched in Ti thus has geodynamic and economic implications.

A lithogeochemical study was undertaken to characterize the lithologic units within the Hope Bay Greenstone Belt. Samples were collected from a wide range of rock types including intrusive and extrusive rocks with compositions ranging from ultramafic to felsic. At least two samples were collected from each stratigraphic suite in the study area; in many cases in excess of four samples were taken. All rocks in the study area have been metamorphosed to various degrees with the majority metamorphosed to low greenschist grade. Areas of low strain were preferentially sampled and primary volcanic features, such as pillows or volcanic clasts, were usually visible. Localized high strain (shear zones) and hydrothermal alteration (carbonitization, sericitization, albitisation, silicification) were avoided. Sampling of felsic rocks included coherent flow and pyroclastic material although, in some cases, resedimented syn-eruptive volcaniclastic material was sampled and is believed to closely represent volcanic chemistry. Mafic volcanic rock samples were taken from the core of pillows avoiding pillow selvages and pillow breccias due to their susceptibility to alteration. Some areas of alteration are impossible to avoid, in particular rocks of the Discovery Basalt Suite or Patch Basalt Suite as these lithologic units are preferentially pervasively hydrothermally altered. To minimize effects of metamorphism and alteration immobile elements, identified in other studies, will be relied upon to compare rock groups. Condie (1976) identified a number of elements as not being affected by seafloor alteration and low grade metamorphism; these elements include Ti, Y, Zr, Zn, Cr, V, Sr, Sc, Hf, Co, Nb, Ni and REE's. These are the elements that will be focused on in the geochemical discrimination in this chapter.

3.2 Lithogeochemistry

3.2.1 Analytical Methods

A total of one hundred and five lithogeochemical samples were taken in the field and sent directly to ALS Chemex in North Vancouver. Samples were crushed and pulverized using carbon steel to a size of better than 95% of less than 106 micron in size. Major elements were determined by X-ray fluorescence (XRF) and L.O.I. was determined by weight loss during the fusion of the disk. An additional 38 elements were determined using Inductively Coupled Plasma - Mass Spectroscopy (ICP - MS) using a lithium metaborate fused disk. Additional geochemical and isotopic characterisation of some of the original lithogeochemical samples is presented in section 3.3. In addition to field screen, discussed above, these samples were geochemical screened to determine the lowest degrees of alteration. These 'least altered' samples were selected to represent each volcanic suite encountered. In addition to ALS Chemex quality controls, which were within acceptable values, internal standards were included with the sample shipments and the results are presented in Appendix C. In addition to quality control conducted at ALS Chemex, a subset of samples, mentioned above, was analyzed at the Pacific Center for Isotopic and Geochemical Research (PCIGR), the results of this along with a discussion can be found in Appendix C.

3.2.2 General Chemical Classification

The rocks in the Hope Bay Greenstone Belt range in composition from rhyolite to basalt based on Zr/TiO_2 vs SiO_2 (Winchester, 1977) and total alkali's vs silica (TAS) (Le Bas et al., 1986) (Figure 3.1a 3.1b). A SiO_2 histogram of the samples collected in this study shows three peaks at 47, 68 and 79. These peaks correspond to the mafic volcanic rocks and two groups of felsic volcanic rocks (Figure 3.2a). After MacLean and Barrett (1993) the rocks of the Hope Bay Greenstone Belt are tholeiitic, transitional or calc-alkaline. The mafic volcanic rocks have principally tholeiitic compositions with three samples in the transitional field. The felsic rocks form two groups, with most of the samples being of calc-alkaline affinity and a number of samples with very high Zr values falling into the tholeiitic field (Figure 3.2b).

3.2.3 Mafic Volcanic Rocks

Mafic volcanic rocks of the Hope Bay Greenstone Belt make up the majority of lithologies (n=66). The SiO_2 content ranges from 39 to 57% with a median of 47% SiO_2. Textural examination of the two outliers with >54% SiO_2 shows that they have undergone silicification. The mafic rock types in the Hope Bay Greenstone Belt are difficult to identify using IUGS classification as it is based on major elements such as Fe, Mg, K, Ca, Si which can be mobile during alteration and metamorphism (Condie, 1976; Kerrich and Wyman, 1996). These elements have seen varying degrees of mobility, depending on type and extent of alteration, but due to precautions mentioned above many samples are believed to be fairly representative of the original composition.

A relatively rare feature observed in the Hope Bay Greenstone Belt is the titanium enrichment trends in the mafic volcanic rocks. In a Al_2O_3 vs TiO_2 plot, three trends could be identified corresponding to the normal/LREE-enriched basalt group and the Ti-enriched basalt group, the Ti-enriched Al-depleted basalt group (Figure 3.3a). These groups are evident in a series of major element plots (Figure 3.4).

A classification scheme that was developed for unaltered Archean rocks of the Abitibi Greenstone Belt is the modified AFM diagram (Jensen, 1976; Grunsky at al., 1992). Least altered rocks from this study area plot as andesites, normal basalts and Fe basalts in this modified AFM diagram (Figure 3.3b). These groups can be further subdivided using REE chemistry to define the normal basalt and LREE-enriched basalt groups (see below). On the basis of the discrimination tools discussed above to filter the geochemical data from mafic rocks, we can assign a proper rock name (Figure 3.5). The rock names are the normal basalt, LREE-enriched basalt, Fe-,Ti-enriched basalt, Fe- and Ti-enriched Al-depleted basalt groups. Titanium concentrations of these rocks are easily observed on a TiO_2 histogram where the basalts show a bimodal distribution with peaks at 1% and 1.6% TiO_2 corresponding to the median of the normal-LREE-enriched basalt group and Ti-enriched basalt group (Figure 3.6a).

3.2.3.1 Normal Basalt Group

The normal basalt group is the most abundant basalt group in the Hope Bay Greenstone Belt and is represented throughout the stratigraphy. This group (n=36) is characterized by TiO_2= 0.39-1.12%, Al_3O_2/TiO_2= 16.55 (Figure 3.3a). It also has a Y/Zr ratio that falls in the tholeiitic field of MacLean and Barrett (1993). A selection of other element ratios, presented on Table 3.1, shows the chemical characteristics of this normal basalt group. The subset of samples from this study has values that are typical of the larger dataset from the entire Hope Bay Greenstone Belt (Miramar Geochemical Database, 2007) (Figure 3.4and 3.7). REE from the normal basalt group have flat patterns with $[La/Yb]_N$= 1.03, $[La/Sm]_N$= 0.94 and $[Gb/Yb]_N$= 1.02 and lack a Eu anomaly (Eu/Eu*=1.01) (Figure 3.8a). On a number of tectonic discrimination diagrams, the normal basalt group plot within the fields of ocean floor - calc-alkaline – volcanic arc (Figure 3.9a), island arc tholeiite – MORB – calc-alkaline (Figure 3.9b) or MORB – volcanic arc (Figure 3.10).

3.2.3.2 Light Rare Earth (LREE) Enriched Basalt Group

Based on their rare earth element patterns, a group of basalts with similar Al_2O_3 vs TiO_2 ratios to the normal basalt group can be identified and is named the Light Rare Earth Enriched (LREE) basalt group (Figure 3.8). The LREE-enriched basalt group is found in a number of locations throughout the belt and is believed to be restricted to the middle to upper stratigraphic positions. The LREE-enriched basalt group is almost identical to normal group in major element chemistry such as TiO_2 = 0.95% and Al_2O_3/TiO_2 = 18.18. It differs from the normal group by enrichment in the light REE's, Th, Zr and Nb and depletion in V and minor depletion in Fe_2O_3 (Figure 3.7 and 3.4). The LREE-enriched basalt group has a steeper sloped REE profile than the normal basalt group with chondrite normalized values of 14 to 55 times and ratios of $[La/Yb]_N$= 3.91, $[La/Sm]_N$= 2.21 and $[Gb/Yb]_N$= 1.14, and has a moderate negative Eu anomaly (Eu/Eu*=0.69) (Figure 3.8b). The LREE-enriched basalt group plots as calc-alkaline basalts (Figure 3.9) or within plate basalts (Figure 3.10) on tectonic discrimination diagrams.

3.2.3.3 Ti-enriched Basalt Group

The Ti-enriched basalt group (n=21) is known in five localities in the Hope Bay Greenstone Belt where they are named the Boston Basalt, Kennet Tarn, Patch, Doris, Boston and Bend basalt suites and are restricted to the lower portion of the stratigraphy of the belt. This group is characterized by higher TiO_2 (1.22-1.91%) and low Al_2O_3/TiO_2 (6.05-11.48). In addition to being enriched in Ti relative to normal basalts, this group is enriched in other incompatible elements such as Zr, Th, Nb and the REE's (Figure 3.7 and 3.4). The Ti-enriched group exhibits some complicated behavior of Y and V. For example, the Doris basalt suite is depleted in V and has extreme enrichment in Y compared to the other suites in the Ti-enriched basalt group (Figure 3.7).

The Ti-enriched basalt group has a flat REE profile that is approximately 20 times chondrites (Figure 3.8c) with $[La/Yb]_N$= 1.33, $[La/Sm]_N$= 1.06 and $[Gb/Yb]_N$= 1.11 and slight Eu anomaly (Eu/Eu*=0.96). The tectonic discrimination diagrams show a signature of ocean floor - calc-alkaline – volcanic arc (Figure 3.9a) or MORB (Figure 3.9b and Figure 3.10).

3.2.3.4 Ti-enriched Al-depleted Basalt Group

The Ti-enriched Al-depleted basalt group is only found in the central and north part of the Hope Bay Greenstone Belt where they are part of the Patch Basalt Suite. This group is identifiable in the large Miramar database and is observed in this study by two samples. This group of basalts are discussed in greater detail in a thesis on the Naartok Deposit by Therriault (2006). One of these samples has MgO contents of close to 18% which is in the range of a komatiite. Volcanic textures consistent with komatiitic lavas are also observed (Therriault, 2006), but REE profiles as well as other trace elements are not constant with komatiites. The extremely high MgO contents observed are likely a result of an olivine cumulate within the basalt flow. This group (n=2) is characterized by high to extremely high TiO_2 content (2.22 - 3.45%) and has varying degrees of Al-depletion. This gives an extremely low Al_2O_3/TiO_2 ratio's (3.07-3.85) (Figure 3.3). In addition to being enriched in Ti, relative to normal basalts, this group is enriched in many incompatible elements including Zr, Y, Nb and LREE's. There are also notable enrichments in Cr, Ni, Fe and V, with samples showing extreme enrichments in Ni and Cr. The rocks are enriched in LREE's and depleted in HREE which gives them a steep slope ranging from 13 to 70 times chondrites (Figure 3.8d). It has chondrite normalized ratios of $[La/Yb]_N$= 4.80, $[La/Sm]_N$= 1.54 and $[Gb/Yb]_N$= 2.36 and moderate Eu anomaly (Eu/Eu*=0.46). The Ti-enriched Al-depleted basalt group plots as within plate basalts (Figure 3.9a and Figure 3.10) or above MORB (Figure 3.9b).

3.2.4 Felsic Volcanic Rocks

The stratigraphy framework outlined in Chapter 2 will be used as a guide when discussing the felsic geochemistry. The rocks are divided into five suites; Flake Lake (2716 Ma and 2697 Ma), Square Lake (2690 Ma), Windy Lake (2686 Ma), Koignuk River (2677 Ma) and Clover Lake (2663 Ma), based on geochronology, geographic location and field relationships. The felsic volcanic rocks (n=32) have SiO_2 contents that range from 55 to 78.3% with an average of 66% SiO_2. Almost all of the samples with <62% SiO_2 have been identified as having a significant component of physical reworking and the samples >62% SiO_2 better represent primary volcanic chemistry. Based on chemistry the felsic volcanic rocks are not as easily subdivided as the mafic volcanic rocks but two main groups are observed. The first felsic group is referred to as the calc-alkaline felsic group and includes the Square Lake, Windy Lake, Koignuk River and Clover Lake suites (Figure 3.2b). The second group is the tholeiitic felsic group and is made up of the Flake Lake Suite (Figure 3.2b).

3.2.4.1 Flake Lake Suite

The Flake Lake Suite is the oldest episode of felsic volcanism in the belt (2697.6 to 2716 Ma) and has a unique chemical signature. This suite is set apart from the other felsic suites by an extremely high concentration of incompatible elements Zr, Y, Th, Hf and REE's as well as low Al content (Figure 3.11). A selection of other element ratios is presented on Table 3.2 which shows the chemical characteristics of this suite. Rhyolites of Flake Lake Felsic Suite are of tholeiitic affinity using the Zr vs Y plot after MacLean and Barrett (1993) (Figure 3.1b). The REE patterns are relatively flat with minor LREE enrichment; these rocks are the most REE enriched in the Hope Bay Greenstone Belt, at approximately >100 time chondrite with $[La/Yb]_N$= 1.9, $[La/Sm]_N$= 1.86 and $[Gb/Yb]_N$= 0.87 (Figure 3.12a). This suite has a very pronounced negative Eu anomaly (Eu/Eu*= 0.55), likely due to Eu substituting into plagioclase (Weill and Drake 1973). There are two groups within the Flake Lake Suite that can be identified based on REE profiles. One group contains most of the samples showing a lower enrichment in REE's whereas three samples have sub parallel and significantly more enriched profiles (Figure 3.12a). These two groups do not correspond to any spatial or temporal relationships and most likely represent differing mineralogy. Identified by Hebel (1999), this tholeiitic rhyolite was the first of its type identified in the Slave Province. According to the classification of Lesher et al. (1986) Flake Lake Suite would be called a FIIIa rhyolite (Figure 3.13). In the Superior Province, rhyolites with this unique chemistry are intimately associated with volcanic hosted massive sulfides deposits such as Noranda and Kidd creek (Bleeker et al., 1999).

3.2.4.2 ca. 2690 Ma Dacite

These samples are part of a heterogeneous package of felsic volcanic rocks that is found intercalated with the Wolverine Basalts. Three samples taking suggest an age similar to that of the Square Lake Suite (2690 Ma) which is ~20 km south of the location that these samples were taken. These samples plot as calc-alkaline dacites and have similar compositions as the Windy Lake and Koignuk Suites (Figure 3.1 & 3.11). The chondrite normalized REE profiles are relatively depleted compared with other dacites, with a moderately slope with $[La/Yb]_N$= 8.46, $[La/Sm]_N$= 2.63 and $[Gb/Yb]_N$= 2.38 and has positive Eu anomaly (Eu/Eu*= 1.13) (Figure3.12b REE diagrams). The samples from this study are comparable to the type Square Lake section but have 5 times lower chondrite normalized REE values in the LREE. The samples collected in this study were deposited in a submarine environment and are interpreted at being resedimented syn-eruptive volcaniclastic deposits.

3.2.4.3 Windy Lake Suite

The Windy Lake Suite extends along the entire 82 km length of the Hope Bay Greenstone Belt. It has coherent volcanic, volcaniclastic and sedimentary facies rocks. The samples analyzed as part of this study are calc-alkaline dacites with average SiO_2 = 66% and Zr/Y =15.72 (MacLean and Barret, 1993). The chondrite normalized REE profiles show moderate fractionation with a slope $[La/Yb]_N$= 16.47. A moderate enrichment in the LREE $[La/Sm]_N$= 3.96 and $[Gb/Yb]_N$= 2.64 and a minor negative Eu anomaly (Eu/Eu*= 0.87) is also observed in this suite (Figure3.12c). A group of three samples of the Windy Lake Suite located on the Doris Discovery Transect has more fractionated REE profiles $[La/Yb]_N$= 25.6. These samples indicate that the Windy Lake Felsic Suite may have had a number of volcanic centers that taped a variety of magma sources. Hebel (1999) identified two groups in the Windy Lake Suite, the first (FG-1) is a dacite with a composition similar to other calc-alkaline felsic suites in the belt with SiO_2 = 69% and TiO_2= 0.53% and moderately fractionated REE's. The second group (FG-2) is a calc-alkaline rhyolite which is set apart by high SiO_2 (=79%) and low TiO_2 (=0.11%), a large enrichment in the LREE's $[La/Yb]_N$ = 71.2, HREE enrichment ($[La/Sm]_N$ = 6.0, and $[Gd/Yb]_N$ = 5.0, and a minor negative Eu anomaly (Eu/Eu* = 0.9). The rhyolite (FG-2) group of the Windy Lake Suite was not observed in the course of mapping and is confined to a 2.5 km by 500 m locality in the middle of the belt. This group is not representative of the Windy Lake Suite with dacite (FG-1) comprising over >90% of this suite.

3.2.4.4 Koignuk Suite

The Koignuk Suite (2677 Ma) is the second of the two regionally extensive felsic volcanic units and is found along the western side of the Hope Bay Greenstone Belt. This suite has an average SiO_2 content of 67% and a Zr/Y= 12.2, consistent with a calc-alkaline dacite composition (MacLean and Barret, 1993). The compositions of these rocks are homogenous throughout the entire 40 km length of the belt. Chemical compositions of this suite are similar to the Windy Lake Suite, but the average compositions of the Koignuk suite have more Fe, V and Ti (Figure 3.11). The chondrite normalized REE profiles show a moderate amount of fractionation $[La/Yb]_N$= 11.34 , with moderate enrichment in the LREE $[La/Sm]_N$= 3.85 and $[Gb/Yb]_N$= 2.05 and has a minor negative Eu anomaly (Eu/Eu*= 0.92) (Figure 3.12d). The REE profiles from the Koignuk Suite are less fractionated than the Windy Lake Suite.

3.2.4.5 Clover Lake Suite

Three small outcrops in the middle of the Clover Valley comprise the Clover Lake Suite. As the youngest volcanic rocks identified in the belt (2663 Ma; Hebel, 1999), it has a distinctive chemical signature. This suite is characterized by extremely high SiO_2 (75%) and a Zr/Y=16.6, indicating a calc-alkaline rhyolite. This rhyolite differs from all other felsic volcanic suites in the Hope Bay Greenstone Belt by having a steep REE profile and, except for Rb, is extremely depleted in all trace elements (Figure 3.11 and Figure 3.12e). The chondrite normalized REE profiles show a very high degree of fractionation $[La/Yb]_N$= 36.34, with moderate enrichment in the LREE $[La/Sm]_N$= 4.45 and $[Gb/Yb]_N$= 4.85 and has a large Eu anomaly (Eu/Eu*= 0.45).

3.2.4.6 Clover Epiclastics

A final group of felsic volcanic rocks identified is called the Clover epiclastics. These rocks occur in the same geographical area as the Clover Lake Felsic Suite. The volcanic textures are not particularly clear but this deposit is interpreted as a secondary volcanic deposit, meaning that the original magma composition is not preserved. This group of rocks contains relatively high concentrations of compatible elements such as V, Fe and Ti, but generally low concentrations of incompatible elements (Figure 3.11). The REE profiles have a moderate slope $[La/Yb]_N$=5.61 with some enrichment in the LREE $[La/Sm]_N$=2.82 no enrichment in the HREE $[Gd/Yb]_N$=1.62 and no europium anomaly (Eu/Eu*=1.00) (Figure 3.12f).

3.2.5 Chemostratigraphic Columns

The geochemical results can be integrated with the structural-stratigraphic columns, from Chapter 2, to examine the geochemical evolution of the Hope Bay Greenstone Belt. This time horizon of 2686 Ma is the first time that belt wide felsic volcanism is observed and is a logical location to break the belt into two domains. This age of 2686 Ma represents the transition period in the belts history where mafic dominated volcanism is replaced by interbedded felsic and mafic volcanism with lesser sedimentation.

Cycles of volcanism (mafic and felsic) are often difficult to subdivide as stratigraphic columns are not continuous. This is problematic in the south part of the belt because the structural-stratigraphic columns are not continuous and there may be pieces of belt stratigraphy missing. In the south part of the belt, the volcanic packages have a pattern of alternating mafic – felsic volcanism capped by sedimentary rocks (Figure 3.14). The older domain in the south part of the Hope Bay Greenstone Belt contains intercalated normal tholeiites, Ti-enriched tholeiites and tholeiitic rhyolites. In this study only the Ti-enriched tholeiites and tholeiitic rhyolites were encountered but the Bend Basalt Suite contains intercalated Ti-enriched and normal basalts. The area around Flake Lake is the only location where this complicated mixture of tholeiitic rhyolites, Ti-enriched basalts and normal basalts are seen and is a good example of bimodal volcanism. The volcanism in the lower domain basalts are likely plume dominated. The source of the tholeiitic rhyolites may be in a back arc setting and is elaborated on in the discussion.

In the south part of the belt the younger domain (<2686 Ma) is made up of normal basalts, LREE-enriched basalts and calc-alkaline dacites are observed. This sequence is capped by the Clover Lake Sedimentary Suite and a calc-alkaline Clover Lake rhyolite. There are two sequences of calc-alkaline dacites (Windy Lake Felsic and Koignuk Suites) overlain by mafic volcanic suites (Member Basalt and Clover West Basalt Suites) in this domain. The stratigraphic repetition of these sequences that have similar chemistry and magma sources shows that there were multiple cycles of mafic and felsic volcanism in the south part of the belt.

The north part of the belt has a relatively continuous stratigraphic record (Figure 3.15). Similar to the south part of the stratigraphy there are two domains based on the time horizon of 2686 Ma. The older domain is composed almost entirely of a number of

Ti-enriched basalt – normal basalt cycles. The base of the stratigraphy in the north part of the belt contains Ti-enriched basalts of the Doris Group with is overlain by a normal basalt suite overlain by the Patch Basalt Suite where Ti-enriched basalt and Ti-enriched Al-depleted basalt groups are found together. The trace element compositions of the two suites of basalt enriched in titanium vary. The Doris Group is depleted in V and enriched in Y and Zr compared all the other titanium basalt suites. The upper parts of the stratigraphy of the older domain are dominated by normal basalts with minor intervals of Ti-enriched basalts at the top of the older domain. This continuous succession of basalt stratigraphy shows that there were multiple cycles of Ti-enriched basaltic separated by normal basaltic volcanism.

The younger domain (<2686 Ma) in the north part of the belt is made up of calc-alkaline, normal basalts and LREE-enriched basalts. The two calc-alkaline felsic suites (the Windy Lake and Koignuk Suites) have similar major and trace element compositions and are separated by basalts that have normal and LREE-enriched chemical signatures. Local Ti-enriched basalts are also found outside the transect area. The upper limit of the Windy Lake Felsic Suite sedimentation is 2678 Ma which means that the basalts overlying it are coeval with the Koignuk Felsic Suite. Above these volcanics is the Conglomerate Hill Sedimentary Suite (2670 Ma) which contains argillites and conglomerates. These are intruded by sills of the late mafic intrusions which are a xenolith rich suite.

The north and south parts of the belt are comparable in stratigraphic succession (Chapter 2) as well as geochemical evolution. In older domain (>2686 Ma) the normal and Ti-enriched groups can be correlated across the entire belt while Ti-enriched Al-depleted basalt group is restricted to the north part of the belt and the tholeiitic rhyolite, of the Flake Lake Suite, is restricted the south part of the belt. Chemical groups of the younger domain (<2686 Ma) can be correlated across the belt. In both parts of the belt calc-alkaline Koignuk and Windy Lake Felsic Suites are separated by mafic volcanism. Both of these felsic suites are local associated with LREE-enriched basalts which could be the result of mixing. The northern and southern parts or the Hope Bay Greenstone Belt have similar geochemical signatures and can be successfully correlated.

3.3 Isotope and High Resolution Trace Element Geochemistry (PCIGR)

High-resolution trace element and Hf-Nd isotopic compositions of 35 samples were measured at the Pacific Centre for Isotopic and Geochemical Research (PCIGR) at the University of British Columbia. The samples are a subset of the larger dataset and are representative samples from the mafic and felsic volcanic suites and were selected avoiding alteration. The procedures of sample preparation, dissolution, column chemistry and analysis are presented in Appendix B.

3.3.1 Results of Lu-Hf and Sm-Nd Geochemistry

The analytical results and other calculated data such as initial ratios at the time of emplacement and epsilon values for samples are presented in Table 3.3. Rock suites identified previously will be referred to in the discussion of various binary plots and histograms showing distribution of model ages. $^{147}Sm/^{144}Nd$ vs $^{143}Nd/^{144}Nd$ plot shows three main groups; the normal and Ti-enriched basalt groups which has higher $^{143}Nd/^{144}Nd$ and $^{147}Sm/^{144}Nd$ ratios, the calc-alkaline felsic, LREE-enriched enriched basalt and Ti-enriched Al-depleted basalt groups which have much lower ratios and the group of samples the tholeiitic rhyolite group (Figure 3.16). The third group, the tholeiitic rhyolites of the Flake Lake Suite plots between the other two main groups and also shows a distribution disturbance around the isochron line.

A plot of $^{176}Lu/^{177}Hf$ vs $^{176}Hf/^{177}Hf$ shows a similar grouping of samples as observed in the Sm-Nd plot. Calc-alkaline felsic and Ti-enriched Al-depleted basalt group have lower $^{176}Hf/^{177}Hf$ and $^{176}Lu/^{177}Hf$ ratios whereas the normal and Ti-enriched basalts have higher ratios (Figure 3.17). Ideally all the samples that have been part of a closed isotopic system should fall on a line (isochron) on the Sm-Nd and Lu-Hf isochron. Samples that do not fall on, or close to, the isochron may be explained by either analytical problems, inhomogeneities of the sample or the isotopic system may have been disturbed by alteration. This problem is not seen in the Sm-Nd samples as the results are within an acceptable range on the isochron diagram. The Lu-Hf results have 6 samples that exhibit abnormal behaviour. These samples are from the Flake Lake Suite, the Windy Basalts, Member Basalts and Wolverine Basalts (Figure 3.17). These samples are labeled the "isotopically disturbed group" and will be excluded from further discussion as they likely represent an open system and do not represent primary isotopic compositions. Alteration in all the samples and the disturbed group will be examined in closer detail in the next section (3.3.2 Alteration and Isotopic Disequilibrium).

Examining the initial ratio of $^{143}Nd/^{144}Nd$ and $^{176}Hf/^{177}Hf$ at 2.68Ga, $(^{143}Nd/^{144}Nd)_{@2.68Ga}$ vs. $(^{176}Hf/^{177}Hf)_{@2.68Ga}$, samples from the Hope Bay Greenstone Belt shows the presence of distinct groups. The calc-alkaline felsic rocks overlap with the Ti-enriched basalt group whereas the normal basalt group has lower $(^{143}Nd/^{144}Nd)_{@2.68Ga}$ values and the isotopically disturbed group have low $(^{176}Hf/^{177}Hf)_{@2.68Ga}$ values (Figure

3.18). The tholeiitic rhyolite group (Flake Lake Suite) has a wide range of $(^{143}Nd/^{144}Nd)_{@2.68Ga}$, from 0.50906 to 0.50947, as well as a large range of $(^{176}Hf/^{177}Hf)_{@2.68Ga}$ values, from 0.28107 to 0.28206. The Ti-enriched Al-depleted basalt group has similar $(^{143}Nd/^{144}Nd)_{@2.68Ga}$ values to the calc-alkaline group but with lower $(^{176}Hf/^{177}Hf)_{@2.68Ga}$. The LREE-enriched basalt sample plots similarly to the calc-alkaline felsic groups.

In the previous section (3.2.3) four basalt groups were determined using a number of discrimination diagrams, these groups are called Normal basalt, LREE-enriched Basalt, Ti-enriched Basalt and Ti-enriched Al-depleted basalt groups. A plot of Al_3O_2/TiO_2 vs. $\varepsilon_{Nd(i)}$ (Figure 3.19) shows that the normal basalt group range in ε_{Nd} value from 2.1 to 5.5, the Ti-enriched basalt group have a similar range of $\varepsilon_{Nd(i)}$ 1.7 to 4.6 and the Ti-enriched Al-depleted basalt group has values of 3.8 and 3.6. These samples have no overall correlation between $\varepsilon_{Nd(i)}$ and Ti-enrichment.

Examining the Al_3O_2/TiO_2 vs. $\varepsilon_{Hf(i)}$ plot, the normal basalt group has a large range in $\varepsilon_{Hf(i)}$ values (Figure 3.20). The normal basalt group ranges from -12.8 to 4.4 and has 6 samples with values of ε_{Hf} <-2, which have been identified as being isotopically disturbed. The Ti-enriched basalt group has a range in $\varepsilon_{Hf(i)}$ values from -1.6 to 4.6 and the Ti-enriched Al-depleted basalt group has $\varepsilon_{Hf(i)}$ values of 4.4 and 3.4.

3.3.1.1 Model Ages

It is assumed that the Earth's crust has been created from the mantle by magmatism. When the first piece of the crust was created, it had the $^{143}Nd/^{144}Nd$ or $^{176}Lu/^{177}Hf$ ratio of the mantle. The assumption can be made that the mantle has the same Nd and Hf isotopic history as Chondritic Uniform Reservoir (CHUR) or Depleted Mantle

(DM). This means a piece of crust will have the same $^{143}Nd/^{144}Nd$ or $^{176}Hf/^{177}Hf$ as the mantle when it is created. If we know the present day Sm/Nd and $^{143}Nd/^{144}Nd$ ratio or Lu/Hf and $^{176}Hf/^{177}Hf$ ratio of a rock, we can calculate Hf and Nd model ages. The point at which the line describing the evolution of the sample intersects the line describing the evolution of DM or CHUR gives the model age, τ_{DM} or τ_{CHUR} (Figure 3.21).

The model ages calculated for Nd and Hf relative to both CHUR and DM (Table 3.3). The τ_{CHUR} for Nd ($^{Nd}\tau_{CHUR}$) yielded 11 meaningless ages (negative). Examining $(^{143}Nd/^{144}Nd)_{@2.68Ga}$ vs $^{Nd}\tau_{CHUR}$ the normal basalt group has ages of less than 1.5 Ga whereas the majority of the samples plot between 2 and 3 Ga (Figure 3.22). The calc-alkaline felsic group has very homogenous values with an average $^{Nd}\tau_{CHUR}$ of 2.47 Ga. The Ti-enriched basalt group has an average $^{Nd}\tau_{CHUR}$ of 2.25 Ga whereas the normal basalt group has an average $^{Nd}\tau_{CHUR}$ of 1.25Ga. The model ages for $^{Nd}\tau_{CHUR}$ have a weakly bimodal distribution with peaks at 2.15Ga and 2.55Ga (Figure 3.23). The group at 2.15Ga is dominated by basalts while the group at 2.55Ga is made up of felsic volcanic rocks.

Examining the $(^{143}Nd/^{144}Nd)_{@2.68Ga}$ vs $^{Nd}\tau_{DM}$ diagram, a number of overlapping groups can be identified (Figure 3.24). The Normal basalt group has a range of model ages from 2.25 to 3 Ga with an average of 2.68Ga and the Ti-enriched basalt group ranges in model ages from 2.5 to 3.25Ga with an average of 2.9Ga. The calc-alkaline felsic group is very homogenous with Koignuk Felsic Suite and Windy Felsic Suite having an average $^{Nd}\tau_{DM}$ of 2.78 and 2.9Ga respectively. The tholeiitic felsic group (the Flake Lake Felsic Suite) has a wide range of model ages and $(^{143}Nd/^{144}Nd)_{@2.68Ga}$ values with an average $^{Nd}\tau_{DM}$ of 3.16Ga. The model ages for $^{Nd}\tau_{DM}$ show a normal distribution with a median of 2.75Ga (Figure 3.25). The calc-alkaline felsic group is older than the U/Pb ages of the rocks whereas the rest of the groups overlap the U/Pb ages.

The τ_{CHUR} for Hf (${}^{Hf}\tau_{CHUR}$) yielded 6 ages that were meaningless as they were zero or negative. The plot of $({}^{176}Hf/{}^{177}Hf)_{@2.68Ga}$ vs ${}^{Hf}\tau_{CHUR}$ shows the normal basalt group has a wide range of model ages with an average ${}^{Hf}\tau_{CHUR}$ of 2.0Ga and the Ti-enriched basalt group having a average ${}^{Hf}\tau_{CHUR}$ of 2.64Ga (Figure 3.26). The calc-alkaline felsic group has a tight range of model ages with an average ${}^{Hf}\tau_{CHUR}$ of 2.45Ga whereas the tholeiitic felsic group has a moderate range of model ages with an average ${}^{Hf}\tau_{CHUR}$ of 2.18Ga. On the histogram, the ${}^{Hf}\tau_{CHUR}$ has a poorly defined bimodal distribution with peaks at 2.1 and 2.55Ga (Figure 3.27). The basalt groups are distributed across the histogram while the calc-alkaline felsic group makes up the majority of the peak at 2.55Ga.

The $({}^{176}Hf/{}^{177}Hf)_{@2.68Ga}$ vs ${}^{Hf}\tau_{DM}$ has the majority of model ages between 2 and 3Ga with all the groups having a great deal of overlap (Figure 3.28). The normal basalt group has an average ${}^{Hf}\tau_{DM}$ of 3.17Ga and the Ti-enriched basalt group has an average ${}^{Hf}\tau_{DM}$ of 3.6Ga. The felsic rocks have an extremely homogenous Hf model ages (avg ${}^{Hf}\tau_{DM}$ = 2.47Ga) and the tholeiitic felsic group and an average ${}^{Hf}\tau_{DM}$ of 1.86Ga. Examining the histogram the ${}^{Hf}\tau_{DM}$ have a bimodal distribution with peaks at 2.1 and 2.55Ga (Figure 3.29). The basalts make up the majority of the peak at 2.1Ga whereas the peak at 2.55Ga is made up of both basalts and felsic volcanic rocks.

The initial $\varepsilon_{Nd(i)}$ vs $\varepsilon_{Hf(i)}$ plot has three main groups, the disturbed group of samples with unrealistically low ratios of Hf, the tholeiitic felsic group and the main cluster of samples (Figure 3.30). Within the main group, the Normal and LREE-enriched basalt groups have higher $\varepsilon_{Nd(i)}$ values (avg = 3.7) and slightly lower $\varepsilon_{Hf(i)}$ values (avg =

2.1). Also in the main group, the Ti-enriched basalt group has average $\varepsilon_{Nd(i)}$ = 3.2 and $\varepsilon_{Hf(i)}$ = 2.8 and Ti-enriched Al-depleted basalt group has average $\varepsilon_{Nd(i)}$ = 3.7 and $\varepsilon_{Hf(i)}$ = 3.9. The calc-alkaline felsic group has an average $\varepsilon_{Hf(i)}$ = 4.5 and $\varepsilon_{Nd(i)}$ = 2.7. The tholeiitic felsic group has a large range of values of $\varepsilon_{Nd(i)}$ = -1.9- 6.0 and $\varepsilon_{Hf(i)}$ = -0.1 - 35.3 with no clear isotopic signature.

3.3.2 Alteration and Isotopic Disequilibrium

The group identified as being isotopically disturbed needs to be examined in further detail to determine the reason for its abnormal behaviour. Element molar ratios can be useful when examining hydrothermal alteration to albite or sericite. An increase in the molar ratio of K to Al can indicate alteration to sericite, $KAl_3Si_3O_{10}(OH)_2$, whereas an increase in the ratio of Na to Al can indicate alteration to albite, $NaAlSi_3O_8$ (S. Halley, pers comm., 2007). The least altered samples will have very low <0.03 K/Al molar ratios and between 0.2 and 0.4 Na/Al molar ratios. Three of the six samples identified as being in isotopic disequilibria have experienced low degrees of sericite alteration (Figure 3.31).

In the Hope Bay Greenstone Belt, the Hf isotopic system was identified as being more affected by the disturbance than the Nd system. Loss on Ignition (LOI) is commonly a good proxy for hydrothermal alteration as many primary silicates are hydrated and CO_2 is added. Examining the ε_{Hf} vs LOI diagrams, the isotopically disturbed group of samples are identified by their extremely low ε_{Hf} values but have a wide range of LOI. In the isotopically disturbed group of samples, there is no correlation between LOI and ε_{Hf} value (Figure 3.32).

The mineral systematics of the Hf system are not completely understood and the low grade alteration/metamorphism of minerals to epidote and chlorite seem to affect the closure of the Hf isotopes (D. Weis, pers comm., 2007). The background greenschist metamorphism produces abundant chlorite and epidote in the Hope Bay Greenstone Belt and may be responsible for the disturbance in the Hf system (Gebert, 1991). A number of thin sections of the isotopically disturbed samples were compared to that of other basalts that were not disturbed and the mineralogy was relatively similar with all samples containing chlorite ±epidote. A detailed study of alteration and metamorphism is beyond the scope of this study and these 6 basalts that appear isotopically disturbed will be excluded from the final discussion.

3.3.3 Isotopic Sources of the Hope Bay Greenstone Belt

The Sm-Nd and Lu-Hf isotopes in the Hope Bay Greenstone Belt as petrogenetic tracers have been useful in fingerprinting the volcanic groups. (Figure 3.16 and 3.17). Both plots show the Ti-enriched basalt and the normal basalt groups have isotopic compositions close to today's depleted mantle and bulk silicate earth. Samples from the calc-alkaline group have the lowest radiogenic ratio and plot lowest on the graph with the LREE-enriched basalt and Ti-enriched Al-depleted basalt group having intermediate ratios (Figure 3.16 and 3.17). The tholeiitic felsic group has isotopic compositions between the two clusters described above but many of the tholeiitic felsic group samples do not fall on the 2.68Ga isochron which indicates that these samples exhibit odd systematics.

$(^{143}Nd/^{144}Nd)_{@2.68Ga}$ vs $(^{176}Hf/^{177}Hf)_{@2.68Ga}$ has no clear trend for Hf isotopes but the Nd isotopes show groupings of rock types. The normal basalt group has higher $(^{143}Nd/^{144}Nd)_{@2.68Ga}$ ratios whereas the calc-alkaline felsic and Ti-enriched basalt groups have lower ratios. The Ti-enriched Al-depleted basalt group lies between the two areas (Figure 3.33). The fact that no pattern exists in the $(^{176}Hf/^{177}Hf)_{@2.68Ga}$, indicates that Nd and Hf isotopes were not behaving the same in the system.

There are no clear trends for the $\varepsilon_{Nd(i)}$ and $\varepsilon_{Hf(i)}$ vs Al_2O_3/TiO_2 (Figure 3.19 and 3.20). In these plots, there is a large variation in the Al_2O_3/TiO_2 ratios but there is no correlation with the Nd or Hf isotopic composition (Figure 3.34). Samples from the Ti-enriched Al-depleted basalt group and the Ti-enriched basalt groups appear to have more homogenous Hf isotopic compositions than the normal group(Figure 3.34).

The $^{Nd}\tau_{DM}$ of samples from the Hope Bay Greenstone Belt, indicate that the crystallization of the rock occurred between 2.8 and 2.9Ga. This differs from the $^{Nd}\tau_{CHUR}$ peaks which are at 2.1 to 2.2Ga for the normal basalt group and 2.5 to 2.6 for the calc-alkaline felsic group. From U/Pb dating of zircons, the age range of magmatism is from 2716 to 2662 Ma, and overall the $^{Nd}\tau_{DM}$ is a good estimate of the time at which the magma that created these rocks was extracted from the mantle. Examining only the calc-alkaline felsic group the $^{Nd}\tau_{CHUR}$ is a good approximation of the model age.

$^{Hf}\tau$ of from the Hope Bay Greenstone Belt have mixed results as expected from their disturbed systematics, with only the calc-alkaline felsic samples coming close to the accurate U/Pb ages. Examining the Hf model ages, both the $^{Hf}\tau_{DM}$ and $^{Hf}\tau_{CHUR}$ do not give ages close to the known time of crystallization. The basalt groups have very young model ages and the calc-alkaline felsic group gives a better approximation of the age as they overlap the U/Pb ages.

Overall the $^{Nd}\tau_{DM}$ appears to give the best distribution of ages and has a peak that is close to the crystallization age of the rocks (~2.68Ga). Examining only the calc-alkaline felsic group, the $^{Hf}\tau_{DM}$ appears to be a good approximation of the age of crystallization.

The $\varepsilon_{Nd(i)}$ vs $\varepsilon_{Hf(i)}$ show a weak negative correlation when the isotopically disturbed samples are removed (Figure 3.35). All the basalt groups overlap with respect to $\varepsilon_{Nd(i)}$ and $\varepsilon_{Hf(i)}$ but much of the normal basalt group appears to be $\varepsilon_{Hf(i)}$ depleted and enriched in $\varepsilon_{Nd(i)}$ compared to the other two groups. This is unusual, as these samples that have been shown to have similarities to MORB, which comes from a DM source typically has a depleted $\varepsilon_{Nd(i)}$ and depleted $\varepsilon_{Hf(i)}$ values. Vervoort and Blinchert-Toft (1999) identified that in the early Archean, the mantle had a narrow range in $\varepsilon_{Hf(i)}$ values but a very wide range in $\varepsilon_{Nd(i)}$ values, which results in a horizontal trend oblique to the juvenile array. Vervoort and Blinchert-Toft (1999) attribute the dispersion in the $\varepsilon_{Nd(i)}$ of these rocks to a later disturbance in the Sm-Nd isotope system and does not represent initial isotopic variations in the early Earth. A similar pattern of a horizontal trend oblique to the juvenile array is observed in the samples from the Hope Bay Greenstone Belt. It is not clear if the Hf or Nd isotopes are shifted away from the juvenile whole rock mantle array identified by Vervoorti and Blinchert-Toft (1999). There is a group of basalts that is isotopically disturbed in Hf which are discussed above and named the isotopically disturbed group. There is little evidence to suggest that all the rocks in the Hope Bay Greenstone Belt have experienced an isotopic disturbance in Hf. The normal basalt group is the group that has the largest shift away from the juvenile whole rock mantle array.

The calc-alkaline felsic group is fairly homogenous with respect to $\varepsilon_{Nd(i)}$ and is less homogenous with respect to $\varepsilon_{Hf(i)}$. The Ti-enriched Al-depleted basalt and Ti-enriched basalt groups have isotopic compositions that are transitional between the calc-alkaline and the normal basalt group.

The tholeiitic rhyolite group (the Flake Lake Felsic Suite) was omitted from much of the discussion above since it has highly variable Hf and Nd isotopic composition. The highly variable isotopic compositions observed in these rocks are consistent with highly variable trace element values (Figure 3.11).

3.4 Discussion

On a regional scale, geochemical fingerprinting of the volcanic rocks has defined a number of chemically distinct suites that are restricted to particular portions of the stratigraphy. These suites appear to have slightly different sources of formation.

3.4.1 Mafic Volcanic Rocks

Mafic rocks in the Hope Bay Greenstone Belt have a number of chemically distinct suites, many of which are stratigraphically restricted. These suites include the normal basalt, LREE-enriched basalt, Ti-enriched basalt and Ti-enriched Al-depleted basalt groups. The elevated Ti content of the Ti-enriched basalt and Ti-enriched Al-depleted basalt groups are not observed in any other greenstone belt in the SSP. There is only one locality with similar rocks on the continent, found in the Abitibi Greenstone Belt (Stone et al., 1987; Xie et al., 1993).

The normal and Ti-enriched basalts are similar to rocks erupted by decompression melting of the mantle due to their flat REE profiles however they are not N-MORB or E-MORB (Hofmann, 2003). The lack of any other part of an ophiolite sequence would support the idea that these rocks are not from a mid ocean ridge setting. Since differing REE patterns Ti-enriched basalts and normal basalts likely originated from the same melting regime (decompression melting) the enrichment in incomparable elements resulted from enriched mantle being incorporated to the melt. This may infer that the mantle beneath the Hope Bay Greenstone Belt was inhomogeneous. The isotopic evidence is consistent with trace and REE patterns and shows that the Ti-enriched basalt group has an enriched source compared to the normal basalt group. The Ti-enriched Al-depleted basalt group is the result of high degrees of melting of the mantle. It has been suggested that this group is the result of a complicated interaction between plume and mantle melting, with an enriched mantle likely being involved (Therriault 2006). This idea does not fit well with the geology which suggests quick transition between some of the Ti enriched and normal basalt groups. The Ti-enriched Al-depleted basalt group has a REE signature similar to ocean island basalts (OIB); this hypothesis has limited support by the isotopic evidence, as the Ti-enriched Al-depleted basalt group has similar isotopic ratios to the calc-alkaline felsic volcanic rocks. The LREE-enriched basalt group is the rock type closest to andesites in the belt and is similar to primitive arc basalts (Kelemen et al., 2003).

Examining the chemo-stratigraphic columns, we see that the Ti-enriched mafic volcanic rocks lie in the lower portions of the volcanic stratigraphy of the Hope Bay Greenstone Belt (Figure 3.14 and 3.15). Ti-enriched mafic volcanic rocks host the

Naartok and Doris Deposits and are locally found in the Boston Deposit. Normal basalts are found throughout the stratigraphy with the LREE-enriched group restricted to the middle and upper portions. The Ti-enriched mafic volcanic rocks (Ti-enriched Al-depleted basalt group and Ti-enriched basalt group) are highly prospective for gold mineralization and are easily identified using geochemical screening (Figure 3.5).

3.4.2 Felsic Volcanic Rocks

Felsic rocks are made up of four calc-alkaline suites and one tholeiitic suite. The felsic calc-alkaline suites include the Square Lake Suite, Windy Lake Suite, Koignuk Suite and Clover Lake Suite. These four suites are formed by similar magmatic processes though they are distinct volcanic events and are separated by mafic volcanism. This group of rocks has geochemical signature similar to a volcanic arc setting (Kelemen et al., 2003). The Square Lake Suite, Windy Lake Suite and Koignuk Suite are similar and could result from dehydration of slab and hydration of the mantle similar to that we see in modern volcanic arcs (Bebout, 2003).

A felsic tholeiite suite named the Flake Lake suite is of rhyolitic composition. The relatively unfractionated REE profile indicates that the garnet did not fractionate from the liquid nor was it a residual phase (Weill and Drake, 1973). The petrogenesis of this rock has not been resolved but these two scenarios may explain their compositions. The first scenario includes a primitive source mafic magma which evolved at a shallow level in the crust drawing mafic magmas out of the chamber with little crustal assimilation until rhyolite erupted. The second scenario is the partial melting of a dry mafic tholeiitic crustal source generating a rhyolitic melt, leaving a residue dominated by plagioclase and clinopyroxene (Thy et al., 1990). Tholeiitic rhyolites of the Kidd Creek

Assemblage in the Abitibi greenstone belt have similar chemical characteristics to the Flake Lake Felsic Suite and are intruded by gabbro sills and overlain by the basaltic volcanic rocks (Bleeker et al., 1999). One key difference between the two units is the Kidd Creek rhyolites are associated with komatiites but no true komatiites are found in the Hope Bay Greenstone Belt.

3.4.3 Correlating Geochemistry within the Hope Bay Greenstone Belt

Geochemical signatures of the volcanic suites in the Hope Bay Greenstone Belt are similar in the north and south parts of the belt. Mafic volcanic rock groups dominate the stratigraphy, with normal basalt, LREE-enriched basalt and Ti-enriched basalt groups found in both the south and north parts of the belt and Ti-enriched Al-depleted basalt group restricted to a continuous stratigraphic package (the Patch Basalt Suite) in the north part of the belt. Calc-alkaline felsic packages of the Windy Felsic and Koignuk Suite are regionally continuous units found along the entire length of the belt. Chemical compositions of these units are extremely homogenous over their entire range. Restricted to the south part of the belt, the Clover Lake Suite is found in only one location whereas the tholeiitic Flake Lake Suite has a great deal of geochemical variability. Found in the middle belt with local beds in the north part of the belt, the Square Lake Suite is the oldest calc-alkaline volcanism in the Hope Bay Greenstone Belt at 2690 Ma. The Hf and Nd isotopes have proven useful in identifying the sources of magma for the rocks of the Hope Bay Greenstone Belt. Geochemical groups identifying the major and trace element analysis are confirmed by Nd and Hf isotopic composition.

3.4.4 Comparisons to other Greenstone Belts

In the Slave Structural Province, the Yellowknife Greenstone Belt has been compared to the Hope Bay Greenstone Belt (Hebel, 1999; Sherlock et al., 2001). It has a number of similarities in age and basic geology but differs in the number of volcanic cycles and range of rock compositions. The Yellowknife Greenstone Belt does not contain rocks similar to the tholeiitic rhyolites or Ti-enriched Al-Depleted basalts (Bleeker, 1999; Cousens, 2000; Cousens et al., 2006). However, the Kam Group of the Yellowknife Greenstone Belt does locally contain some Ti-enriched basalts similar to those found in the Hope Bay Greenstone Belt (Cousens, 2000).

Located in the eastern Superior Province, the Abitibi Greenstone Belt is the best documented greenstone belt in Canada. There are numerous similarities between these greenstone belts, including the presence of tholeiitic rhyolites and Ti-enriched Al-depleted basalts (Stone et al., 1987; Xie et al., 1993; Bleeker et al., 1999; Ayer et al., 1999). Differences between the two belts include the lack of large faults and komatiites in the Hope Bay Greenstone Belt (Ayer et al., 1999). The Abitibi has two main tectonic models; the "oceanic island arc subduction zone" model (Jackson and Fyon 1991; Kerrich et al., 1999; Ayer et al., 2002; Wyman et al. 2002) and the (para) autochthonous model (Thurston, 2002, Ayer et al. 2002).

3.5 Summary

The combination of field relationships, from a number of discrete transects across the Hope Bay Greenstone Belt, and U-Pb geochronology has allowed the creation of a revisted stratigraphic framework (Chapter 2). This model is used as a base for lithologic and isotope geochemical techniques, which characterize the volcanic suites of the Hope Bay Greenstone Belt.

An examination of the lithogeochemistry and isotope geochemistry in the Hope Bay Greenstone Belt shows that mafic and felsic volcanic rocks have a range of chemical signatures. The majority of rock types in the belt are common to greenstone belts in the Canadian Shield including basalts, with lesser andesites, dacites and rhyolites. However the Hope Bay Greenstone Belt has a number of rock types that are rare or undocumented in greenstone belts. These rare rock types include the relatively minor Ti-enriched Al-depleted basalt (Patch Basalt Suite) which is part of a larger Ti enriched group and tholeiitic rhyolite groups (Flake Lake Felsic Suite).

The integration of the stratigraphic framework (Chapter 2) and the geochemical results allow us to understand the chemical evolution of the belt. Many mafic volcanic groups and felsic volcanic suites are restricted to particular portions of the stratigraphy. The lower portions of the stratigraphic (>2686 Ma) contain high Ti basalt groups as well as normal basalt groups and the anomalous tholeiitic rhyolite of the Falk Lake Suite. The upper portions of the stratigraphy contain calc-alkaline dacites with minor calc-alkaline rhyolite, normal basalt and LREE basalt. The distribution of these geochemical packages has implications for the tectonic evolution of the belt as well as mineral exploration. There are important tectonomagmatic changes that occur between the deposition of the rocks in the upper and lower parts of the stratigraphy. The observations can be generalized to conclude that the rocks found in the lower part of the stratigraphy have sourced from high degrees of partial melting of the mantle possibly with the influence of a plume. The rocks that make up the upper part of the stratigraphy are a mixture of primitive arc basalts and calc-alkaline rocks which are sourced from lower degrees of partial melting of crust or the mantle. From these observations it could be inferred that the Hope Bay Greenstone Belt has gone from a plume dominated setting to an island-arc setting. In addition to this, some of the basalts in the lower parts of the stratigraphy are enriched in Ti (plus a series of incompatible elements) which can be explained by the melting of an inhomogeneous mantle.

The results of Sm-Nd and Lu-Hf isotopic analysis show that there are significant differences between volcanic groups. The calc-alkaline group plot in a homogenous array with some samples falling on the juvenile mantle whole rock array. The normal basalt group has some problems with isotopic disequilibrium. Nonetheless this group has a negative correlation of $\varepsilon_{Hf(i)}$ and $\varepsilon_{Nd(i)}$ values. The Ti-enriched Al-depleted basalts and Ti-enriched basalt groups have isotopic compositions that are transitional between the calc-alkaline and the normal basalt group.

The association of particular lithologic suites and gold deposition in the Hope Bay Greenstone Belt suggest that fluid-rock interaction and wall rock sulphidation are the most important mechanisms for depositing gold (Mikucki, 1998). These rock groups have high Ti contents and are named the Ti-enriched basalt group and the Ti-enriched Al-depleted basalt group. These basalt groups are found in the Bend Basalt Suite and Kennet Tarn Basalt Suite which do not host gold deposits and the Boston Basalt Suite, Doris Basalt Suite and Patch Basalt Suite which each host gold deposits. All these basalt suites containing Ti-enriched basalts represent a high exploration potential.

Table 3.1: Average inter-Element ratios for four basalt groups from six transects of the Hope Bay Greenstone belt

Basalt Group	LREE Basalts (n=6)	σ	normal Basalts (n=36)	σ	Ti enriched Basalts (n=19)	σ	Ti enriched Al depleted basalt-basaltic komattite (n=2)	σ
SiO_2	48.3	3.87	46.5	4.40	48.9	3.81	40.5	1.62
Al_2O_3	17.10	1.72	14.25	1.57	13.40	1.42	10.06	4.57
Fe_2O_3	10.80	2.33	12.35	1.70	14.45	2.91	17.28	3.01
TiO_2	0.96	0.11	0.88	0.14	1.50	0.14	2.84	0.87
MgO	5.86	1.78	6.22	3.02	3.72	1.45	12.95	6.99
Zr	107.38	29.13	54.34	14.44	99.16	21.12	142.00	25.46
Y	21.58	4.14	18.67	3.57	33.63	6.34	26.20	7.64
Al_3O_2/TiO_2	18.18	3.43	16.55	2.28	8.96	1.10	3.46	0.55
TiO_2/V	41.74	5.81	30.41	2.52	67.28	52.37	67.97	1.27
TiO_2/Y	448.67	44.88	474.41	55.57	478.58	120.48	1079.54	17.30
TiO_2/Zr	97.65	39.55	167.11	30.56	153.66	31.56	197.33	25.87
Ti/V	145.57	17.57	198.32	16.48	124.17	52.34	88.17	1.64
Nb/Yb	2.59	0.63	1.14	0.20	1.60	1.22	9.64	0.51
Ce/Y	1.44	0.29	0.43	0.07	0.54	0.21	1.58	0.50
Ti/Nb	3.64	0.71	1.58	0.31	2.04	0.66	4.55	0.05
Zr/Y	5.20	1.94	2.97	0.91	3.23	1.23	5.51	0.64
Mg#	51.49	7.51	50.50	7.24	33.89	7.15	56.82	10.16
Eu/Eu*	0.69	0.12	1.01	0.06	0.96	0.16	0.46	0.02
$(La/Yb)_N$	3.91	0.22	1.03	0.07	1.33	0.36	4.80	0.03
$(La/Sm)_N$	2.21	0.22	0.94	0.13	1.06	0.16	1.54	0.36
$(Gd/Yb)_N$	1.40	0.92	1.02	0.21	1.11	0.70	2.36	1.42

Table 3.2: Average sellected element and inter-Element ratios for six felsic groups from six transects of the Hope Bay Greenstone belt

	Flake Lake Suite (n=7)	σ	Square Lake Suite (n=2)	σ	Windy Lake Suite (n=9)	σ	Koignuk Suite (n=11)	σ	Clover Epiclastics (n=4)	σ	Clover Lake Suite (n=1)
SiO_2	74.85	2.68	66.52	2.22	65.85	3.033	62.91	3.967	57.45	1.277	75.08
Al_2O_3	11.19	0.60	15.49	0.615	14.85	0.985	15.63	1.009	15.76	1.263	12.90
Fe_2O_3	4.37	2.13	2.87	0.651	3.77	1.075	5.77	1.945	7.30	0.675	0.79
TiO_2	0.23	0.08	0.33	0.106	0.43	0.083	0.56	0.095	0.72	0.173	0.09
Zr	361.43	113.96	102.25	10.96	146.62	53.35	143.32	24.2	146.38	16.73	56.50
Nb	25.39	23.34	2.00	0	5.67	3.048	6.36	2.157	6.60	1.233	3.00
V	14.86	18.59	48.00	21.21	51.67	28.39	81.36	28.03	121.00	24.95	8.00
Nb	25.39	23.34	2.00	0	5.67	3.048	6.36	2.157	6.60	1.233	3.00
La	34.97	17.99	6.75	0.778	23.58	10.25	17.67	3.888	13.35	1.282	10.70
Nb/Yb	1.81	0.79	3.67	0.471	5.32	0.906	5.78	1.46	4.00	1.054	15.00
La/Yb	2.88	0.33	12.47	3.017	24.25	10.62	16.70	5.1	8.26	2.522	53.50
Zr/Y	3.90	0.79	15.72	2.861	13.86	3.983	12.20	3.159	9.20	2.002	16.62
Al_3O_2/TiO_2	56.17	24.66	50.65	18.42	35.26	6.256	28.68	3.898	22.47	3.362	143.33
TiO_2/1000*Nb	1536.53	2267.36	65.00	21.21	131.25	67.74	113.85	25.06	93.16	15.92	333.33
TiO_2/Zr	6.68	2.76	32.53	13.86	31.59	7.793	39.41	8.588	48.87	7.28	15.93
TiO_2/Y	27.04	12.75	491.47	124.8	443.74	180.4	465.94	93.21	440.16	44.22	264.71
TiO_2/V	239.14	150.60	69.62	8.673	108.01	62.72	71.24	11.8	59.97	9.898	112.50
Ce/Y	0.82	0.06	2.13	0.023	4.62	2.141	3.00	0.812	2.07	0.708	6.29
$(La/Yb)_N$	1.96	0.22	8.47	2.05	16.47	7.217	11.34	3.465	5.61	1.713	36.34
$(La/Sm)_N$	1.86	0.23	2.63	0.071	3.97	0.356	3.86	0.647	2.82	0.365	4.45
$(Gd/Yb)_N$	0.88	0.07	2.39	0.515	2.65	0.831	2.05	0.33	1.62	0.283	4.85
Eu/Eu*	0.56	0.11	1.14	0.17	0.87	0.10	0.93	0.08	1.00	0.12	0.45

Table 3.3: Hf and Nd isotopic compositions of rocks from the Hope Bay Greenstone Belt.

Sample no.1	84536	84541	84544	202915	84545	84572	84574	84573	84557	84576	84577	84579
Suite	Member basalts	Member basalts	Member basalts	Boston Basalt	Clover east basalts	Clover east basalts	Clover east basalts	Clover Lake Suite	Clover west basalts	Clover west basalts	Clover west basalts	Clover west basalts
Rock Type	Normal Basalt	Normal Basalt	Normal Basalt	Normal Basalt	Normal Basalt	Normal Basalt	LREE Basalt	Rhyolite	Normal Basalt	Normal Basalt	Normal Basalt	Normal Basalt
Northing	442606	441884	441320	441033	439452	438902	438811	438196	436704	437337	437045	436006
Easting	7514639	7514093	7512181	7504174	7507669	7507363	7506770	7506733	7502763	7505892	7505239	7505604
Lu (ppm)	0.29	0.41	0.34	0.24	0.25	0.21	0.25	0.05	0.38	0.38	0.41	0.41
Hf (ppm)	1.02	1.90	1.28	1.16	1.15	0.74	2.76	2.10	1.55	1.75	1.51	1.46
Lu/Hf	0.284	0.215	0.266	0.206	0.217	0.284	0.092	0.021	0.248	0.218	0.273	0.279
$^{176}Lu/^{177}Hf$	0.0404	0.0305	0.0379	0.0293	0.0309	0.0403	0.0130	0.0030	0.0352	0.0309	0.0388	0.0396
$^{176}Hf/^{177}Hf$ (m)	0.283187	0.282739	0.282877	0.282544	0.282746	0.283154	0.281860	0.281328	0.282933	0.282771	0.282746	0.282742
2σ	0.000014	0.000009	0.000006	0.000010	0.000013	0.000026	0.000005	0.000005	0.000011	0.000014	0.000006	0.000005
$^{176}Hf/^{177}Hf$ (i)	0.28112	0.28118	0.28094	0.28104	0.28116	0.28109	0.28119	0.28117	0.28113	0.28119	0.28076	0.28071
ε_{Hf} (i)	1.6	3.7	-4.7	-1.0	3.3	0.6	4.4	3.6	2.1	4.1	-11.1	-12.8
t_{CHUR} (Ga)	3.00	0.65	1.20	3.06	0.59	2.80	2.37	2.51	4.14	0.04		
t_{DM} (Ga)	8.84	2.06	5.57	2.78	2.11	6.52	2.43	2.53	1.97	1.98	13.93	36.65
Sm (ppm)	2.04	2.62	2.10	1.58	1.52	1.40	2.94	1.64	2.80	2.98	2.56	2.55
Nd (ppm)	6.30	8.49	6.57	5.30	4.75	4.44	13.30	8.95	9.70	10.27	8.08	7.33
Sm/Nd	0.324	0.309	0.320	0.298	0.320	0.315	0.221	0.183	0.289	0.290	0.317	0.348
$^{147}Sm/^{144}Nd$	0.1958	0.1866	0.1935	0.1802	0.1935	0.1906	0.1336	0.1107	0.1745	0.1754	0.1916	0.2103
$^{143}Nd/^{144}Nd$ (m)	0.512835	0.512626	0.512789	0.512555	0.512746	0.512808	0.511727	0.511289	0.512445	0.512464	0.512774	0.512990
2σ	0.000007	0.000008	0.000005	0.000006	0.000006	0.000005	0.000005	0.000004	0.000006	0.000006	0.000004	0.000004
$^{143}Nd/^{144}Nd$ (i)	0.50937	0.50933	0.50937	0.50937	0.50933	0.50944	0.50936	0.50933	0.50936	0.50936	0.50939	0.50927
ε_{Nd} (i)	4.2	3.2	4.0	4.1	3.2	5.4	4.0	3.3	3.9	3.9	4.4	2.1
t_{CHUR} (Ga)		0.18		0.77			2.19	2.38	1.33	1.25		3.87
t_{DM} (Ga)	2.66	2.92	2.71	2.69	3.02	2.25	2.69	2.74	2.73	2.72	2.57	7.10

All Hf isotopic ratios determined by MC-ICP-MS, Nd isotopic ratios determined by TIMS, and concentration data by HR-ICP-MS at the PCIGR, UBC. Initial ratios calculated at 2.68 Ga using $\lambda^{144Sm} = 6.54 \times 10^{-12}$ (Lugmair & Marti, 1978) and $\lambda^{176}Lu = 1.865 \times 10^{-11}$ y^{-1} (Scherer et al., 2001).

Epsilon values and model ages calculated using $^{177}Hf/^{176}Hf_{CHUR} = 0.282772$ and $^{176}Lu/^{177}Hf_{CHUR} = 0.0332$ (Blichert-Toft & Albarède, 1997) $^{177}Hf/^{176}Hf_{DM} = 0.28325$ and $^{176}Lu/^{177}Hf_{DM} = 0.0384$ (Salters and Stracke 2004); and $^{143}Nd/^{144}Nd_{CHUR} = 0.512638$ and $^{147}Sm/^{144}Nd_{CHUR} = 0.1967$ (DePaolo & Wasserburg, 1976), $^{143}Nd/^{144}Nd_{DM} = 0.5131$ and $^{147}Sm/^{144}Nd_{DM} = 0.2137$(Salters and Stracke 2004).

Table 3.3: Hf and Nd isotopic compositions of rocks from the Hope Bay Greenstone Belt.

Sample no.1	84581	200611	84502	84514	84589	84591	202910	84515	84516	84538	84585	84586
Suite	Clover west basalts	Clover west basalts	Flake Lake Suite	Flake Lake Suite	Flake Lake Suite	Flake Lake Suite	Gas Cache	Bend Basalt	Bend Basalt	Bend Basalt	Koignuck Suite	Koignuck Suite
Rock Type	Normal Basalt	Normal Basalt	Felsic	Felsic	Felsic	Felsic	Ti Enriched Al Depleted Basalt	Ti Enriched Basalt	Ti Enriched Basalt	Ti Enriched Basalt	Dacite	Dacite
Northing	436498	435180	445855	446046	445066	444650	436986	444625	443962	443331	434569	433606
Easting	7504990	7505521	7519179	7518893	7513292	7515305	7532167	7514723	7515325	7515307	7505768	7505416
Lu (ppm)	0.28	0.21	1.90	2.16	1.29	1.90	0.36	0.71	0.49	0.40	0.17	0.19
Hf (ppm)	0.94	0.89	10.94	13.90	10.80	10.80	4.80	3.10	1.93	1.36	3.75	4.30
Lu/Hf	0.298	0.230	0.174	0.155	0.119	0.176	0.075	0.229	0.255	0.294	0.046	0.045
$^{176}Lu/^{177}Hf$	0.0423	0.0327	0.0247	0.0221	0.0169	0.0250	0.0106	0.0325	0.0363	0.0418	0.0066	0.0064
$^{176}Hf/^{177}Hf$ (m)	0.283144	0.282777	0.282360	0.282499	0.282930	0.282348	0.281737	0.282860	0.282885	0.283327	0.281537	0.281559
2σ	0.000012	0.000009	0.000004	0.000004	0.000004	0.000003	0.000004	0.000006	0.000005	0.000009	0.000005	0.000004
$^{176}Hf/^{177}Hf$ (i)	0.28097	0.28110	0.28110	0.28137	0.28206	0.28107	0.28119	0.28119	0.28102	0.28119	0.28120	0.28123
ε_{Hf} (i)	-3.4	1.1	0.9	10.6	35.3	-0.1	4.4	4.3	-1.6	4.1	4.6	5.8
t_{CHUR} (Ga)	2.14	-0.62	2.53	1.30		2.70	2.40		1.93	3.36	2.43	2.37
t_{DM} (Ga)	0.73	2.41	2.57	1.80	0.42	2.66	2.45	1.78	3.19	6.07	2.47	2.42
Sm (ppm)	2.08	1.68	10.10	11.80	14.80	17.90	9.16	4.70	3.18	3.01	2.70	2.72
Nd (ppm)	6.80	6.00	34.00	44.00	72.80	82.00	42.10	16.10	10.10	9.30	14.00	13.90
Sm/Nd	0.306	0.280	0.297	0.268	0.203	0.218	0.218	0.292	0.315	0.324	0.193	0.196
$^{147}Sm/^{144}Nd$	0.1849	0.1693	0.1796	0.1621	0.1229	0.1319	0.1315	0.1765	0.1904	0.1957	0.1166	0.1183
$^{143}Nd/^{144}Nd$ (m)	0.512595	0.512427	0.512239	0.512036	0.511640	0.511631	0.511682	0.512368	0.512760	0.512785	0.511387	0.511382
2σ	0.000005	0.000006	0.000005	0.000005	0.000006	0.000007	0.000005	0.000007	0.000007	0.000007	0.000004	0.000008
$^{143}Nd/^{144}Nd$ (i)	0.50933	0.50943	0.50906	0.50917	0.50947	0.50930	0.50936	0.50925	0.50939	0.50932	0.50933	0.50929
ε_{Nd} (i)	3.2	5.3	-1.9	0.2	6.0	2.7	3.8	1.7	4.6	3.2	3.2	2.5
t_{CHUR} (Ga)	0.56	1.18	3.54	2.64	2.06	2.36	2.23	2.04			2.37	2.43
t_{DM} (Ga)	2.92	2.47	4.03	3.27	2.52	2.82	2.71	3.18	2.53	3.07	2.75	2.81

All Hf isotopic ratios determined by MC-ICP-MS, Nd isotopic ratios determined by TIMS, and concentration data by HR-ICP-MS at the PCIGR, UBC. Initial ratios calculated at 2.68 Ga using $\lambda^{144Sm} = 6.54\times10^{-12}$ (Lugmair & Marti, 1978) and $\lambda^{176}Lu = 1.865\times10^{-11}$ y^{-1} (Scherer et al., 2001).

Epsilon values and model ages calculated using $^{177}Hf/^{176}Hf_{CHUR} = 0.282772$ and $^{176}Lu/^{177}Hf_{CHUR} = 0.0332$ (Blichert-Toft & Albarède, 1997) $^{177}Hf/^{176}Hf_{DM} = 0.28325$ and $^{176}Lu/^{177}Hf_{DM} = 0.0384$ (Salters and Stracke 2004); and $^{143}Nd/^{144}Nd_{CHUR} = 0.512638$ and $^{147}Sm/^{144}Nd_{CHUR} = 0.1967$ (DePaolo & Wasserburg, 1976), $^{143}Nd/^{144}Nd_{DM} = 0.5131$ and $^{147}Sm/^{144}Nd_{DM} = 0.2137$(Salters and Stracke 2004).

Table 3.3: Hf and Nd isotopic compositions of rocks from the Hope Bay Greenstone Belt.

Sample no.1	200632	202929	202940	202943	84626	202930	84521	84551	202931	202918	200649
Suite	Koignuck Suite	Patch Lake Mafics	Patch Lake Mafics	Patch Lake Mafics	Windy Basalts	Windy Basalts	Windy Felsics	Windy Felsics	Windy Felsics	Wolverine Basalts	Wolverine Basalts
Rock Type	Dacite	Ti Enriched Basalt	Ti Enriched Al Depleted Basalt	Ti Enriched Basalt	Normal Basalt	Normal Basalt	Felsic	Felsic/sedimentry	felsic	Normal Basalt	Normal Basalt
Northing	434808	433764	434297	433968	433898	433092	438992	439610	432493	434048	436630
Easting	7505652	7551849	7550413	7551527	7550638	7551626	7514291	7511094	7551376	7547623	7545657
Lu (ppm)	0.14	0.49	0.42	0.46	0.26	0.38	0.20	0.09	0.11	0.24	0.39
Hf (ppm)	4.20	2.22	4.78	2.01	1.31	1.46	3.59	3.07	3.26	0.98	1.31
Lu/Hf	0.032	0.222	0.087	0.229	0.201	0.261	0.057	0.031	0.034	0.247	0.298
$^{176}Lu/^{177}Hf$	0.0046	0.0316	0.0124	0.0325	0.0285	0.0370	0.0080	0.0043	0.0048	0.0350	0.0424
$^{176}Hf/^{177}Hf$ (m)	0.281463	0.282785	0.281802	0.282849	0.282609	0.282666	0.281549	0.281467	0.281391	0.282914	0.282937
2σ	0.000005	0.000007	0.000005	0.000008	0.000012	0.000008	0.000006	0.000004	0.000041	0.000030	0.000005
$^{176}Hf/^{177}Hf$ (i)	0.28123	0.28117	0.28117	0.28118	0.28115	0.28077	0.28114	0.28124	0.28114	0.28112	0.28076
ε_{Hf} (i)	5.6	3.5	3.4	4.0	2.7	-10.8	2.4	6.2	2.6	1.7	-10.9
t_{CHUR} (Ga)	2.40		2.44	-6.37	1.83		2.54	2.37	2.55	3.97	0.95
t_{DM} (Ga)	2.44	2.04	2.49	1.85	2.30	7.51	2.56	2.42	2.56	2.10	-4.09
Sm (ppm)	2.38	3.35	9.40	2.86	1.82	2.47	3.70	1.80	2.00	1.49	2.09
Nd (ppm)	12.50	10.54	43.50	9.00	6.32	7.70	20.40	8.80	9.90	4.70	6.35
Sm/Nd	0.190	0.318	0.216	0.318	0.288	0.320	0.181	0.205	0.202	0.317	0.329
$^{147}Sm/^{144}Nd$	0.1151	0.1923	0.1306	0.1921	0.1741	0.1936	0.1096	0.1236	0.1221	0.1917	0.1991
$^{143}Nd/^{144}Nd$ (m)	0.511337	0.512755	0.511653	0.512703	0.512513	0.512775	0.511233	0.511316	0.511437	0.512823	0.512922
2σ	0.000007	0.000007	0.000005	0.000005	0.000006	0.000006	0.000007	0.000006	0.000007	0.000005	0.000007
$^{143}Nd/^{144}Nd$ (i)	0.50930	0.50935	0.50934	0.50931	0.50943	0.50935	0.50930	0.50913	0.50928	0.50943	0.50940
ε_{Nd} (i)	2.8	3.8	3.6	2.8	5.4	3.7	2.6	-0.6	2.3	5.3	4.7
t_{CHUR} (Ga)	2.42		2.27		0.85		2.45	2.75	2.45		16.52
t_{DM} (Ga)	2.78	2.80	2.73	3.13	2.44	2.83	2.79	3.08	2.83	2.25	2.37

All Hf isotopic ratios determined by MC-ICP-MS, Nd isotopic ratios determined by TIMS, and concentration data by HR-ICP-MS at the PCIGR, UBC. Initial ratios calculated at 2.68 Ga using $\lambda^{144Sm} = 6.54 \times 10^{-12}$ (Lugmair & Marti, 1978) and $\lambda^{176}Lu = 1.865 \times 10^{-11}$ y^{-1} (Scherer et al., 2001).

Epsilon values and model ages calculated using $^{177}Hf/^{176}Hf_{CHUR} = 0.282772$ and $^{176}Lu/^{177}Hf_{CHUR} = 0.0332$ (Blichert-Toft & Albarède, 1997) $^{177}Hf/^{176}Hf_{DM} = 0.28325$ and $^{176}Lu/^{177}Hf_{DM} = 0.0384$ (Salters and Stracke 2004); and $^{143}Nd/^{144}Nd_{CHUR} = 0.512638$ and $^{147}Sm/^{144}Nd_{CHUR} = 0.1967$ (DePaolo & Wasserburg, 1976), $^{143}Nd/^{144}Nd_{DM} = 0.5131$ and $^{147}Sm/^{144}Nd_{DM} = 0.2137$(Salters and Stracke 2004).

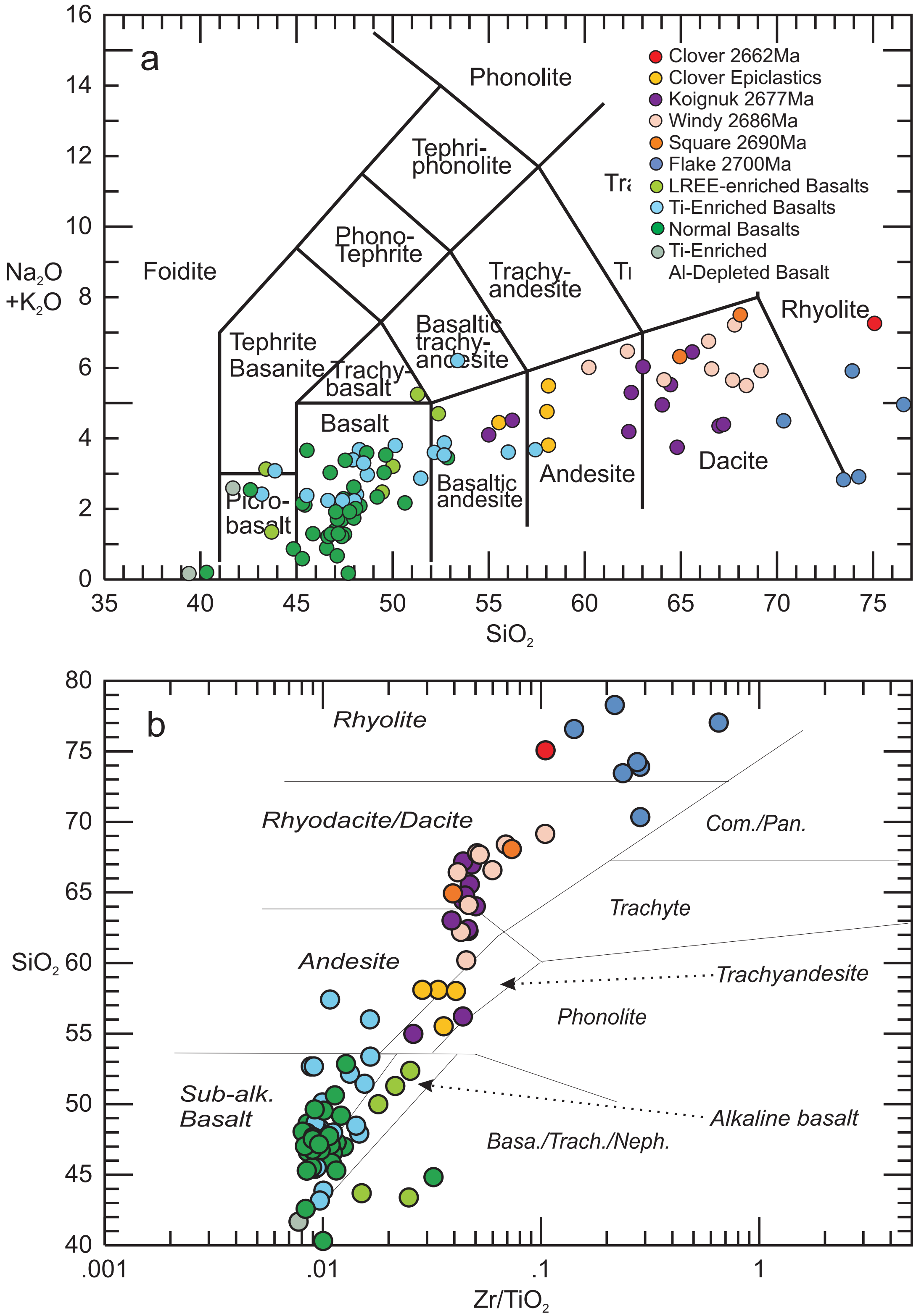

Figure 3.1: **a)** Alkali vs SiO_2 plot of volcanic rocks in this study after Le Bas et al. (1986) **b)** SiO_2 vs Zr/TiO_2 plot of volcanic rocks from the Hope Bay Greenstone Belt in this study after Winchester and Floyd (1977)

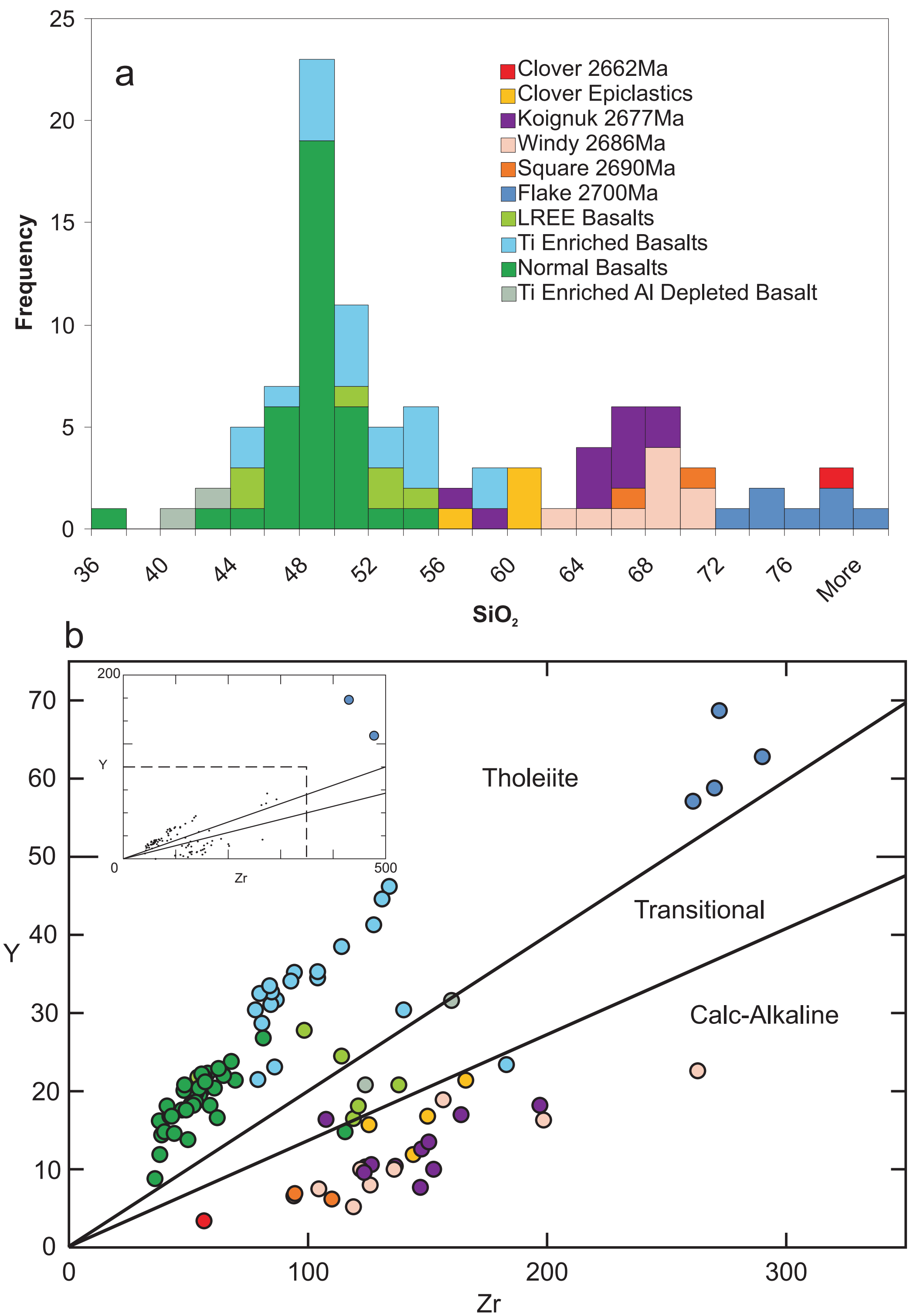

Figure 3.2: **a)** Histogram of SiO_2 for samples from mafic and felsic volcanic lithologies of the Hope Bay Greenstone Belt **b)** Zr vs. Y of samples from mafic and felsic volcanic lithologies of the Hope Bay Greenstone Belt MacLean and Barret (1993)

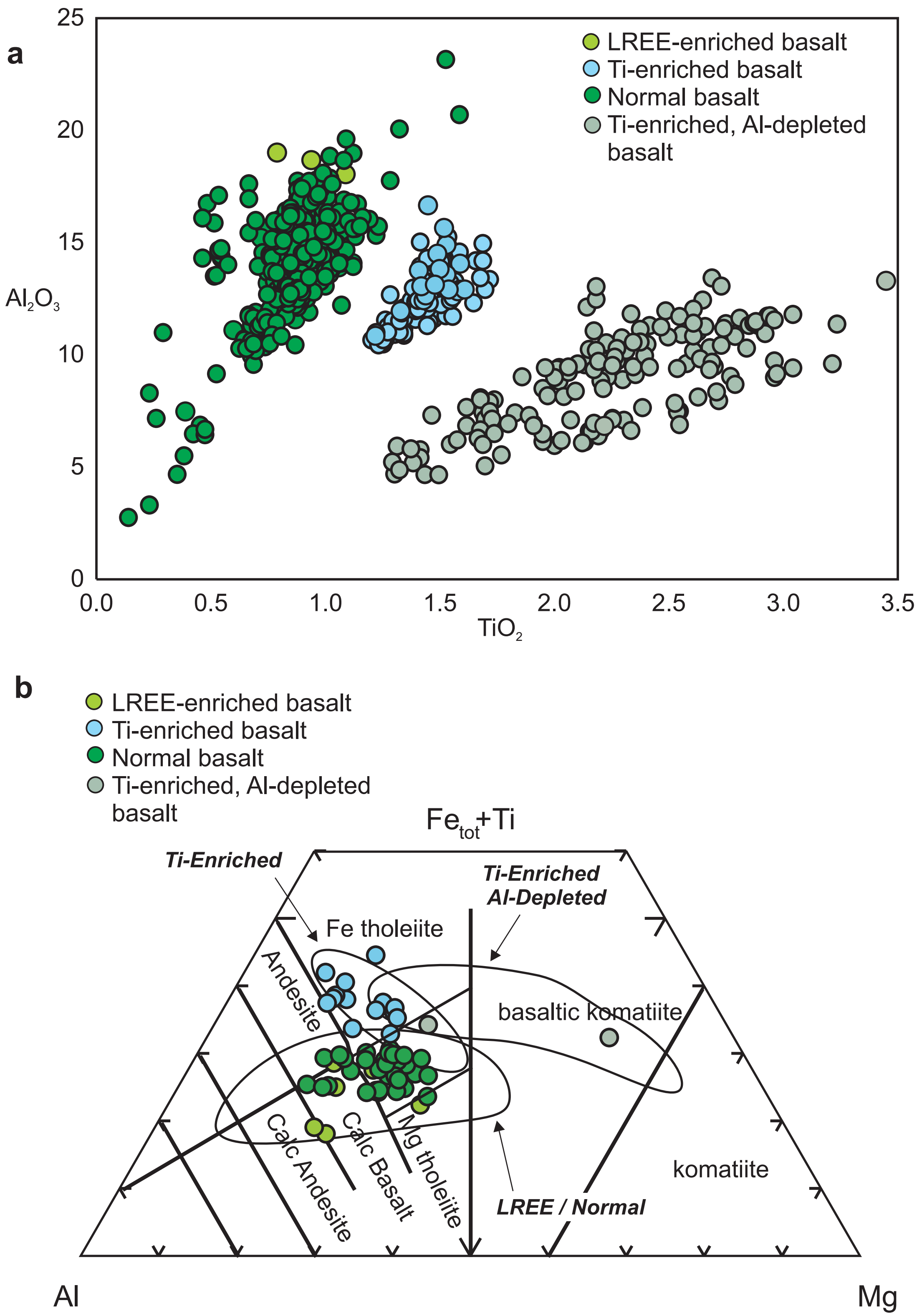

Figure 3.3: **a)** Al_3O_2 vs TiO_2 plot of all basalts in the Hope Bay Greenstone Belt, from this study and Mirimar Dataset **b)** Modified AFM diagram of least altered rocks from the Hope Bay Greenstone Belt (Jensen; 1976; Grunsky at al. 1992)

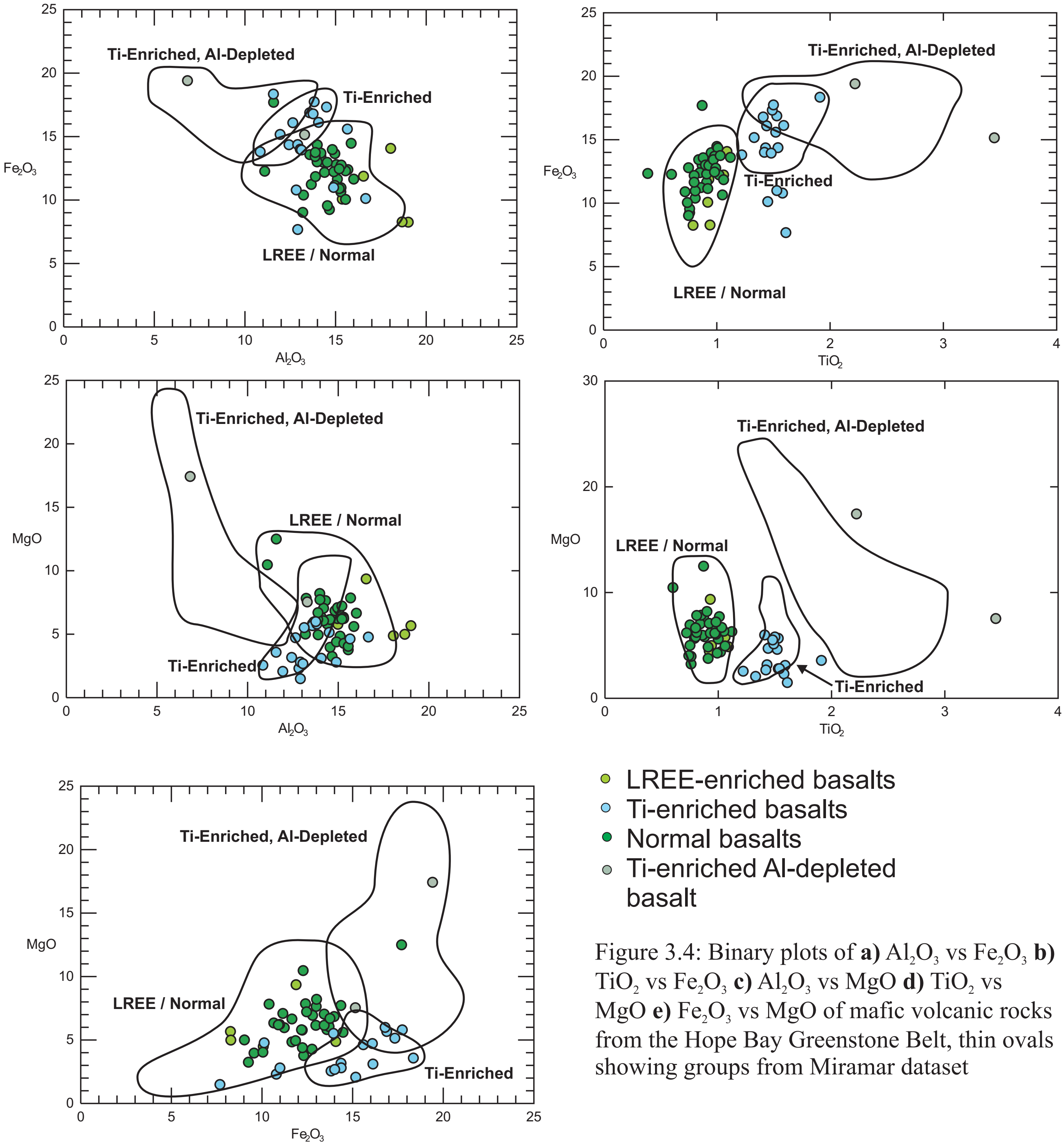

Figure 3.4: Binary plots of **a)** Al_2O_3 vs Fe_2O_3 **b)** TiO_2 vs Fe_2O_3 **c)** Al_2O_3 vs MgO **d)** TiO_2 vs MgO **e)** Fe_2O_3 vs MgO of mafic volcanic rocks from the Hope Bay Greenstone Belt, thin ovals showing groups from Miramar dataset

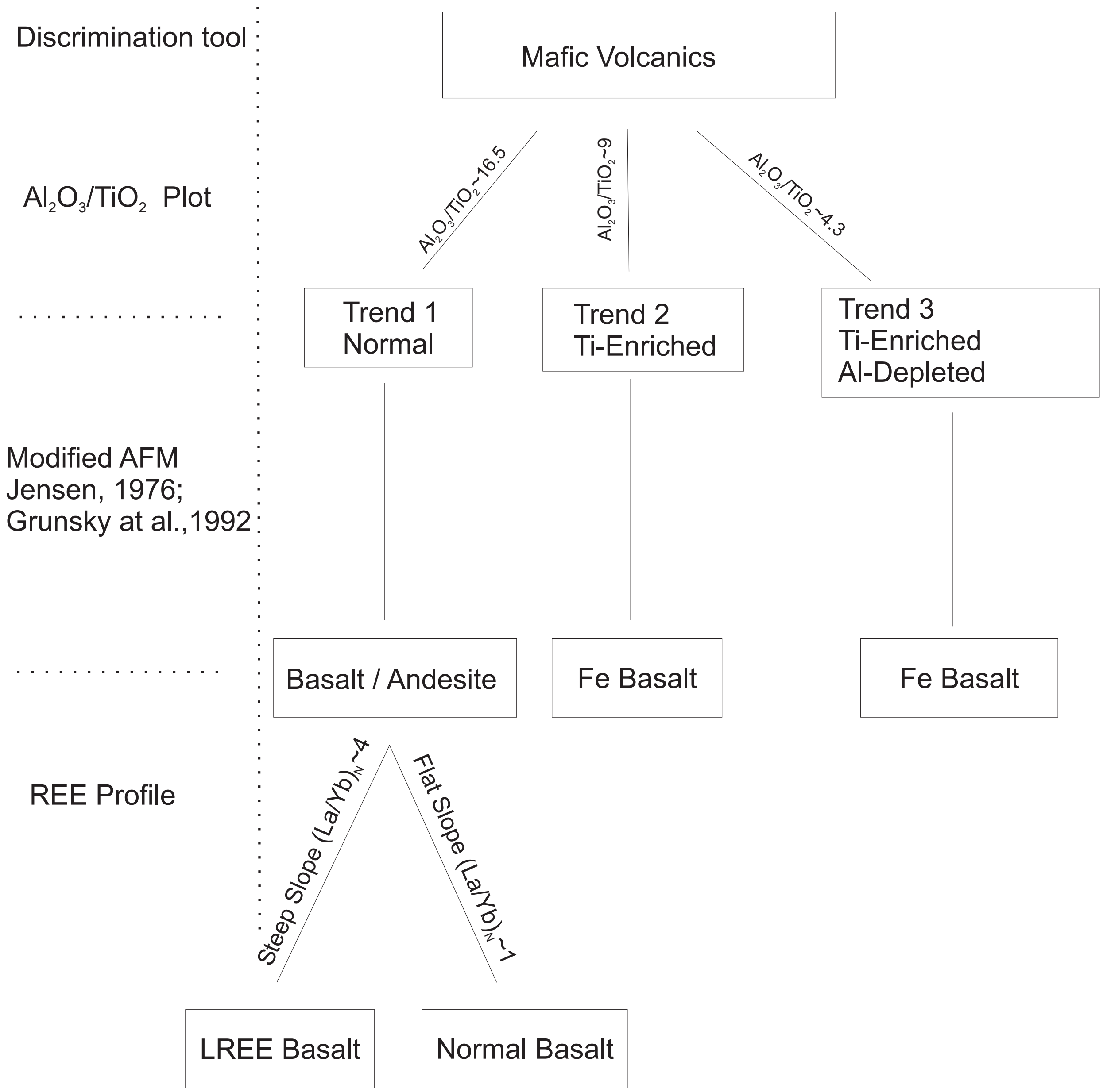

Descriptive Name	LREE-enriched Basalt	Normal Basalt	Fe-, Ti-Enriched Basalt	Fe-, Ti-Enriched, Al-Depleted Basalt
Group Name for this study	LREE- enriched Basalt Group	Normal Basalt Group	Ti-Enriched Basalt Group	Ti-Enriched, Al-Depleted Basalt Group
Short name for figures	LREE	Normal	Ti-enriched	Ti-enriched, Al-depleted

Figure 3.5 Flow diagram describing filtering of geochemical data to determining mafic volcanic groups

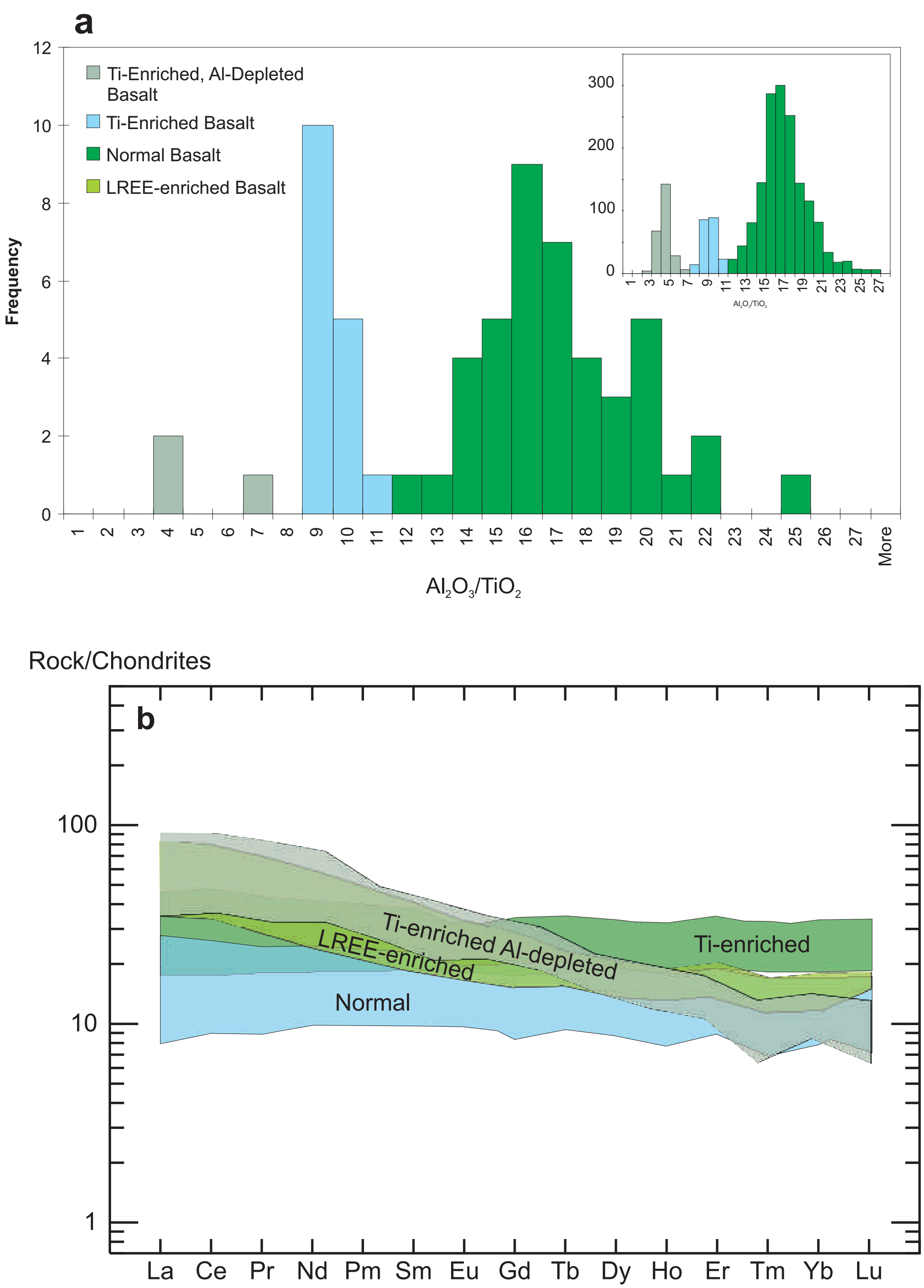

Figure 3.6: **a)** Histogram of TiO_2 concentration of mafic volcanic rocks from the Hope Bay Greenstone Belt **b)** Chondrite normalized REE diagrams of mafic volcanic rocks from the Hope Bay Greenstone Belt with basalt groups labelled

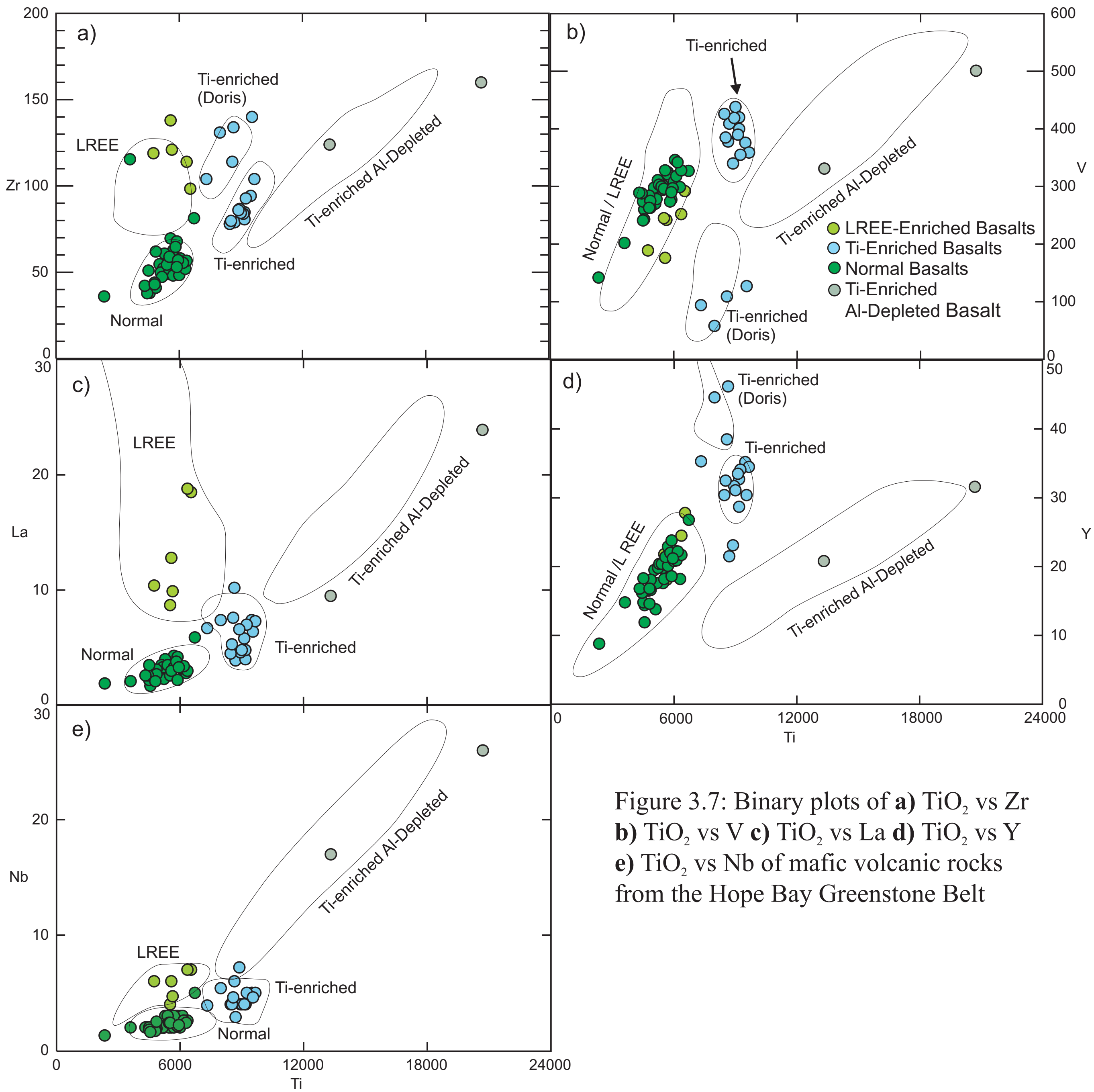

Figure 3.7: Binary plots of **a)** TiO_2 vs Zr **b)** TiO_2 vs V **c)** TiO_2 vs La **d)** TiO_2 vs Y **e)** TiO_2 vs Nb of mafic volcanic rocks from the Hope Bay Greenstone Belt

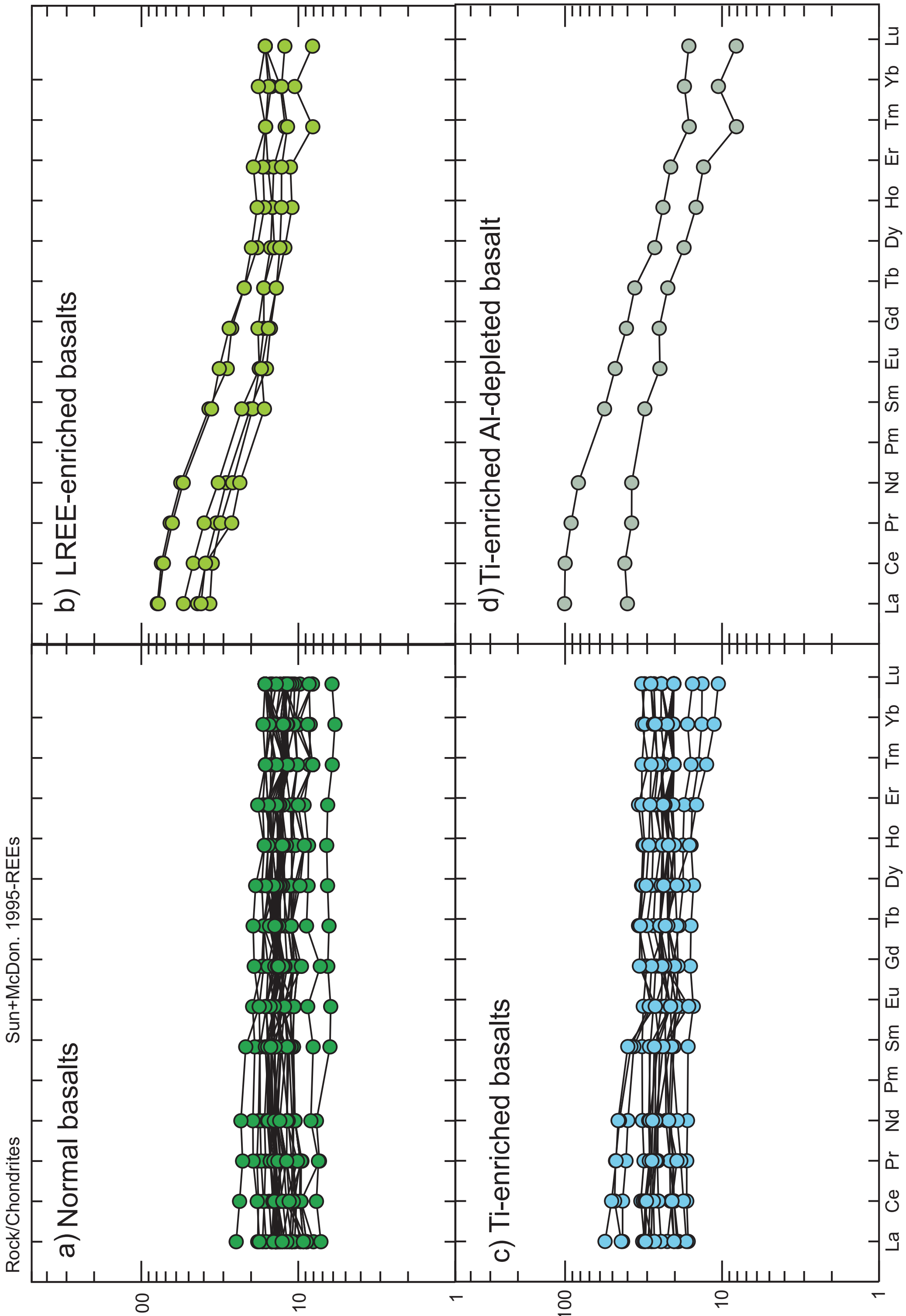

Figure 3.8: Chondrite normalized REE diagrams of **a)** LREE-enriched basalts **b)** Ti-enriched basalts **c)** Normal Basalts **d)** Ti-enriched Al-depleted basalts-basaltic komatiite from the Hope Bay Greenstone Belt after Sun and McDonough (1995)

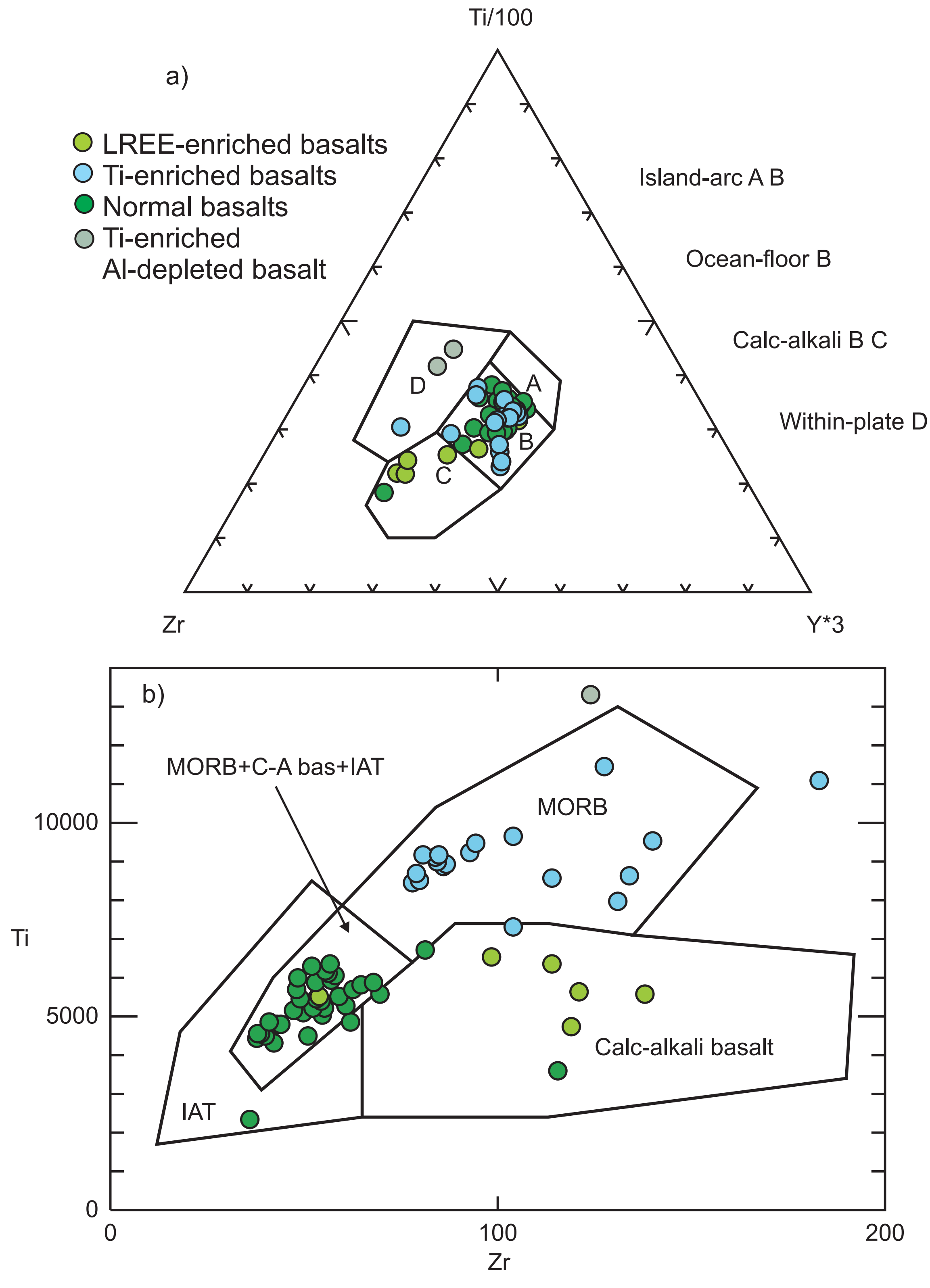

Figure 3.9: **a)** Tectonic discrimination diagram after Pearce and Cann (1973) of mafic volcanic rocks from the Hope Bay Greenstone Belt. A B: Island Arc, B: Ocean Floor B C: Calc Alkaline, D: Within Plate **b)** Tectonic discrimination diagram after Pearce and Cann (1973) of mafic volcanic rocks from the Hope Bay Greenstone Belt. IAT: Island Arc Tholeiite, MORB: Mid Ocean Ridge Basalt, C-a bas: Calc-alkaline Basalt

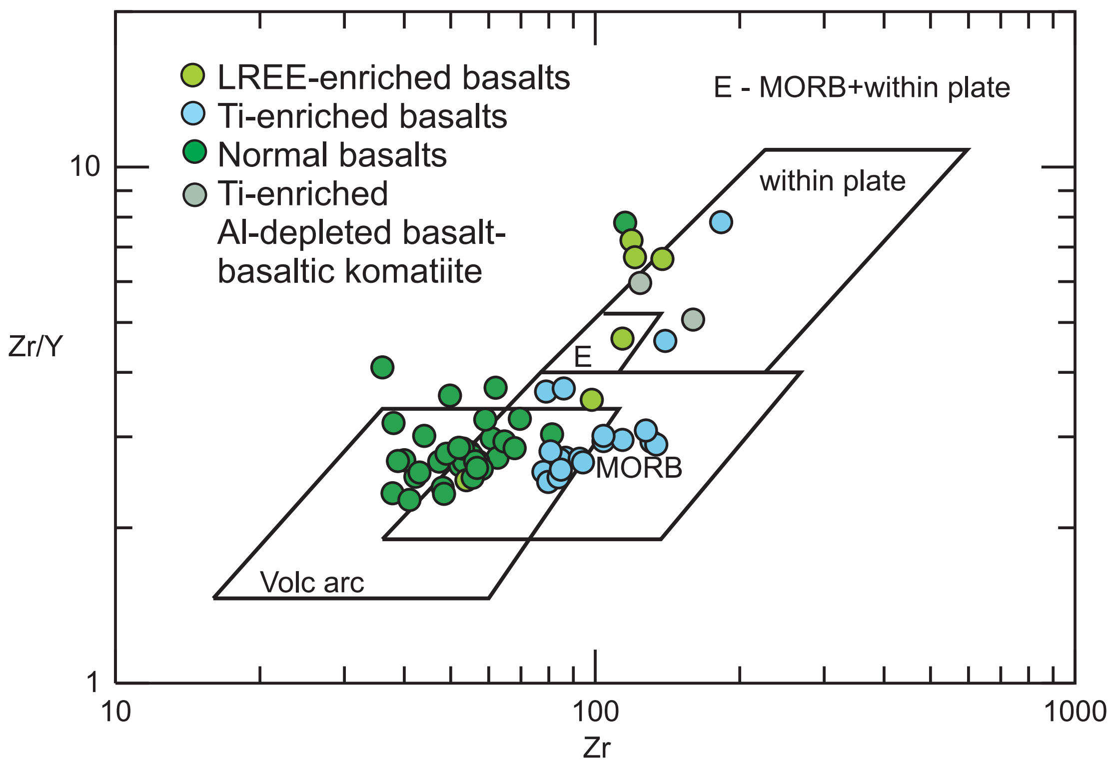

Figure 3.10 Tectonic discrimination diagram after Pearce and Norry (1979) for basalt samples collected during the course of this study. MORB: Mid Ocean Ridge Basalt

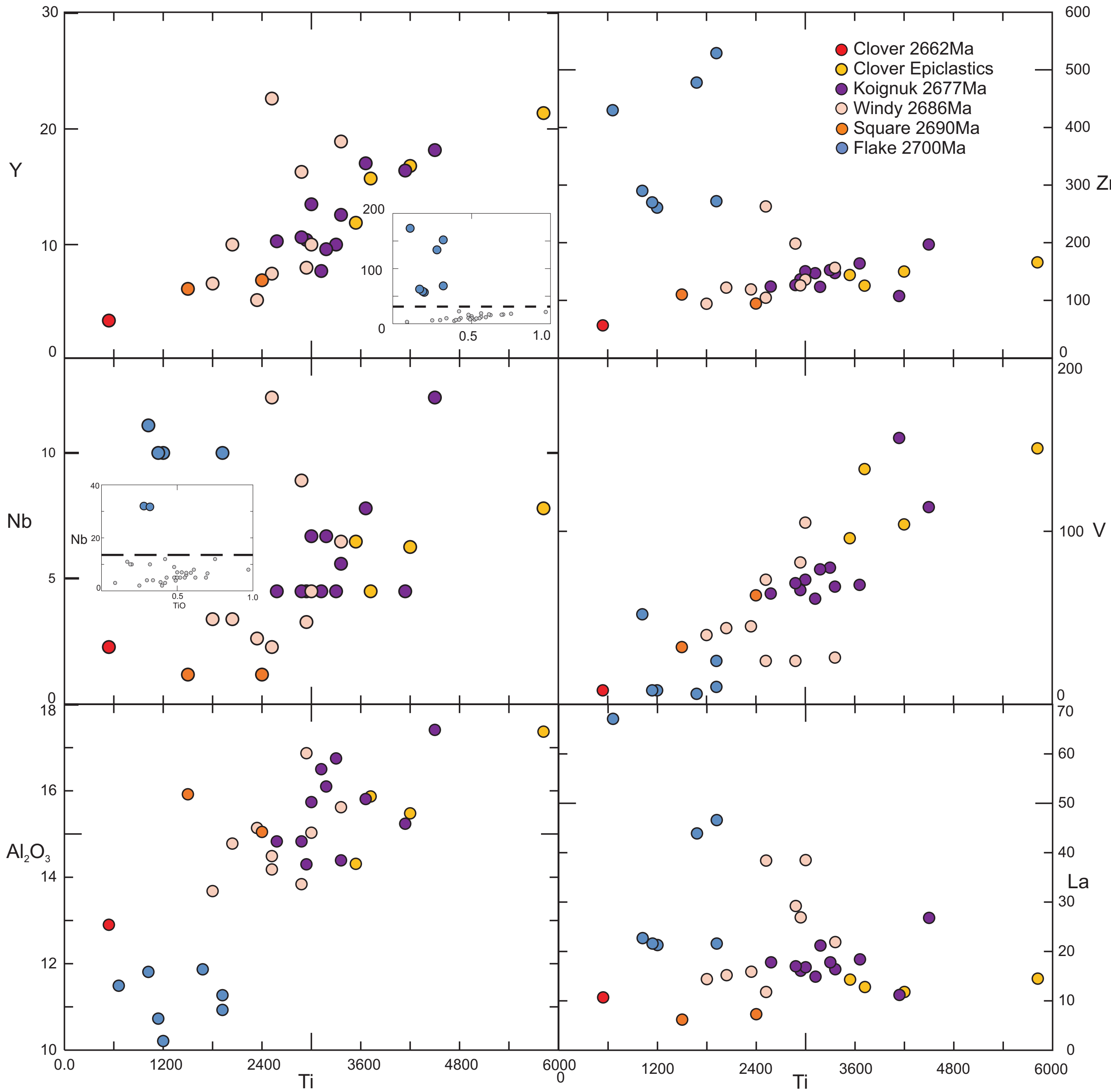

Figure 3.11: Binary plots of felsic volcanic rocks from the Hope Bay Greenstone Belt, Y vs. TiO_2 and Zr vs. TiO_2 and Nb vs. TiO_2 and V vs. TiO_2 and Al_3O_2 vs. TiO_2 and La vs. TiO_2

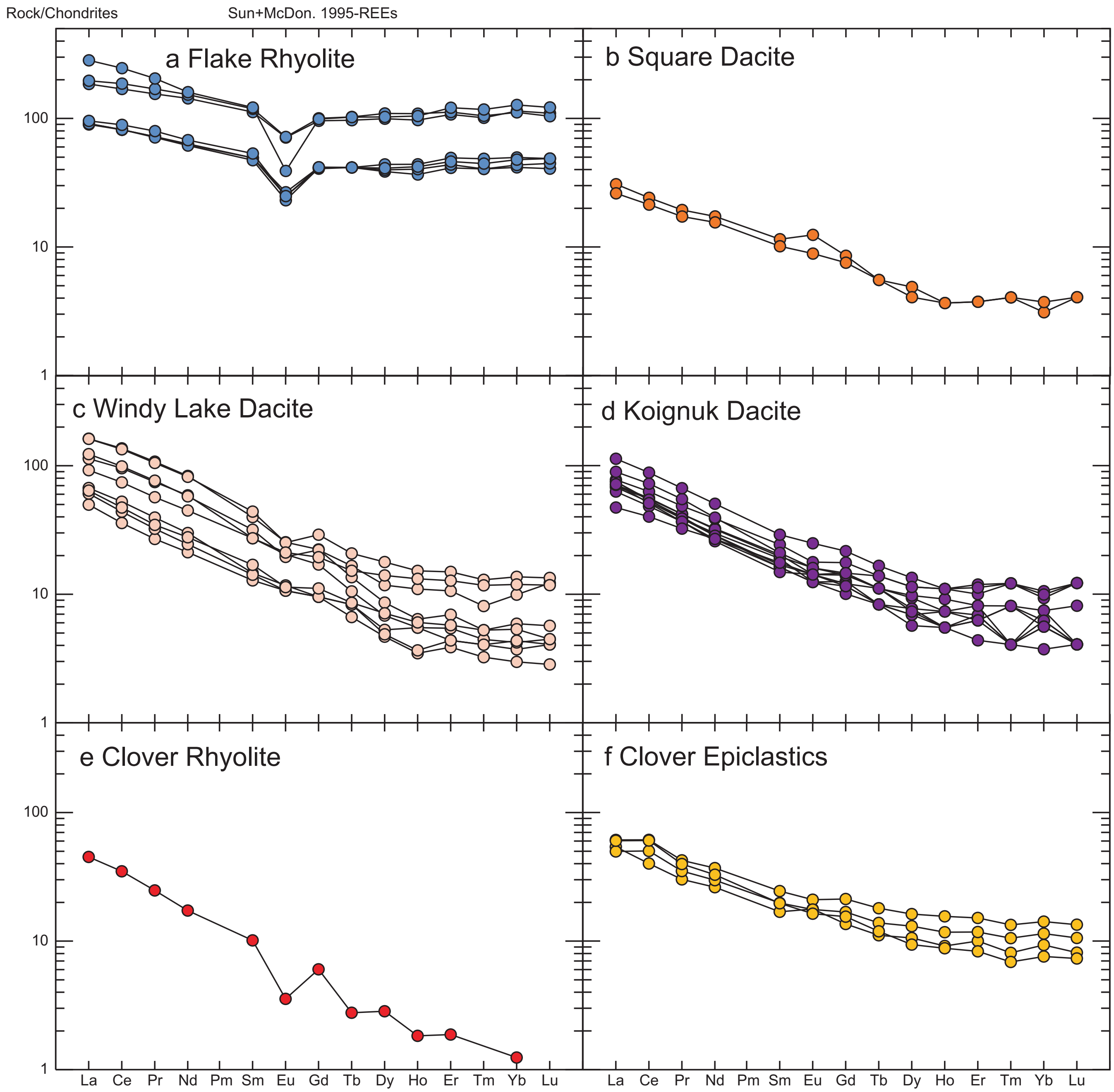

Figure 3.12 Chondrite normalized REE diagram (Sun and McDunough 1995) for the 6 felsic volcanic suites encountered in the Hope Bay Greenstone Belt

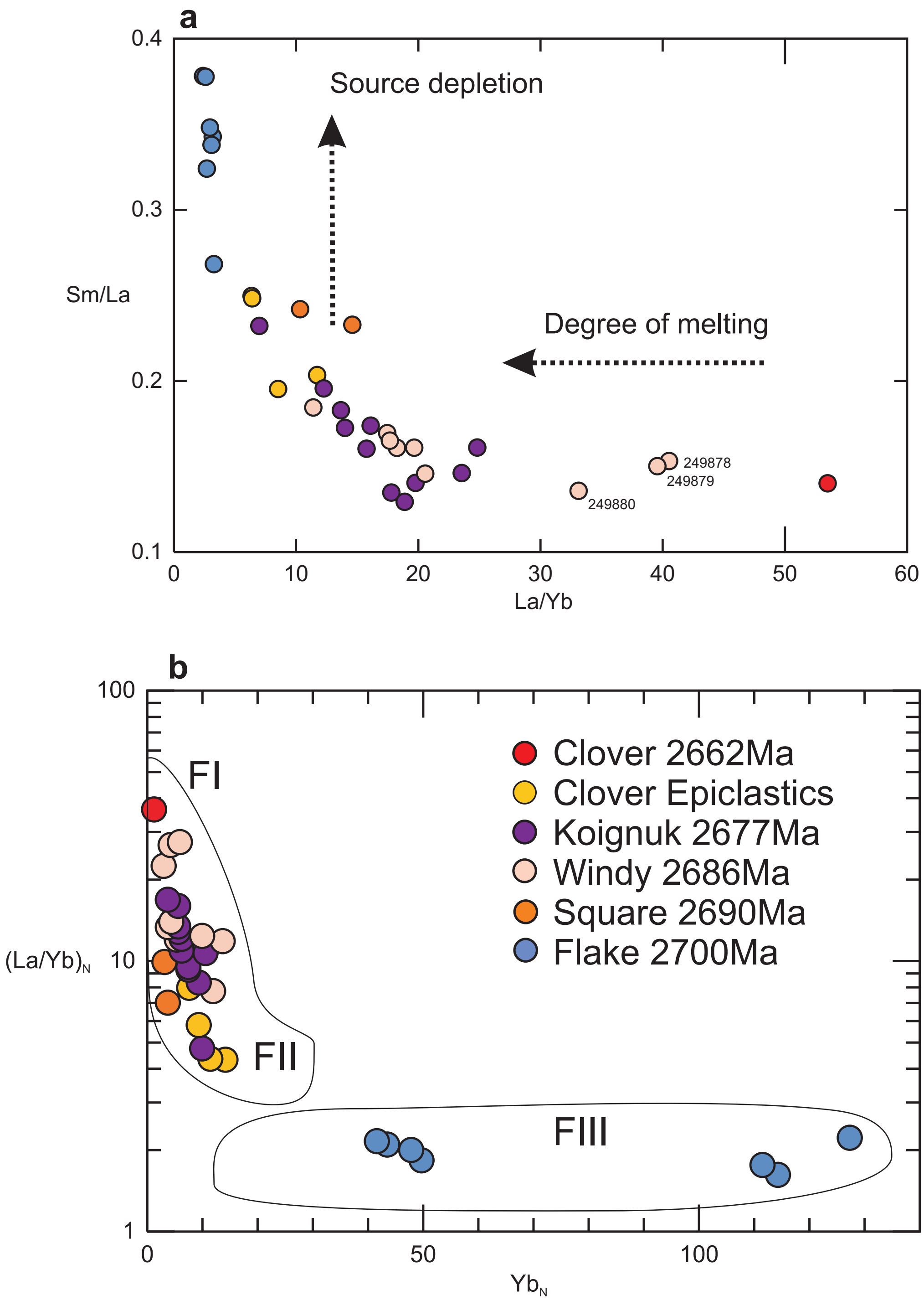

Figure 3.13: **a)** Sm/La ratio is a measure of source depleting after Plank (2005) and the La/Yb ratio is a measure of the degree of melting of mafic rocks after Cameron et al. (2002) **b)** La/Yb$_N$ vs La$_N$ of felsic volcanic rocks from Hope Bay Greenstone Belt with envelopes of FI FII and FIII rock types from Lesher et al. (1985)

Flake and CloverTransects

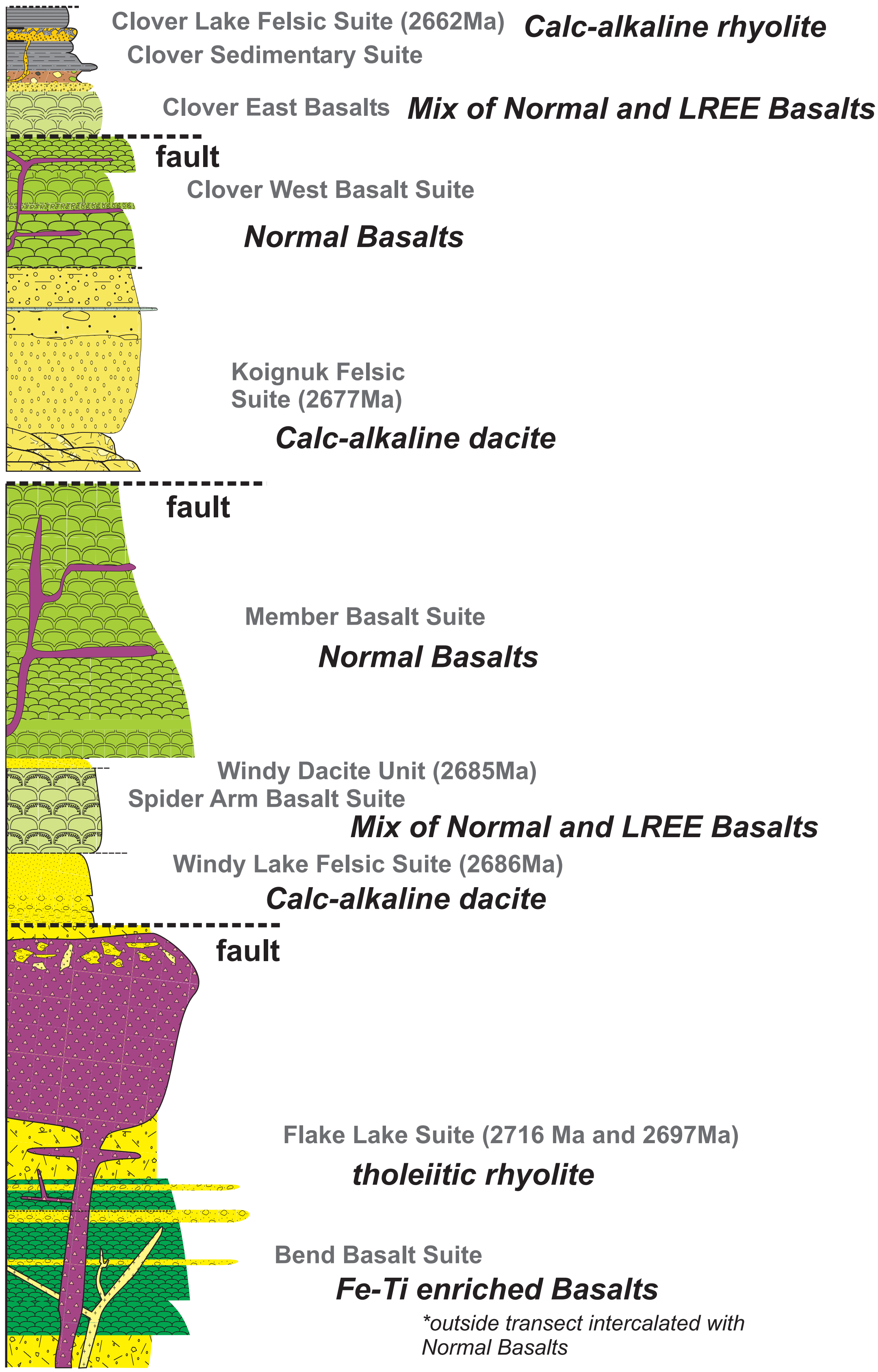

Figure 3.14: Chemo-stratigraphic reconstruction of the south part of the Hope Bay Greenstone Belt. Width of column does not represent clast or pillow size but instead is

Figure 3.15: Chemo-stratigraphic reconstruction of the north part of the Hope Bay Greenstone Belt. Width of column does not represent clast or pillow size but instead is used to easily distinguish different packages for rocks.

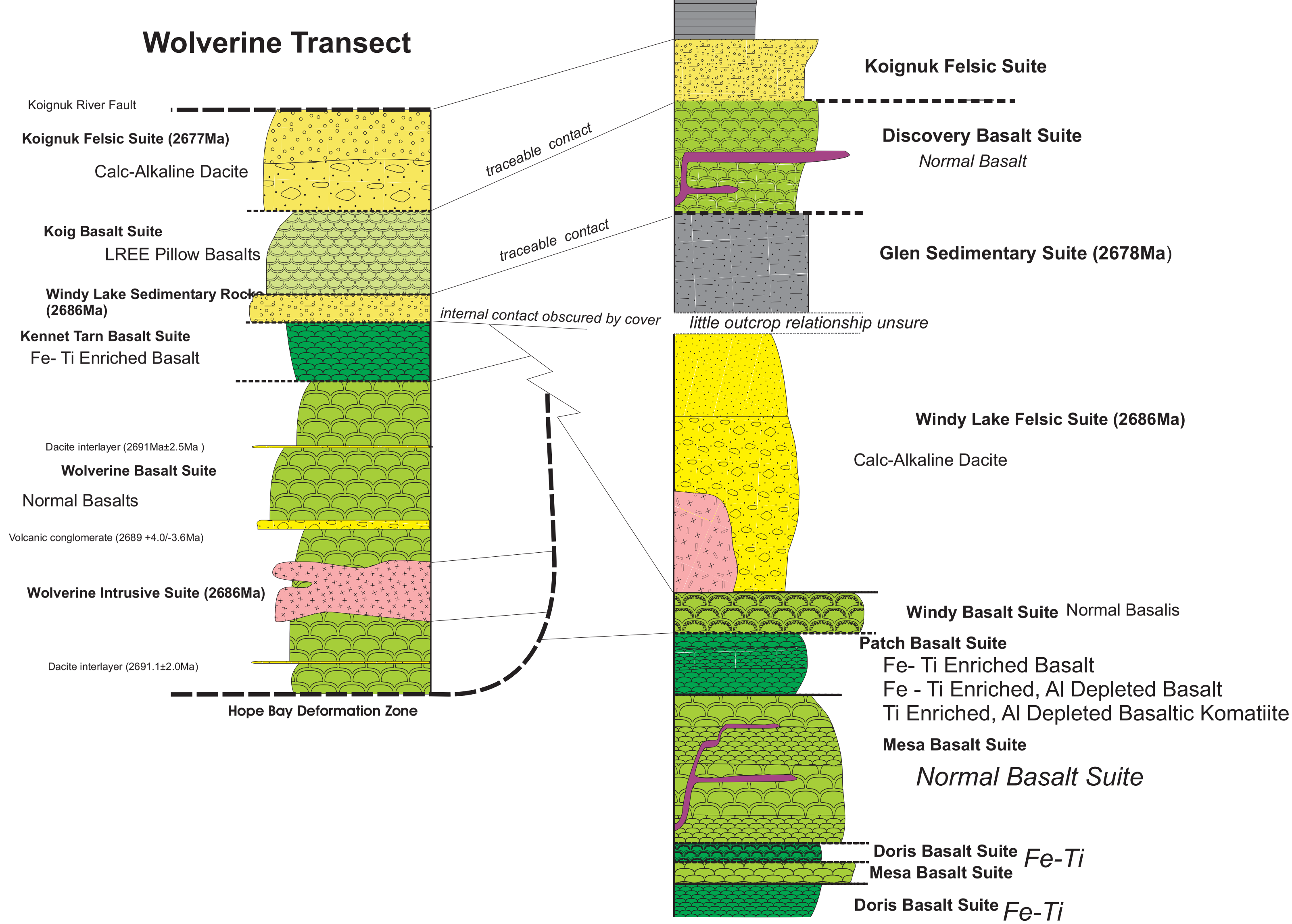

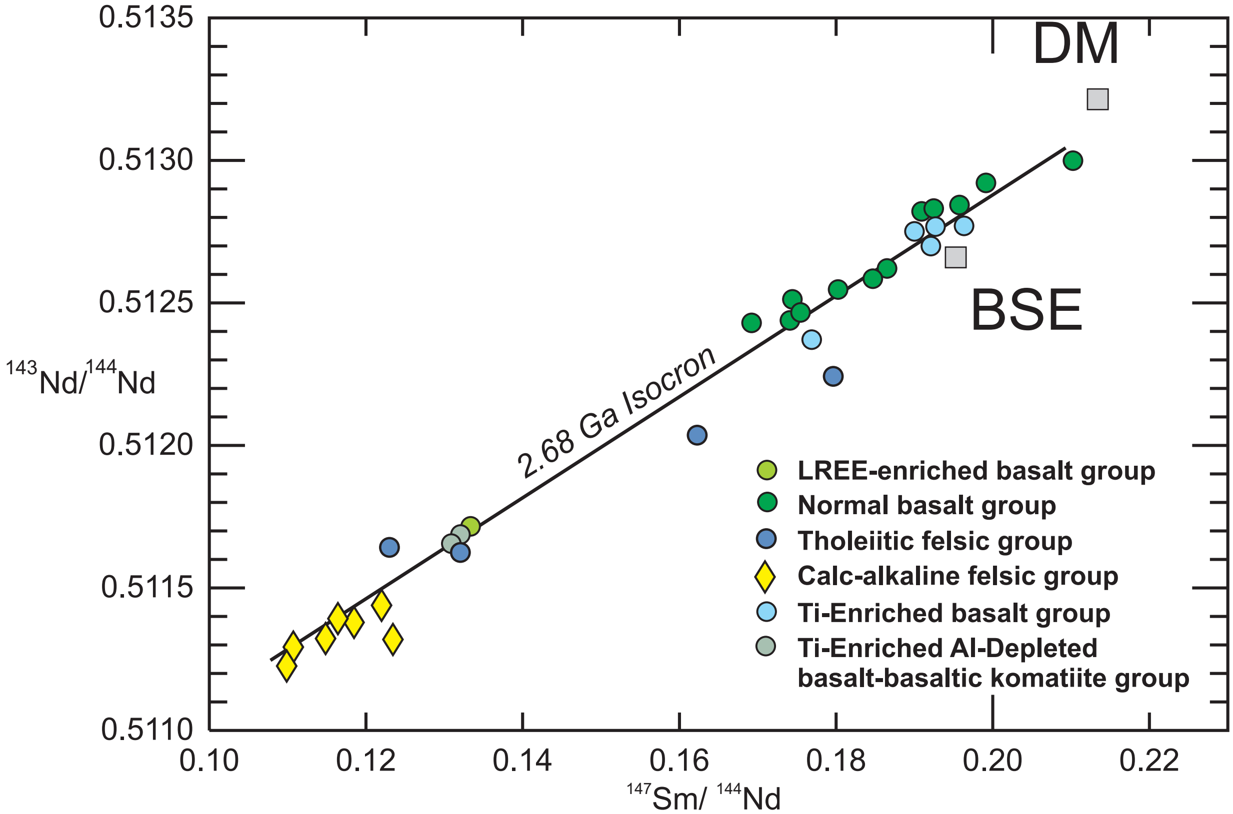

Figure 3.16: $^{143}Nd/^{144}Nd$ vs $^{147}Sm/^{144}Nd$ plot with rock groups, with 2.68Ga reference isochron as solid black line. abbreviations: BSE= Bulk Silicate Earth, DM = Depleted Mantle,

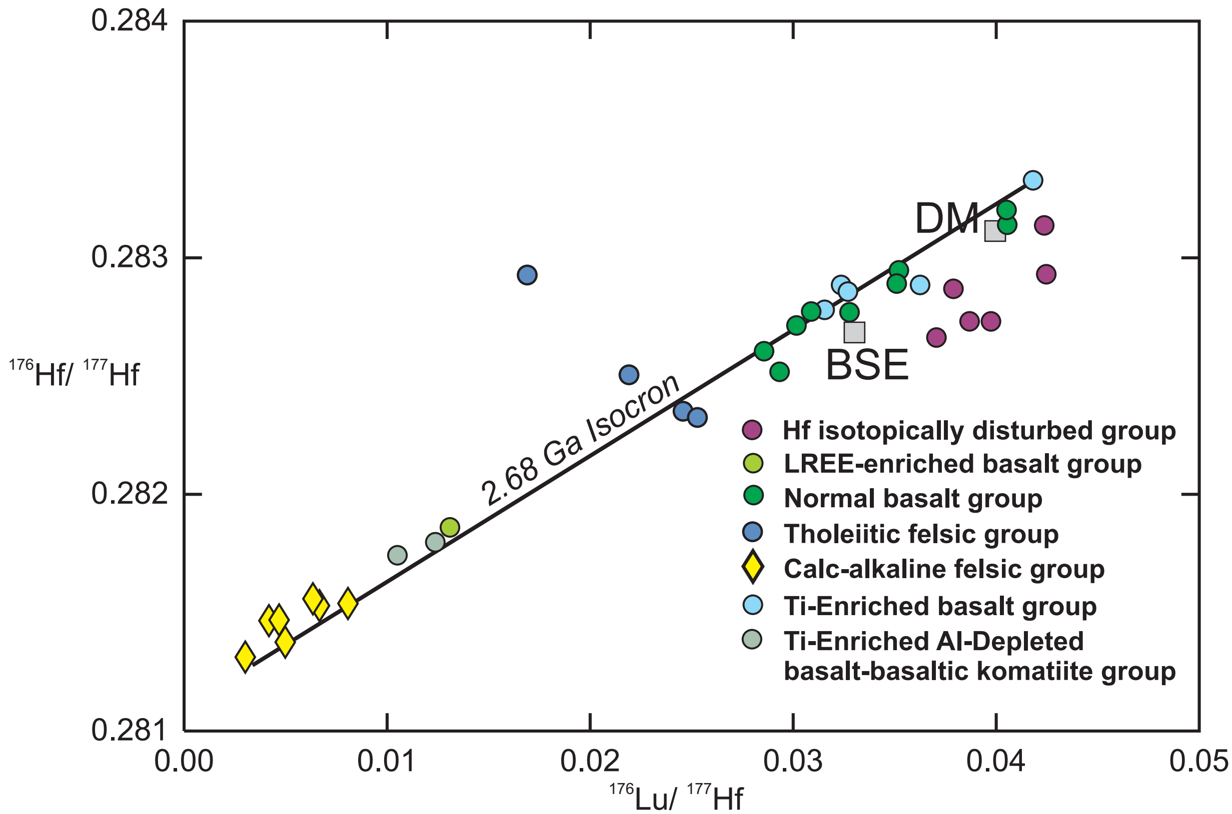

Figure 3.17: $^{176}Hf/^{177}Hf$ vs $^{176}Lu/^{177}Hf$ plot with rock groups, with 2.68Ga reference isochron as solid black line. abbreviations: BSE= Bulk Silicate Earth, DM = Depleted Mantle,

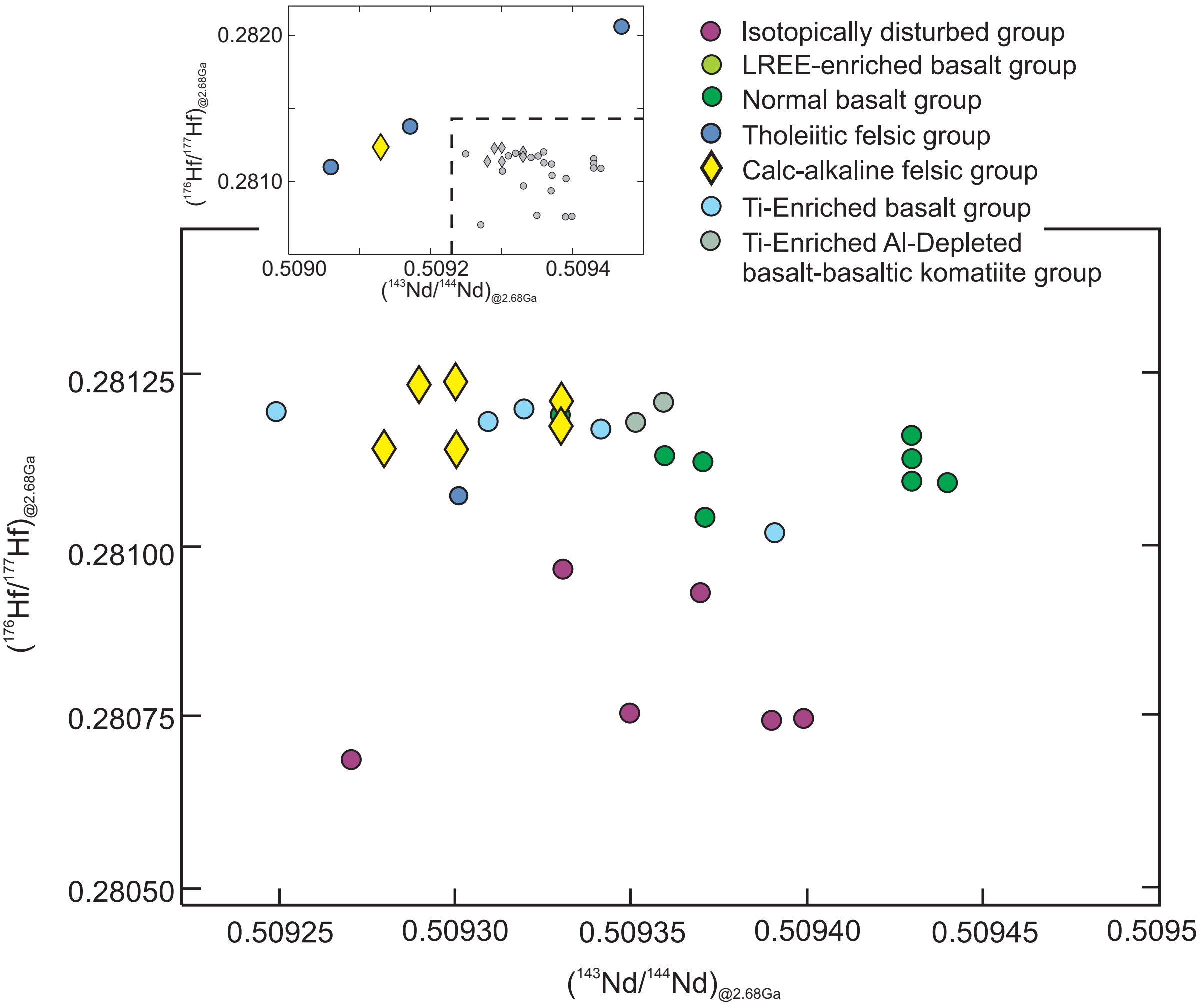

Figure 3.18: $(^{143}Nd/^{144}Nd)_{@2.68Ga}$ vs $(^{176}Hf/^{177}Hf)_{@2.68Ga}$ plot for all samples from the Hope Bay Greenstone Belt

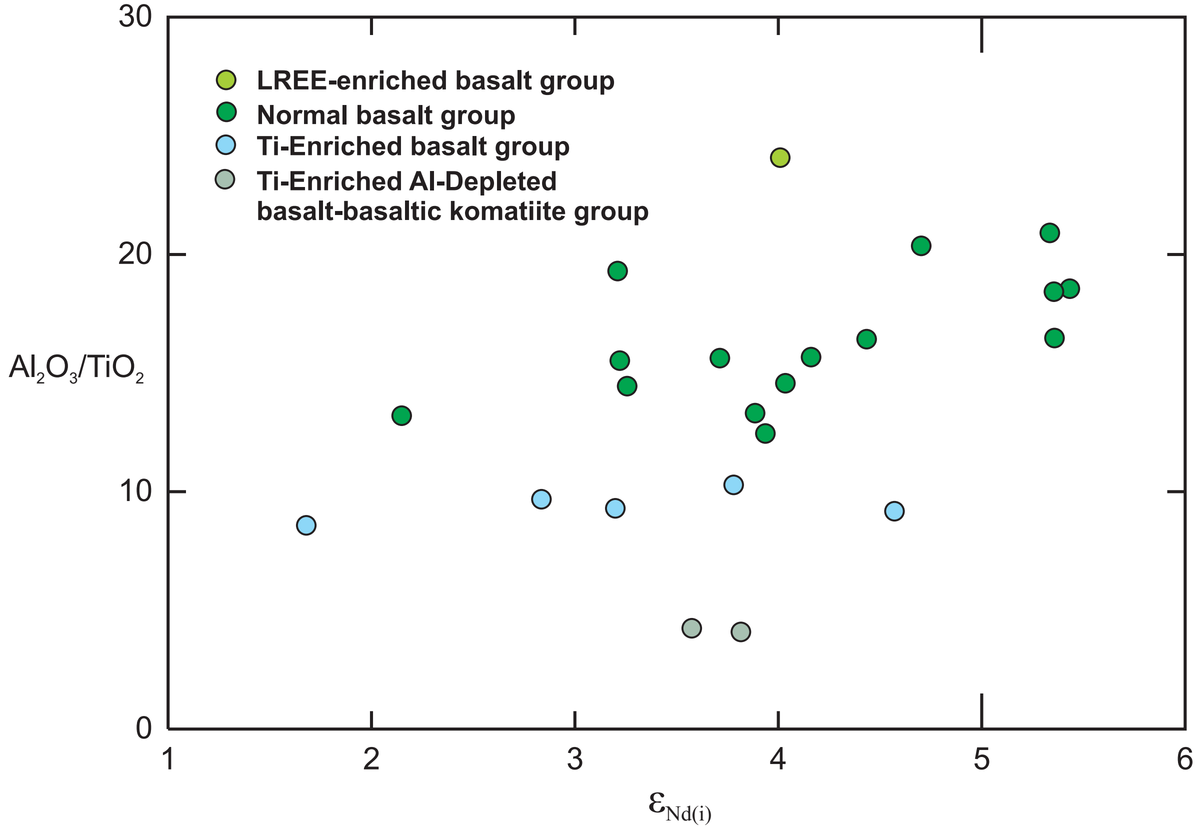

Figure 3.19: $\varepsilon_{Nd(i)}$ vs Al_2O_3/TiO_2 plot with rock groups, relevant samples labelled

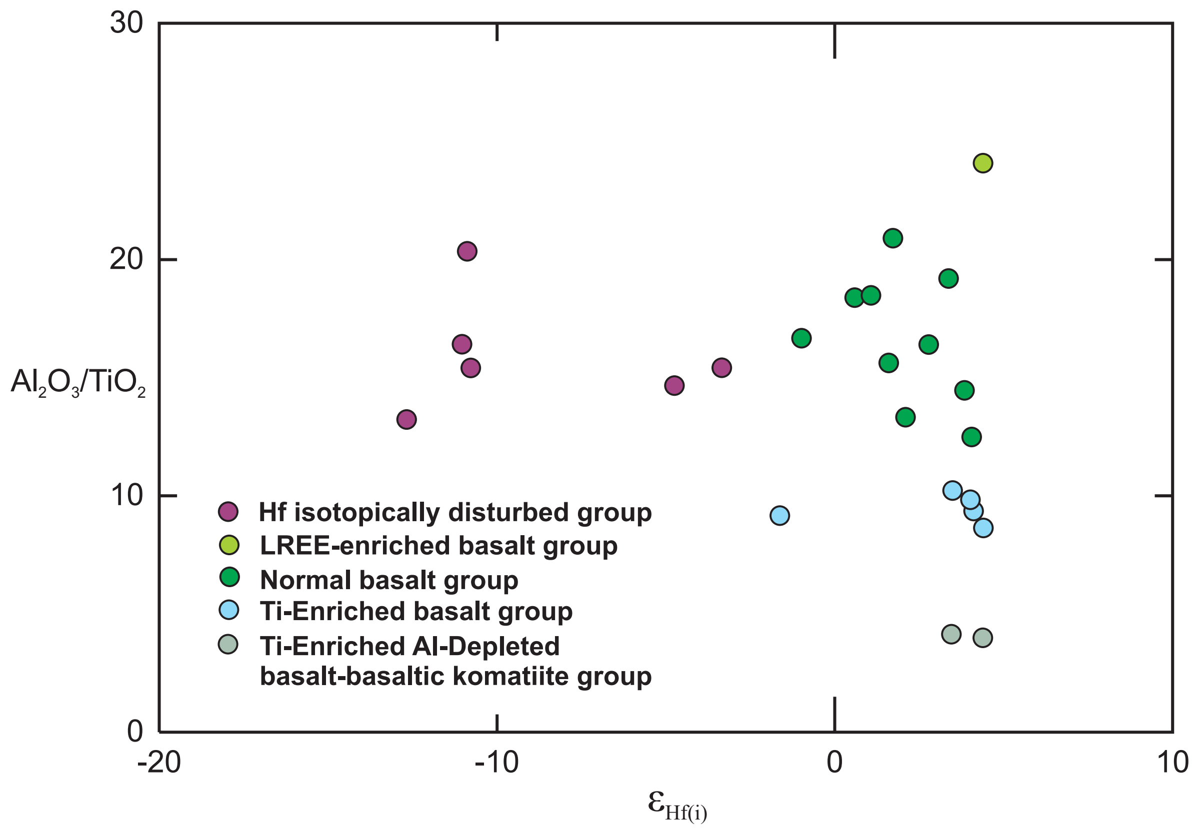

Figure 3.20: $\varepsilon_{Hf(i)}$vs Al_2O_3/TiO_2 plot with rock groups, relevant samples labelled

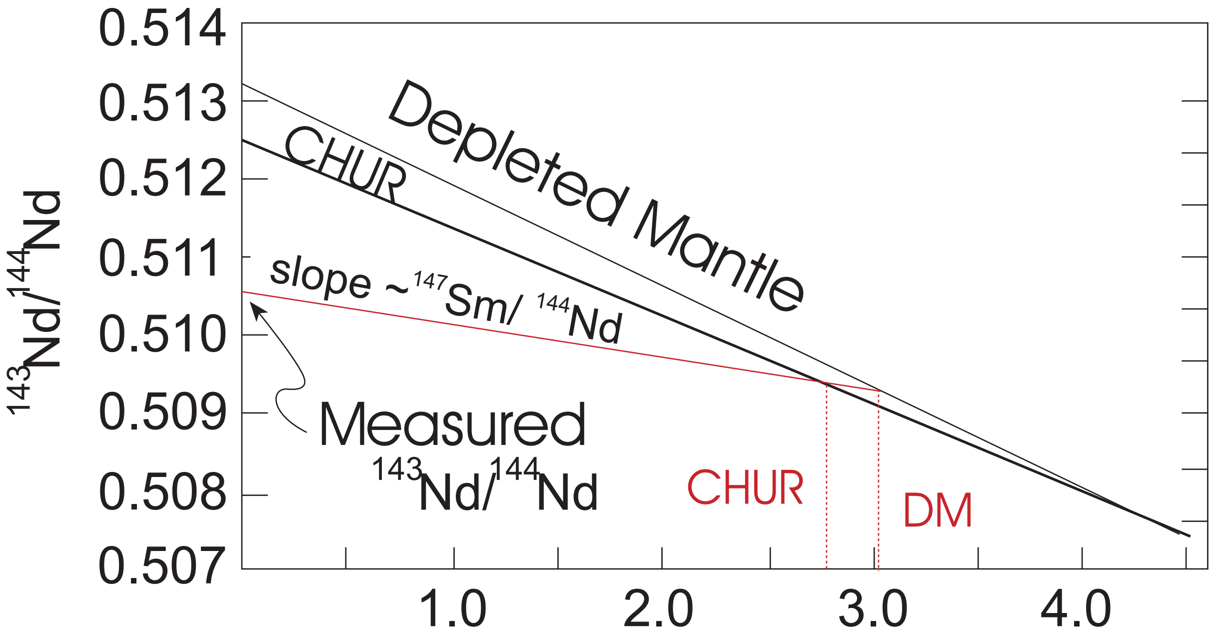

Figure 3.21: plot of Sm-Nd model ages. The $^{143}Nd/^{144}Nd$ is extrapolated backward (slope depending on Sm/Nd) until it intersects a mantle or chondritic growth curve. In this example, the CHUR model age is 3.05 Ga while the depleted mantle model age is 3.3 Ga.

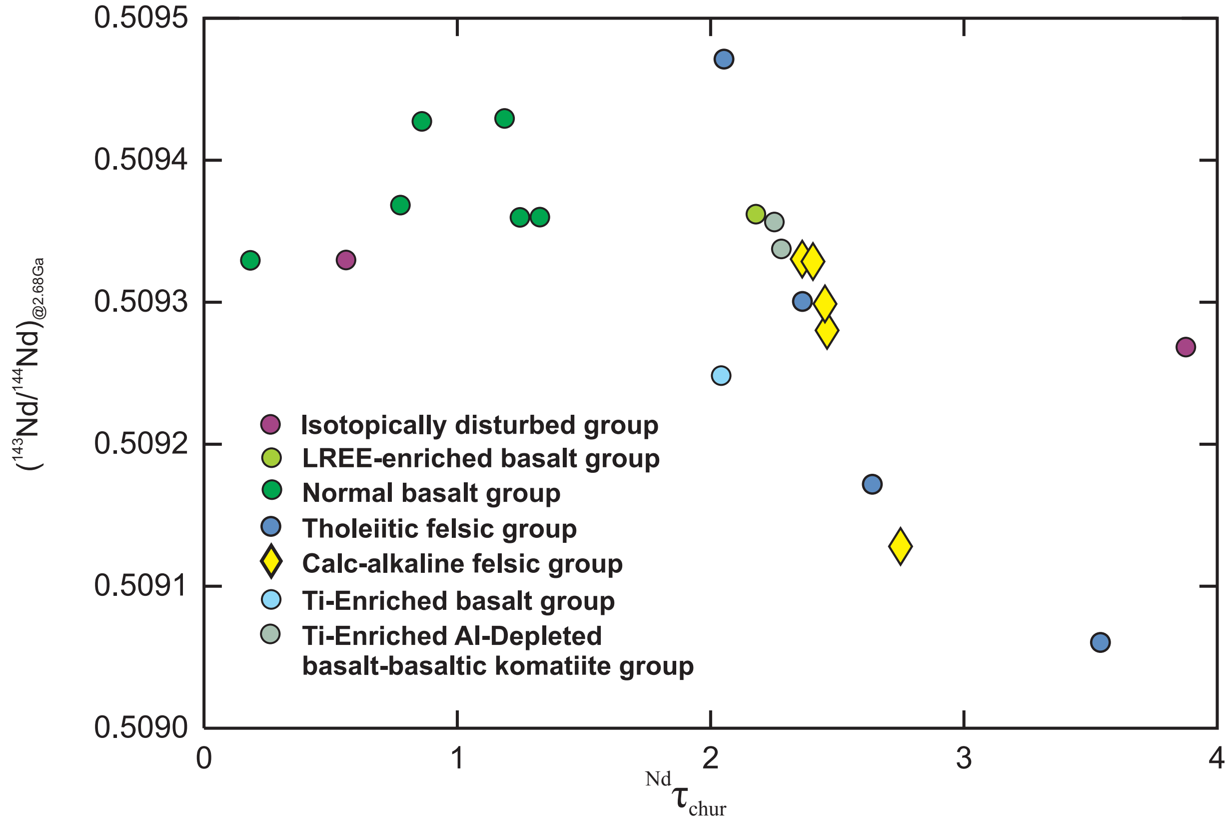

Figure 3.22: $(^{143}Nd/^{144}Nd)_{@2.68Ga}$ vs $^{Nd}\tau_{CHUR}$ plot of rocks from the Hope Bay Greenstone Belt

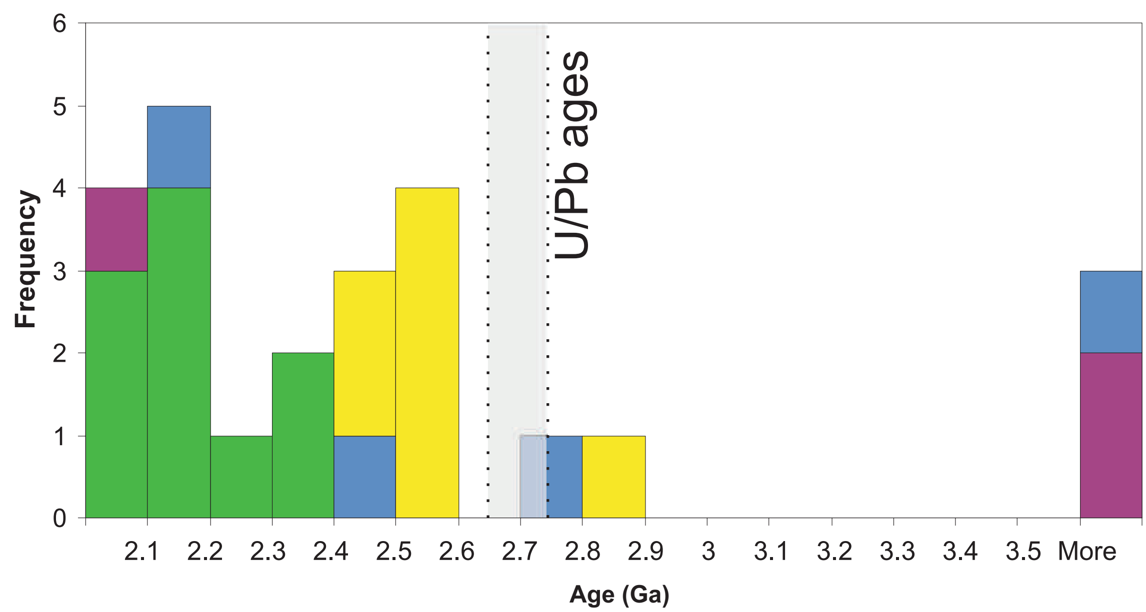

Figure 3.23: $^{Nd}\tau_{CHUR}$ histogram of rocks from the Hope Bay Greenstone Belt

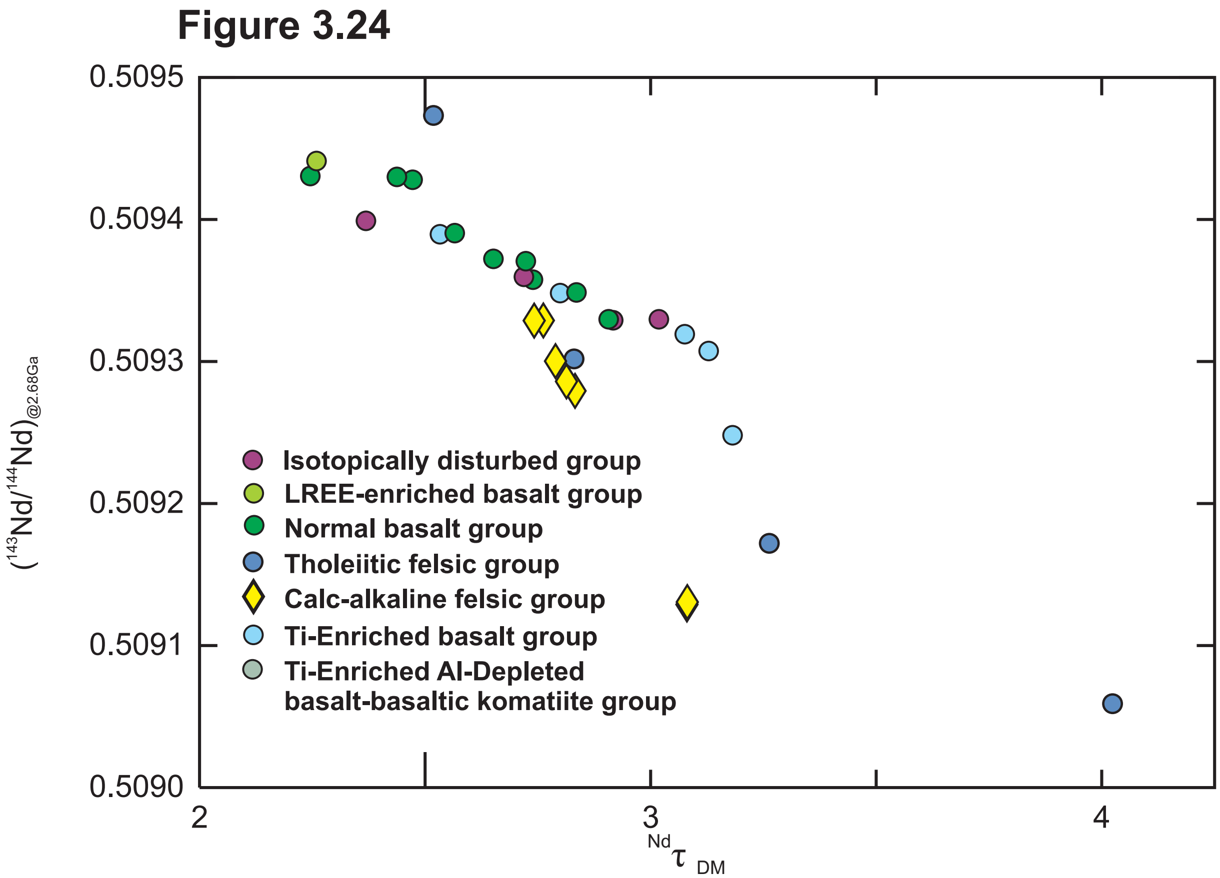

Figure 3.24: $(^{143}Nd/^{144}Nd)_{@2.68Ga}$ vs $^{Nd}\tau_{DM}$ plot of rocks from the Hope Bay Greenstone Belt

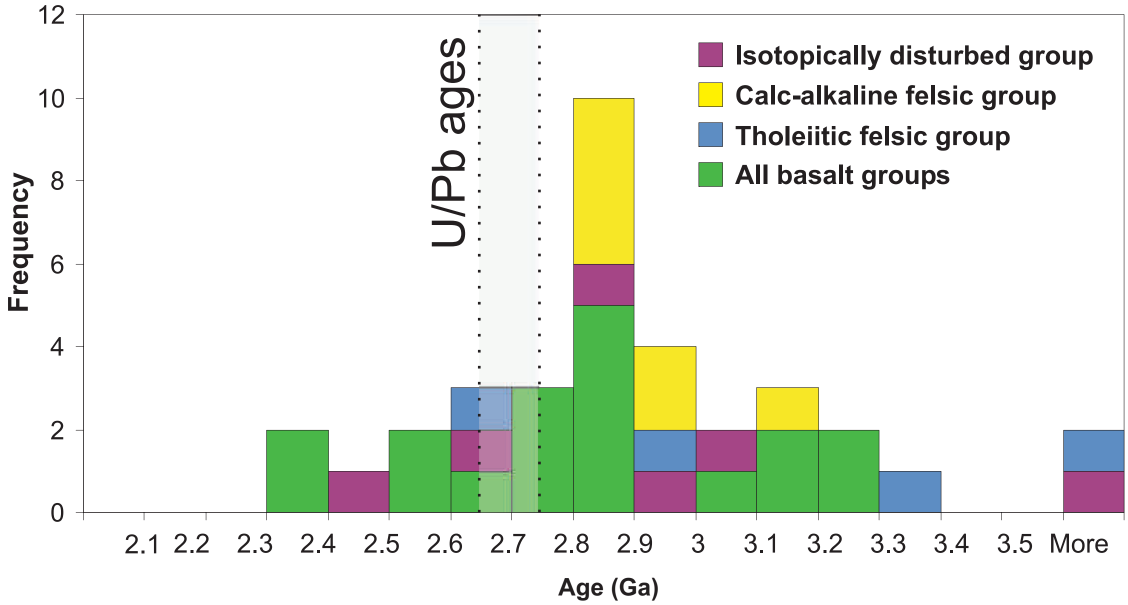

Figure 3.25: $^{Nd}\tau_{DM}$ histogram of rocks from the Hope Bay Greenstone Belt

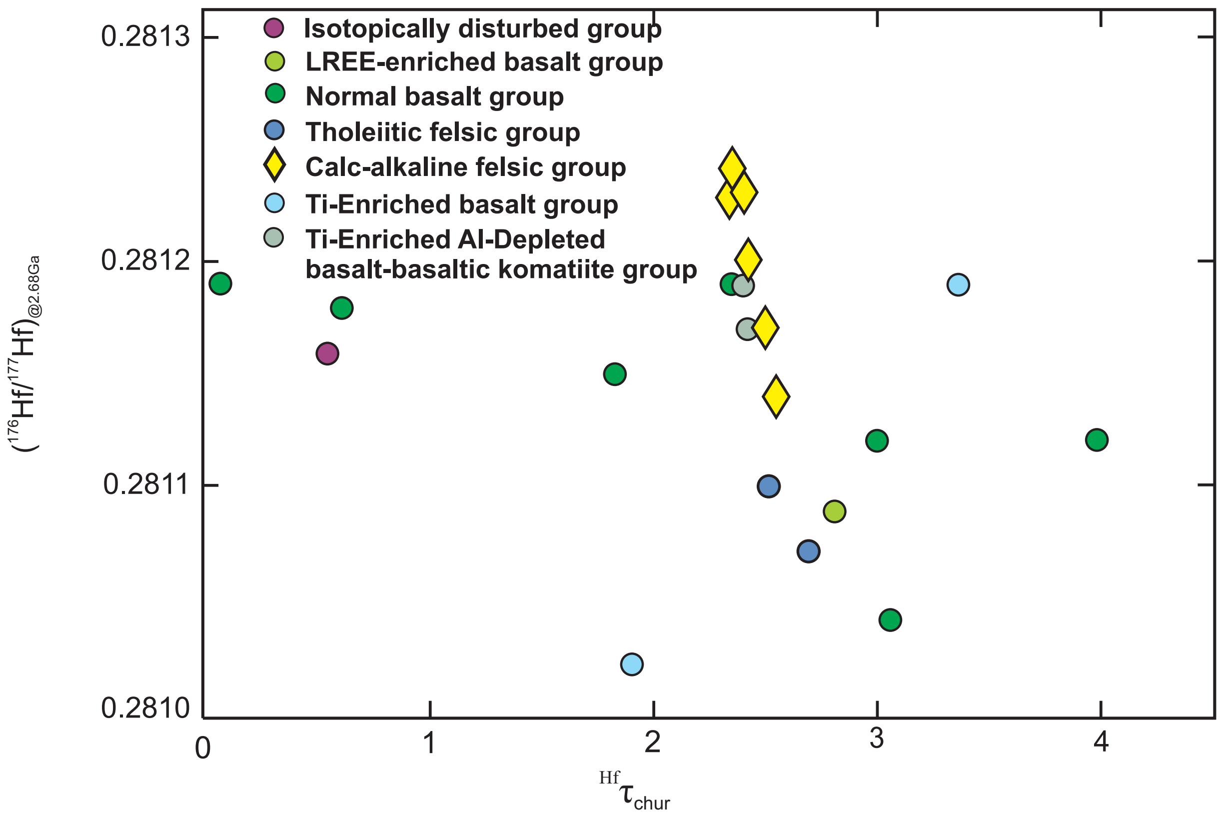

Figure 3.26: $(^{176}Hf/^{177}Hf)_{@2.68Ga}$ vs $^{Hf}\tau_{CHUR}$ plot of rocks from the Hope Bay Greenstone Belt

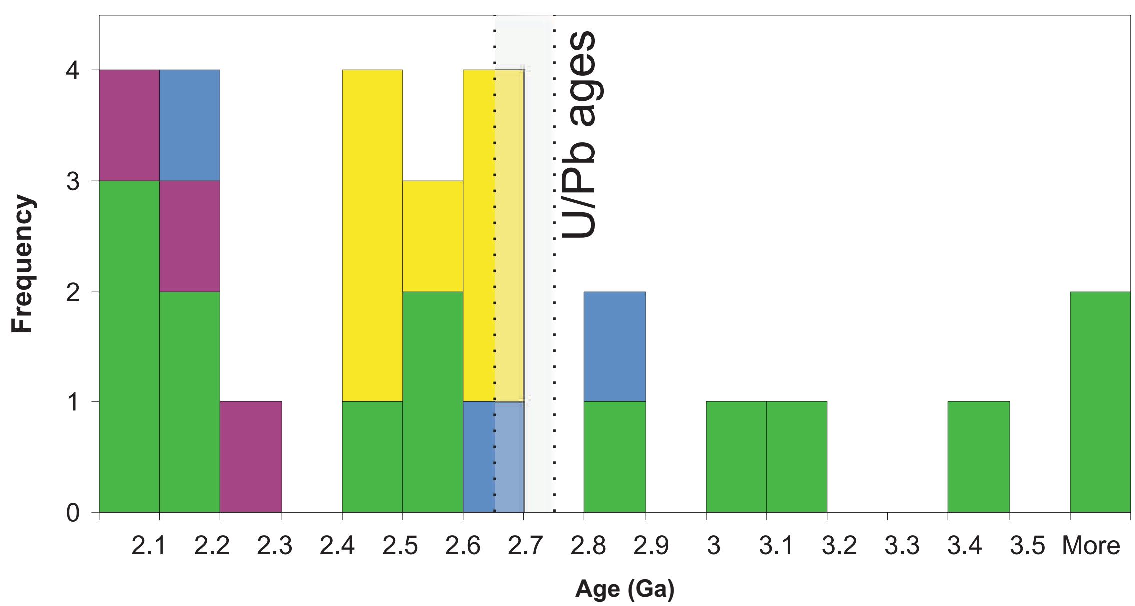

Figure 3.27: $^{Hf}\tau_{CHUR}$ histogram of rocks from the Hope Bay Greenstone Belt

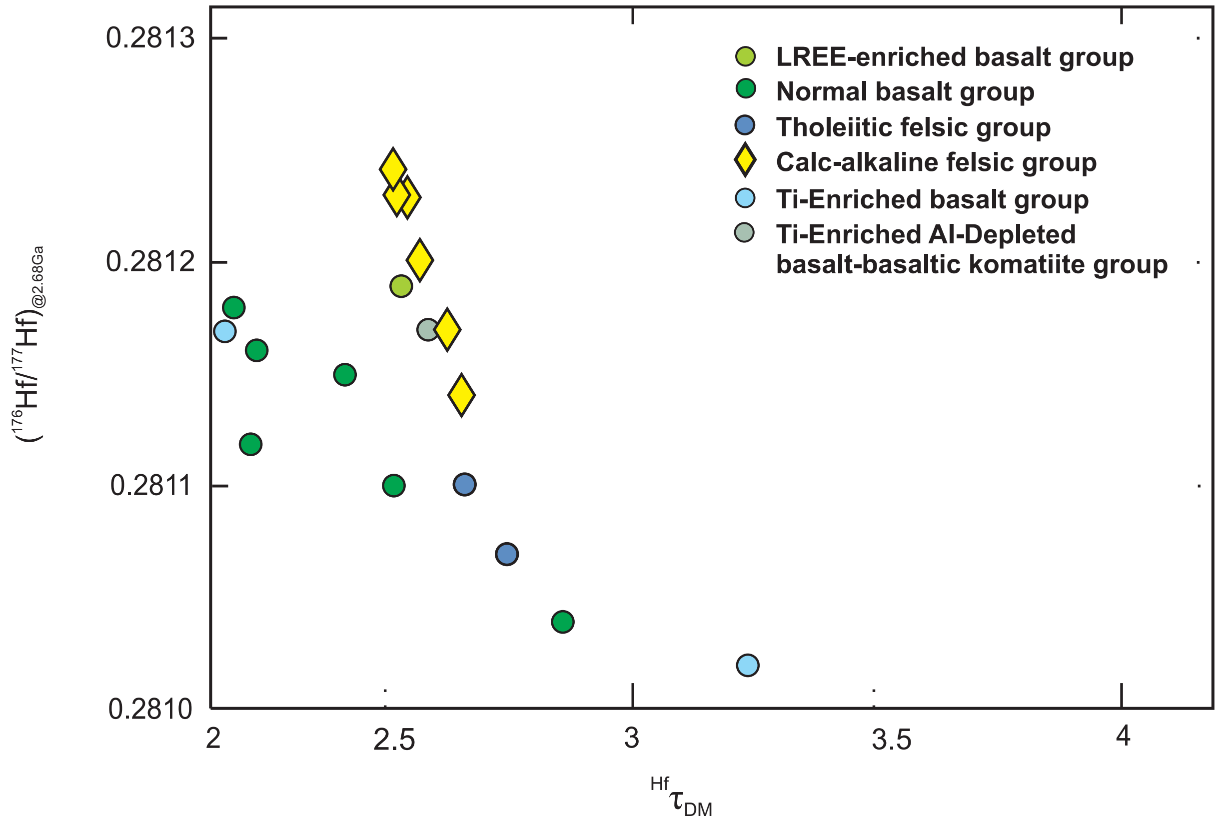

Figure 3.28: $(^{176}Hf/^{177}Hf)_{@2.68Ga}$ vs $^{Hf}\tau_{DM}$ plot of rocks from the Hope Bay Greenstone Belt

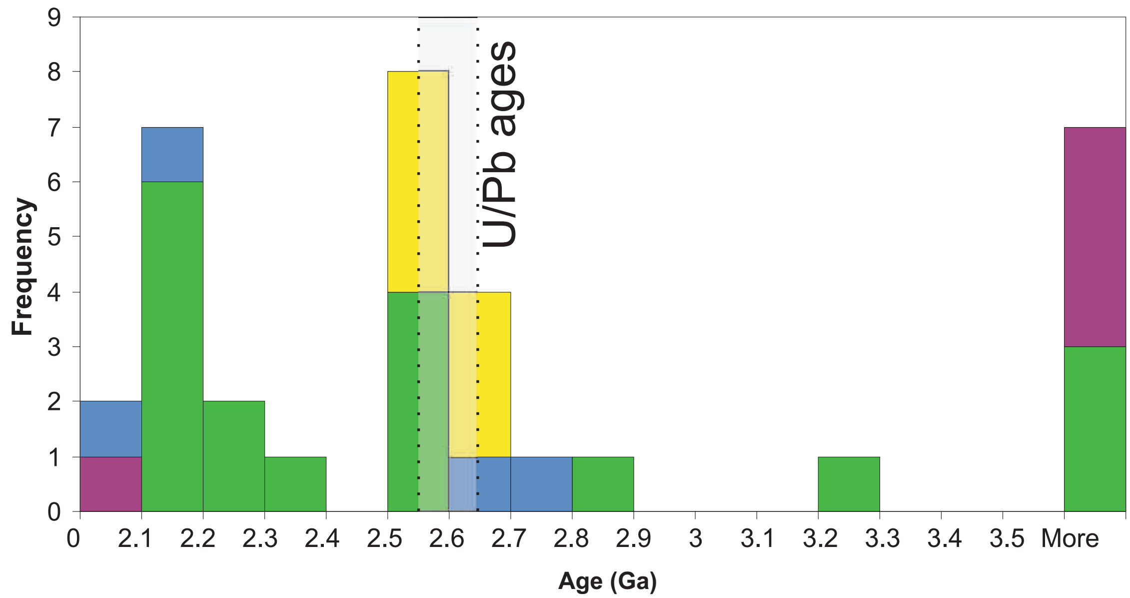

Figure 3.29: $^{Hf}\tau_{DM}$ histogram plot of rocks from the Hope Bay Greenstone Belt

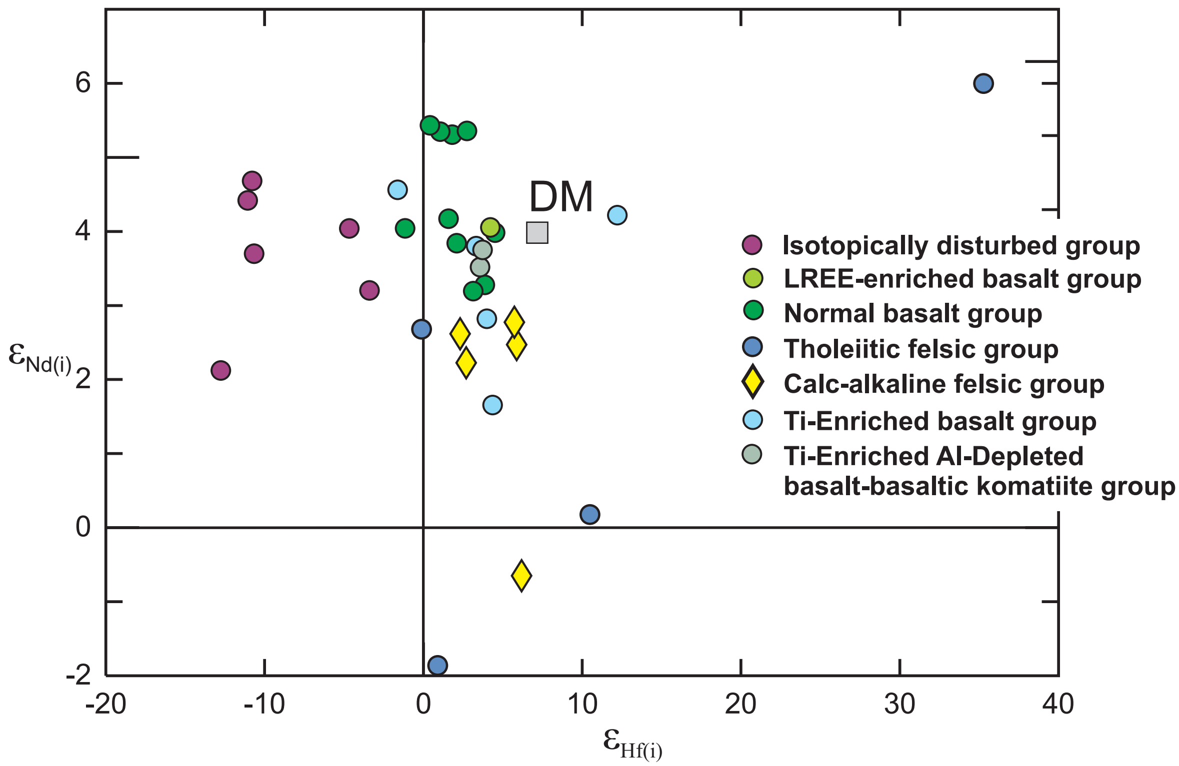

Figure 3.30: $\varepsilon_{Nd(i)}$ vs $\varepsilon_{Hf(i)}$ plot of rocks from the Hope Bay Greenstone Belt

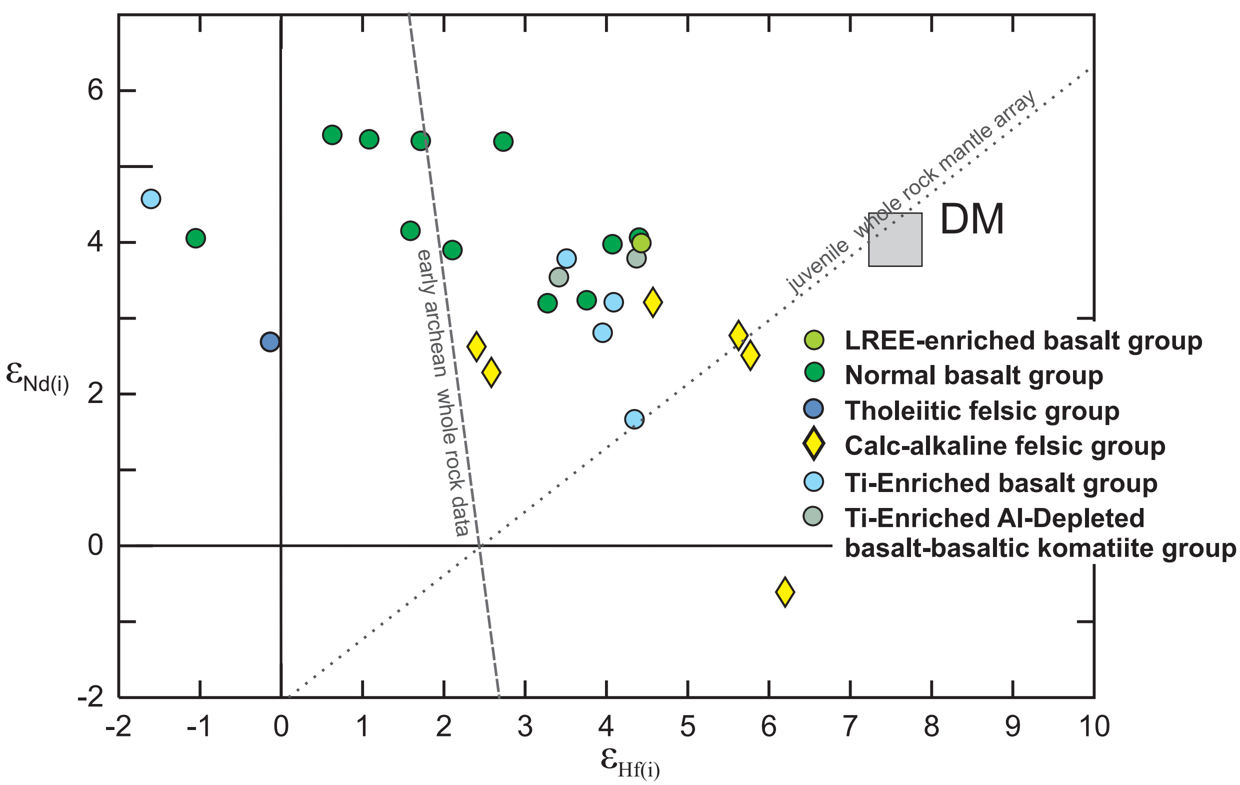

Figure 3.35 $\varepsilon_{Nd(i)}$ vs $\varepsilon_{Hf(i)}$ plot of rocks from the Hope Bay Greenstone Belt with the isotopically disturbed samples removed Juvenile Mantle Array from Vervoorti and Blinchert-Toft (1999), DM value calculated from Salters and Stracke (2004)

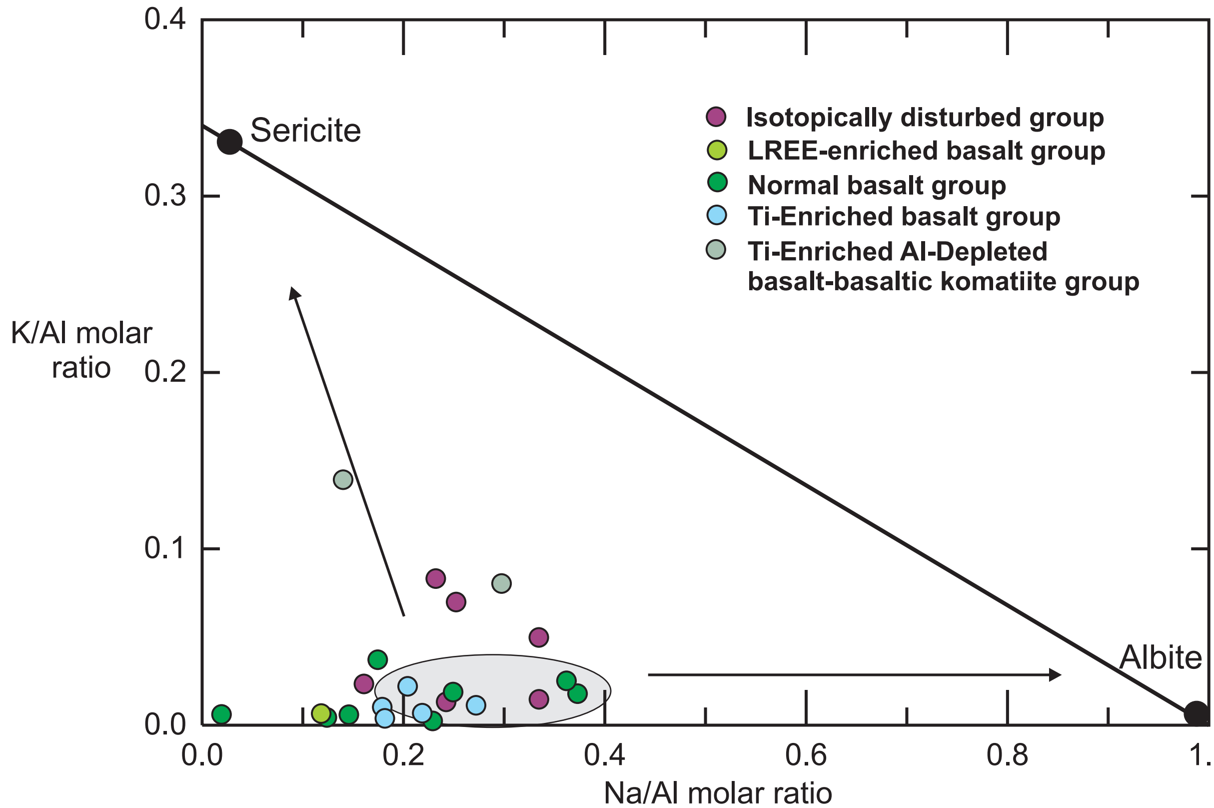

Figure 3.31 K/Al vs Na/Al molar ratio diagram with the least altered area shaded and paths of alteration to sericite and albite indicated with arrows

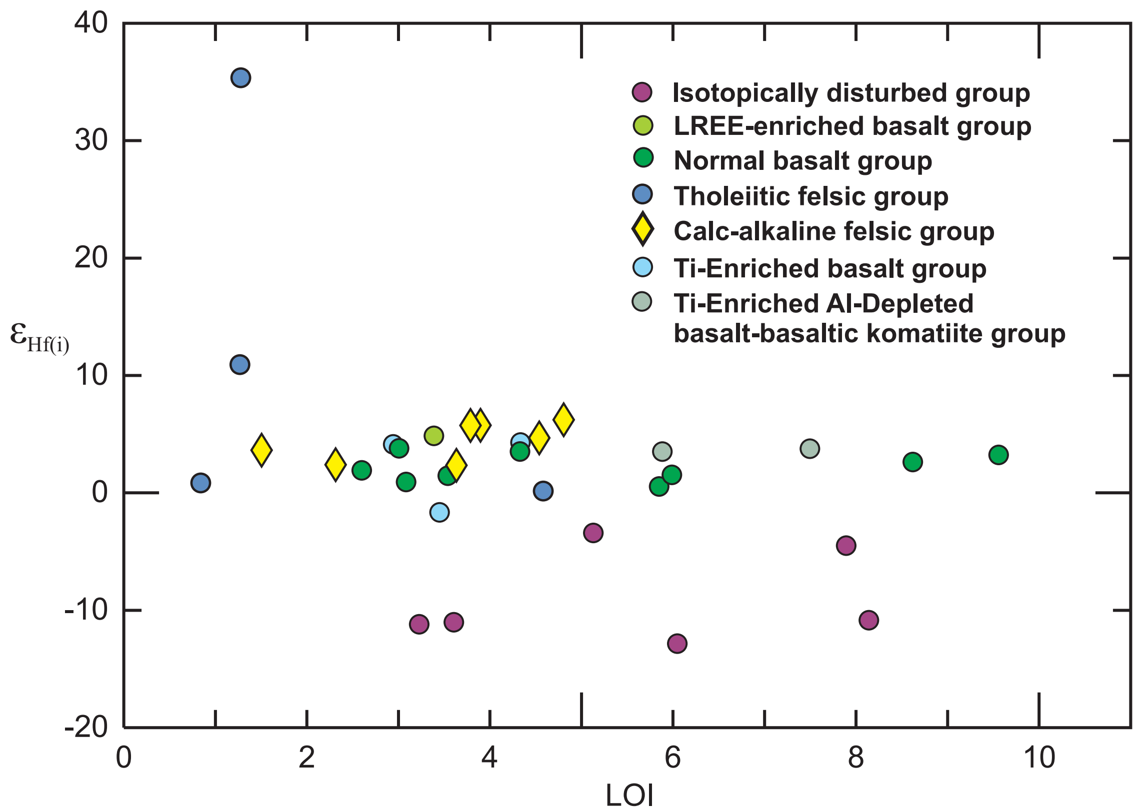

Figure 3.32 $\varepsilon_{Hf(i)}$ vs LOI plot of samples from The Hope Bay Greenstone Belt

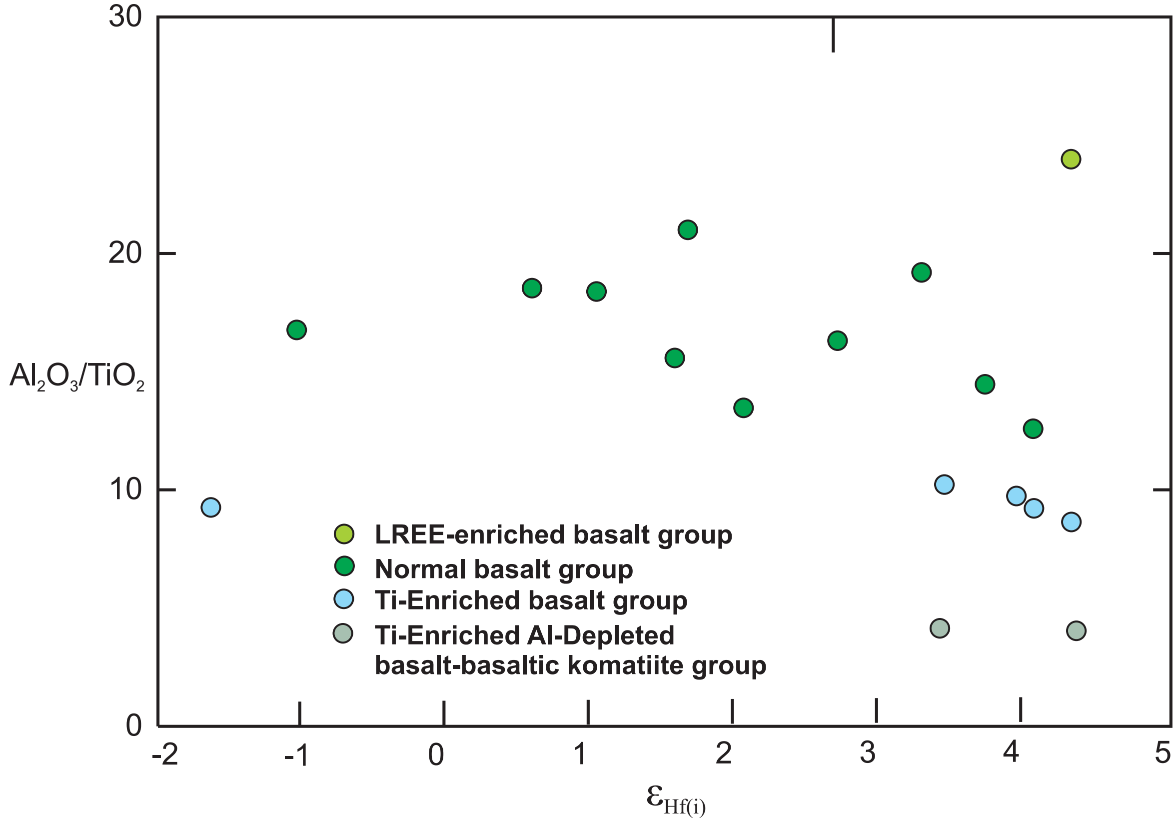

Figure 3.34 $\varepsilon_{Hf(i)}$ vs Al_2O_3/TiO_2 plot with basalt sample and isotopically disturbed samples removed, from the Hope Bay Greenstone Belt,

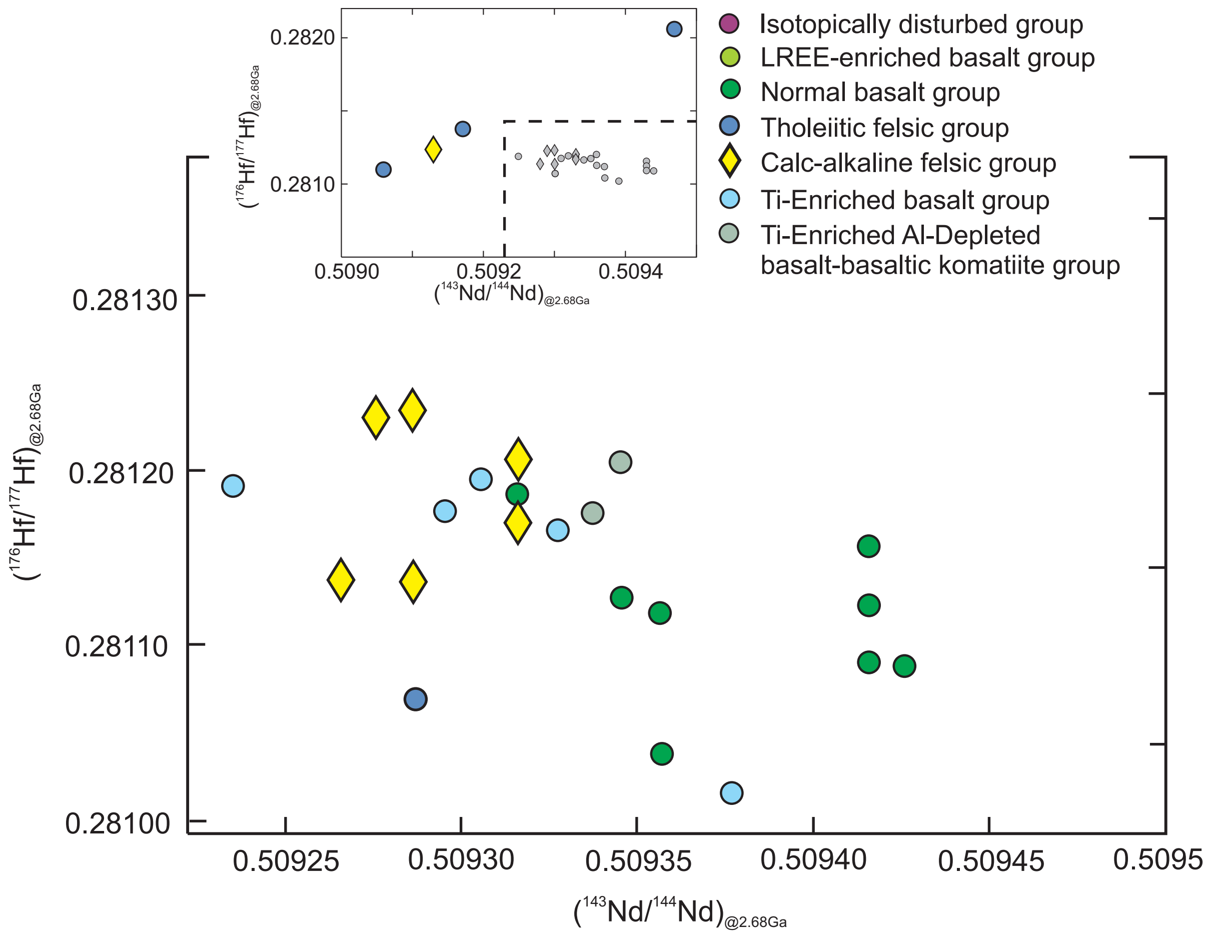

Figure 3.33 $^{143}Nd/^{144}Nd)_{@2.68Ga}$ vs $(^{176}Hf/^{177}Hf)_{@2.68Ga}$ with basalt sample and isotopically disturbed samples removed, from the Hope Bay Greenstone Belt

CHAPTER 4

Conclusions and Suggestions for Further Work

4.1 Conclusion

The creation of a detailed tectonic evolutionary framework for the formation of supracrustal successions has been accomplished by mapping six strategically located transects aided by geochronology, lithogeochemistry, and isotope geochemistry. The Hope Bay Greenstone Belt is characterised by cycles of mafic and felsic volcanism. U-Pb geochronology from this study supports the previous work that indicated felsic volcanism occurred over 53 m.y. (2716 to 2663 Ma). The stratigraphy of the north part of the belt is relatively continuous, broadly younging to the west. This differs from the south part of the belt where there are a number of stratigraphic packages that are juxtaposed against each other by faults. Despite the shuffling of the stratigraphy in the south part of the belt, the Windy Lake Felsic Suite and Koignuk Felsic Suite can be correlated between the north and south parts of the belt.

Chemical compositions of volcanic rocks range from basalt to rhyolite. The felsic suites can be subdivided based on field characteristics, geochronology and geochemical signatures. The Flake Lake Suite is made up of tholeiitic rhyolites whereas the Koignuk, Windy and Square Suites are calc-alkaline dacites. Mafic volcanic rocks are subdivided into four main groups based on chemical composition. The isotopic results show that the Ti-enriched Al-depleted basal and Ti-enriched basalt groups have isotopic compositions that are transitional between the calc-alkaline and the normal basalt group. These Ti-enriched basalt groups are restricted to discrete stratigraphic suites that commonly vary along strike due to faults or are pinched out stratigraphically. The lower portions of the stratigraphy (older than 2690 Ma) are dominated by mafic volcanic rocks. Basalts with elevated Ti content are almost all found in this lower portion or the Hope Bay Greenstone

Belt stratigraphy. Normal basalts are found throughout the stratigraphy with the LREE enriched basalts restricted to the upper part of the stratigraphy (younger than 2690 Ma). The Hope Bay Greenstone Belt has many similarities to other well documented greenstone belts in the Canadian Shield such as the Yellowknife Greenstone Belt and the Abitibi Greenstone Belt. These include age, rock types, stratigraphy and duration of volcanism. This being said, the Hope Bay Greenstone Belt is a unique greenstone belt with respect to the majority of gold (~10 million oz) deposited in two basalt suites with elevated Ti content. The connection between basalts enriched in Ti and gold, which has been observed previously in the Hope Bay Greenstone Belt, provides the highest exploration potential in the belt for large gold deposits.

4.2 Further work

Results from this study have addressed many questions surrounding the evolution of the Hope Bay Greenstone Belt. There are still a number of questions that are unresolved as well as new questions being raised which include:

- The Hope Bay Sedimentary Suite is located on an island to the north of the belt. What is its relationship between this suite and the rest of the Hope Bay Greenstone Belt?
- Broadly, the north and south parts have similar stratigraphy. The north part of the Hope Bay Greenstone Belt has more voluminous high Ti basalts than the south part of the belt. Does this represent the inhomogeneities of the mantle or different geodynamic settings for the north and south part of the belt?
- The Flake Lake Suite is found in the south part of the belt associated with Ti-enriched basalts but basalts enriched in Ti in the north part of the belt have no associated felsic

volcanism. Is the Flake Lake Suite rhyolites and Ti-enriched basalts a genetic relationship? (Petrologic modeling could shed light on this)

- The sedimentary rocks dated on the east and west limbs of the Boston anticline have significantly different ages. Is there a unconformity and/or faulting in the Boston stratigraphy? Due to lack of outcrop this answer may be difficult to answer, but further dating and examination of outcrops may shed light on the answer to this question.
- What is the age of the Clover Sedimentary Suite, surrounding the Clover Lake Felsic Suite? It is inferred to be 2662 Ma from the date on the Clover Lake Felsic Suite but direct dating of the detrital zircons would be useful.
- In much of the greenstone belt there is a significant steeply dipping stretching lineation suggesting vertical movement but there are areas that thrusts are inferred. What geodynamic processes were at work on the Hope Bay Greenstone Belt? (horizontal or vertical tectonics)
- The majority of the SSP is made up of intrusive rocks with greenstone belts making up ~5% of the rock types. In the Archean earth what made up the other 95% more greenstone belt type rocks, ocean basins or continents?
- Detailed petrologic modeling of the Ti enriched Basalt suites was not part of this study. Is it possible through batch melting or factional melting to create these usual basalt suites? How do these Ti basalt suites fit with what we know about Archean mantle dynamics?

Bibliography

Ayer J., Amelin Y., Corfu F., Kamo S., Ketchum J., Kwok K., Trowell N. 2002, Evolution of the southern Abitibi greenstone belt based on U–Pb geochronology: autochthonous volcanic construction followed by plutonism, regional deformation and sedimentation, Precambrian Research, **115**: 63–95

Batiza, R.and White, J.D.L., 2000. Submarine lavas and hyaloclastite. In: H. Siguredsson, B. Houghton, H. Rymer and J. Stix, Editors, Encyclopedia of Volcanoes, Academic press, London, pp. 361–381.

Bebout, G.E., 2003. Trace Element and Isotopic Fluxes/Subducted Slab In H. D. Holland and K. K. Turekian (eds). Treatise on Geochemistry, Volume 3.20. Elsevier, p.1-50.

Bevier, M.L., and Gebert, J.S. 1991. U-Pb geochronology of the Hope Bay-Elu Inlet area, Bathurst Block, Northeastern Slave Structural Province, N.W.T.. Canadian Journal of Earth Sciences, **28**: 1925-1930.

Bleeker, W., Ketchum, J.W.F., Jackson, V.A., and Villeneuve, M.E. 1999. The central slave basement complex; part I, its structural topology and autochthonous cover; NATMAP slave province project. Canadian Journal of Earth Sciences, **36**: 1083-1109.

Bleeker, W., Parrish, R.R., Sager-Kinsman, S., 1999. High precision U–Pb Geochronology of the late Archean Kidd Creek deposit and surrounding Kidd volcanic complex. Econ. Geol. Monogr. 10, 43–69.

Bleeker, W., Parrish, R.R., Sager-Kinsman, S., 1999. High precision U–Pb Geochronology of the late Archean Kidd Creek deposit and surrounding Kidd volcanic complex. Economic Geology Monograph. **10**: 43–69.

Bleeker, W. 2003. The late archean record; a puzzle in ca. 35 pieces; A tale of two cratons; the Slave-Kaapvaal workshop, Lithos, **71**: 99-134.

Bleeker, W., Ketchum, J., Davis, B., Sircombe, K., Stern, R., and Waldron, J. 2004. The Slave Craton from on top: the crustal view. *In* The Lithoprobe Celebratory Conference: From Parameters to Processes - Revealing the Evolution of a Continent Abstract. 5p.

Bleeker, W., and Hall, B. 2007 In: The Slave Craton: Geological and Metallogenic Evolution Goodfellow W.D. (ed.) Mineral Resources of Canada: A Synthesis of Major Deposit-types, District Metallogeny, the Evolution of Geological Provinces, and Exploration Methods. Geological Survey of Canada and Geological Association of Canada. pp. 849-881.

Blichert-Toft, J., and Albarède, F. 1997. The Lu-Hf isotope geochemistry of chondrites and the evolution of the mantle-crust system. Earth and Planetary Science Letters **148**: 243–258.

Bowring, S.A., and Williams, I.S., 1999. Priscoan (4.00-4.03 Ga) orthogneisses from northwestern Canada: Contributions to Mineralogy and Petrology, **134:** p. 3-16.

Carpenter, R.L. and Sherlock, R.S. 2001. Preliminary geochemical analysis of volcanic rocks in the Wolverine-Madrid corridor. Department of Indian and Northern Affairs Canada - Nunavut Minerals Section, 12p.

Carpenter, R.L., Sherlock, R.S., Quang, C., Kleespies, P. and McLeod, R. 2003. Geology of the Doris North gold deposits, northern Hope Bay volcanic belt, Slave Structural Province, Nunavut. Geological Survey of Canada, Current Research 2003-C6, 10p.

Chown, E.H., Daigneault, R. & Mueller, W. 1992. Tectonic evolution of the Northern Volcanic Zone, Abitibi Belt, Quebec. Canadian Journal of Earth Sciences, **29**: 2211-2225.

Condie, K.C., 1976. Trace-element geochemistry of Archean greenstone belts Earth-Science Reviews, **12-4**: 393-417

Corfu, F. 1993. The evolution of the southern Abitibi greenstone belt in light of precise U--Pb geochronology. Economic Geology, **88**: 1323-1340.

Cousens, B.L. 2000. Geochemistry of the Archean Kam Group, Yellowknife Greenstone Belt, Slave Province, Canada. Geology, **108**: 181–197

Cousens, B., Falck, H., Ootes, L., Jackson, V., Mueller, W., Corcoran, P., Finnigan, C., van Hees, E., Facey, C. and Alcazar A. 2006. Regional Correlations, Tectonic Settings, and Stratigraphic Solutions in the Yellowknife Greenstone Belt and Adjacent Areas from Geochemical and Sm-Nd Isotopic Analyses of Volcanic and Plutonic Rocks. Special Publication - Geological Association of Canada. Mineral Deposits Division, vol.3, pp.70-95.

Daniel F. Weill; Michael J. Drake, 1973, Europium Anomaly in Plagioclase Feldspar: Experimental Results and Semiquantitative Model, Science, **180-4090**: 1059-1060.

Davis, W.J., and Hegner, E., 1992, Neodymium isotopic evidence for the tectonic assembly of late Archean crust in the Slave Province, Northwest Canada: Contributions to Mineralogy and Petrology, **111-4**: 493-504.

Davis, W.J. and Bleeker, W. 1999. Timing of plutonism, deformation, and metamorphism in the Yellowknife Domain, Slave Province, Canada. Canadian Journal of Earth Sciences, **36:** 1169–1187.

DePaolo, D.J. & Wasserburg, G.J. 1976. Nd isotopic variations and petrogenetic models. Geophysical Research Letters **3**: 249–252.

Donaldson C.H., 1982, Spinifex-textured komatiites: a review of textures, compositions and layering. In Arndt N.T. and Nisbet E.G. (Eds.). Komatiites, Allen and Unwin, London, pp. 213–244.

Easton R.M., Johns G.W., 1986. Volcanology and mineral exploration the application of physical volcanology and facies studies, Ontario Geological Survey, Miscellaneous Papers 129; 2-39

Ferguson, M.E., Waldron, J.W.F, and Bleeker, W., 2005, The Archean deep-marine environment: turbidite architecture of the Burwash Formation, Slave Province, Northwest Territories: Canadian Journal of Earth Sciences, **42**: 935–954

Fraser, J.A. 1964. Geological notes on northeastern District of Mackenzie, Northwest Territories. Geological Survey of Canada, Paper 63-40, 20p.

Gebert, J.S. 1993. Geology and mineral potential of the Archean Hope Bay and Elu Inlet volcanic belts, Northeastern Slave Structural Province, District of Mackenzie, N.W.T. Northern Affairs Program, Northwest Territories Geology Division, EGS Paper 1993-1, 103p

Gebert, J.S. 1999. Hope Bay project, exploration overview. Unpublished summary report, BHP minerals, 367p.

Gerstenberger, H., Haase, G. 1997. A highly effective emitter substance for mass spectrometric Pb isotope ratio determinations. Chemical Geology. **136**: 309–312.

Grunsky, E.C., Easton, R.M., Thurston, P.C. and Jensen, L.S. 1992. Characterization and statistical classification of Archean volcanic rocks of the Superior Province using major element geochemistry. *In* Geology of Ontario. Edited by P.C. Thurston, H.R. Williams, R.H. Sutcliffe and G.M. Stott. Ontario Geological Survey Special Volume 4, 1397-1438.

Hrabi, R.B., Grant, J.W., Berclaz, A., Duquette, D. and Villeneuve, M.E., 1994. Geology of the northern half of the Winter Lake supracrustal belt, Slave Province, Northwest Territories; in Current Research 1994-C; Geologic Survey of Canada, pp. 13–22.

Heaman, L.M., Kjarsgaard, B.A., and Creaser, R.A. 2003, The timing of kimberlite magmatism in North America: implications for global kimberlite genesis and diamond exploration: Lithos, **71**: 153-184.

Hebel, M.U. 1999. U-Pb geochonology and lithogeochemistry of the Hope Bay greenstone belt, Slave Structural Province, Northwest Territories, Canada. Unpublished M.Sc. thesis, University of British Columbia, 95p.

Helmstaedt, H., Padgham,W.A. 1986.Anewlook at the stratigraphy of the Yellowknife Supergroup at Yellowknife, NWT: implications for the age of gold-bearing shear zones and Archean basin evolution. Canadian Journal of Earth Sciences. **23**: 454–475.

Henderson, J.B. 1985, Geology of the Yellowknife-Hearne Lake area, District of Mackenzie: a segment across an Archean basin: Geological Survey of Canada Memoir 414, Geological Survey of Canada, 135 p.

Henderson, J.R., Kerswill, J. A., Henderson, M.N., Villeneuve, M., Petch, C.A., Dehls, J.F., O'Keefe, M.D. 1994. Geology, geochronology, and mineral occurrences of the High Lake greenstone belt (parts of NTS 76 L and M) Slave Province, Northwest Territories Exploration Overview, vol.1994, pp.37-38

Henderson. J.B. 1970. Stratigraphy of the Yellowknife Supergroup, Yellowknife Bay-Prosperous Lake area, District of Mackenzie, Geological Survey of Canada, Paper 70-26.

Hoffman, A.W. 2003. Sampling Mantle Heterogeneity through Oceanic Basalts: Isotopes and Trace Elements. In H. D. Holland and K. K. Turekian (eds). Treatise on Geochemistry, Volume 2. Elsevier, p.61-101

Hoffman, P.F. 1989. Precambrian geology and tectonic history of North America. In A.W. Bally and Palmer, A.R. (eds), The Geology of North America-An Overview. Geological Society of America, Boulder, Colorado, p 447-512.

Huppert, H.E. and Sparks, R.S.J., 1988. The generation of granitic magmas by intrusion of basalt into continental crust, Journal of Petrology **29**(3):599-624

Isachsen, C.E., and Bowring, S.A., 1994, Evolution of the Slave Craton: Geology, **22-10**: 917-920.

Jackson, S.L., and Fyon, J.A. 1991. The western Abitibi Subprovance in Ontario; in Geology of Ontario, Ontario Geologic Survey, Special Volume 4 Part I, p. 405-475

Jenner, G.A., 1996. Trace Element geochemistry of igneous rocks: geochemical nomenclature and analytical geochemistry. In Wyman, D.A., ed., Trace Element

Geochemistry of Volcanic Rocks: Application for Massive Sulphide Exploration: Geological Association of Canada, Short Course Notes, v.12 p. 51-77.

Jensen, L.S. 1976. A new cation plot for classifying subalkalic volcanic rocks. Ontario Division of Mines, Miscellaneous Paper 66, 22p.

Kelemen, P. B.; Hanghøj, K.; Greene, A. R. 2003. One View of the Geochemistry of Subduction-related Magmatic Arcs, with an Emphasis on Primitive Andesite and Lower Crust In H. D. Holland and K. K. Turekian (eds). Treatise on Geochemistry, Volume 3. Elsevier, p. 593-659

Kerrich, R. and Wyman, D.A., 1996. The trace element systematics of igneous rocks in mineral exploration an overview. In Wyman, D.A., ed., Trace Element Geochemistry of Volcanic Rocks: Application for Massive Sulphide Exploration: Geological Association of Canada, Short Course Notes, v.12 p. 1-50.

Kerrich, R., Polat, A., Wyman, D., and Hollings P. 1999. Trace element systematics of Mg-, to Fe-tholeiitic basalt suites of the Superior Province: implications for Archean mantle reservoirs and greenstone belt genesis, Lithos, 46; 163-187

Ketchum, J.W.F., Bleeker, W., and Stern, R.A. 2004, Evolution of an Archean basement complex and its autochthonous cover, southern Slave Province, Canada: Precambrian Research, **135**: 149-176.

King, J.E., and Helmstaedt, H. 1997. The Slave Province, North-West Territories, Canada. In M.J. De Wit, and L.D. Ashwal. (eds), Greenstone Belts. Oxford Monographs on Geology and Geophysics; no. 35. p 459-479.

Krogh, T.E, 1982. Improved accuracy of U-Pb zircon ages by the creation of more concordant systems using an air abrasion technique. Geochimica et Cosmochimica Acta, **46**: 637-649.

Kusky, T.M. 1989. Accretion of the Archean Slave province. Geology, **17**: 63–67.

Kusky, T.M., 1990. Evidence for Archean ocean opening and closing in the southern Slave province. Tectonics **9**: 1533–1563.

Le Bas, M.J., Le Maitre, R.W., Streckeisen, A., Zanettin, B.A., 1986. Chemical classification of volcanic rocks based on the total alkali-silica diagram. Journal of Petrology, **27-3**: 745-750

LeCheminant, A.N., and Heaman, L.M. 1989. Mackenzie igneous events, Canada: Middle Proterozoic hotspot magmatism associated with ocean opening. Earth and Planetary Science Letters, **96**: 38–48.

Lee, J.K.W., Williams, I.S., Ellis, D.J. 1997. Pb, U and Th diffusion in natural zircon Nature, **390-6656**: 159-162.

Ludwig K.R., 2003. Isoplot 3.00, A Geochronological Toolkit for Microsoft Excel. University of California at Berkely, kludwig@bgc.org.

Lugmair, G.W. and Marti, K. 1978. Lunar initial $^{143}Nd/^{144}Nd$: Differential evolution of the lunar crust and mantle. Earth and Planetary Science Letters **39**: 349–357

MacLean, W.H., Barrett, T.J. 1993. Lithogeochemical techniques using immobile elements, Journal of Geochemical Exploration, **48-2**: 109-133

Madsen, J.K., Sherlock, R. and Lindsay, D., 2006, The Geology, Geochemistry and Mineralization of the Naartok gold deposits; Hope Bay Belt, Nunavut Canada, Geological Association of Canada/Mineralogical Association of Canada Meeting, Program with Abstracts 32, p 52

Martel, E., Lin, S., 2006, Structural evolution of the Yellowknife greenstone belt, with emphasis on the Yellowknife River fault zone and the Jackson Lake Formation, Special Publication - Geological Association of Canada. Mineral Deposits Division, vol.3, pp.95-115,

McPhie J., Doyle M.G., Allen R.L., 1993. Volcanic Textures: A guide to the interpretation of textures in volcanic rocks. Hobart: CODES, University of Tasmania p.198

Mikucki, E.J., 1998. Hydrothermal transport and depositional processes in Archean lode-gold systems: A review, Ore Geology Reviews **13**; 307-321.

Mortensen., J.K., Relf, C., Davis, W.J., and King, J.E. 1992. U-Pb zircon ages from the Shallow Bay volcaniclastic belt, Contwoyto Lake area, NWT: Age constraints for Lupin-type iron formation. Radiogenic Age and Isotope Studies: Report 5, Geological Survey of Canada, Paper 91-2, p 9-15.

Padgham, W.A. 1985. Observations and speculations on supracrustal successions in the Slave Structural Province. In L.D. Ayres, P.C Thurston, K.D. Card, and W. Weber (eds), Evolution of Archaean Sequences. Geological Association of Canada. Special Paper 28, p 133-151.

Padgham, W.A., and Fyson, W.K. 1992. The Slave Province: a distinct Archean craton. Canadian Journal of Earth Sciences, **29**: 2072-2086.

Padgham, W.A. 1995. Evolution of the Slave Craton discussion. Geology, **23-9**: 863-864

Padgham, W.A. 1996. Slave conglomerate dating. Northern affairs program Northwest Territories Geology Division EGS paper 1996-12, 85 p.

Parrish, R., Roddick, J.C., Loveridge, W.D., and Sullivan, R.W., 1987, Uranium-lead analytical techniques at the geochronology laboratory, Geological Survey of Canada. *In* Radiogenic Age and Isotopic Studies, Report 1, Geological Survey of Canada, Paper 87-2, p. 3-7.

Pearce, J.A. and Cann, J.R. 1973. Tectonic setting of basic volcanic rocks determined using trace element analysis. Earth and Planetary Science Letters, **19**: 290-300.

Pearce, J.A. and Norry, M.J. 1979. Petrogenetic implications of Ti, Zr, Y, and Nb variations in volcanic rocks. Contributions to Mineralogy and Petrology, **69**: 33-47.

Pearce, J.A., 1996. Users Guide to Basalt Discrimination Diagrams. In Wyman, D.A., ed., Trace Element Geochemistry of Volcanic Rocks: Application for Massive Sulphide Exploration: Geological Association of Canada, Short Course Notes, v.12 p. 79-113.

Roddick, J.C., 1987, Generalized numerical error analysis with application to geochronology and thermodynamics. Geochimica et Cosmochimica Acta, **51**: 2129-2135.

Salters, V. and Stracke, A. 2004. Composition of the depleted mantle. Geochemistry, Geophysics, Geosystems 5, 27p.

Scherer, E., Munker, C., and Mezger, K. 2001, Calibrating the Lu-Hf clock, Science, **293**: 683–686.

Sherlock, R.L., Carpenter, R.L., Bardoux, M., Flood, E. and Kleespies, P. 2002. Volcanic relationships and gold mineralization in the Wolverine-Madrid corridor, Hope Bay Volcanic Belt, Nunavut. Geological Survey of Canada, Current Research 2002-C9, 11p.

Sherlock, R.S. and Lindsay, D.W. 2002. Volcanic stratigraphy of the QSP area, Hope Bay volcanic belt, Nunavut. Geological Survey of Canada, Current Research 2002-C8, 9p.

Sherlock, R.L., Carpenter, R.L., and Quang, C. 2003a. Volcanic stratigraphy, structural geology, and gold mineralization in the Wolverine-Doris corridor, northern Hope Bay Volcanic Belt, Nunavut. Geological Survey of Canada, Current Research 2003-C7, 11p.

Sherlock, R.L. and Carpenter, R.L. 2003b. Bedrock geology of the Wolverine-Doris corridor, northern Hope Bay Volcanic Belt. GSC open file 1553, 1 sheet.

Sherlock, R.L. and Sandeman, H.A. 2004a. Volcanic stratigraphy and structural geology of the area of the Boston gold deposit, Hope Bay Volcanic Belt, Nunavut. Geological Survey of Canada, Current Research, no. 2004-C2, 11p.

Sherlock, R.L. and Sandeman, H.A. 2004b. Volcanic stratigraphy and structural geology of the Boston area, Hope Bay Volcanic Belt, Nunavut. Geological Survey of Canada, Open File 4601, 1 sheet.

Stemler, J.U. 2000. A fluid inclusion and stable isotopic examination of the Boston greenstone belt hosted, Archean lode gold deposit, Hope Bay volcanic belt, Nunavut, Canada. Unpublished M.Sc. thesis, University of Alberta, 212p.

Stemler J. U., Richards J. P. and Muehlenbachs K., 2006, A fluid inclusion and stable isotopic investigation of the Boston lode-gold deposit, Hope Bay volcanic belt, Nunavut Exploration and Mining Geology, **15** (1-2):101-121

Stern, R.A., Bleeker, W., 1998. Age of the world's oldest rocks refined using Canada's SHRIMP. The Acasta gneiss complex, Northwest Territories, Canada. Geoscience Canada **25-1**: 27– 31.

Sterritt, V.A., 2003, Petrographyic and Mineralogica Investigation of the Doris and Madrid Gold Deposit Hope Bay Greenstone Belt, Nunavut, Unpublished Report, Queens University, 51p.

Stone, W.E., Jensen, L.S. and Church, W.R. 1987. Petrography and geochemistry of an unusual Fe-rich basaltic komatiite from Boston Township, northeastern Ontario.Canadian Journal of Earth Sciences, **24:** 2537-2550.

Stubley, M.P. 2002. Bedrock geology of the Discovery-Twin Peaks area, Hope Bay Volcanic Belt, Slave craton. Unpublished report to Miramar Hope Bay Ltd., December 2002, 39p.

Stubley, M.P., 2005. Slave Craton: Interpretive bedrock compilation; Northwest Territories Geoscience Office, NWT-NU Open File 2005-01.

Sun, S., McDonough, W.F. 1989. Chemical and isotopic systematics of oceanic basalts: implications for mantle compositions and processes. In Saunders, A.D. and Norry, M.J., Magmatism in the Ocean Basins, Geological Society Special Publication. No. 42, p. 313-345.

Therriault, R., 2006. Geology, Geochemistry, and Gold mineralization of the Madrid Gold Deposit, Hope Bay Volcanic Belt Nunavut, Canada Unpublished M.Sc. thesis, University of Western Ontario, 233p.

Thirlwall, M.F., 2000. Inter-laboratory and other errors in Pb isotope analyses investigated using a ^{207}Pb–^{204}Pb double spike: Chemical Geology, **163**: 299–322.

Thompson, P.H., Culshaw, N., Buchanan, J.R. and Manojlovic, P. 1986. Geology of the Slave Province and Thelon Tectonic Zone in the Tinney Hills-Overby Lake (west half) map area, District of Mackenzie. In Current Research, Part A, Geological Survey of Canada, paper 86-1A, pp. 275-289.

Thompson, P.H. 1996. Regional geology of Archean granitoid rocks adjacent to the Hope Bay Volcanic Belt, northeastern Slave province, Canadian Shield. Unpublished report to BHP Minerals, 39p.

Thompson, P. H. 1997. Regional geology of Archean granitoid rocks adjacent to the Hope Bay and Elu Inlet volcanic belts, northeastern Slave structural province, Canadian Shield. Unpublished report to BHP Minerals, November 12, 1997, 58p.

Thorpe, R.I., Cumming, G.L., and Mortensen, J.K., 1992, A significant Pb isotope boundary in the Slave Province and its probable relation to ancient basement in the western Slave Province; in Project Summaries, Canada-Northwest Territories Mineral Development Agreement 1987-91: Geological Survey of Canada, Open File 2484, p. 179-184.

Thurston, P.C., 2002. Autochonous development of Superior Province greenstone belts?; Precambrian Research **115**; 11-36

Thy, P., Beard, J.S., and Lofgren, G.E., 1990. Experimental constraints on the origin of Icelandic rhyolites; Journal of Geology, v.98, p. 417-421

van Breemen, O., Davis, W.J., and King, J.E. 1992. Temporal distribution of granitoid plutonic rocks in the Slave Province, Northwest Canadian Shield, Canadian Journal of Earth Sciences **29**: 2186-2199.

Villeneuve, M.E., Henderson, J.B., Hrabi, R.B., Jackson, V.A., Relf, C., 1997. 2.70–2.58 Ga plutonism and volcanism in the Slave Province, District of MacKenzie, Northwest Territories. In: CurrentResearch, Geological Survey of Canada, Paper 1997-F, pp. 107–119.

Winchester, J.A. and Floyd, P.A. 1977. Geochemical discrimination of different magma series and their differentiation products using immobile elements. Chemical Geology, 20: 325-343.

Wyman D.A., Kerrich R., Polat A., 2002 Assembly of Archean cratonic mantle lithosphere and crust: plume–arc interaction in the Abitibi–Wawa subduction–accretion complex, Precambrian Research **115**: 37–62.

Xie, Q., Kerrich, R. and Fan, J. 1993. HFSE/REE fractionations recorded in three komatiite-basalt sequences, Archean Abitibi greenstone belt: Implications for multiple plume sources and depths. Geochimica et Cosmochimica Acta, **57:** 4111-4118.

APPENDIX A:

Geochronology Methods and Sample Description

A1 Analytical Methods

All sample preparation, geochemical separations and mass spectrometry were done at the Pacific Centre for Isotopic and Geochemical Research in the Department of Earth and Ocean Sciences, University of British Columbia. Zircon was separated from samples using conventional crushing, grinding, and Wilfley table techniques, followed by final concentration using heavy liquids and magnetic separations. Zircons were selected on the basis of grain quality, size, magnetic susceptibility and morphology. All zircon was air abraded prior to dissolution to minimize the effects of post-crystallization Pb-loss, using the technique of Krogh (1982). Single zircon grains were dissolved in sub-boiled 48% HF and 14 M HNO_3 (ratio of ~10:1, respectively) in the presence of a mixed ^{233}-^{235}U-^{205}Pb tracer; zircons for 40 hours at 240°C in 300 μL PTFE or PFA microcapsules contained in high pressure vessels (Parr™ acid digestion vessels with 125 mL PTFE liners). Sample solutions were then dried to salts at ~130°C. Zircon residues were redissolved in ~100 μL of sub-boiled 6.2 M HCl for 12 hours at 210°C in high pressure vessels. These solutions were transferred to 7 mL PFA beakers, dried to a small droplet after addition of 2 μL of 0.5 N H_3PO_4 . Samples were then loaded on single, degassed zone refined Re filaments in 5 μL of a silicic acid/phosphoric acid emitter (Gerstenberger and Haase, 1997). Isotopic ratios were measured using a modified single collector VG-54R thermal ionization mass spectrometer equipped with an analogue Daly photomultiplier. Measurements were done in peak-switching mode on the Daly detector. Analytical blanks during the course of this study were 0.2 pg for U and for Pb in the range of 1-3 pg. U fractionation was determined directly on individual runs using the ^{233}-^{235}U tracer, and Pb isotopic ratios were corrected for fractionation of 0.23%/amu, based on replicate analyses of the NBS-982 Pb standard and the values recommended by Thirlwall (2000). Reported precisions for Pb/U and Pb/Pb dates were determined by numerically propagating all analytical uncertainties through the entire age calculation using the technique of Roddick (1987). Standard concordia diagrams were constructed, and regression intercepts, concordia ages and weighted means calculated with Isoplot 3.00 (Ludwig, 2003). Unless otherwise noted, all errors are quoted at the 2σ level.

A2 Sample descriptions and Results

The descriptions and discussion below accompany the results of the anaylsis (Table 2.3), the U/Pb concordia plots (Figure 2.13) and map of sample locations (Figure 2.14).

a) AJS-01 Flake Lake Suite, quartz rhyolite volcaniclastic

This sample is from south of Flake Lake and collected east outside of the Flake transect. The rubble outcrop is several hundred meters in diameter and is composed of banded rhyolite with 10% ~1 mm quartz phenocrysts. Four analysed grains had low U concentrations (28.9-31.4 ppm) and gave concordant and overlapping results, with a concordia intercept of 2697.6±8.9 Ma (with U/Pb decay error and 95% confidence). This sample does not exhibit lead loss, and has large errors on each fraction attributed to both low U contents in the zircons. This age is taken as a good estimate of the crystallization of this rock.

b) AJS-05 Windy Lake Felsic Suite,

This 15 m wide intermediate to felsic unit lies northeast of Spider Lake, and is bounded by the Member Basalt Suite to the northeast and the Spider Arm Basalt Suite to the southwest. This rock is composed of grey lapilli in a siliceous feldspar rich matrix, with sparse quartz phenocrysts. Five clear and colorless zircon grains weighing between 4 and 7 μg were analyzed. The majority of zircons are low in U and contain between 46.3 to 91.9 ppm. Four of the five anaylses are concordant and nearly overlapping, with the four analyses yielding a concordia intercept of 2685±2.0 Ma. A five point regression through all data give a upper intercept of 2685.8± 2.3 and lower intercept of 1607±200 Ma. Due to the limited dispersion of the data, the concordia intercept at 2685±2.0 Ma is considered the best estimate of the age of this rock.

c) AJS-04 Square Lake Suite, quartz-feldspar dacite tuff

This sample was collected from a thin (<3 m) felsic unit found between Wolverine and Patch Lakes, on the Wolverine Transect. This felsic feldspar phyric fragmental unit has lapilli size fragments in a siliceous feldspar rich matrix. In outcrop, it is bounded by mafic volcanic rocks of the Wolverine Basalt Suite, and subsequently folded. Three clear and colorless zircon grains, ranging in weight from 2 to 5 μg, were analysed. One yields a concordant result with a $^{207}Pb/^{206}Pb$ age of 2690.5±2.3 Ma, whereas the remaining two gave discordant results. A three point linear regression gives an upper intercept of 2691.1±2.0 Ma and a lower intercept of 237 Ma. The upper intercept of 2691.1±2.0 Ma is interpreted as the crystallization age of this tuff.

d) AJS-03 Square Lake Suite, quartz-feldspar dacite tuff

A thin felsic unit is found as two small outcrops to the south of the Naartok Deposit to the north of the Wolverine transect. This unit is bounded on both sides by pillow basalts of the Wolverine Basalt Suite. This feldspar phyric volcaniclastic rock has many angular feldspar grains with some quartz eyes. The zircons selected for anaylsis were clear and colorless, with four fractions ranging in mass from 2-7 μg. Variably discordant results (5.3-1.0%) are attributed to minor Pb loss. A linear regression gives an upper intercept of 2691.7 ±2.5 Ma and a lower intercept of 250±180 Ma. The former is interpreted as the crystallization age of this tuff.

e) AJS-06 Boston Sedimentary Suite

This sample from the shore of Spider Lake and is part of the west limb of the Boston Anticline. The quartz wacke is surrounded by wacke beds and thin argillite beds, all of which have been folded on an outcrop scale. Five clear and colorless zircon grains selected for anaylsis range in weight from 2 to 8 μg. One analysis is concordant with a $^{207}Pb/^{206}Pb$ date of 2690 Ma, while the remaining vary from 1.9 to 7.6% discordant, with $^{207}Pb/^{206}Pb$ ages of 2685.2 ± 4.0 Ma, 2675.8 ± 2.5 Ma, 2695.3 ± 3.6 Ma, and 2687.5 ± 6.0 Ma. The youngest $^{207}Pb/^{206}Pb$ date of 2675.8 ± 2.5 Ma provides a maximum estimate for deposition.

f) LMB-55 Glen Lake Sedimentary Unit

This siltstone sample was taken from an outcrop to the south of Discovery Bay. This sedimentary unit is located between the Discovery Basalt Suite to the west and the Windy Lake Felsic Suite to the east. Five clear and colorless zircon grains selected for anaylsis range in weight from 3 to 8 µg. Three of the grains were low in U, ranging from 53.6 to 83.9, with the remaining samples containing 113.9 and 110.5. The four low U analyses were found to be concordant to slightly reversely discordant, with $^{207}Pb/^{206}Pb$ dates of 2683.7 ±1.9 Ma, 2679.4 ±1.7 Ma, 2682.1 ±1.9 Ma and 2683.3 ±1.7Ma. One sample was found to be 16.6% discordant with $^{207}Pb/^{206}Pb$ age of 2678.4±2.8 Ma. The youngest $^{207}Pb/^{206}Pb$ date of 2678.4±2.8 Ma provides a maximum estimate of deposition.

g) LMB-56 Conglomerate Hill Sedimentary Suite

This sample taken on the east shore of Hope Bay from a sandstone interbedded with a pebbly conglomerate. The sample is mostly made up of white to cream feldspar grains and few clear quartz grains. Five clear and colorless zircon grains selected for anaylsis range in weight from 3 to 13 µg. All of the grains are low in U, ranging from 27.3 to 107.1 ppm . These samples were found to be concordant to slightly reversely discordant, with$^{207}Pb/^{206}Pb$ dates of 2684.4 ±1.8 Ma, 2675.8 +2.1/-2.2 Ma, 2677.9 ±1.7 Ma, 2670.6 ±2.5 Ma and 2682.1 ±2.5 Ma. The youngest $^{207}Pb/^{206}Pb$ date of 2670.6 ±2.5 Ma provides a maximum estimate for deposition.

APPENDIX B:

Procedures of Geochemical-Isotopic Analysis PCIGR

Quality Assurance and Dissolution Procedures

Samples with large grain sizes will not homogenize during dissolution so original sample powders, which were ground by ALS Chemex, were inspected under microscope to confirm that particle sizes were less than 60um in diameter. Procedural duplicates (84577, 84514) were included to monitor data reproducibility. The USGS reference material G-2 granite was analyzed to monitor the accuracy of the concentration results. Both trace element and isotopic compositions for each sample were determined from a single digestion procedure.

Digestion

The samples were split into two groups, 1) those that do contain refractory minerals (zircon bearing) and 2) those that do not contain refractory minerals. Samples identified as containing refractory minerals underwent high temperature dissolution. This involved sample powder (100 to 150 mg) being mixed with 5.0 mL of 48% HF and 1.0 mL of 14 N HNO_3 and placed in steel-jacketed acid-washed high-pressure PTFE bombs and placed in an oven at 190^{o}C for 5 days. Digested samples were dried on a hotplate overnight at 130^{O}C, reconstituted in 6.0 mL of 6 N HCl and re-bombed for 24 hours at 190^{O}C. Samples that lacked refractory minerals underwent standard hotplate dissolution. This procedure involved rock powders (100 to 250 mg) being placed in 15 mL screw-top Savillex® PFA beakers with 10.0 mL of 48% HF and 1.0 mL of 14 N HNO_3. The beakers were then placed on a hotplate for 48 hours at 130^{O}C and were occasionally placed in an ultrasonic bath to aid in complete digestion. After digestion, samples were dried down overnight on a hotplate at 130^{o}C, reconstituted in 6.0 mL of 6 N sub-boiled

HCl and re-dissolved for 24 hours at 130°C. Dissolved samples in of both groups were transferred to Savillex® and dried on a hotplate. Each sample was then re-dissolved in HCl (4 g) on a hotplate and an aliquot for trace element analysis was removed and placed in a separate Savillex® beaker. The remaining sample solution was kept for isotope ratio determination (see column chemistry procedures below).

Trace Element Anaylsis Procedure

Detailed procedures and instrument analytical operating parameters can be found in Petorius et al. (2005). The trace element aliquot was diluted by 800 to 2000 times in 1% HNO_3 with 1 ppb In as in internal standards. Trace element concentrations were analyzed on a Thermo Finnigan Element2 high resolution inductively coupled plasma mass spectrometer (HR-ICP-MS). Trace element concentrations from PCIGR are shown in Table 3.4. Two to three procedural blanks included in each batch of ten samples analyzed and were within acceptable values. Results for USGS reference material (G-2) are within error (2σ) of the range of previously published values (Robinson et al., 1986; Totland et al., 1992; Govindaraju, 1994; Liang et al., 2000; Raczek et al., 2000; Meisel et al., 2001; Pretorius et al., 2006). A comparison and brief discussion of trace element results from PCIGR and ALS Chemex can be found in Appendix E.

Sm-Nd and Lu-Hf Column Chemistry Procedure

The following Hf separation procedures are modified from Patchett and Tatsumoto (1980) and Blichert-Toft et al. (1997). The REE (including Nd) were separated from Hf using a Teflon® column with Biorad AG 50W-X8 100-200 mesh resin and a progressively increasing concentration of HCl from 1.5 N to 4.0 N. The Hf separate was then passed through a polypropylene column and a Savillex™ column, using a 0.1 N HF / 0.5 N HCl solution and Biorad AG 1-X8 100-200 mesh resin, and a 0.3 N HF / 2.5 N HCl solution and Biorad AG 50W-X8 200-400 mesh resin, respectively. Nd was separated from the REE in a separate quartz column using 0.16 N HCl and HDEDE-coated Teflon® beads.

Instrumentation and Analysis

The Nd isotopic measurements were made on a Thermo Finnigan Triton-TI thermal ionization mass spectrometer (TIMS) in static mode with relay matrix rotation on double Be-Ta filaments. The results are shown in Table 2.5. The measured compositions of each sample are the mean of 135 analyses (as blocks of 15 cycles). Samples were measured in 3 batches over four days. During the analysis of each batch the La Jolla Nd standard was measured six times giving a mean value of $^{143}Nd/^{144}Nd = 0.511855 \pm 0.000006$ (2σ), 0.511863 ± 0.000009 (2σ) and 0.511829 ± 0.000009 (2σ) for the three batches, respectively. Two procedural duplicates are within analytical error (2σ). All measurements were corrected for internal mass fractionation using $^{146}Nd/^{144}Nd = 0.7219$. The Nd isotopic compositions of the USGS G-2 reference material are within analytical error (2σ) of previously reported results (Weis et al., 2006).

The Hf isotopic compositions were analyzed in static mode on the PCIGR Nu Plasma multi-collector inductively coupled plasma mass spectrometer (MC-ICP-MS) in the "dry" plasma mode using a desolvating nebulizer (DSN). Measured ratios and age-corrected values are shown in Table 2.5. The measured compositions of each sample are the mean of 60 analyses (3 blocks of 20 cycles). The measured Hf isotopic ratios were corrected for interferences by monitoring Lu and Yb beams throughout each analysis. Samples were measured in 3 separate batches over three days. Standard sample bracketing of the Hf JMC 475 in-house standard gave a mean value of $^{176}Hf/^{177}Hf$ = 0.282163 ± 0.000012 (2σ; n=12), 0.282174 ± 0.000009 (2σ; n=12) and 0.282172 ± 0.000004 (2σ n=13) for both the three batches respectively; these values are within the range of previously published values (Blichert-Toft et al., 1997; Chauvel & Blichert-Toft, 2001; Goolaerts et al., 2004). The three procedural duplicates are within analytical error (2σ). All reported values were normalized to $^{176}Hf/^{177}Hf$ = 0.282160 as suggested by Vervoort & Blichert-Toft (1999). The Hf isotopic compositions of the USGS G-2 reference material are within analytical error (2σ) of previously reported results (Weis et al., 2006).

References:

Patchett P. J. and Tatsumoto M. (1980), A routine high-precision method for Lu-Hf isotope geochemistry and chronology. Contr. Mineral. Petrol., 75, 263-267.

Blichert-Toft J., Chauvel C., and Albarède F. (1997), Separation of Hf and Lu for high-precision isotope analysis of rock samples by magnetic sector-multiple collector ICP-MS. Contrib. Mineral. Petrol., 127, 248-260.

Vervoort J. D. and Blichert-Toft J. (1999), Evolution of the depleted mantle: Hf isotope evidence from juvenile rocks through time. Geochim. Cosmochim. Acta 63, 533-556.

Weis D., Kieffer B., Maerschalk C., Barling J., de Jong J., Williams G., Hanano D., Pretorius W., Mattielli N., Scoates J.S., Goolaerts A., Friedman R. and Mahoney J.B. (2006), High-precision isotopic characterization of reference materials by TIMS and MC-ICP-MS. Geochem. Geophys. Geosyst., 7,

APPENDIX C:

Major and Trace Element Abundances of Samples from the Hope Bay Greenstone Belt, (ALS CHEMEX)

Appendix C: Major oxide and Trace element concentrations by XRF and ICP-MS (ALS Chemex) for samples from the Hope Bay Greenstone Belt

Sample	84585	84586	200630	200632	202914	202926	202927	202932	84520
Rock Type	Calc-Alkaline Dacite	Calc-Alkaline Dacite	Calc-Alkaline Dacite	Calc-Alkaline Dacite	Calc-Alkaline Dacite	Calc-Alkaline Dacite	Calc-Alkaline Dacite	Calc-Alkaline Dacite	Calc-Alkaline Dacite
UTME	434569	433606	434584	434808	433145	434967	434965	434944	441602
UTMN	7505760	7505408	7505520	7505648	7505904	7506416	7506416	7506352	7510752
Suite	Koignuck Felsic Suite	Koignuck Felsic Suite	Koignuck Felsic Suite	Koignuck Felsic Suite	Koignuck Felsic Suite	Koignuck Felsic Suite	Koignuck Felsic Suite	Koignuck Felsic Suite	Koignuck Felsic Suite
SiO_2	62.29	64.46	65.59	62.42	64.03	64.80	66.99	67.21	63.03
TiO_2	0.49	0.56	0.52	0.55	0.50	0.61	0.43	0.48	0.53
Al_2O_3	14.30	14.39	16.50	16.75	15.74	15.81	14.83	14.83	16.10
Fe_2O_3	9.76	4.93	3.39	5.14	5.23	5.41	4.52	4.32	4.78
MnO	0.10	0.07	0.07	0.05	0.04	0.05	0.04	0.06	0.07
MgO	2.47	1.93	1.20	2.81	3.37	2.45	1.54	1.52	2.13
CaO	1.59	3.41	2.07	3.08	3.33	5.55	5.07	3.31	3.30
Na_2O	1.31	4.10	4.51	4.10	3.75	2.58	4.14	3.32	4.35
K_2O	2.88	1.42	1.94	1.20	1.20	1.17	0.21	1.08	1.68
P_2O_5	0.11	0.12	0.16	0.11	0.14	0.20	0.09	0.11	0.20
Cr_2O_3	0.01	0.01	0.01	0.01	0.02	0.02	0.02	0.01	<0.01
SrO	<0.01	0.01	0.02	0.03	0.02	0.03	0.03	0.03	0.03
BaO	0.02	0.02	0.04	0.02	0.02	0.03	0.01	0.02	0.04
LOI	4.53	3.85	3.95	3.81	2.34	1.22	1.87	3.15	3.41
Total	99.85	99.27	99.98	100.10	99.74	99.93	99.79	99.44	99.66
V	66	68	61	79	72	69	64	70	78
Cr	80	90	90	110	190	180	140	120	80
Co	19.8	12.3	7.3	15.3	15.4	13.8	9.7	8.5	13.1
Ni	42	22	25	41	51	21	28	20	24
Cu	27	24	7	34	72	22	5	23	24
Zn	75	71	53	86	62	48	36	60	54
Cs	0.8	0.5	1.4	0.9	0.3	1.4	0.2	1.1	1.4
Rb	26.4	30.5	30.9	27.3	19.6	24.9	2.7	23.7	43.6
Sr	27.7	141.5	124.5	231.0	192.0	235.0	247.0	230.0	244.0
Ba	144.0	190.0	311.0	265.0	272.0	185.5	71.3	185.0	336.0
Nb	5.0	6.0	5.0	5.0	7.0	8.0	5.0	5.0	7.0
Zr	136.5	147.5	147	152.5	150.5	164	124	126.5	123.5
Hf	4	4	4	4	4	4	4	4	3
Y	10.4	12.6	7.7	10.0	13.5	17.0	10.3	10.6	9.6
La	16.1	16.4	14.9	17.8	16.8	18.4	17.8	17.0	21.2
Ce	31.9	33.8	29.6	32.9	34.3	38.5	33.3	31.3	44.4
Pr	3.6	3.9	3.4	3.7	3.9	4.5	3.6	3.4	5.1
Nd	13.6	14.8	12.2	13.1	14.6	17.7	13.0	11.8	18.0
Sm	2.8	3.0	2.4	2.5	2.9	3.6	2.4	2.2	3.1
Eu	0.7	0.8	0.7	0.8	0.9	1.0	0.7	0.8	0.9
Gd	2.5	2.8	2.0	2.4	2.9	3.5	2.3	2.3	2.8
Tb	0.3	0.4	0.3	0.4	0.4	0.5	0.3	0.3	0.4
Dy	1.9	2.3	1.4	1.9	2.4	2.8	1.7	1.7	1.8
Ho	0.3	0.4	0.3	0.4	0.5	0.6	0.3	0.4	0.3
Er	1.1	1.3	0.7	1.1	1.3	1.6	1.0	1.0	1.0
Tm	0.1	0.1	0.1	0.1	0.2	0.3	0.2	0.2	0.1
Yb	1.0	1.2	0.6	0.9	1.2	1.5	1.0	0.9	0.9
Lu	0.1	0.1	0.1	0.1	0.2	0.3	0.1	0.1	0.1
Pb	<5	13	<5	5	9	<5	<5	<5	<5
Th	2.0	2.0	2.0	3.0	2.0	2.0	3.0	3.0	3.0
U	0.6	0.6	<0.5	0.7	0.5	0.6	0.6	0.6	0.8
Ga	17	17	19	20	19	19	18	18	17
Sn	1	1	1	2	<1	<1	<1	<1	1
Ta	0.5	0.5	0.5	0.5	0.6	0.6	0.5	0.5	0.5
W	1	<1	<1	1	1	1	1	<1	1

Appendix C: Major oxide and Trace element concentrations by XRF and ICP-MS (ALS Chemex) for samples from the Hope Bay Greenstone Belt

Sample	84546	202923	1001	1002	202931	249878	249879	249880	84550
Rock Type	Calc-Alkaline Dacite	Calc-Alkaline Dacite	Calc-Alkaline Dacite	Calc-Alkaline Dacite	Calc-Alkaline Dacite	Calc-Alkaline Dacite	Calc-Alkaline Dacite	Calc-Alkaline Dacite	Calc-Alkaline Dacite
UTME	441040	431433	433414	434907	432493	431446	430929	430653	440476
UTMN	7512112	7548960	7549968	7546448	7551376	7560720	7561216	7557888	7512448
Suite	Koignuck Felsic Suite	Koignuck Felsic Suite	Square Lake	Square Lake	Windy Felsics	Windy Felsics	Windy Felsics	Windy Felsics	Windy Felsics
SiO_2	56.23	55.00	64.95	68.09	66.44	60.21	62.22	67.79	68.41
TiO_2	0.75	0.69	0.40	0.25	0.42	0.50	0.49	0.39	0.48
Al_2O_3	17.41	15.24	15.05	15.92	14.49	15.03	16.87	15.14	13.84
Fe_2O_3	7.69	8.30	3.33	2.41	2.82	5.17	5.19	3.27	3.04
MnO	0.09	0.10	0.05	0.02	0.06	0.06	0.07	0.03	0.06
MgO	3.44	5.21	1.18	1.01	2.27	2.87	2.22	0.89	1.09
CaO	6.24	4.92	3.40	1.37	2.54	4.14	3.34	1.87	2.56
Na_2O	2.80	3.92	4.66	6.00	4.64	4.40	4.38	6.57	2.62
K_2O	1.71	0.18	1.66	1.50	2.11	1.61	2.09	0.65	2.88
P_2O_5	0.25	0.14	0.06	0.07	0.07	0.24	0.18	0.11	0.06
Cr_2O_3	0.01	0.02	0.00	0.00	0.03	0.01	<0.01	<0.01	0.01
SrO	0.03	0.02	0.01	0.01	0.01	0.05	0.07	0.05	0.02
BaO	0.04	0.02	0.05	0.03	0.03	0.03	0.05	0.04	0.06
LOI	3.34	6.22	4.02	2.58	3.60	5.23	2.31	2.59	4.84
Total	100.05	99.97	98.82	99.26	99.54	99.55	99.49	99.39	99.98
V	114	154	63	33	72	105	82	45	25
Cr	130	180	60	20	110	80	40	30	90
Co	21.2	30.3	10.6	6.3	6.7	17.4	13.4	8.4	5.2
Ni	46	116	31	57	24	45	32	14	10
Cu	48	27	21	12	33	21	10	<5	12
Zn	83	82	77	54	32	56	58	41	55
Cs	1.1	0.4	3.9	0.8	0.9	1.1	1.2	0.6	1.9
Rb	47.3	3.8	53.3	38.6	34.6	38.4	46.7	13.9	52.8
Sr	264.0	130.0	86.0	121.0	86.9	408.0	629.0	325.0	141.5
Ba	428.0	86.1	451.0	249.0	335.0	311.0	367.0	199.5	463.0
Nb	12.0	5.0	2.0	2.0	3.0	5.0	3.9	3.3	9.0
Zr	197	107.5	94.5	110	104.5	136	126	119	198.5
Hf	5	3	3	3	3	3.7	3.4	3.4	5
Y	18.2	16.4	6.9	6.2	7.5	10.0	8.0	5.2	16.3
La	26.8	11.2	7.3	6.2	11.8	38.5	26.9	15.9	29.2
Ce	54.1	24.6	14.8	13.1	22.0	83.7	58.7	32.2	60.6
Pr	6.2	3.0	1.8	1.6	2.5	10.0	6.9	3.7	7.1
Nd	23.1	12.3	7.9	7.1	9.7	38.1	26.9	13.7	26.4
Sm	4.3	2.6	1.7	1.5	1.9	5.9	4.0	2.2	4.7
Eu	1.4	0.8	0.7	0.5	0.6	1.4	1.2	0.7	1.1
Gd	4.3	2.9	1.7	1.5	1.9	4.4	3.4	1.9	4.4
Tb	0.6	0.5	0.2	0.2	0.3	0.5	0.4	0.2	0.6
Dy	3.3	2.8	1.2	1.0	1.3	2.1	1.7	1.2	2.9
Ho	0.6	0.6	0.2	0.2	0.3	0.4	0.3	0.2	0.6
Er	1.9	1.8	0.6	0.6	0.7	1.1	0.9	0.6	1.7
Tm	0.3	0.3	0.1	0.1	0.1	0.1	0.1	0.1	0.2
Yb	1.7	1.6	0.5	0.6	0.6	1.0	0.7	0.5	1.6
Lu	0.3	0.3	0.1	0.1	0.1	0.1	0.1	0.1	0.3
Pb	6	<5	9	<5	<5	<5	5	<5	5
Th	4.0	1.0	2.0	1.0	2.0	5.0	3.5	2.6	4.0
U	0.8	<0.5	0.5	0.5	0.5	0.97	0.79	0.61	0.9
Ga	22	17	21	22	18	17.5	20.1	16.3	16
Sn	2	<1	1	1	<1	1	1	1	1
Ta	0.7	<0.5	0	0	<0.5	0.4	0.4	0.4	0.6
W	2	1	3	2	1	1	1	3	2

Appendix C: Major oxide and Trace element concentrations by XRF and ICP-MS (ALS Chemex) for samples from the Hope Bay Greenstone Belt

Sample	84551	249517	249521	249522	84573	1004	249533	249534	249535
Rock Type	Calc-Alkaline Dacite	Calc-Alkaline Dacite	Calc-Alkaline Dacite	Calc-Alkaline Dacite	Calc-Alkaline Rhyolite	Epiclastic Andesites	Epiclastic Andesites	Epiclastic Andesites	Epiclastic Andesites
UTME	439610	440384	439611	439587	438196	437602	437714	437627	437691
UTMN	7511088	7512368	7512016	7511424	7506720	7503312	7504816	7504080	7503024
Suite	Windy Felsics	Windy Felsics	Windy Felsics	Windy Felsics	Clover Lake felsics	Clover Sediments	Clover Sediments	Clover Sediments	Clover Sediments
SiO_2	67.69	69.17	66.60	64.12	75.08	58.11	58.11	55.53	58.03
TiO_2	0.30	0.42	0.34	0.56	0.09	0.62	0.97	0.70	0.59
Al_2O_3	13.68	14.18	14.78	15.62	12.90	15.87	17.37	15.48	14.31
Fe_2O_3	3.08	3.32	2.86	5.21	0.79	7.61	6.69	8.10	6.79
MnO	0.04	0.06	0.05	0.09	0.02	0.09	0.05	0.06	0.32
MgO	0.99	0.67	1.59	0.93	0.42	4.41	4.11	3.94	5.42
CaO	3.76	2.57	2.63	3.52	0.61	5.75	1.99	3.21	2.12
Na_2O	4.33	4.23	3.76	3.64	3.11	3.50	5.12	3.85	4.62
K_2O	1.32	1.69	2.21	2.02	4.15	0.31	0.37	0.60	0.14
P_2O_5	0.07	0.09	0.09	0.19	0.04	0.08	0.19	0.15	0.15
Cr_2O_3	0.01	<0.01	<0.01	<0.01	0.01	0.00	<0.01	<0.01	0.03
SrO	0.04	0.02	0.02	0.04	<0.01	0.03	0.03	0.02	0.02
BaO	0.03	0.05	0.02	0.04	0.08	0.02	0.01	0.02	0.02
LOI	4.79	3.05	5.10	3.61	1.50	2.48	4.24	6.99	5.77
Total	100.15	99.53	100.05	99.59	98.81	98.90	99.24	98.65	98.32
V	40	25	44	27	8	136	148	104	96
Cr	80	30	20	10	140	180	10	50	240
Co	6.8	5.2	7.8	8.9	1.4	28.4	27.0	20.5	24.3
Ni	12	6	12	8	5	90	20	45	134
Cu	7	<5	<5	6	<5	62	46	76	32
Zn	47	72	35	87	31	85	102	437	164
Cs	0.6	1.2	1.4	1.6	1.8	0.6	0.4	0.8	0.3
Rb	31.6	48.7	49.2	48.9	85.2	9.3	7.3	13.9	2.4
Sr	284.0	195.0	195.5	307.0	39.0	279.0	214.0	145.5	120.0
Ba	296.0	361.0	294.0	380.0	670.0	109.5	132.5	157.0	187.5
Nb	4.0	12.0	4.0	6.8	3.0	5.0	8.0	6.6	6.8
Zr	94.1	263	122	156.5	56.5	125.5	166	150	144
Hf	3	6.8	3.5	4.5	2	4	4.5	4	3.7
Y	6.6	22.6	10.0	18.9	3.4	15.7	21.4	16.8	11.9
La	14.4	38.4	15.2	21.9	10.7	12.8	14.5	11.8	14.3
Ce	26.9	82.4	29.0	45.5	21.4	24.6	37.6	30.8	37.1
Pr	3.0	9.8	3.2	5.3	2.3	2.8	3.9	3.3	3.7
Nd	11.2	37.5	12.7	20.5	7.9	12.0	16.9	13.6	15.0
Sm	2.1	6.5	2.5	4.0	1.5	2.5	3.6	2.9	2.9
Eu	0.6	1.4	0.6	1.2	0.2	1.0	1.2	1.0	0.9
Gd	1.9	5.8	2.2	3.9	1.2	2.7	4.2	3.4	3.1
Tb	0.3	0.8	0.3	0.6	0.1	0.4	0.7	0.5	0.4
Dy	1.2	4.4	1.8	3.5	0.7	2.6	4.0	3.2	2.3
Ho	0.2	0.8	0.3	0.7	0.1	0.5	0.9	0.6	0.5
Er	0.7	2.4	0.9	2.0	0.3	1.6	2.4	1.9	1.3
Tm	0.1	0.3	0.1	0.3	<0.1	0.2	0.3	0.3	0.2
Yb	0.7	2.2	0.9	1.9	0.2	1.5	2.3	1.8	1.2
Lu	0.1	0.3	0.1	0.3	<0.1	0.2	0.3	0.3	0.2
Pb	<5	6	<5	11	<5	5	<5	<5	48
Th	3.0	5.8	3.0	3.7	3.0	2.0	2.6	2.2	2.5
U	0.5	1.3	0.62	0.95	1.1	0.6	0.6	0.46	0.5
Ga	17	18.8	21.3	22.3	18	18	21.2	17.7	16
Sn	1	2	1	2	1	1	1	1	1
Ta	<0.5	0.8	0.4	0.6	<0.5	0	0.6	0.5	0.4
W	2	7	2	5	2	1	1	2	3

Appendix C: Major oxide and Trace element concentrations by XRF and ICP-MS (ALS Chemex) for samples from the Hope Bay Greenstone Belt

Sample	84547	84548	84549	84574	249536	202922	249537	249539	249540
Rock Type	LREE basalt	LREE basalt	LREE basalt	LREE basalt	LREE basalt	LREE basalt	normal basalt	normal basalt	normal basalt
UTME	440554	440432	441038	438811	437719	431509	441162	441436	442186
UTMN	7511728	7512352	7512032	7506768	7502992	7549024	7504896	7503088	7502096
Suite	LREE Basalts	LREE Basalts	LREE Basalts	Clover East Basalts	Clover East Basalts	Koig Basalts	Boston Basalt	Boston Basalt	Boston Basalt
SiO_2	43.70	50.01	49.46	52.38	51.30	43.41	23.98	46.79	50.64
TiO_2	1.09	1.06	0.92	0.79	0.94	0.93	0.39	0.80	0.75
Al_2O_3	18.04	14.98	15.37	19.01	18.67	16.54	7.47	16.00	13.19
Fe_2O_3	14.07	12.22	10.07	8.26	8.28	11.88	12.34	11.65	9.03
MnO	0.28	0.18	0.18	0.12	0.13	0.12	0.16	0.19	0.26
MgO	4.88	5.78	4.49	5.67	4.99	9.36	20.97	6.66	5.01
CaO	11.33	8.71	10.42	5.53	5.02	4.17	3.02	12.25	10.69
Na_2O	1.27	3.12	2.42	4.32	5.20	2.90	0.49	1.26	2.06
K_2O	0.08	0.09	0.06	0.38	0.05	0.23	0.16	0.03	0.11
P_2O_5	0.24	0.29	0.12	0.16	0.09	0.16	0.03	0.06	0.05
Cr_2O_3	0.05	0.01	0.05	0.01	0.01	0.02	0.38	0.05	0.15
SrO	0.06	0.04	0.03	0.04	0.03	0.01	0.01	0.02	0.02
BaO	<0.01	0.01	0.01	0.02	0.01	0.01	<0.01	<0.01	0.01
LOI	5.23	3.01	5.55	3.37	3.75	10.20	28.80	3.84	7.08
Total	100.30	99.49	99.15	100.05	98.47	99.95	98.20	99.61	99.05
V	292	252	245	189	242	176	142	263	241
Cr	250	100	350	110	140	220	2860	340	1080
Co	65.9	43.7	59.0	33.1	35.6	44.8	105.0	50.2	63.6
Ni	141	42	239	92	81	172	917	171	244
Cu	98	56	77	70	10	51	8	112	110
Zn	106	91	83	94	84	119	253	95	81
Cs	0.1	0.3	0.1	0.8	0.2	0.3	0.4	0.1	0.1
Rb	0.9	1.3	0.7	12.7	0.4	5.7	7.4	0.4	2.5
Sr	524.0	321.0	237.0	370.0	270.0	73.1	75.4	224.0	160.5
Ba	15.0	51.2	21.4	214.0	62.1	137.0	26.0	10.2	52.5
Nb	7.0	7.0	4.0	6.0	4.7	6.0	1.3	1.8	2.0
Zr	98.4	114	53.9	119	121	138	36	43	51
Hf	3	3	2	3	3.1	4	1	1.3	1.4
Y	27.8	24.5	21.8	16.5	18.1	20.8	8.8	16.8	18.3
La	18.5	18.8	8.7	10.4	9.9	12.8	1.9	2.1	3.5
Ce	44.5	45.8	21.7	23.8	24.0	28.7	5.9	7.0	9.4
Pr	5.9	6.1	2.9	3.1	2.5	3.7	0.7	0.9	1.1
Nd	24.8	25.7	12.0	13.2	10.8	14.8	3.5	4.8	6.0
Sm	5.3	5.5	2.9	3.0	2.4	3.4	0.9	1.6	1.8
Eu	1.8	1.6	1.0	0.9	1.0	1.0	0.4	0.7	0.8
Gd	5.5	5.3	3.3	3.0	3.1	3.6	1.3	2.3	2.6
Tb	0.8	0.8	0.6	0.5	0.5	0.6	0.2	0.4	0.5
Dy	4.9	4.5	3.7	3.0	3.2	3.5	1.6	3.0	3.2
Ho	1.0	0.9	0.8	0.6	0.7	0.8	0.4	0.7	0.7
Er	3.1	2.7	2.5	1.8	2.1	2.3	1.0	2.0	2.1
Tm	0.4	0.4	0.4	0.2	0.3	0.3	0.2	0.3	0.3
Yb	2.9	2.5	2.4	1.7	2.1	2.1	0.9	2.0	1.9
Lu	0.4	0.4	0.4	0.2	0.3	0.4	0.2	0.3	0.3
Pb	<5	<5	<5	17	<5	<5	8	<5	<5
Th	1.0	1.0	1.0	1.0	1.7	1.0	0.3	0.2	0.3
U	<0.5	<0.5	<0.5	<0.5	0.34	<0.5	<0.05	<0.05	<0.05
Ga	21	18	18	19	19.4	14	9	16.3	14.3
Sn	1	1	1	1	1	<1	<1	<1	1
Ta	<0.5	<0.5	<0.5	<0.5	0.4	0.5	0.1	0.1	0.1
W	2	2	1	1	15	1	28	10	12

Appendix C: Major oxide and Trace element concentrations by XRF and ICP-MS (ALS Chemex) for samples from the Hope Bay Greenstone Belt

Sample	249541	84545	84572	84580	84575	84576	84577	84578	84579
Rock Type	normal basalt	normal basalt	normal basalt	normal basalt	normal basalt	normal basalt	normal basalt	normal basalt	normal basalt
UTME	441048	439452	438902	437808	437265	437337	437045	436744	436006
UTMN	7502736	7507664	7507360	7503584	7506128	7505888	7505232	7506272	7505600
Suite	Boston Basalt	clover east basalts	clover east basalts	clover east basalts	clover west basalts	clover west basalts	clover west basalts	clover west basalts	clover west basalts
SiO_2	47.69	48.65	44.84	47.44	45.85	49.20	47.34	47.13	40.32
TiO_2	0.98	0.76	0.60	0.91	0.95	1.12	0.87	0.84	0.87
Al_2O_3	15.20	14.66	11.09	15.10	14.96	14.08	14.30	14.19	11.58
Fe_2O_3	12.46	9.25	12.27	11.65	13.66	13.61	12.99	13.43	17.70
MnO	0.20	0.20	0.24	0.25	0.22	0.20	0.21	0.22	0.31
MgO	7.22	3.25	10.47	4.85	6.23	6.31	7.64	7.04	12.50
CaO	9.27	9.70	13.66	11.65	12.37	10.25	10.78	11.76	10.41
Na_2O	0.16	3.22	0.79	2.06	1.22	2.11	1.39	1.59	0.14
K_2O	0.02	0.37	0.08	0.23	0.08	0.23	0.30	0.12	0.06
P_2O_5	0.06	0.06	0.04	0.07	0.08	0.10	0.08	0.06	0.06
Cr_2O_3	0.04	0.03	0.13	0.04	0.01	0.01	0.04	0.04	0.06
SrO	0.02	0.01	0.01	0.02	<0.01	0.02	0.01	0.01	0.01
BaO	<0.01	0.01	<0.01	0.01	<0.01	0.01	0.01	<0.01	<0.01
LOI	4.90	9.54	5.85	4.94	3.56	2.99	3.23	2.96	6.06
Total	98.22	99.70	100.05	99.21	99.20	100.25	99.19	99.39	100.10
V	290	260	202	302	325	327	302	298	311
Cr	330	280	1040	310	190	100	300	300	460
Co	49.1	46.9	59.2	50.9	50.7	51.9	52.1	49.9	57.2
Ni	120	113	294	132	75	67	114	110	115
Cu	112	114	81	130	114	138	124	116	101
Zn	105	69	75	76	97	102	85	87	118
Cs	0.0	0.6	0.1	<0.1	0.1	0.2	0.1	<0.1	0.1
Rb	0.2	9.3	0.6	2.6	0.9	3.9	4.2	0.7	0.5
Sr	119.5	79.4	92.3	157.0	50.7	208.0	90.5	170.0	69.8
Ba	4.8	88.3	11.2	28.8	10.2	37.6	31.2	10.5	5.2
Nb	2.1	2.0	2.0	2.0	3.0	5.0	2.0	2.0	2.0
Zr	53	38.8	115.5	53.2	62.6	81.3	55.3	54.7	52.3
Hf	1.6	1	3	2	2	2	2	2	2
Y	18.6	14.4	14.8	19.8	22.9	26.8	20.0	19.5	19.8
La	2.2	2.5	2.1	3.2	4.3	5.9	3.3	3.1	2.3
Ce	7.3	6.3	5.9	8.1	11.0	14.5	8.3	8.2	6.6
Pr	0.9	1.0	0.9	1.2	1.7	2.1	1.3	1.3	1.1
Nd	5.4	4.9	4.8	6.3	8.2	10.6	6.6	6.3	6.0
Sm	1.7	1.6	1.6	2.1	2.6	3.2	2.3	2.1	2.2
Eu	0.7	0.6	0.6	0.8	0.9	1.0	0.7	0.7	0.8
Gd	2.6	2.0	2.0	2.7	3.1	3.8	2.8	2.7	2.6
Tb	0.5	0.4	0.4	0.5	0.5	0.7	0.5	0.5	0.5
Dy	3.4	2.6	2.5	3.2	3.9	4.6	3.4	3.4	3.3
Ho	0.7	0.5	0.5	0.7	0.8	0.9	0.7	0.7	0.7
Er	2.2	1.7	1.7	2.2	2.6	2.9	2.2	2.2	2.1
Tm	0.3	0.2	0.2	0.3	0.3	0.4	0.3	0.3	0.3
Yb	2.3	1.6	1.6	2.1	2.4	2.7	2.1	2.0	2.0
Lu	0.3	0.2	0.3	0.3	0.4	0.4	0.3	0.3	0.3
Pb	<5	<5	<5	<5	7	<5	<5	<5	<5
Th	0.3	<1	<1	<1	<1	<1	<1	<1	<1
U	<0.05	<0.5	<0.5	<0.5	<0.5	<0.5	<0.5	<0.5	<0.5
Ga	15.1	14	13	16	18	17	15	16	15
Sn	<1	1	1	1	1	1	1	1	1
Ta	0.1	<0.5	<0.5	<0.5	<0.5	<0.5	<0.5	<0.5	<0.5
W	10	2	1	<1	1	3	3	1	3

Appendix C: Major oxide and Trace element concentrations by XRF and ICP-MS (ALS Chemex) for samples from the Hope Bay Greenstone Belt

Sample	84581	200611	249882	249895	84536	84540	84541	84543	84544
Rock Type	normal basalt	normal basalt	normal basalt	normal basalt	normal basalt	normal basalt	normal basalt	normal basalt	normal basalt
UTME	436498	435180	429172	431933	442606	442213	441884	441742	441320
UTMN	7504976	7505520	7557632	7548784	7514624	7514256	7514080	7513408	7512176
Suite	clover west basalts	clover west basalts	Discovery basalts	Koig Basalts	Member Basalt	Member Basalt	Member Basalt	Member Basalt	Member Basalt
SiO_2	45.31	47.98	42.60	47.17	47.01	47.50	47.30	46.57	45.43
TiO_2	0.88	0.85	0.76	0.99	0.93	1.01	0.98	0.97	1.02
Al_2O_3	13.58	15.68	14.55	15.31	14.54	13.99	14.19	13.87	14.90
Fe_2O_3	13.58	12.40	9.56	12.76	12.97	14.35	13.70	13.43	12.23
MnO	0.26	0.16	0.25	0.22	0.19	0.21	0.22	0.21	0.20
MgO	5.82	7.86	3.97	4.28	6.16	7.72	6.06	6.16	4.39
CaO	12.32	9.32	9.35	11.04	12.85	10.20	11.18	9.73	11.38
Na_2O	2.00	2.37	1.94	1.21	1.32	1.22	1.57	0.84	2.08
K_2O	0.16	0.25	0.60	0.09	0.07	0.06	0.14	0.05	0.03
P_2O_5	0.07	0.07	0.06	0.06	0.08	0.07	0.16	0.14	0.08
Cr_2O_3	0.02	0.03	0.03	0.03	0.04	0.06	0.08	0.04	0.03
SrO	0.01	0.02	0.02	0.02	0.01	0.01	0.01	0.01	0.01
BaO	<0.01	<0.01	0.02	0.01	<0.01	0.01	<0.01	0.01	<0.01
LOI	5.15	3.10	16.30	5.93	3.58	3.28	4.32	7.35	7.91
Total	99.16	100.10	100.00	99.12	99.76	99.69	99.89	99.38	99.71
V	303	270	243	297	328	346	277	274	318
Cr	140	290	260	240	320	310	270	270	250
Co	48.6	51.2	44.4	55.0	48.6	50.1	45.4	45.4	47.4
Ni	69	137	129	141	106	88	92	92	84
Cu	110	97	86	126	118	118	92	100	120
Zn	90	90	66	91	84	100	91	99	89
Cs	0.1	0.1	0.8	0.2	<0.1	<0.1	0.1	0.1	<0.1
Rb	1.7	4.3	20.2	1.0	0.3	0.3	1.4	0.3	0.2
Sr	95.8	177.5	91.7	192.0	141.0	142.5	115.0	153.0	101.0
Ba	46.6	59.4	70.4	11.4	7.0	11.3	33.4	7.4	12.8
Nb	3.0	2.0	1.6	2.2	2.0	3.0	3.0	3.0	3.0
Zr	60.8	49.8	38	57	69.6	58	67.9	64.7	56.2
Hf	2	1	1.2	1.6	2	2	2	2	2
Y	20.4	13.8	11.9	21.2	21.4	22.3	23.8	22.0	20.9
La	4.0	3.5	1.7	3.3	3.0	3.2	4.2	3.8	3.3
Ce	10.1	8.0	4.7	8.8	8.2	8.5	11.2	10.2	8.9
Pr	1.5	1.1	0.7	1.4	1.3	1.4	1.8	1.6	1.4
Nd	7.5	5.4	3.8	6.7	6.8	7.0	8.9	8.0	7.2
Sm	2.3	1.7	1.2	2.2	2.3	2.4	2.8	2.6	2.3
Eu	0.8	0.7	0.5	0.8	0.9	0.8	1.1	1.0	0.9
Gd	2.8	1.9	1.4	2.8	2.9	3.1	3.4	3.3	2.8
Tb	0.5	0.4	0.3	0.5	0.5	0.6	0.6	0.6	0.5
Dy	3.5	2.4	2.1	3.6	3.6	3.7	4.2	3.8	3.7
Ho	0.7	0.5	0.5	0.8	0.8	0.8	0.9	0.8	0.8
Er	2.3	1.6	1.5	2.4	2.5	2.5	2.7	2.5	2.4
Tm	0.3	0.2	0.2	0.4	0.3	0.4	0.4	0.4	0.3
Yb	2.3	1.4	1.4	2.3	2.4	2.4	2.5	2.4	2.3
Lu	0.3	0.9	0.2	0.4	0.4	0.4	0.4	0.4	0.4
Pb	<5	<5	<5	<5	<5	<5	<5	<5	<5
Th	<1	<1	0.4	0.3	<1	<1	<1	<1	<1
U	<0.5	<0.5	0.14	0.06	<0.5	<0.5	<0.5	<0.5	<0.5
Ga	16	17	13.8	16.4	18	18	17	17	17
Sn	1	1	1	1	1	1	1	1	1
Ta	<0.5	<0.5	0.2	0.2	<0.5	<0.5	<0.5	<0.5	<0.5
W	7	1	1	3	1	3	2	2	1

Appendix C: Major oxide and Trace element concentrations by XRF and ICP-MS (ALS Chemex) for samples from the Hope Bay Greenstone Belt

Sample	249515	249516	249518	200688	202930	249877	202918	202924	202925
Rock Type	normal basalt	normal basalt	normal basalt	normal basalt	normal basalt	normal basalt	normal basalt	normal basalt	normal basalt
UTME	442856	442674	440391	432023	433092	432139	434048	434608	434037
UTMN	7514880	7515328	7512816	7559392	7551616	7560224	7547616	7552736	7552736
Suite	Member Basalt	Member Basalt	Member Basalt	Windy Basalts	Windy Basalts	Windy Basalts	Wolverine Basalts	Wolverine Basalts	Wolverine Basalts
SiO_2	45.54	47.11	45.30	48.30	49.56	52.86	46.63	47.98	48.07
TiO_2	1.06	1.03	0.81	0.86	0.90	0.81	0.74	0.95	1.00
Al_2O_3	13.89	13.88	15.30	13.66	13.98	13.23	15.55	14.82	15.86
Fe_2O_3	11.85	13.75	10.97	11.23	13.01	10.39	10.05	13.98	14.47
MnO	0.19	0.22	0.18	0.17	0.21	0.16	0.23	0.20	0.22
MgO	4.95	6.70	6.23	5.97	8.21	7.83	4.04	6.85	5.61
CaO	8.52	11.48	12.50	10.52	6.95	6.27	15.18	9.37	9.11
Na_2O	3.57	0.60	0.53	1.69	1.96	3.12	1.15	1.60	1.92
K_2O	0.09	0.07	0.06	0.40	1.07	0.33	0.07	0.14	0.09
P_2O_5	0.07	0.08	0.06	0.08	0.08	0.10	0.05	0.07	0.08
Cr_2O_3	0.03	0.03	0.04	0.02	0.04	0.04	0.03	0.04	0.04
SrO	0.01	0.02	0.02	0.01	0.01	0.01	0.01	0.02	0.01
BaO	0.01	0.01	0.01	0.01	0.02	0.01	<0.01	0.01	0.01
LOI	9.24	4.34	6.85	7.31	3.62	3.56	5.98	3.28	3.40
Total	99.01	99.33	98.86	100.20	99.62	98.72	99.71	99.31	99.90
V	328	342	275	278	300	263	288	321	308
Cr	270	280	380	140	390	320	230	320	300
Co	47.2	54.1	56.1	42.5	44.7	42.8	55.3	49.5	52.2
Ni	88	88	170	73	82	87	136	82	134
Cu	94	148	111	110	101	83	120	120	68
Zn	87	114	84	84	94	74	120	99	110
Cs	0.0	0.0	0.0	0.1	0.2	0.1	<0.1	0.1	0.1
Rb	0.5	0.6	0.5	4.3	22.1	4.1	0.7	1.8	0.9
Sr	60.4	184.5	166.5	92.6	101.5	56.8	121.5	109.5	116.5
Ba	16.1	9.0	7.9	55.5	227.0	47.1	15.7	20.7	23.7
Nb	2.6	2.6	1.9	2.0	3.0	2.5	2.0	2.0	2.0
Zr	56.7	55.5	41	47.3	54.4	62	37.8	48.1	48.4
Hf	1.8	1.7	1.4	2	2	1.9	1	1	2
Y	21.7	22.2	18.1	17.6	20.4	16.6	16.2	20.1	20.8
La	3.0	3.4	2.7	3.3	3.5	3.1	2.6	3.3	3.3
Ce	7.0	8.7	6.7	8.5	8.8	8.2	6.5	8.4	8.3
Pr	1.1	1.3	1.0	1.3	1.3	1.2	1.0	1.2	1.3
Nd	6.0	7.1	5.3	6.4	6.9	6.3	5.0	6.2	6.6
Sm	2.2	2.3	1.9	2.1	2.3	1.9	1.7	2.1	2.2
Eu	0.9	0.9	0.7	0.8	0.6	0.7	0.7	0.7	0.8
Gd	2.7	2.8	2.2	2.6	2.7	2.4	2.1	2.7	2.5
Tb	0.5	0.5	0.4	0.5	0.6	0.5	0.4	0.5	0.5
Dy	4.0	3.9	3.1	3.1	3.4	3.1	2.7	3.4	3.4
Ho	0.9	0.9	0.7	0.7	0.8	0.7	0.6	0.7	0.8
Er	2.5	2.5	2.0	2.0	2.2	2.0	1.8	2.2	2.3
Tm	0.3	0.4	0.3	0.3	0.3	0.3	0.3	0.3	0.3
Yb	2.5	2.5	2.0	1.9	2.1	1.9	1.7	2.1	2.2
Lu	0.3	0.4	0.3	0.3	0.4	0.3	0.3	0.3	0.4
Pb	<5	<5	<5	20	<5	<5	22	<5	<5
Th	0.3	0.3	0.2	<1	<1	0.5	<1	<1	<1
U	0.08	0.07	<0.05	<0.5	<0.5	0.08	<0.5	<0.5	<0.5
Ga	15.9	18.6	16.6	15	13	12.8	16	16	16
Sn	1	1	1	1	1	1	<1	<1	<1
Ta	0.2	0.5	0.2	<0.5	<0.5	0.3	<0.5	<0.5	<0.5
W	5	22	3	<1	2	2	1	1	1

Appendix C: Major oxide and Trace element concentrations by XRF and ICP-MS (ALS Chemex) for samples from the Hope Bay Greenstone Belt

Sample	202947	249861	249862	249873	249874	249876	1000	84529	84531
Rock Type	normal basalt	normal basalt	normal basalt	normal basalt	normal basalt	normal basalt	Tholeiitic rhyolite	Tholeiitic rhyolite	Tholeiitic rhyolite
UTME	435158	432850	433623	434765	434352	432439	445023	445059	444299
UTMN	7546512	7559168	7559232	7559328	7559584	7558864	7515104	7516832	7516352
Suite	Wolverine Basalts	Wolverine Basalts	Wolverine Basalts	Wolverine Basalts	Wolverine Basalts	Wolverine Basalts	Flake	Flake	Flake
SiO_2	46.75	47.36	49.64	47.04	47.53	47.76	70.35	78.30	73.46
TiO_2	0.72	0.75	0.80	1.05	0.91	0.92	0.28	0.20	0.19
Al_2O_3	15.20	15.04	14.39	15.29	15.55	14.96	11.87	10.21	10.73
Fe_2O_3	10.90	12.79	12.18	10.65	12.30	11.15	5.84	2.08	8.09
MnO	0.19	0.21	0.20	0.19	0.18	0.21	0.04	0.10	0.03
MgO	6.19	6.94	5.81	6.34	3.77	7.09	1.64	0.46	0.87
CaO	10.51	12.49	8.82	8.53	7.81	10.71	1.07	2.23	0.28
Na_2O	2.96	1.13	3.34	1.86	3.28	1.68	3.06	1.47	0.36
K_2O	0.07	0.09	0.19	0.06	0.10	0.24	1.44	1.96	2.47
P_2O_5	0.05	0.06	0.06	0.09	0.08	0.07	0.04	0.03	0.03
Cr_2O_3	0.04	0.04	0.02	0.03	0.03	0.03	0.00	0.02	0.02
SrO	0.03	0.03	0.02	0.03	0.01	0.01	0.01	0.01	<0.01
BaO	0.01	0.01	<0.01	<0.01	0.01	0.01	0.02	0.03	0.03
LOI	6.23	3.05	4.35	7.06	6.92	4.11	2.81	1.45	2.07
Total	99.85	99.97	99.79	98.22	98.47	98.95	98.46	98.55	98.62
V	289	274	284	299	294	296	6	8	8
Cr	360	310	150	240	240	250	10	180	140
Co	50.5	52.1	57.0	45.8	55.7	48.4	3.4	1.4	10.8
Ni	138	136	105	107	121	111	248	6	5
Cu	106	108	146	117	146	126	18	6	95
Zn	84	86	92	95	91	92	356	39	36
Cs	0.1	0.1	0.1	0.1	0.1	0.1	0.6	0.7	1.4
Rb	0.7	0.8	2.0	0.4	1.3	4.3	32.9	36.1	45.7
Sr	269.0	220.0	99.6	123.0	70.5	93.2	109.5	94.6	13.6
Ba	12.2	11.9	21.6	10.4	12.4	51.4	245.0	182.0	233.0
Nb	2.0	1.8	1.7	2.4	2.4	2.4	32.0	10.0	10.0
Zr	42.2	40	44	52	49	59	478	261	270
Hf	1	1.3	1.4	1.8	1.6	1.8	16	8	8
Y	16.8	14.8	14.6	18.2	17.6	18.2	134.0	57.1	58.8
La	2.6	2.2	2.1	2.8	2.9	2.6	43.9	21.3	21.6
Ce	6.5	6.0	5.9	7.7	8.3	7.3	104.0	50.0	50.1
Pr	0.9	0.9	0.9	1.3	1.3	1.2	14.4	6.7	6.7
Nd	4.8	4.8	4.8	6.5	6.6	6.2	65.5	29.0	28.6
Sm	1.6	1.6	1.6	2.1	2.0	1.9	16.6	7.3	7.3
Eu	0.7	0.6	0.6	0.9	0.8	0.7	4.0	1.4	1.5
Gd	2.1	2.2	2.1	2.7	2.4	2.4	19.1	8.1	8.3
Tb	0.4	0.4	0.4	0.6	0.5	0.5	3.5	1.5	1.5
Dy	2.7	2.7	2.8	3.5	3.2	3.3	24.5	9.5	9.8
Ho	0.6	0.6	0.6	0.7	0.7	0.7	5.3	2.0	2.2
Er	1.7	1.7	1.8	2.2	2.1	2.2	17.2	6.6	7.0
Tm	0.2	0.3	0.3	0.3	0.3	0.3	2.5	1.0	1.0
Yb	1.7	1.7	1.7	2.0	2.0	2.1	18.4	6.7	7.0
Lu	0.2	0.2	0.3	0.3	0.3	0.3	2.7	1.0	1.1
Pb	<5	<5	<5	<5	<5	<5	5	8	<5
Th	<1	0.4	0.4	0.4	0.5	0.5	6.0	4.0	4.0
U	<0.5	0.11	0.09	0.09	0.07	0.07	1.7	0.9	1
Ga	15	15.6	14	16.5	16.4	16.5	32	16	17
Sn	1	1	1	1	1	1	6	4	4
Ta	<0.5	0.2	0.2	0.2	0.3	0.3	2	0.7	0.7
W	2	1	2	2	2	3	1	2	2

Appendix C: Major oxide and Trace element concentrations by XRF and ICP-MS (ALS Chemex) for samples from the Hope Bay Greenstone Belt

Sample	84532	84534	249520	84528	200687	200694	84533	84537	84538
Rock Type	Tholeiitic rhyolite	Tholeiitic rhyolite	Tholeiitic rhyolite	Tholeiitic rhyolite	Ti-enriched Al-depleted basalt	Ti-enriched Al-depleted basalt	Ti-enriched basalt	Ti-enriched basalt	Ti-enriched basalt
UTME	444251	443735	446542	444998	432195	431903	444112	443002	443331
UTMN	7516016	7515408	7518416	7516672	7559808	7558768	7516032	7515792	7515296
Suite	Flake	Flake	Flake	Flake	Patch Lake Mafics	Patch Lake Mafics	bend High Ti	bend High Ti	bend High Ti
SiO_2	76.59	73.92	74.25	77.05	41.69	39.40	51.46	48.27	48.12
TiO_2	0.32	0.17	0.32	0.11	3.45	2.22	1.44	1.49	1.50
Al_2O_3	11.27	11.81	10.93	11.49	13.29	6.83	12.64	14.50	13.82
Fe_2O_3	3.44	4.30	4.68	2.13	15.15	19.41	16.09	17.33	17.74
MnO	0.04	0.04	0.08	0.02	0.24	0.20	0.21	0.28	0.22
MgO	0.61	0.76	2.06	0.47	7.54	17.43	4.72	5.14	5.80
CaO	0.73	1.26	1.39	0.59	8.35	6.75	7.21	6.04	7.34
Na_2O	4.03	4.63	0.73	3.38	0.27	0.12	2.55	3.52	2.26
K_2O	0.93	1.28	2.18	1.98	2.32	0.05	0.32	0.16	0.15
P_2O_5	0.04	0.03	0.02	0.01	0.29	0.21	0.18	0.12	0.10
Cr_2O_3	0.02	0.02	<0.01	0.02	0.05	0.20	0.01	<0.01	<0.01
SrO	0.01	0.01	0.02	0.01	0.02	<0.01	0.01	0.01	0.01
BaO	0.02	0.03	0.04	0.05	0.10	<0.01	0.02	0.01	0.01
LOI	1.30	0.99	2.26	1.55	5.98	6.73	2.56	3.25	2.97
Total	99.33	99.24	98.96	98.85	98.75	99.56	99.43	100.10	100.05
V	25	52	10	<5	501	331	378	419	438
Cr	200	180	10	150	370	1440	90	70	70
Co	3.7	3.6	1.9	1.2	64.5	96.2	45.5	54.3	49.5
Ni	7	5	5	5	244	759	47	44	41
Cu	6	5	<5	6	200	188	98	126	103
Zn	31	40	234	72	175	104	128	144	137
Cs	0.2	0.1	0.4	0.3	0.3	0.1	0.2	0.1	0.1
Rb	17.4	13.4	35.8	37.4	40.9	1.6	7.4	1.3	0.9
Sr	57.6	69.9	43.8	31.3	192.0	20.0	109.0	67.9	88.4
Ba	143.0	322.0	369.0	444.0	925.0	8.5	104.0	29.6	20.1
Nb	10.0	11.0	31.7	73.0	26.0	17.0	6.0	4.0	4.0
Zr	272	290	529	430	160	124	134	86.7	84.4
Hf	9	9	16	18	5	4	4	3	3
Y	68.7	62.8	152.0	173.0	31.6	20.8	46.2	31.7	31.1
La	21.6	22.7	46.6	67.1	23.9	9.5	10.2	4.6	4.8
Ce	50.2	54.7	114.5	151.0	61.2	25.5	26.4	12.4	13.1
Pr	6.6	7.4	15.8	19.0	8.5	3.5	3.8	1.9	2.0
Nd	28.1	31.0	70.0	73.2	37.6	17.2	18.2	10.0	10.4
Sm	7.0	7.9	17.6	18.0	8.3	4.6	5.4	3.4	3.4
Eu	1.3	1.4	4.0	2.2	2.7	1.4	1.6	1.1	1.1
Gd	8.2	8.3	20.0	19.7	8.1	5.0	6.4	4.3	4.3
Tb	1.5	1.5	3.7	3.7	1.3	0.8	1.2	0.8	0.8
Dy	10.8	10.1	26.9	25.3	6.6	4.3	7.9	5.5	5.4
Ho	2.4	2.3	6.0	5.7	1.3	0.8	1.7	1.2	1.2
Er	7.9	7.4	18.0	19.4	3.4	2.1	5.2	3.6	3.5
Tm	1.2	1.1	2.6	2.9	0.4	0.2	0.8	0.5	0.5
Yb	8.0	7.7	18.0	20.5	2.8	1.7	5.0	3.5	3.4
Lu	1.2	1.2	2.6	3.0	0.4	0.2	0.8	0.5	0.5
Pb	<5	<5	<5	<5	11	<5	<5	<5	<5
Th	4.0	4.0	5.9	13.0	2.0	1.0	1.0	<1	<1
U	1.1	1.1	1.3	3.2	0.5	<0.5	<0.5	<0.5	<0.5
Ga	16	15	30.9	28	25	16	20	16	19
Sn	3	3	4	9	2	2	1	1	1
Ta	0.7	0.7	1.8	4.4	1.5	0.8	<0.5	<0.5	<0.5
W	2	2	2	2	<1	1	1	2	1

Appendix C: Major oxide and Trace element concentrations by XRF and ICP-MS (ALS Chemex) for samples from the Hope Bay Greenstone Belt

Sample	84539	249538	249899	249900	249863	249864	249865	249875	200686
Rock Type	Ti-enriched basalt	Ti-enriched basalt	Ti-enriched basalt	Ti-enriched basalt	Ti-enriched basalt	Ti-enriched basalt	Ti-enriched basalt	Ti-enriched basalt	Ti-enriched basalt
UTME	442749	441271	427635	428999	433660	433603	433396	433823	432383
UTMN	7515680	7504672	7557104	7556944	7559232	7558960	7558512	7559040	7559392
Suite	Bend High Ti	Boston Ti	Discovery basalts	Discovery basalts	Doris Basalts	Doris Basalts	Doris Basalts	Doris Basalts	Patch Lake Mafics
SiO_2	46.63	43.19	53.38	52.68	52.17	47.93	56.02	48.49	50.14
TiO_2	1.41	1.48	1.85	1.45	1.43	1.59	1.33	1.22	1.58
Al_2O_3	13.76	13.12	15.50	16.66	12.43	14.06	11.94	10.84	12.83
Fe_2O_3	16.79	13.94	5.62	10.12	14.36	16.12	15.17	13.81	10.79
MnO	0.23	0.21	0.16	0.16	0.13	0.25	0.20	0.34	0.24
MgO	5.99	5.52	1.87	4.78	3.17	3.11	2.07	2.56	2.31
CaO	9.08	8.45	7.46	2.97	5.48	5.51	4.24	6.84	9.58
Na_2O	2.09	2.02	5.94	2.71	3.54	3.35	3.51	2.33	2.88
K_2O	0.15	0.40	0.27	0.82	0.06	0.04	0.10	0.97	0.92
P_2O_5	0.13	0.11	0.33	0.12	0.22	0.27	0.31	0.20	0.12
Cr_2O_3	0.02	0.05	0.01	0.04	<0.01	<0.01	<0.01	<0.01	<0.01
SrO	0.01	0.01	0.03	0.02	0.02	0.01	0.02	0.01	0.01
BaO	<0.01	0.01	0.02	0.02	<0.01	0.02	0.02	0.02	0.01
LOI	3.63	9.82	7.10	6.79	6.43	6.99	4.57	11.20	8.73
Total	99.93	98.33	99.53	99.32	99.43	99.25	99.49	98.81	100.15
V	426	340	192	409	109	127	58	94	376
Cr	60	150	120	80	10	10	10	10	60
Co	50.8	52.8	42.6	45.8	27.9	34.7	23.1	25.6	37.2
Ni	42	97	145	58	6	5	9	5	43
Cu	86	113	104	93	29	9	49	23	96
Zn	117	111	95	154	112	153	148	121	112
Cs	0.1	0.2	0.5	1.1	0.1	0.1	0.1	0.4	0.3
Rb	1.5	1.6	6.8	19.2	0.6	0.3	1.2	21.2	21.8
Sr	143.0	104.5	202.0	107.0	54.3	72.0	98.0	93.9	60.3
Ba	35.7	8.4	113.0	104.0	10.2	9.5	46.5	133.5	160.0
Nb	4.0	7.2	11.3	2.9	4.6	4.6	5.4	3.9	5.0
Zr	78	86	183	79	114	140	131	104	94.3
Hf	2	2.6	4.7	2.1	3.7	4.4	4	3.3	3
Y	30.4	23.1	23.4	21.5	38.5	30.4	44.6	35.3	35.2
La	4.5	6.6	10.4	3.9	7.6	6.4	7.4	6.7	7.4
Ce	12.4	19.5	29.7	10.3	18.5	16.8	20.2	17.1	19.0
Pr	2.0	2.4	4.4	1.6	2.7	2.5	2.9	2.5	2.7
Nd	9.9	11.8	20.6	7.6	13.4	12.1	14.7	12.2	13.2
Sm	3.4	3.2	5.6	2.4	4.2	3.5	4.8	3.9	4.3
Eu	1.3	1.0	1.6	0.9	1.5	0.9	1.8	1.4	1.2
Gd	4.3	4.1	5.6	3.2	5.3	4.6	6.0	4.8	5.0
Tb	0.8	0.7	0.8	0.6	1.1	0.9	1.2	1.0	0.9
Dy	5.2	4.4	4.8	3.7	6.9	6.0	8.0	6.5	5.9
Ho	1.1	1.0	0.9	0.9	1.5	1.3	1.7	1.3	1.3
Er	3.4	2.8	2.3	2.5	4.5	4.3	5.5	4.2	3.9
Tm	0.5	0.4	0.3	0.4	0.6	0.6	0.7	0.6	0.6
Yb	3.3	2.7	1.8	2.2	4.3	4.4	5.2	4.0	3.6
Lu	0.5	0.4	0.3	0.3	0.7	0.7	0.8	0.6	0.5
Pb	<5	<5	<5	6	<5	<5	<5	<5	55
Th	<1	0.8	0.7	0.3	1.2	1.6	1.3	1.1	1.0
U	<0.5	0.13	0.18	0.08	0.27	0.48	0.29	0.28	<0.5
Ga	19	17	22	21.8	19.8	22.9	19.6	19	17
Sn	1	1	2	1	1	1	1	1	1
Ta	<0.5	0.5	0.8	0.2	0.4	0.5	0.5	0.3	<0.5
W	3	34	2	2	2	2	2	<1	<1

Appendix C: Major oxide and Trace element concentrations by XRF and ICP-MS (ALS Chemex) for samples from the Hope Bay Greenstone Belt

Sample	200689	200693	200695	202920	202921	202928	202929
Rock Type	Ti-enriched basalt	Ti-enriched basalt	Ti-enriched basalt	Ti-enriched basalt	Ti-enriched basalt	Ti-enriched basalt	Ti-enriched basalt
UTME	432139	432233	432500	432982	432510	433673	433764
UTMN	7559312	7558880	7556688	7547952	7548208	7552864	7551840
Suite	Patch Lake Mafics	Patch Lake Mafics	Patch Lake Mafics	Patch Lake Mafics	Patch Lake Mafics	Patch Lake Mafics	Patch Lake Mafics
SiO_2	52.69	57.43	48.68	45.53	48.00	43.88	47.39
TiO_2	1.53	1.61	1.53	1.42	1.91	1.54	1.52
Al_2O_3	14.89	12.91	13.57	13.05	11.57	12.91	15.65
Fe_2O_3	10.99	7.68	16.88	14.01	18.35	14.37	15.59
MnO	0.20	0.15	0.22	0.29	0.24	0.22	0.26
MgO	2.80	1.49	5.67	2.68	3.58	2.81	4.63
CaO	6.32	7.28	7.05	10.89	6.37	10.20	6.51
Na_2O	2.67	1.87	2.85	2.31	1.95	3.03	1.94
K_2O	1.20	1.81	0.12	0.07	0.28	0.05	0.30
P_2O_5	0.11	0.12	0.11	0.13	0.20	0.14	0.12
Cr_2O_3	0.01	0.01	<0.01	0.01	<0.01	0.01	0.01
SrO	0.01	0.01	0.02	0.01	0.01	0.01	0.01
BaO	0.02	0.05	0.02	<0.01	0.01	0.01	0.02
LOI	6.70	7.69	2.68	9.48	7.52	10.35	5.89
Total	100.15	100.10	99.40	99.89	100.00	99.53	99.84
V	400	359	420	385	291	355	390
Cr	120	80	50	70	40	80	160
Co	46.8	36.8	48.8	43.5	48.1	41.2	46.9
Ni	65	47	38	41	8	38	82
Cu	112	92	115	102	112	82	87
Zn	102	73	132	395	152	136	122
Cs	0.3	0.7	0.1	0.1	0.8	<0.1	0.2
Rb	31.5	48.0	1.2	0.6	2.9	0.4	6.9
Sr	51.6	43.0	166.0	85.7	102.5	124.5	128.0
Ba	276.0	409.0	31.3	32.3	23.9	14.6	66.0
Nb	4.0	5.0	4.0	4.0	11.0	5.0	4.0
Zr	80.7	104	84.8	79.8	127.5	92.8	83.9
Hf	3	3	3	3	4	3	3
Y	28.7	34.5	32.7	32.5	41.3	34.1	33.5
La	4.0	7.3	4.8	5.3	13.2	7.0	5.8
Ce	10.8	18.6	12.8	12.8	31.0	17.6	15.6
Pr	1.7	2.6	1.8	1.9	4.4	2.6	2.4
Nd	8.8	12.7	10.0	9.7	21.0	13.2	11.7
Sm	3.1	4.0	3.1	3.0	5.9	3.8	3.7
Eu	1.1	1.2	1.2	1.1	1.5	1.2	1.5
Gd	3.8	4.8	4.0	3.8	6.7	4.7	4.4
Tb	0.7	0.9	0.8	0.8	1.2	0.9	0.9
Dy	4.9	5.8	5.3	5.0	7.5	5.8	5.7
Ho	1.1	1.2	1.1	1.2	1.6	1.3	1.2
Er	3.3	3.8	3.7	3.7	4.6	3.8	3.6
Tm	0.5	0.5	0.5	0.6	0.7	0.6	0.5
Yb	3.3	3.6	3.6	3.5	4.3	3.6	3.6
Lu	0.5	0.5	0.5	0.6	0.7	0.6	0.6
Pb	105	<5	<5	<5	<5	6	<5
Th	<1	1.0	<1	<1	1.0	1.0	<1
U	<0.5	<0.5	<0.5	<0.5	<0.5	<0.5	<0.5
Ga	19	20	18	17	19	17	21
Sn	2	2	1	<1	<1	<1	<1
Ta	<0.5	<0.5	<0.5	<0.5	0.7	<0.5	<0.5
W	<1	1	1	1	1	1	1

APPENDIX D:

High Resolution Trace Element Abundances of Samples From the Hope Bay Greenstone Belt, (PCIGR)

Appendix D: Trace element concentrations by HR-ICP-MS (PCIGR) for samples from the Hope Bay Greenstone Belt

Sample no.1	84536	84541	84544	202915	84545	84572	84574	84573	84557
Suite	Member basalts	Member basalts	Member basalts	Boston Basalt	Clover east basalts	Clover east basalts	Clover east basalts	Clover Lake Suite	Clover west basalts
Rock Type	Normal Basalt	Normal Basalt	Normal Basalt	Normal Basalt	Normal Basalt	Normal Basalt	LREE Basalt	Rhyolite	Normal Basalt
Northing	442606	441884	441320	441033	439452	438902	438811	438196	436704
Easting	7514639	7514093	7512181	7504174	7507669	7507363	7506770	7506733	7502763
Sc	36.5	41.4	38.0	42	32.6	32.5	25.6	2.788	41.5
V	351	314	373	318	282	242	211.5	6.8	343
Cr	256	242	172	203	221	893	104	174	56
Co	50.3	47	50	48.7	49.3	60.3	33.9	1.2	52.0
Ni	97	90	84.2	91.4	116	290	89.4	3.5	64.1
Cu	104.4	87	118.0	62.5	107.2	76	61.3	3.4	109
Zn	89	111	100	64.6	77	85	88	32	112
Cs	0.016	0.045	0.03	0.77	0.62	0.105	0.69	1.9	0.150
Rb	0.202	1.58	0.173	14.10	10.99	0.68	11.88	95	2.3
Sr	153	129	108	66	91	103	342	42.5	110
Ba	9.77	35.7	13.9	108	94	11.4	204.1	681	44.7
Nb	2.77	3.7	3.04	2.9	2.30	2.0	6.12	3.0	4.42
Zr	36.4	77	49.8	44.2	42	23.1	111	55	58.5
Hf	1.023	1.9	1.28	1.163	1.15	0.74	2.76	2.1	1.546
Y	18.8	24.0	18.7	12.6	14.0	13.71	15.8	4.17	23.8
La	3.06	4.18	3.20	2.72	2.51	2.18	11.1	12.90	5.43
Ce	8.2	11.50	8.62	7.4	6.40	5.82	25.0	25.5	14.3
Pr	1.26	1.747	1.33	1.11	0.97	0.893	3.22	2.72	2.1
Nd	6.3	8.49	6.57	5.30	4.75	4.44	13.3	8.95	9.7
Sm	2.04	2.62	2.103	1.58	1.52	1.40	2.94	1.64	2.8
Eu	0.791	0.98	0.773	0.56	0.540	0.494	0.94	0.190	0.92
Gd	2.73	3.47	2.80	1.94	2.06	1.956	2.979	1.20	3.5
Tb	0.49	0.611	0.50	0.348	0.369	0.350	0.474	0.172	0.61
Dy	3.40	4.34	3.45	2.13	2.5	2.428	3.01	0.835	4.5
Ho	0.74	0.93	0.75	0.52	0.56	0.526	0.618	0.140	0.96
Er	2.10	2.75	2.20	1.55	1.64	1.52	1.74	0.357	2.8
Tm	0.308	0.398	0.328	0.236	0.24	0.219	0.251	0.048	0.386
Yb	1.96	2.62	2.19	1.54	1.61	1.51	1.67	0.32	2.6
Lu	0.291	0.408	0.341	0.24	0.25	0.210	0.253	0.045	0.383
Pb	0.672	0.517	0.290	0.355	0.223	0.347	2.30	2.391	0.406
Th	0.242	0.339	0.275	0.272	0.237	0.174	1.4	0.38	0.48
U	0.047	0.062	0.051	0.048	0.043	0.0329	0.279	1.28	0.078
Li	9.4	11.7	11.8	45.9	20.5	16.2	11.5	8.4	26.9
Ga	15.3	15.4	15.7	15.9	13.0	11.31	18.33	19.3	13.3
Mo	0.465	0.47	0.38	0.22	0.20	0.41	0.38	1.037	0.434
Cd	0.087	0.17	0.146	0.06	0.073	0.058	0.11	0.04	0.094
Sn	0.38	0.43	0.64	0.31	0.275	0.358	0.543	0.147	0.48
Sb	0.116	0.032	0.018	0.378	0.288	0.12	0.476	0.83	0.263
Ta	0.159	0.222	0.167	0.190	0.134	0.113	0.407	0.29	0.267
W	0.056	0.127	0.049	0.117	0.062	0.042	0.109	0.229	0.35
Bi	0.0075	0.00559	0.006	0.0109	0.0046	0.0075	0.0136	0.168	0.00526

Appendix D: Trace element concentrations by HR-ICP-MS (PCIGR) for samples from the Hope Bay Greenstone Belt

Sample no.1	84576	84577	84579	84581	200611	84502	84514	84589	84591
Suite	Clover west basalts	Clover west basalts	Clover west basalts	Clover west basalts	Clover west basalts	Flake Lake Suite	Flake Lake Suite	Flake Lake Suite	Flake Lake Suite
Rock Type	Normal Basalt	Normal Basalt	Normal Basalt	Normal Basalt	Normal Basalt	Felsic	Felsic	Felsic	Felsic
Northing	437337	437045	436006	436498	435180	445855	446046	445066	444650
Easting	7505892	7505239	7505604	7504990	7505521	7519179	7518893	7513292	7515305
Sc	39.0	57	51.9	38	36.6	6.74	0.77	0.246	1.79
V	383	300	300	326	308	40.0	9.4	1.59	16.1
Cr	82.6	290	454	107	258	121.1	129	88	98
Co	57.0	56	58.3	50.5	54	8.05	5.0	0.477	4
Ni	63.7	112	108.3	66.1	131	5.43	8.2	3.0	4
Cu	124.4	116	92.4	93	88	15.17	16	7.6	14.3
Zn	98.1	82	115	92	77	93	27	20.6	109
Cs	0.203	0.14	0.08	0.097	0.14	0.21	0.0383	0.118	0.421
Rb	3.70	5.0	0.382	1.83	4.7	12.17	3.90	3.4	31.3
Sr	196.7	106	72.7	99	185.3	75	232	38.4	46.2
Ba	36.6	31.7	6.8	48	62	147	63.8	29.8	156
Nb	4.4	2.4	2.333	3.58	2.395	14.5	23	40.5	28.8
Zr	59	56	54.9	35	28.0	388	497	314	371
Hf	1.75	1.51	1.463	0.94	0.89	10.94	13.9	10.8	10.8
Y	25.1	23.8	23.2	17.9	13.81	101	116	64	102
La	6.05	4.29	2.89	3.80	3.65	19.4	28	63.0	61.1
Ce	14.95	11.15	8.619	9.9	9.0	48.1	71	137	149
Pr	2.13	1.656	1.38	1.44	1.26	7.3	9.7	17.7	19.7
Nd	10.27	8.08	7.33	6.8	6.0	34.0	44	72.8	82
Sm	2.98	2.56	2.55	2.08	1.68	10.1	11.8	14.8	17.9
Eu	0.95	0.931	1.003	0.76	0.70	2.1	3.0	1.7	3.2
Gd	3.75	3.52	3.46	2.63	2.15	13.2	14.6	14.5	17.7
Tb	0.656	0.629	0.63	0.471	0.372	2.4	2.7	2.3	2.9
Dy	4.53	4.24	4.24	3.3	2.53	16.5	18.3	14.1	18.6
Ho	0.97	0.912	0.90	0.70	0.54	3.74	4.20	2.92	4.0
Er	2.74	2.736	2.663	2.1	1.55	11.4	13.2	8.43	12.1
Tm	0.415	0.384	0.394	0.300	0.221	1.75	2.04	1.2	1.8
Yb	2.61	2.63	2.62	1.91	1.43	11.9	13.89	8.43	12.2
Lu	0.381	0.412	0.408	0.28	0.205	1.9	2.16	1.288	1.9
Pb	0.69	0.421	0.467	0.43	0.8	2.93	1.86	1.8	1.9
Th	1.10	0.07	<lod	0.346	0.31	3.7	5.16	10.6	8.7
U	0.120	0.02	<lod	0.067	0.061	0.831	1.149	0.783	1.642
Li	17.1	31.0	31.5	19.5	17.8	<lod*	0.03	<lod	17.4
Ga	16.41	16.1	15.5	14.4	16.2	15.52	22	13.2	16.2
Mo	0.49	1.0	0.800	0.41	0.3373	2.20	1.8	3.38	5.41
Cd	0.14	0.026	0.165	0.131	0.060	0.17	0.07	0.062	0.158
Sn	0.49	0.3	0.168	0.447	0.33	1.90	1.1	0.93	2.44
Sb	0.73	0.17	1.37	0.29	0.17	0.12	0.223	0.264	0.75
Ta	0.299	0.171	0.177	0.197	0.143	0.77	0.83	1.8	1.49
W	0.364	0.13	0.063	0.221	0.10	0.232	0.262	0.35	0.28
Bi	0.154	<lod	<lod	0.0112	0.0125	0.06	0.078	0.07	0.045

Appendix D: Trace element concentrations by HR-ICP-MS (PCIGR) for samples from the Hope Bay Greenstone Belt

Sample no.1	202910	84515	84516	84538	84585	84586	200632	202929	202940
Suite	Gas Cache	Bend Basalt	Bend Basalt	Bend Basalt	Koignuck Suite	Koignuck Suite	Koignuck Suite	Patch Lake Mafics	Patch Lake Mafics
Rock Type	Ti Enriched Al Depleted Basalt	Ti Enriched Basalt	Ti Enriched Basalt	Ti Enriched Basalt	Dacite	Dacite	Dacite	Ti Enriched Basalt	Ti Enriched Al Depleted Basalt
Northing	436986	444625	443962	443331	434569	433606	434808	433764	434297
Easting	7532167	7514723	7515325	7515307	7505768	7505416	7505652	7551849	7550413
Sc	41.3	40.9	36.6	42.5	7.59	4.7	4.74	39.5	44
V	496	456	428	465	84	78.5	87	427	526
Cr	181.8	54	52	51	73	73.6	76.1	140	242
Co	60.1	49.8	45.0	49.0	23	13.00	14.6	47	69.6
Ni	150.1	40.6	30.0	35	44	21.6	38	78	156.9
Cu	268.9	102	100.1	94	28	27	32	77	199
Zn	192	222	137	141	86	78.8	77.6	104	231
Cs	1.467	0.193	0.03	0.046	0.86	0.530	0.966	0.173	0.388
Rb	25.3	2.1	1	0.93	27	34.6	24.3	7.4	24.71
Sr	230	165	142	91.2	27.0	140	219	130	258
Ba	262	14.4	13.8	18.27	129.8	171.3	194	73	1889
Nb	24.28	6.857	4.47	4.5	5.7	6.89	5.61	4.5	24.6
Zr	187	122	74.5	45.6	153	167	169.8	88	190.9
Hf	4.8	3.1	1.93	1.36	3.75	4.3	4.2	2.22	4.78
Y	31.2	42	28.2	28.0	10.8	12.62	9.5	30.8	34.5
La	28.75	9.64	4.99	4.507	19.2	16.0	16.7	5.66	30.2
Ce	71	25.0	13.4	12.05	35.9	33.0	30.8	15.18	74
Pr	9.60	3.56	2.03	1.83	3.85	3.74	3.46	2.226	10.0
Nd	42.1	16.1	10.1	9.3	14.0	13.9	12.5	10.54	43.5
Sm	9.16	4.7	3.18	3.01	2.7	2.72	2.38	3.353	9.4
Eu	2.76	1.405	1.20	1.00	0.767	0.792	0.749	1.31	3.0
Gd	8.3	5.92	4.22	3.985	2.41	2.57	2.15	4.30	8.6
Tb	1.17	1.07	0.75	0.718	0.350	0.384	0.320	0.776	1.25
Dy	6.7	7.26	5.2	4.9	1.97	2.31	1.9	5.39	7.2
Ho	1.22	1.632	1.12	1.05	0.401	0.460	0.365	1.156	1.35
Er	3.09	4.73	3.32	3.1	1.10	1.29	0.98	3.42	3.47
Tm	0.419	0.72	0.479	0.446	0.158	0.189	0.132	0.501	0.472
Yb	2.56	4.611	3.12	2.8	1.06	1.25	0.86	3.21	2.9
Lu	0.358	0.71	0.493	0.40	0.174	0.193	0.135	0.493	0.417
Pb	2.60	1.517	1.50	0.580	1.27	1.8	2.0	0.539	3.00
Th	3.1	1.03	0.39	0.37	2.6	3.0	3.0	0.41	2.7
U	0.590	0.181	0.083	0.070	0.508	0.627	0.610	0.076	0.507
Li	14.6	16.6	15.0	14.9	42	8.5	17.6	38.7	25.6
Ga	21.86	17.5	17	15.4	18	17.09	18.14	18.9	25.1
Mo	2.41	0.62	0.49	0.364	6.21	1.59	4.6	0.36	2.90
Cd	0.30	0.206	0.158	0.137	0.0429	0.0577	0.134	0.052	0.097
Sn	0.4988	0.82	0.326	0.401	0.42	0.53	0.886	0.507	1.014
Sb	0.20	0.085	0.106	0.04	0.25	0.064	0.11	0.045	0.286
Ta	1.19	0.36	0.240	0.24	0.49	0.53	0.40	0.303	1.12
W	0.154	0.217	0.094	0.074	0.58	0.31	0.24	0.103	0.20
Bi	0.0205	0.060	0.023	0.0061	0.0179	0.0307	0.051	0.0119	0.031

Appendix D: Trace element concentrations by HR-ICP-MS (PCIGR) for samples from the Hope Bay Greenstone Belt

Sample no.1	202943	84626	202930	84521	84551	202931	202918	200649
Suite	Patch Lake Mafics	Windy Basalts	Windy Basalts	Windy Felsics	Windy Felsics	Windy Felsics	Wolverine Basalts	Wolverine Basalts
Rock Type	Ti Enriched Basalt	Normal Basalt	Normal Basalt	Felsic	Felsic/sedimentry	felsic	Normal Basalt	Normal Basalt
Northing	433968	433898	433092	438992	439610	432493	434048	436630
Easting	7551527	7550638	7551626	7514291	7511094	7551376	7547623	7545657
Sc	37.4	35.4	52	5.8	1.56	7.7	30.6	50.9
V	445	305	284	91	41.0	84.4	301	280.6
Cr	106	376	389.5	120	44.3	87.8	201	360
Co	42.8	49	42.5	15	6.1	8.0	54.8	54.7
Ni	53.5	108	72.0	41	8.0	24.8	128.9	165.8
Cu	92	88	81.6	26	6.32	38	104	114.6
Zn	111	78	75.7	60	47.5	29.7	103.5	66.43
Cs	0.046	0.098	0.105	0.57	0.500	0.806	0.043	0.526
Rb	1.20	8.7	23.48	26	31.3	24.9	0.511	29.1
Sr	136	73	94.8	332	257	81.0	120	94.4
Ba	21.0	41.8	201	356	215	282	17.7	113.1
Nb	4.204	2.68	2.395	5.90	3.97	2.93	1.874	1.96
Zr	80	53	53	145.20	118	128	37	44.9
Hf	2.01	1.31	1.458	3.59	3.07	3.26	0.977	1.314
Y	25.55	14.3	22.44	13.8	6.27	7.76	13.2	21.3
La	4.46	3.52	4.03	24.6	9.90	11.9	2.18	2.94
Ce	12.0	9.24	10.66	51	21.44	21.9	6.2	8.1
Pr	1.82	1.33	1.58	5.5	2.32	2.58	0.95	1.236
Nd	9.0	6.32	7.70	20.4	8.8	9.9	4.70	6.35
Sm	2.86	1.82	2.466	3.7	1.8	2.0	1.49	2.091
Eu	1.022	0.628	0.725	1.06	0.523	0.684	0.609	0.747
Gd	3.82	2.30	3.35	3.15	1.54	1.89	2.04	2.942
Tb	0.69	0.401	0.592	0.453	0.210	0.263	0.353	0.538
Dy	4.75	2.68	3.984	2.60	1.2	1.44	2.68	3.71
Ho	1.06	0.582	0.87	0.52	0.238	0.277	0.58	0.817
Er	3.11	1.69	2.55	1.4	0.63	0.77	1.694	2.45
Tm	0.444	0.260	0.36	0.202	0.094	0.107	0.244	0.348
Yb	2.96	1.71	2.54	1.3	0.63	0.698	1.59	2.42
Lu	0.46	0.263	0.380	0.203	0.094	0.111	0.241	0.392
Pb	0.52	0.58	0.479	3.23	2.2	0.621	0.63	1.080
Th	0.377	0.255	0.0380	4.5	2.38	2.9	0.173	0.035
U	0.071	0.047	0.0395	0.92	0.598	0.425	0.041	<lod
Li	22.3	35.0	8.9	1.33	0.80	15.9	9.4	24.8
Ga	17.7	12.9	12.86	20	13.23	18.18	14.167	15.79
Mo	0.36	0.30	0.30	2.93	0.749	1.65	0.333	0.474
Cd	0.130	0.04	0.06	0.063	0.072	0.0341	0.151	0.095
Sn	0.316	0.29	0.0026	0.450	0.428	0.50	0.327	0.26
Sb	0.043	0.05	<lod	0.07	0.200	0.1018	0.125	0.09
Ta	0.242	0.152	0.170	0.504	0.315	0.219	0.110	0.1
W	0.124	0.17	0.0257	0.30	0.08	0.20	0.066	0.012
Bi	0.00384	0.006	<lod	0.10	0.055	0.031	0.012	<lod

APPENDIX E:

Results and Discussion of QA/QC

Analysis of Standards

The standards that were included in the regular sample shipments and the results of the analysis are presented in Table E.1. Overall the results are within acceptable values of error with some elements showing reproducibility problems. The elements that appear to have problems being reproduced include some of the transition metals including Cu, Zn, Ni and Co. These elements often contaminate samples during the crushing and pulverising process.

A Discussion on Comparison of PCIGR and ALS Chemex Analysis

A subset of samples analyzed by ALS Chemex was selected to undergo further geochemical and isotopic determination at the Pacific Centre for Isotopic and Geochemical Research (PCIGR). For methods of analysis of the labs refer to Appendix B. This created duplicate analysis of 35 samples and can examine the (accuracy and precision) reliability and reproducibility of analysis. Binary plots of selected elements with concentration at each lab plotted on the axis and are found in Figure E.1. The majority of elements have high correlations (R^2>0.9), with the exception of Pb, Th, Sn, U, W. Lu, Mo, Hf and Ga. Some of these elements are close to a R^2 of 0.9 and include Lu, Hf and Pb. Concentrations of the Uranium series elements (U, Pb, Th) are all close to, or fall below the detection limit for the ALS Chemex analysis. This would explain the low correlation of U and Th but does not account for the negative correlation in Pb. The high values of Pb and W in the ALS analysis compared to low concentration in the PCIGR analysis suggest Pb and W contamination ALS Chemex samples after the crushing and pulverization (Figure E.1). A number of elements from ALS Chemex show low resolution which results in a “step effect” and includes the elements W, Sn, Pb, U, Th, Lu and Hf. Another effect that is observed in the data from both labs is that of samples with extremely high REE concentrations correlate poorly between the two labs. It may be related to instrumental or dissolution problems of refractory minerals (such as zircon) contained in this rock These are samples from the Flake Lake Suite which is a highly fractionated rhyolite and in Chapter 3 has been shown to be isotopically and geochemical inhomogeneous.

Table E.1: Standards processed at ALS Chemex

	Standard BAS-1 n=4	Sample 249524	% error	Sample 249887	% error	Standard P-1 n=5	Sample 249542	% error
SiO_2	53.30	52.51	1.48	51.83	2.76	70.96	69.08	2.65
TiO_2	1.30	1.36	4.62	1.35	3.85	0.38	0.35	7.89
Al_2O_3	15.40	15.34	0.39	15.47	0.45	14.10	14.46	2.55
Fe_2O_3	10.70	11.11	3.83	10.75	0.47	3.90	3.66	6.15
MnO	0.15	0.14	6.67	0.14	6.67	0.08	0.07	12.50
MgO	7.35	7.38	0.41	6.91	5.99	1.11	1.02	8.11
CaO	7.84	7.99	1.91	7.99	1.91	3.49	3.27	6.30
Na_2O	3.20	3.13	2.19	3.04	5.00	3.80	3.61	5.00
K_2O	0.54	0.55	1.85	0.51	5.56	2.12	1.98	6.60
P_2O_5	0.19	0.23	21.05	0.20	5.26	0.08	0.07	12.50
Total	100.20	99.77	0.43	98.21	1.99	100.56	98.16	2.39
V	155.00	164.00	5.81	176.00	13.55	58.20	57.00	2.06
Cr	220.00	240.00	9.09	240.00	9.09	149.20	130.00	12.87
Co	47.00	51.40	9.36	49.50	5.32	6.20	7.60	22.58
Ni	169.00	191.00	13.02	187.00	10.65	none	6.00	n/a
Cu	61.00	55.00	9.84	58.00	4.92	15.50	8.00	48.39
Zn	104.00	107.00	2.88	81.00	22.12	44.00	52.00	18.18
Cs	0.12	0.10	16.67	0.09	25.00	1.22	0.98	19.67
Rb	6.70	6.60	1.49	5.60	16.42	50.40	45.00	10.71
Sr	436.00	502.00	15.14	457.00	4.82	256.00	218.00	14.84
Ba	167.00	180.50	8.08	176.50	5.69	724.00	704.00	2.76
Nb	7.80	7.60	2.56	6.90	11.54	3.78	3.40	10.05
Zr	91.00	87.00	4.40	84.00	7.69	126.00	133.00	5.56
Hf	2.30	2.40	4.35	2.40	4.35	3.76	3.80	1.06
Yb	1.40	1.41	0.71	1.40	0.00	2.46	2.22	9.76
La	8.80	9.40	6.82	9.30	5.68	13.20	11.00	16.67
Ce	20.00	20.90	4.50	21.60	8.00	28.00	25.90	7.50
Pr	2.80	2.92	4.29	2.96	5.71	3.36	2.70	19.64
Nd	13.00	13.40	3.08	13.20	1.54	13.00	11.20	13.85
Sm	3.50	3.42	2.29	3.52	0.57	2.92	2.48	15.07
Eu	1.30	1.24	4.62	1.25	3.85	0.78	0.77	1.28
Gd	3.70	3.33	10.00	3.28	11.35	3.12	3.01	3.53
Tb	0.57	0.51	10.53	0.57	0.00	0.52	0.50	3.85
Dy	3.10	3.12	0.65	3.15	1.61	3.34	3.08	7.78
Ho	0.61	0.60	1.64	0.60	1.64	0.72	0.70	2.78
Er	1.50	1.61	7.33	1.66	10.67	2.10	2.13	1.43
Tm	0.22	0.21	4.55	0.20	9.09	0.35	0.31	11.43
Y	17.00	16.00	5.88	14.30	15.88	22.80	18.30	19.74
Lu	0.20	0.20	0.00	0.21	5.00	0.40	0.33	17.50
Pb	2.00	<DL	n/a	<DL	n/a	10.20	11.00	7.84
Th	0.83	0.83	0.00	0.85	2.41	4.38	4.18	4.57
U	0.32	0.31	3.13	0.32	0.00	1.48	1.27	14.19
Ga	19.00	20.40	7.37	19.50	2.63	15.00	14.20	5.33
Sn	1.00	1.00	0.00	1.00	0.00	2.44	2.00	18.03
Ta	0.48	0.50	4.17	0.50	4.17	0.30	0.30	0.00

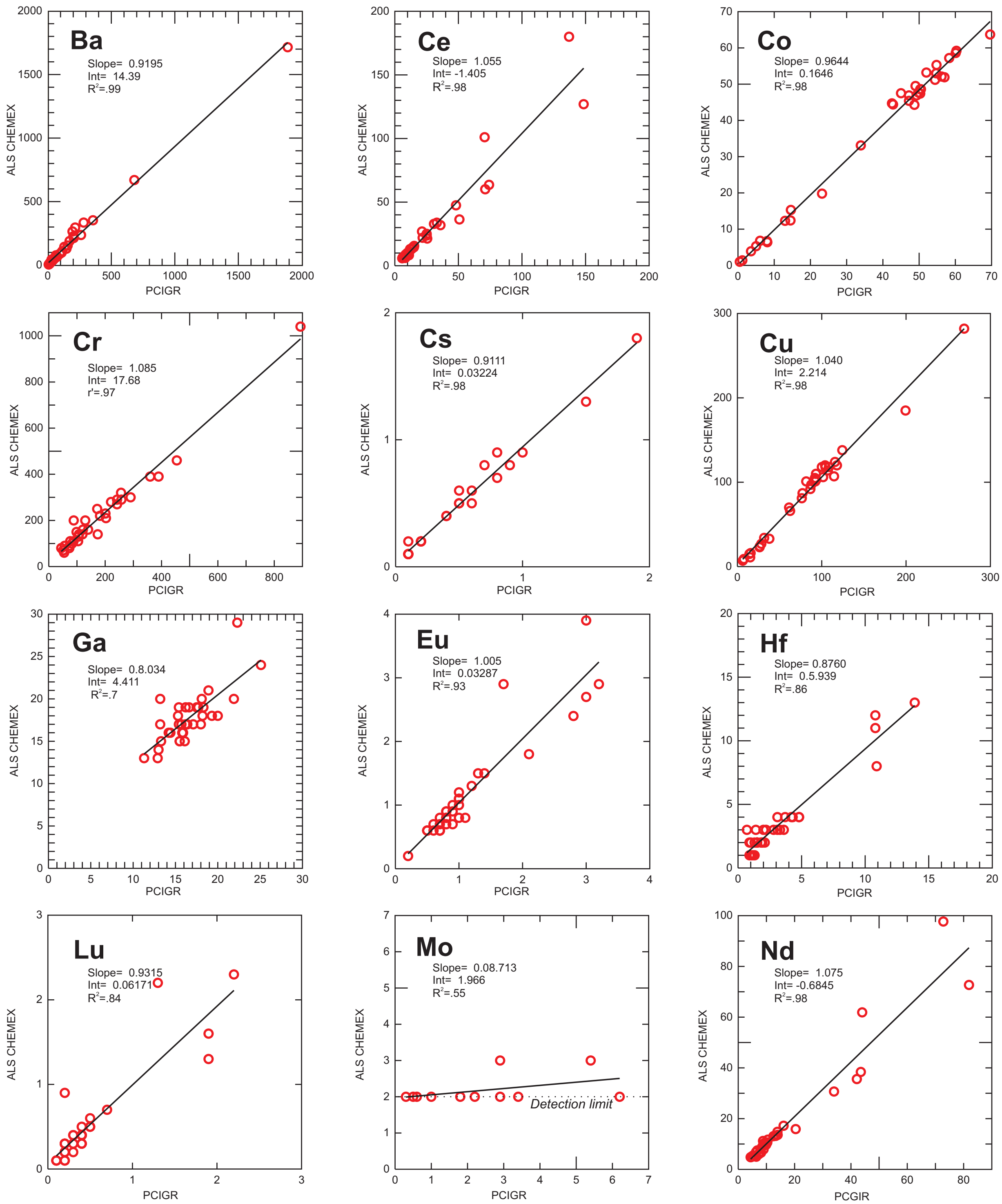

Figure E.1: Comparison of trace element results from PCIGR (HR-ICP-MS) and ALS CHEMEX North Vancouver (ICP-MS). Methods Discussed in Chapter 3, All samples are included in Appendix C (PCIGR) and Appendix D (ALS CHEM). Detection Limit included where necessary.

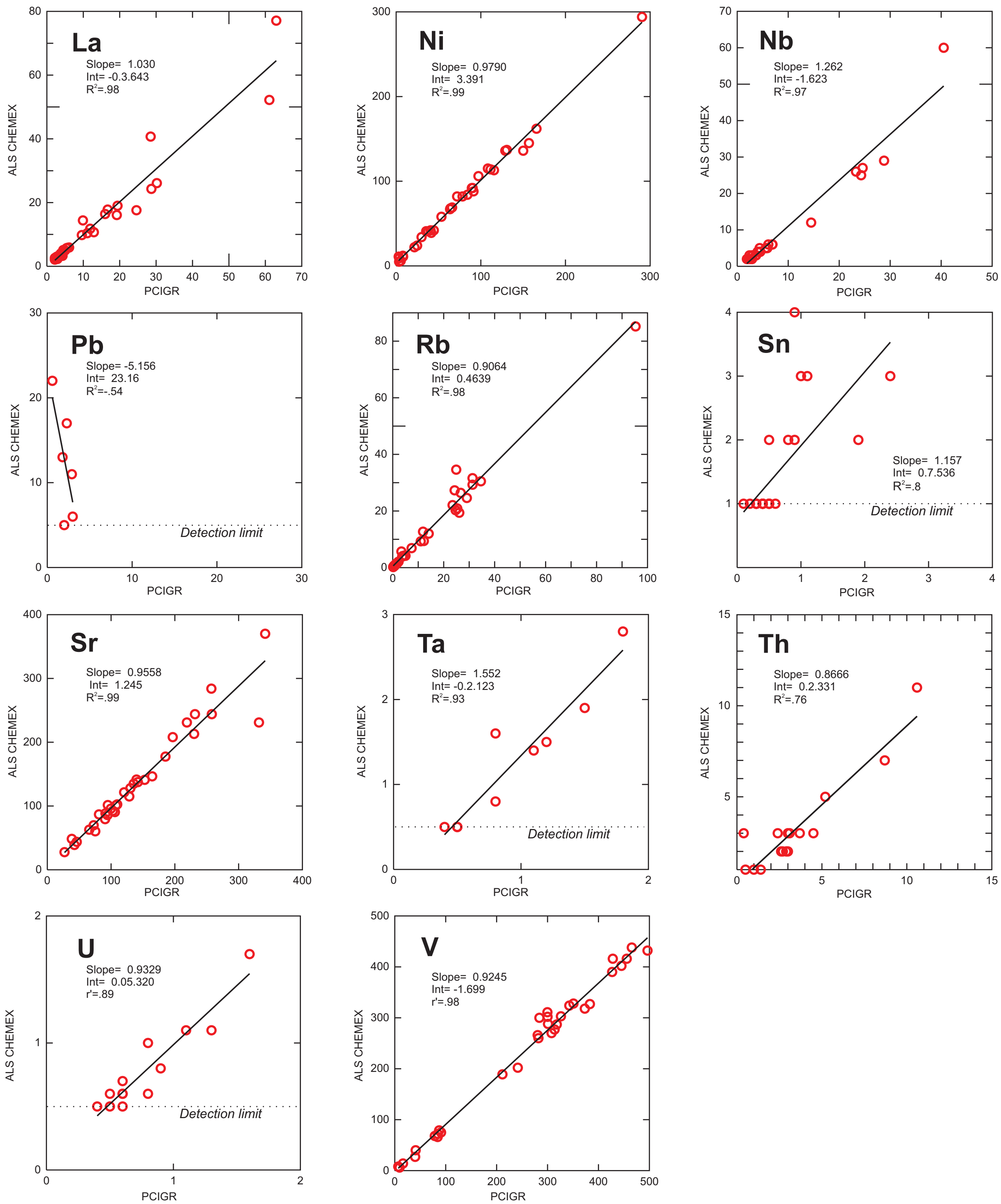

Figure E.1 (continued): Comparison of trace element results from PCIGR (HR-ICP-MS) and ALS CHEMEX North Vancouver (ICP-MS). Methods Discussed in Chapter 3, All samples are included in Appendix C (PCIGR) and Appendix D (ALS CHEM). Detection Limit included where necessary.

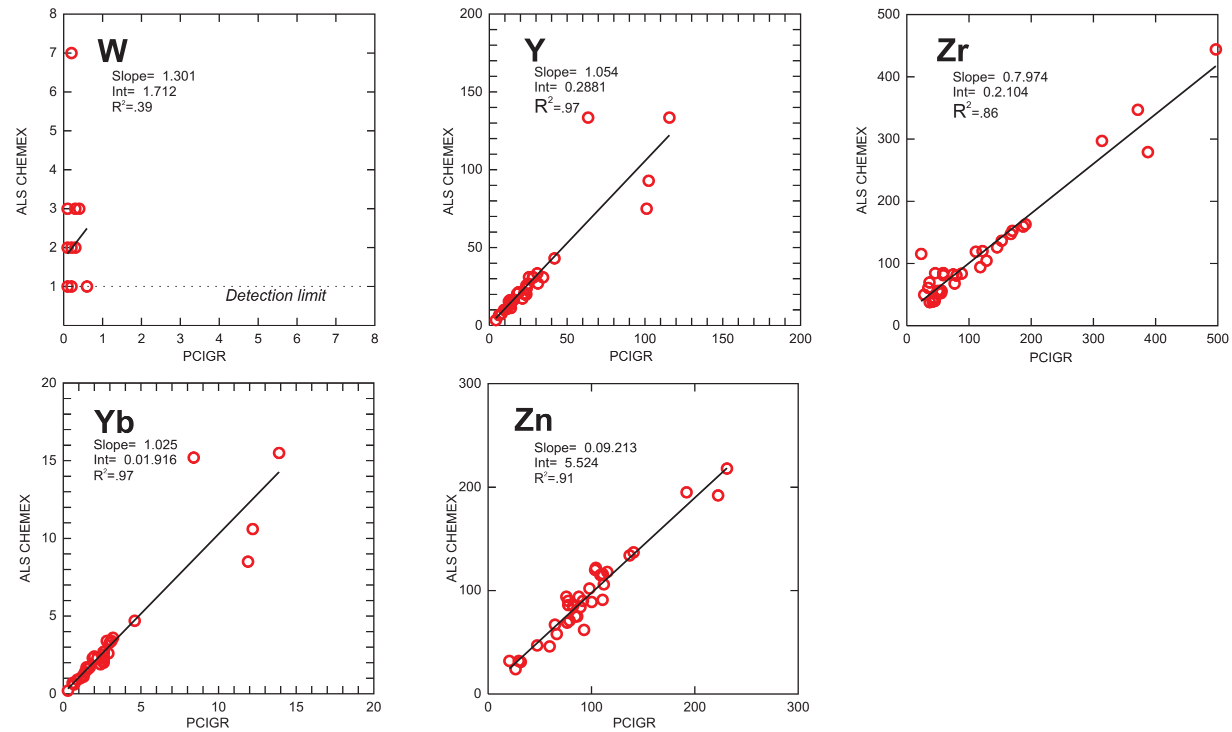

Figure E.1 (continued): Comparison of trace element results from PCIGR (HR-ICP-MS) and ALS CHEMEX North Vancouver (ICP-MS). Methods Discussed in Chapter 3, All samples are included in Appendix C (PCIGR) and Appendix D (ALS CHEM). Detection Limit included where necessary.